

# Boron-Tethered Auxiliaries for Directed C-H functionalisation of Aryl Boronic Esters: Feasibility Studies

Gareth Mark Hughes

**University of East Anglia**

**2022**

This copy of the thesis has been supplied on condition that anyone who consults it is understood to recognise that its copyright rests with the author and that use of any information derived therefrom must be in accordance with current UK Copyright Law. In addition, any quotation or extract must include full attribution.

# Declaration

This thesis is submitted in accordance with the requirements for the degree of Doctor of Philosophy (PhD) from the University of East Anglia

This copy of the thesis has been supplied on condition that anyone who consults it is understood to recognise that its copyright rests with the author and that use of any information derived therefrom must be in accordance with current UK Copyright Law. In addition, any quotation or extract must include full attribution.

School of Chemistry, University of East Anglia March 2022

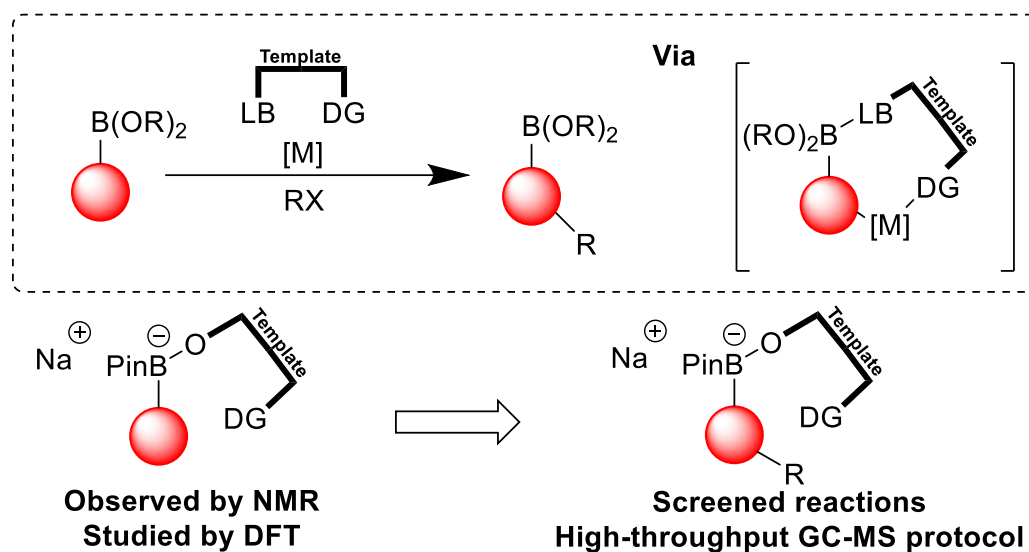
# Acknowledgements

To my supervisor, Thomas Storr, who has been such a supportive and engaging supervisor throughout my PhD. An excellent teacher, mentor, and friend. Garth Jones was also a brilliant help, teaching me to perform the DFT calculations found within this thesis.

In my four years at UEA, I have had the pleasure of being supported by a fantastic group of PhD students, post-docs and academics. I'm very grateful for the advice received. I wish all these people the best of luck in the future.

Most importantly, my partner Katja, has been nothing but supportive during our time in Norwich. You make me laugh and smile and I am lucky to have you.

# Abstract



Transient Interactions between a pinacol boronic ester and bifunctional template, bearing a Lewis basic moiety, were investigated to assess the feasibility of performing directed C-H functionalisation on organoboronic esters whilst maintaining the boronic moiety.

Quantitative conversion was detected for alkoxides coordinating to a fluoroaromatic pinacol boronic ester, characterised by  $^1H$ ,  $^{19}F\{^1H\}$  and  $^{11}B$  NMR, observing a general up-field shift, which is indicative of boronate formation.

DFT calculations (B3LYP/6-31G\*) elucidated that steric factors outweigh trends in  $pK_{a-H}$ , rendering *tert*-butoxide more weakly binding (47 kcal/mol) than methoxide (63 kcal/mol). Synthesis of templates was performed and coordination of these bifunctional alkoxide templates to fluoroaromatic pinacol boronic esters was demonstrated.

A high-throughput screening protocol was developed, utilising GC-MS to rapidly assess the components of crude mixtures. No desired product was observed in these studies but they directed work towards polydentate ligand-substrate binding. A series of *N*-templated iminodiacetic acid (TIDA) ligands were designed.

## **Access Condition and Agreement**

Each deposit in UEA Digital Repository is protected by copyright and other intellectual property rights, and duplication or sale of all or part of any of the Data Collections is not permitted, except that material may be duplicated by you for your research use or for educational purposes in electronic or print form. You must obtain permission from the copyright holder, usually the author, for any other use. Exceptions only apply where a deposit may be explicitly provided under a stated licence, such as a Creative Commons licence or Open Government licence.

Electronic or print copies may not be offered, whether for sale or otherwise to anyone, unless explicitly stated under a Creative Commons or Open Government license. Unauthorised reproduction, editing or reformatting for resale purposes is explicitly prohibited (except where approved by the copyright holder themselves) and UEA reserves the right to take immediate 'take down' action on behalf of the copyright and/or rights holder if this Access condition of the UEA Digital Repository is breached. Any material in this database has been supplied on the understanding that it is copyright material and that no quotation from the material may be published without proper acknowledgement.

# List of Abbreviations

{ <sup>1</sup> H}	Proton Decoupled
AAM	Anthanimide
Ac	Acetate
AMLA	Ambiphilic Metal Ligand Activation
ATR-FTIR	Attenuated Total Reflection – Fourier Transform Infrared Spectroscopy
BDE	Bond Dissociation Energy
Bn	Benzyl
BNCT	Boron Neutron Capture Therapy
BQ	Benzoquinone
Bu	Butyl
CI	Chemical Ionisation
CMD	Concerted Metalation Deprotonation
COD	Cyclooctadiene
coe	Cyclooctene
Cp	Cyclopentadiene
Cp*	Pentamethylcyclopentadiene
CT	Charge Transfer
Cy	Cyclohexyl
CyJohnPhos	2-(Dicyclohexylphosphino)biphenyl
DAN	1,8-Diaminonaphthalene
DavePhos	2-Dicyclohexylphosphino-2'-( <i>N,N</i> -Dimethylamino)biphenyl
dba	Dibenzylideneacetone
DCE	Dichloroethane
DCM	Dichloromethane
DG	Directing Group
DIPEA	<i>N,N</i> -Diisopropylethylamine

DMAE	Dimethyl Aminoethoxide
DMF	Dimethyl Formamide
DMG	Directed Metallation Group
Dmpe	1,2-Bis(dimethylphosphino)ethane
DMSO	Dimethyl Sulfoxide
DoM	Directed <i>Ortho</i> -Metallation
dppf	1,1'-Bis(diphenylphosphino)ferrocene
Dtbpv	4,4'-Di- <i>tert</i> -butyl-2,2'-pipyridine
EI	Electron Ionisation
Et	Ethyl
Fc	Ferrocenyl
FGI	Functional Group Interconversion
FID	Flame Ionisation Detection
GC-MS	Gas Chromatography – Mass Spectrometry
GGA	Generalised Gradient Approximation
Gly	Ethylene Glycol
Gly	Glycine
GTO	Gaussian-Type Orbitals
HFIP	Hexafluoroisopropanol
HIE	Hydrogen Isotope Exchange
HRMS	High Resolution Mass Spectrometry
IES	Internal Electrophilic Substitution
IMes	1,3-Dihydro-1,3-bis(2,4,6-trimethylphenyl)Imidazole-2-ylidene
IR	Infrared
IUPAC	International Union of Pure And Applied Chemistry
i	<i>iso</i> -
LA	Lewis Acid
LB	Lewis Base
LDA	Local Density Approximation
LSDA	Local Spin Density Approximation

M.P.	Melting Point
M/Z	Mass/Charge
<i>m</i> CPBA	<i>Meta</i> -Chloroperbenzoic Acid
Me	Methyl
MeCN	Acetonitrile
Mes	Mesityl
MIDA	<i>N</i> -Methyliminodiacetate
MOM	Methoxy Methyl Ester
NBS	<i>N</i> -Bromosuccinimide
NCS	<i>N</i> -Chlorosuccinimide
NIS	<i>N</i> -Iodosuccinimide
NMO	<i>N</i> -Methylmorpholine <i>N</i> -Oxide
NMP	<i>N</i> -Methyl-2-Pyrrolidone
NMR	Nuclear Magnetic Resonance
NOE	Nuclear Overhauser Effect
NXS	<i>N</i> -Halo Succinimide
PE	Petroleum Ether
PG	Protecting Group
Ph	Phenyl
Pin	Pinacol
Piv	Pivalate
PMB	<i>para</i> -Methoxy Benene
ppm	Parts Per Million
Pr	Propyl
PTSA	<i>Para</i> -Tolylsulfonic Acid
PZA	2-Pyrazol-5-Ylanaline
qNMR	Quantitative Nuclear Magnetic Resonance
R <sub>f</sub>	Retention Factor
RI-NMR	Rapid Injection Nuclear Magnetic Resonance
RuPhos	2-Dicyclohexylphosphino-2',6'-Diisopropoxy-1,1'-Biphenyl



SAR	Structure Activity Relationship
SM	Starting Material
SMCC	Suzuki-Miyaura Cross-Coupling
S <sub>N</sub> Ar	Nucleophilic Aromatic Substitution
STO	Slater-Type Orbitals
t	<i>tert</i> -
T	Temperature
T <sub>1</sub>	Longitudinal Relaxation Constant
TBAF	Tetra-Butyl Ammonium Fluoride
TEA	Triethyl Amine
Tf	Trifluoromethanesulfonyl
TFA	Trifluoroacetate
TFE	Trifluoroethanol
THF	Tetrahydrofuran
TIC	Total Ion Count
TIDA	<i>N</i> -Template Iminodiacetate
TLC	Thin Layer Chromatography
TMS	Trimethyl Silyl
Tol	Tolyl
TPAP	Tetrapropylammonium Perruthate
USA	United States Of America
XPhos	2-(Dicyclohexylphosphino)-2',4',6'-triisopropylbiphenyl

# Contents

<b>1. Carbon-Boron Bond Orthogonality in Transition Metal Catalysed Synthetic Methodologies</b> .....	<b>2</b>
1.1. <i>Boron Chemistry</i> .....	2
1.2. <i>Organoboronic Species</i> .....	4
1.3. <i>Installing Boronic Moieties</i> .....	9
1.4. <i>Transmetallation of Boronic Acids</i> .....	14
1.5. <i>Boronic Acid Protecting Groups</i> .....	20
1.5.1. <i>Boronic Pinacol Esters</i> .....	21
1.5.2. <i>Trifluoroborate salts</i> .....	27
1.5.3. <i>MIDA boronates</i> .....	29
1.5.4. <i>1,8-Diaminonaphthalene Boronic Amides</i> .....	34
1.6. <i>C-H Functionalisation</i> .....	36
1.6.1. <i>Overview</i> .....	36
1.6.2. <i>Mechanistic Insight</i> .....	38
1.7. <i>Directed C-H Functionalisation</i> .....	44
1.7.1. <i>Directed Ortho-Functionalisation</i> .....	44
1.7.2. <i>Distal Directing Auxiliaries</i> .....	46
1.7.3. <i>Traceless Directing Groups</i> .....	48
1.7.4. <i>Transient Directing Groups</i> .....	48
1.7.5. <i>Non-Covalently Bound Directing Groups</i> .....	53
1.8. <i>C-H functionalisation Orthogonal to C-B Bonds</i> .....	58
1.8.1. <i>Substrates with Boronic Moieties</i> .....	58
1.8.2. <i>Boron Tethered Directing Auxiliaries</i> .....	60
1.9. <i>Aims and Objectives</i> .....	67
<b>2. Alkoxy Pinacol Boronates</b> .....	<b>74</b>
2.1. <i>Observing Transient Boron-Ligand Interactions</i> .....	74
2.2. <i>Detecting Lewis Base Co-ordination</i> .....	76
2.3. <i>Quantitative NMR Methodologies</i> .....	78
2.3.1. <i>Developing a <math>^{19}\text{F}\{^1\text{H}\}</math> qNMR Spectroscopic Protocol</i> .....	80
2.3.2. <i>Inversion Recovery Experiment</i> .....	81
2.3.3. <i>Validation of the <math>^{19}\text{F}\{^1\text{H}\}</math> qNMR Spectroscopic Protocol</i> .....	84
2.4. <i>NMR Characterisation</i> .....	86
2.5. <i>Calculation of Dissociation Energies</i> .....	88
2.5.1. <i>DFT Overview</i> .....	88
2.5.2. <i>DFT Dissociation Energies</i> .....	91
2.6. <i>Bifunctional Templates</i> .....	96
2.6.1. <i>Proposed Bifunctional Templates</i> .....	96
2.6.2. <i>Synthesis of Bifunctional Templates</i> .....	100
2.6.3. <i>Substrate-Ligand Complexes</i> .....	106
2.6.4. <i>Ligand-Substrate-Metal Ternary Complexation</i> .....	110
2.7. <i>Screening Studies</i> .....	115
2.7.1. <i>High-throughput analysis by GC-MS</i> .....	115
2.7.2. <i>Screening Results</i> .....	120

<b>3. TIDA-boronates for C-H Functionalisation .....</b>	<b>128</b>
3.1. <i>Polydentate Ligand-Substrate Binding</i> .....	128
3.2. <i>BMIDA Orthogonality in C-H Functionalisation</i> .....	132
3.2.1. Starting Material Synthesis .....	134
3.2.2. Design of Screening Studies .....	138
3.2.3. Screening Results .....	141
3.3. <i>Synthesis of TIDA-Boronates</i> .....	146
<b>4. Conclusions.....</b>	<b>154</b>
4.1. <i>Summary</i> .....	154
4.2. <i>Future Work</i> .....	157
<b>5. References .....</b>	<b>163</b>
<b>6. Appendix .....</b>	<b>171</b>

# Chapter 1

## Carbon-Boron Bond Orthogonality in Transition Metal Catalysed Synthetic Methodologies

# 1. Carbon-Boron Bond Orthogonality in Transition Metal

## Catalysed Synthetic Methodologies

### 1.1. Boron Chemistry

Over the past century, boron chemistry has been applied to a wide range of disciplines, finding applications in materials chemistry, pharmaceuticals, agrochemicals, metallurgy, semiconductors, and chemical syntheses. Boron has a relatively low chemical abundance of 0.001% by weight of the earth's crust compared to an element such as lithium that is twice as abundant (0.002% by weight of the earth's crust).<sup>[1]</sup> Despite this, 10 million tonnes of boron minerals are mined yearly, from major borate reserves located in Turkey (73.4%), Russia (7.8%) and the USA (6.2%); only 3500 tonnes of lithium is mined yearly.<sup>[2]</sup> Access to many boron-containing minerals is improved by their water solubility. The aptly named town of Boron, California supplied approximately 25% of the world's refined borates in 2018;<sup>[3]</sup> Boron, California is located at the edge of the Mojave desert, which was a lakebed until roughly 8,500 years ago.<sup>[4]</sup>

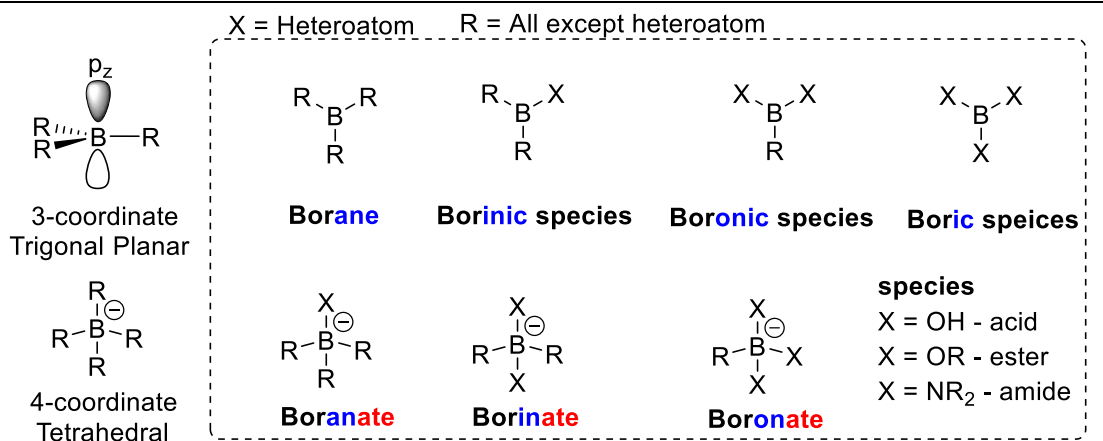
The global applications of boron across a range of distinct industries are numerous. In metallurgy, ferroboration alloys can be added in small quantities to enhance the hardness of steel. In the semiconductor industry, doping of boron to silicon and germanium can modify electrical conductivity. Many land-plants require boron in the form of boric acid or borates to facilitate growth, directing agrochemical outputs.  $^{10}\text{B}$  can capture free neutrons to generate alpha particles (helium nuclei), allowing alpha particle detectors (such as Geiger counters) to be converted to neutron detectors using  $^{10}\text{BF}_3$  gas. In medicine, boron neutron capture therapy (BNCT) injects cancer patients with isotopically enriched  $^{10}\text{B}$ -compounds; patients are then irradiated with a focussed beam of neutrons to promote a controlled production of alpha-particles inside the tumour. Finally, boron is applied in

the ceramic and glass industry, accounting for 65 % of boron minerals consumed in the USA in 2021.<sup>[3]</sup>

Boron has the ability to rapidly convert from a 3-coordinate trigonal planar ( $sp^2$ -hybridised) geometry to a 4-coordinate tetrahedral ( $sp^3$ -hybridised) geometry with an anionic boron centre. This is possible *via* coordination to boron's empty  $p_z$ -orbital, which sits perpendicular to the trigonal planar geometry of a 3-coordinate boron centre. Interaction with this  $p_z$ -orbital is integral to many chemical and biochemical processes.

Some inconsistency in nomenclature is common with boron-compounds, as the IUPAC naming convention does not cover the full range of potential species.<sup>[5]</sup> Lennox *et al.* recently attempted to establish a naming system that is more reflective of naming conventions currently used in the organic literature.<sup>[6]</sup>

The naming convention described by Lennox *et al.* appends different suffixes to a *bor-* root depending on the number of non-heteroatom substituents on a 3-coordinate boron species: *-ane* for three non-heteroatom substituents, *-inic* for two non-heteroatom substituents, *-onic* for one non-heteroatom substituents, and *-ic* for no non-heteroatom substituents. 4-Coordinate derivatives are signified with an additional *-ate* suffix but follow the same convention as the 3-coordinate boron compounds (Scheme 1). It should be noted that some compounds do not fit in the naming convention proposed by Lennox *et al.* For example, boric esters are normally referred to as borates, despite the *-ate* suffix normally indicating a 4-coordinate anionic boron species.

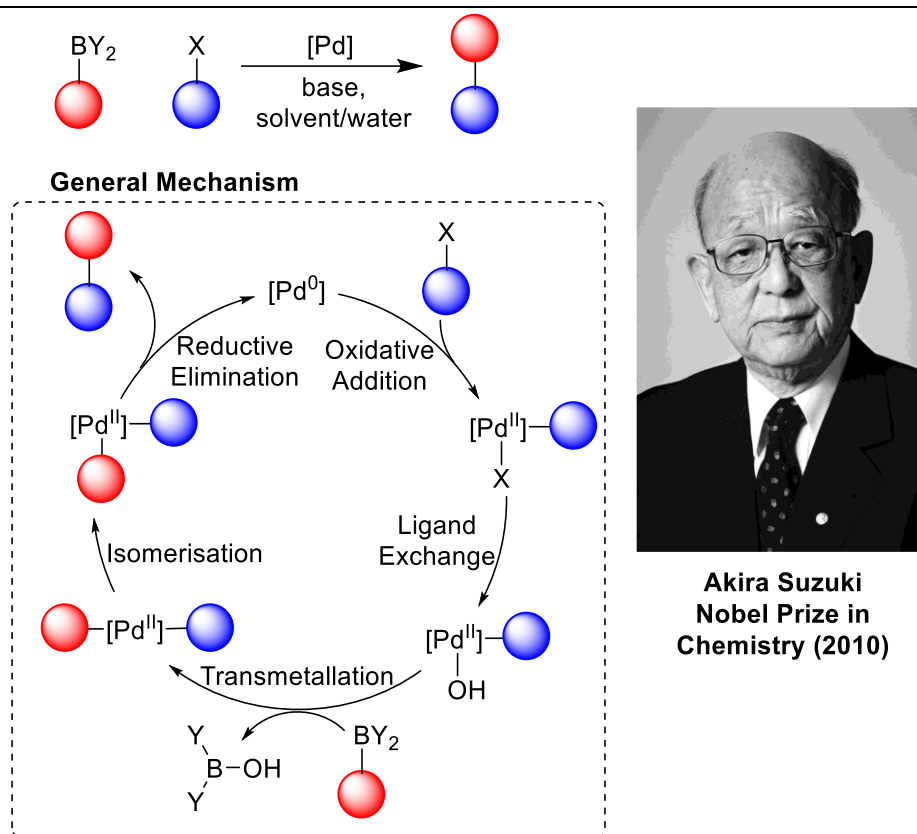


*Scheme 1: General naming system of boron-centred functionalities as proposed by Lennox et al.*

## 1.2. Organoboronic Species

Organoboronic species, are trigonal planar boron-containing moieties with a single organic substituent and two heteroatom substituents. These compounds may be applied in numerous chemical applications contributing to their ubiquity in synthetic chemistry: A quick search of the Reaxys database reveals 272,959 organoboronic species; the Sci-finder database discloses 359,581 organoboronic species.

In synthetic chemistry, the Suzuki-Miyaura cross-coupling reaction (SMCC) is a very important method for carbon-carbon bond formation. The reaction couples an organoboron substrate with an organohalide by palladium catalysis under basic conditions (Scheme 2). The SMCC's significance in modern-day synthetic chemistry earned Akira Suzuki a third share of the 2010 Nobel prize in Chemistry.<sup>[7]</sup>



**Akira Suzuki**  
Nobel Prize in  
Chemistry (2010)

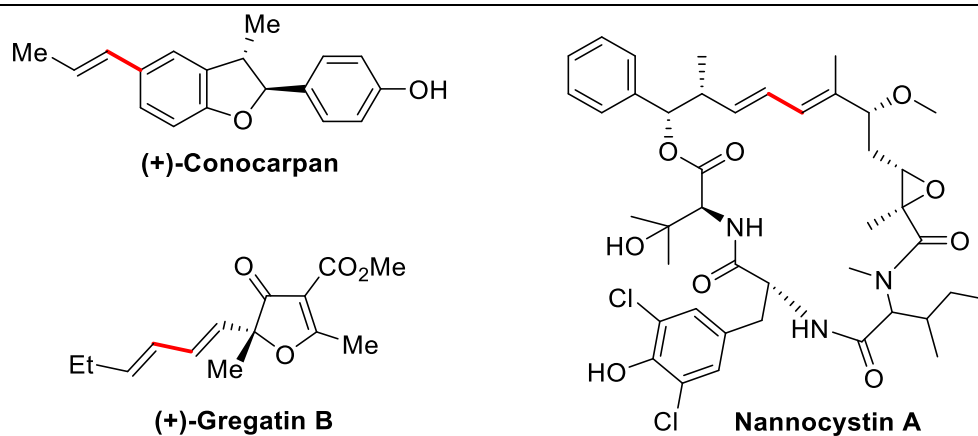
*Scheme 2: The Suzuki-Miyaura cross coupling reaction is a widely utilise Carbon-Carbon bond forming synthetic methodology*

A general SMCC mechanism (Scheme 2) proceeds by oxidative addition of palladium(0) across a carbon-halogen bond yielding an organopalladium(II) species. The organopalladium(II) intermediate then undergoes a ligand exchange to produce an oxo-palladium(II) species, which then performs transmetalation with the organoboronic reagent. This transmetalation generates a palladium(II) species bearing a second organic fragment, which goes on to perform a reductive elimination, regenerating the palladium(0) catalyst and yielding a new carbon-carbon bond.

The Suzuki-Miyaura reaction is prized by synthetic chemists because it uses relatively non-toxic and air-stable reagents, proceeds under mild conditions, has excellent functional group compatibility, gives excellent yields, and can be performed on large scale.<sup>[8]</sup> The scalability of SMCC's have been showcased by Clariant AG, who produce *ortho*-tolyl benzonitrile, an AT II antagonist precursor, using SMCC on multi-tonne scale.<sup>[9]</sup> The functional



group compatibility of SMCC is highlighted in the synthesis of several poly-functional natural products, where it may be employed in the finally synthetic step (Scheme 3).<sup>[10]</sup>

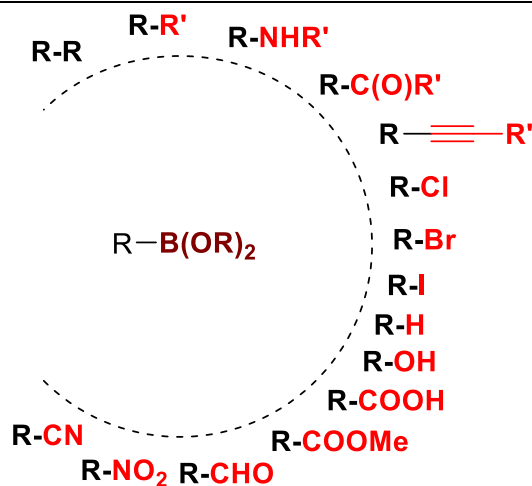


*Scheme 3: Several choice examples of natural products synthesised using Suzuki-Miyaura cross-coupling in the final synthetic step. Bonds formed using SMCC are highlighted in red.*

---

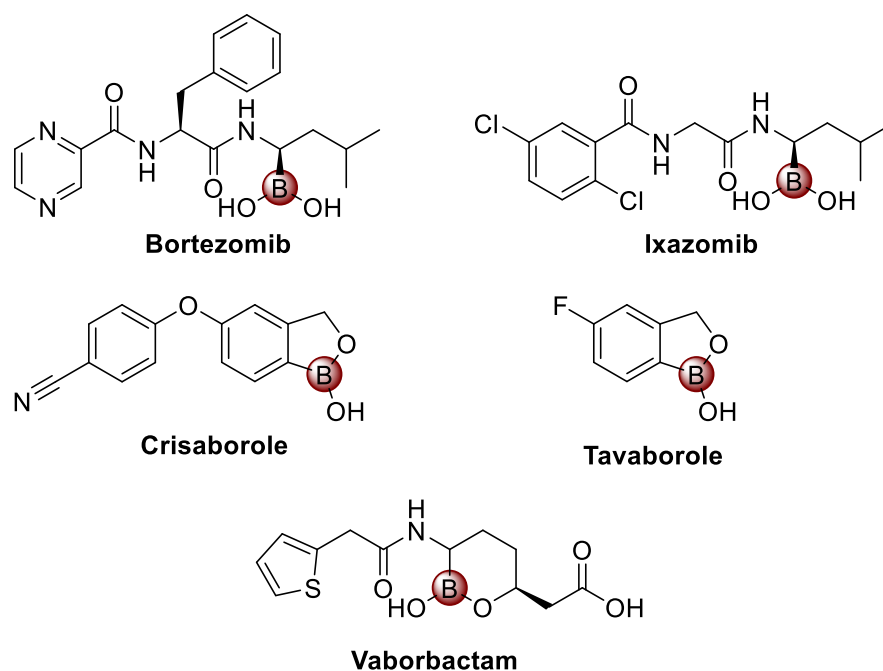
Biaryl motifs are ubiquitous substructures of natural products, pharmaceuticals, agrochemicals and electronic materials. SMCC can achieve the synthesis of symmetrical and unsymmetrical biaryls with high efficiency, rendering SMCC a key reaction for industrial fine-chemical production.<sup>[11]</sup> SMCC reactions are not limited to aryl-aryl couplings, they also have a wide substrate scope covering different carbon-hybridisations. Cross-coupling with alkyl boronic substrate has been disclosed, but may be limited where  $\beta$ -hydride elimination is possible.<sup>[12,13]</sup>

Aside from Suzuki-Miyaura cross-coupling reactions, organoboronic acids have a broad synthetic utility. They are able to undergo a wide range of functional group interconversions (FGIs), making them a stepping-stone to rapidly access numerous synthetic targets (Scheme 4).<sup>[14]</sup>



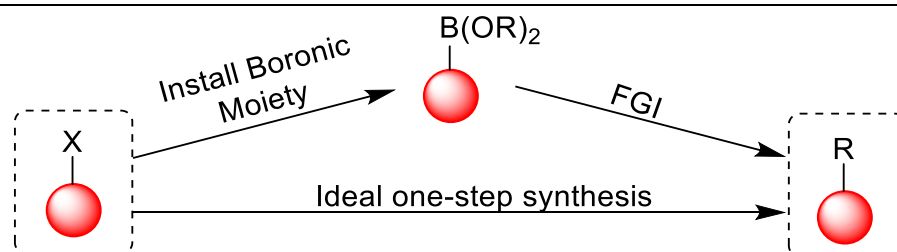
*Scheme 4: Organoboron compounds can undergo a broad range of functional group interconversions. Scheme reproduced from literature.<sup>[14]</sup>*

In pharmaceutical research, boronic acid moieties are currently being studied as bioisosteres for carboxylic acids. Whilst carboxylic acids ( $pK_a \sim 4-5$ ) are deprotonated to charged carboxylates under physiological conditions ( $pH \sim 7.4$ ), boronic acids ( $pK_a \sim 9$ ) remain neutral. Furthermore, their Lewis acid properties can enhance structure activity relationships (SAR) *via* interactions with serine residues in the active sites of some protein targets.<sup>[15]</sup> Bortezomib was first approved in the early 2000's, as an anti-cancer drug for the treatment of multiple myeloma and mantle cell lymphoma, two forms of cancer affecting bone marrow and the lymphatic system respectively. Bortezomib was the first drug on the market to contain a boronic acid.<sup>[16]</sup> Since, numerous boronic acid containing drug candidates have been presented for clinical trials (Scheme 5).



*Scheme 5: A variety of small molecule drugs containing a boronic acid moiety have been approved for treatments.*

In multistep syntheses, boronic acid moieties are often utilised in a transitory manner, meaning that from an initial substrate, a boronic acid moiety is installed and then immediately consumed *via* one of many FGI's. Using boronic moieties in a transitory manner is akin to protecting group strategies; ideally a multistep synthesis would avoid protecting groups, but they are often installed to avoid complications. Optimal syntheses avoid sacrificial groups as they require additional synthetic steps and increase waste (Scheme 6).<sup>[17]</sup>



*Scheme 6: Transitory use of boronic moieties is akin to protecting groups installation, adding additional steps, and lowering atom economy*

Transitory use of boronic moieties does not utilise the functionality as an easily and reversibly modifiable handle to enhance chemistry: Organoboronic species can rapidly undergo exchange of heteroatom substituents; and have an empty coordinative site which can be utilised to control chemical transformations. However, there are only a few examples of compounds bearing boronic moieties being used to enhance chemo-selectivity or stereoselectivity.<sup>[16,18]</sup> Several boronic acid enhanced transition metal catalysed protocols will be described, *vide infra*.

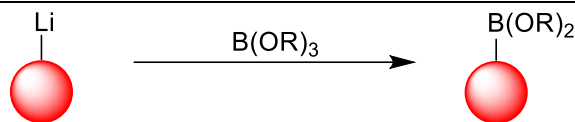
Orthogonality of boronic species is thought to be difficult under transition metal catalysis where transmetallation and radical cleavage pathways can occur, such as in Minisci-type reactions.<sup>[19-21]</sup> A convergent synthesis of, the boronic acid containing drug, bortezomib described by Ivanov *et al.* entirely avoids any transition metal catalysis.<sup>[22]</sup> Their synthesis of bortezomib uses mainly lithiation chemistry which required care to prevent, for example, boron-centred homologation reactions. Furthermore, lithiation chemistry is not desirable for large scale synthesis due to poor substrate scope and exotherms, requiring a sub-ambient reaction temperature. Current research, however, is allowing for controlled ambient temperature lithiation using flow-systems.<sup>[23]</sup>

For brevity, this chapter focuses primarily on transition metal catalysed reactions that do not consume a C-B bond moiety, although non-catalysed C-B orthogonal reactivities have been described in the literature.<sup>[24]</sup>

### 1.3. Installing Boronic Moieties

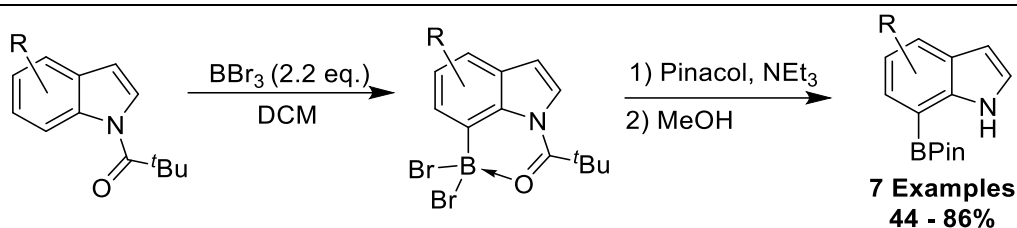
A common approach to formation of a C-B bond is the electrophilic trapping of organolithium or organomagnesium species with boron reagents such as trialkyl boric esters (Scheme 7). The high reactivity of organolithium or organomagnesium intermediates limits substrate scope, preventing the use of substrates with electrophilic or acidic functionalities. In these cases, late-stage installation or deprotection of electrophilic functional groups would be

required post-installation of a boronic moiety. The formation of stabilised lithium and magnesium alkoxides in these reactions creates an exergonic reaction, forming a weak C-B bond ( $\sim 107$  kcal/mol) in exchange of a stronger B-O bond ( $\sim 192$  kcal/mol).<sup>[25]</sup>



*Scheme 7: Borylation may be achieved by quenching of organo-lithium or -magnesium reagents with borates*

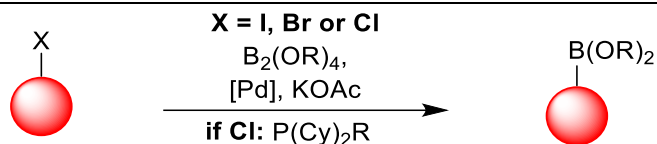
Alternatively, a use of strong electrophiles such as  $\text{BBr}_3$  may be used. Coordination of  $\text{BBr}_3$  to oxygen-centred Lewis bases has been shown to direct borylation to a proximal aryl group *via* electrophilic aromatic substitution.<sup>[26]</sup> As an example, Iqbal *et al.* described an *ortho*-selective borylation of *N*-acyl-indoles, wherein the acyl directs C7-borylation, overriding the nucleophilic favourability of the C3-site exhibited by free indoles (Scheme 8).<sup>[27]</sup>



*Scheme 8: An *N*-pivaloyl directed C7-borylation of indoles using  $\text{BBr}_3$*

Where highly reactive reagents cannot be used due to functional group incompatibilities, softer transition metal catalysed methods can be used. These catalytic methods usually employ diboron reagents rather than cheaper borates; the weak B-B bonds ( $\sim 71$  kcal/mol<sup>[25]</sup>) of diboron reagents are necessary to induce thermodynamic favourability for C-B bond formation. Palladium catalysed Miyaura borylation achieves borylation of aryl halides with diboron reagents, driven by formation of C-B and B-O bonds (Scheme 9). Further developments have permitted borylation of aryl chlorides by addition

of sterically bulky and electron-rich phosphine ligands to permit C-Cl oxidative addition.<sup>[28]</sup> For Miyaura borylation and its contemporary derivatives to be applicable, a halogen must either be installed or maintained from the starting materials as a sacrificial moiety.

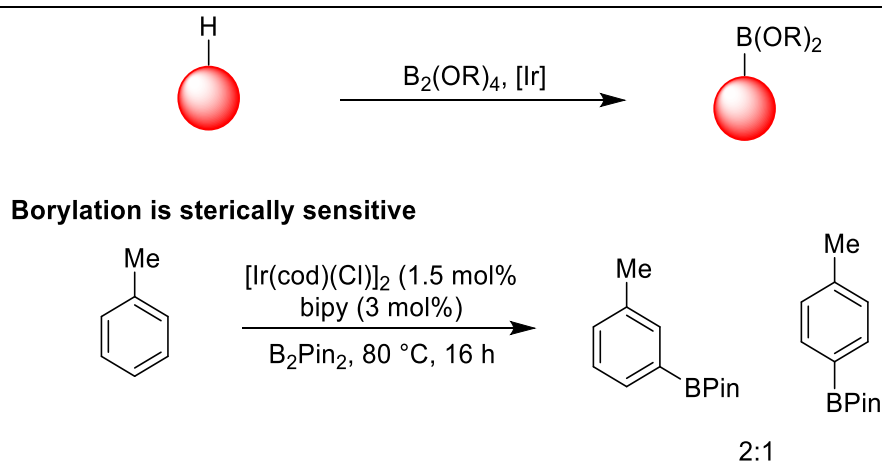


*Scheme 9: C-X Borylation can be achieved via Miyaura Borylation*

---

The borylation of C-H bonds is a highly attractive prospect, as non-acidic C-H bonds are ubiquitous in organic molecules and therefore no preinstallation is required. The challenges of this field of chemistry therefore lie in how to promote the desired borylation in a regioselective manner.

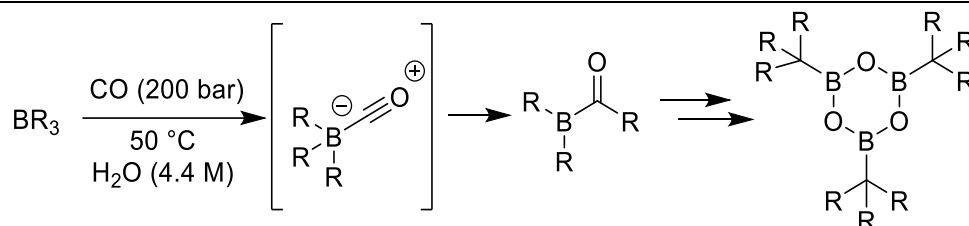
Iridium catalysts can achieve C-H borylations of arenes (Scheme 10). A high steric sensitivity of these catalytic systems often precludes *ortho*-functionalisation, normally affording a 2:1 *meta:para* functionalisation for monosubstituted arenes, 1,3-disubstituted arenes are often highly selective for *meta*-borylation due to its steric accessibility.<sup>[29]</sup> Other metals (Rh, Pd, Fe, etc.) can perform C-H borylations, however, the predictability of site-selectivity and functional group tolerances limits general usage.<sup>[30]</sup>



*Scheme 10: C-H Borylation may be achieved via metal-catalysis*

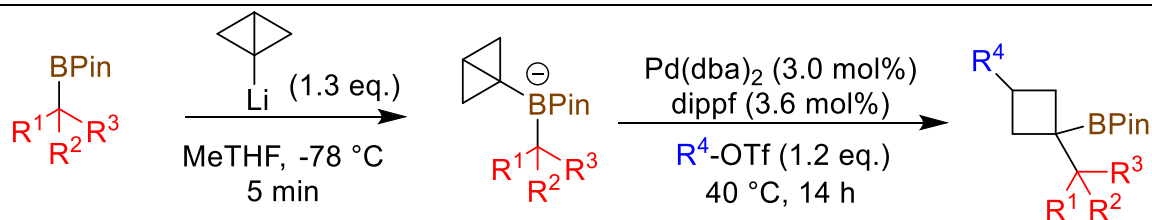
---

Homologation reactions of organoboron reagents can also be considered a sub-class of carbon-boron bond forming chemistries. In organoboron homologation the substrate itself is the boron source, leading to formation of new C-C and C-B bonds. An early example of this type of reactivity, is the reaction of boric esters with carbon monoxide to yield trialkylcarbinyl boroxines.<sup>[31]</sup> Coordination of carbon monoxide to boron's vacant  $p_z$  orbital facilitates an intramolecular transfer of the alkyl constituent *via* a 1,2-migratory shift onto the electrophilic carbon centre (Scheme 11).



Scheme 11: Co-ordination of carbon monoxide to boron facilitates a cascade of 1,2-alkyl migrations from a trialkyl borate producing a boroxime.

Organolithium and organomagnesium reagents can be used to alkylate an organoboronic acid ester substrate, producing a borinate *in situ*. The alkyl migration is then promoted by a proximal electrophilic centre. Transition metals can promote this class of reaction, whilst retaining the C-B bond in the final product. One choice example is the use of a strained bicyclo [1.1.0]butane in the presence of a palladium catalyst. The reaction relieves ring strain *via* a 1,2-migratory insertion forming an organopalladium intermediate which then produces a trisubstituted cyclobutane product (Scheme 12).<sup>[32]</sup>



Scheme 12: Palladium-Catalysed trisubstituted cyclobutane synthesis

As stated before, once installed boronic moieties can be utilised in a range of FGIs. In other words, boronic moieties are reactive to a range of different reaction conditions, and thus are normally used in a transitory manner. However, it will be shown that it is possible to design a multi-step synthesis, using transition metal catalysed reactions, where a boronic acid moiety is maintained from starting materials. To understand how these transition metal catalysed reactions can proceed orthogonally to a boronic moiety, it is important to first understand how C-B bonds are cleaved by transmetallation



## 1.4. Transmetallation of Boronic Acids

Transmetallation of an organoboron reagents is a key step in the catalytic cycles of palladium-catalysed Suzuki-Miyaura<sup>[33-35]</sup>, copper-catalysed Chan-Lam<sup>[36]</sup> and palladium-catalysed copper-mediated Liebskind-Srogl<sup>[37]</sup> cross-coupling reactions. Transmetallation of organoboronic acids to palladium is a facile process, with various other transition metals reported to perform transmetallation at a slower rate.<sup>[34]</sup> Hence a focus will be placed on the transmetallation of organoboronic species with palladium(II) as this is reported to be the quickest. These discussions take place in the context of Suzuki-Miyaura cross-coupling (SMCC) reactions, which have been extensively studied in the literature. A general overview of SMCC's was disclosed in Chapter 0.

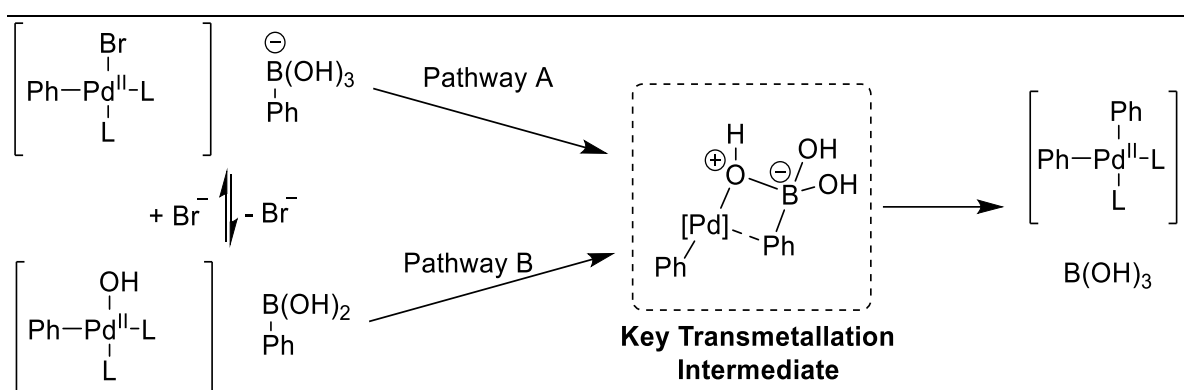
In the catalytic cycle of SMCC, transmetallation transfers the organic component of a organoboronic species onto the metal centre of an organopalladium(II) species. Transmetallation yields a palladium(II) species composed of two organic fragments, which will isomerise to give a *cis*-configuration of organic fragments, prior to reductive elimination to yield a new C-C bond.

When the Suzuki group disclosed the first reaction conditions for the later-termed, Suzuki-Miyaura cross-coupling reaction, it was shown that the reaction requires an oxygen-centred base; such as hydroxide, methoxide, ethoxide or acetate.<sup>[38]</sup> Other organic and inorganic bases can be used but must be employed in conjunction with water to generate hydroxide; fluoride was later found to also promote transmetallation.<sup>[39]</sup> In the absence of base a 2% yield of their desired product was afforded, whilst a "rapid and clean reaction" was realised under basic conditions.<sup>[38]</sup>

Two potential mechanistic pathways (Scheme 13) were investigated,<sup>[40,41]</sup> to explain the role which oxygen-centred bases played in forming a four-membered intermediate which rearranges to perform transmetallation:

**Pathway A.** An “activated” boronate species is formed *in situ* by coordination of an oxygen-centred base to the organoboronic acid. A boronate oxygen then coordinates to palladium. Quarternarisation of the boron weakens the C-B bond increasing its nucleophilicity, thus facilitating transfer of the organic component onto an electrophilic palladium centre.

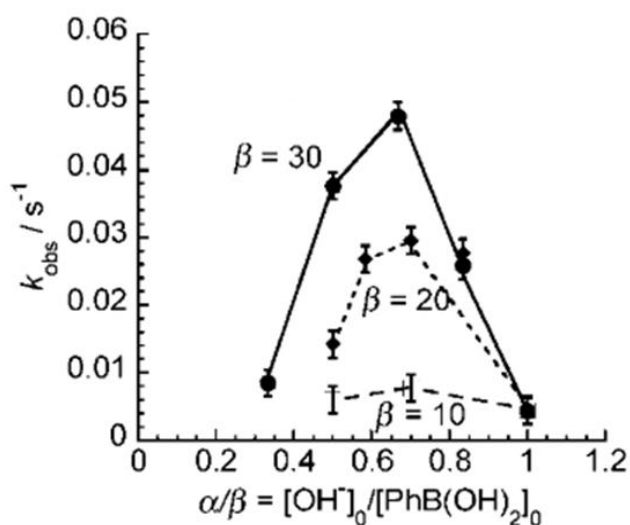
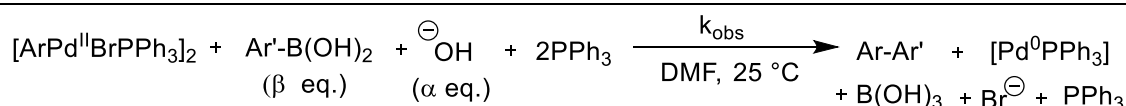
**Pathway B.** Ligation of an oxygen-centred base to palladium forms a highly reactive oxo-palladium species, the oxygen rapidly coordinates to boron forming the key transmetallation intermediate.



*Scheme 13: Two mechanistic pathways were proposed, with equilibrium between the two initial complexes possible*

Kinetic studies performed by Amatore and Jutand shed light on the role of hydroxide in SMCCs. Stoichiometric studies indicated that cross-coupling can proceed from the pathway A complex; reacting  $[PhPd^{II}Br(PPh_3)_2]$  with a trihydroxy boronate,  $[PhB(OH)_3]^-$  to yield biphenyl. Similarly cross-coupling was also afforded from the pathway B complex; reacting a oxo-palladium complex,  $[PhPd^{II}(OH)(PPh_3)_2]$ , with  $PhB(OH)_2$  to yield biphenyl. An equilibrium between the starting states of the two proposed pathways was shown to occur. No reaction occurs when applying both a hydroxopalladium(II) species and the trihydroxy boronate, meaning that once palladium and boron centres are saturated with hydroxide catalytic turn-over is inhibited, therefore hydroxide has both a facilitatory and inhibitory role in the reaction.<sup>[40]</sup>

This can be observed by measuring the rate of transmetallation relative to the ratio of concentrations of the boronic acid reagent and hydroxide anions. The studied showed that the rate was highest when the  $[\text{OH}^-]/\text{PhB}(\text{OH})_2$  ratio was around 0.6. Conversely, the rate was slowed significantly with either a low ( $<0.4:1$ ) or high ( $>1:1$ ) ratio of hydroxide to boronic acid. This indicates that two methods could be approached to diminish the rate of transmetallation, either anhydrous conditions or super-stoichiometric hydroxide loadings (Scheme 14).

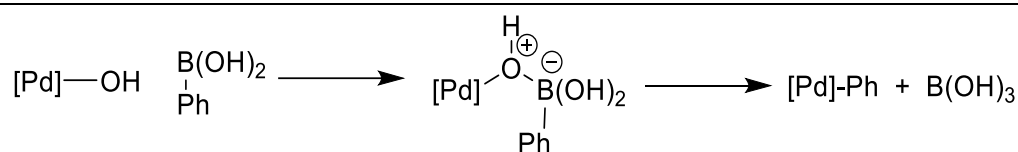


Scheme 14: Hydroxide inhibits transmetallation at high concentration but is necessary for transmetallation to proceed, Figure from Amatore et al. [42]

The concentration of  $[\text{ArPd}^{\text{II}}(\text{OH})\text{L}_2]$  was found to be proportional to the rate-determining transmetallation step. The concentration of bromide was also found to have an inhibitory effect on the reaction, competing with hydroxide for co-ordination to palladium. This information indicated that pathway B was the dominant pathway, with an oxopalladium species as the key intermediate preceding transmetallation.

Later DFT studies indicated that both pathways would converge on a Pd-O-B bridged intermediate (Scheme 15). This high-energy intermediate has

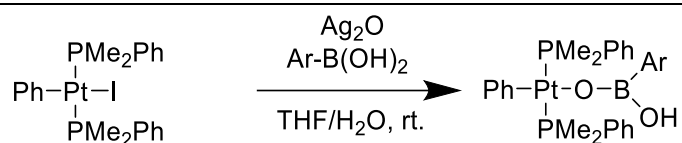
favourable electronics for a rapid transfer of the organic fragment from boron onto palladium with a kinetic barrier calculated to be 14-22 kcal/mol.<sup>[35]</sup>



*Scheme 15: DFT studies indicate that the cross-coupling proceeds via a bridged Pd-O-B intermediate which rapidly decomposes to produce an organopalladium species and a new B-O bond*

---

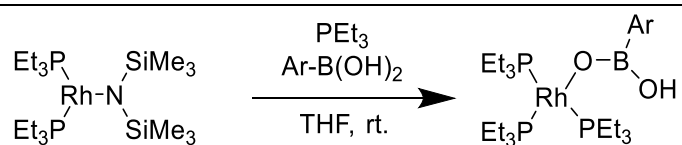
Other M-O-B bridged species have sufficient stabilities to be synthesised and isolated. The equivalent B-O-Pt intermediate can be produced by reaction of *trans*-PtPh(I)(PMe<sub>2</sub>Ph)<sub>2</sub> with 2-methoxyphenyl boronic acid over 4 hours at room temperature in a 50 % yield (Scheme 16). Extending the reaction time to 24 hours yields the transmetallated Pt-Ar species in a 78 % yield which can be characterised by X-ray crystallography.<sup>[43]</sup>



*Scheme 16: Synthesis of an isolatable Pt-O-B bridge complex*

---

Similarly the Hartwig group isolated and synthesised a series of B-O-Rh complexes by treating a Rh(I) silylamido precursor, {(PEt<sub>3</sub>)<sub>2</sub>Rh-[N(SiMe<sub>3</sub>)<sub>2</sub>]}

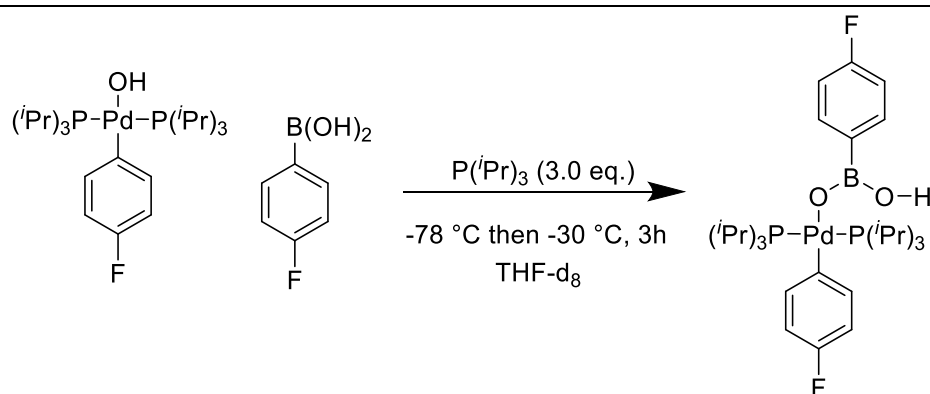
 with various aryl boronic acids at room temperature (Scheme 17).<sup>[44]</sup> These species were characterised by X-ray crystallography, and their stabilities were found to be determined by the electronics of the organoboron species, with electron-rich species found to react slightly slower than electron-deficient species.


*Scheme 17: Synthesis of an isolatable Rh-O-B bridge complex*

---

The short half-life of the Pd-O-B linked intermediate, resulting from its low barrier for transfer of the organic constituent, makes them difficult to study. Thus, the composition of this class of intermediate is difficult to observe experimentally using techniques such as electrospray mass spectrometry and traditional NMR techniques. These elusive intermediates were, however, characterised by rapid injection NMR (RI-NMR). With this approach, structural and kinetic information of the intermediates was obtained.<sup>[45,46]</sup>

4-Fluorophenyl boronic acid, *trans*-(*i*Pr<sub>3</sub>P)<sub>2</sub>(4-FC<sub>6</sub>H<sub>4</sub>)Pd(OH) and two additional equivalents of *i*Pr<sub>3</sub>P were injected at -78 °C in *d*<sub>8</sub>-THF. The solution was gradually heated to -30 °C upon which quantitative conversion to a Pd-O-B linked intermediate was observed (Scheme 18). The bonding connectivity of the intermediate was established by NOE experiments (Nuclear Overhauser Effect). Strong through-space couplings of both the palladium and boron-bound fluoro-aromatics to the *i*Pr<sub>3</sub>P ligands were observed. The boron atom was assigned with a tricoordinate geometry, as identified by the chemical shift in <sup>11</sup>B NMR which is in-line with the synthesised tricoordinate B-O-Pt<sup>[43]</sup> and B-O-Rh<sup>[44]</sup> species previously discussed.



Scheme 18: A key pre-transmetallation intermediate was formed at - 78 °C

---

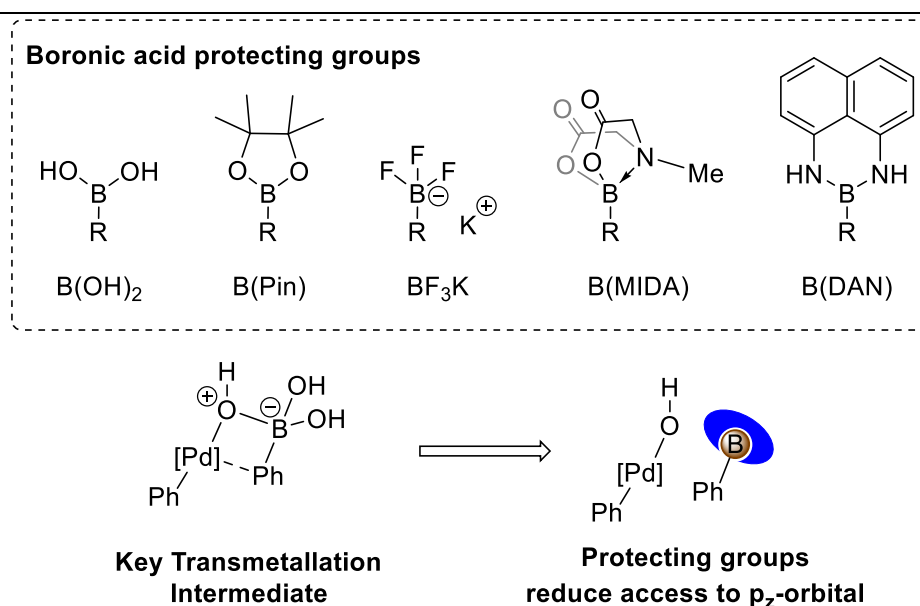
Further evidence to show the boronate pathway, pathway A, is the slower route was also found. When starting the study with *trans*-(*i*Pr<sub>3</sub>P)<sub>2</sub>(4-FC<sub>6</sub>H<sub>4</sub>)PdI and the tetracoordinate 4-fluorophenyl trihydroxy boronate only a

10% conversion was realised, with the low reaction temperatures inhibiting the hydroxide exchange necessary to form the oxopalladium(II) intermediate.

The studies outlined in this chapter are of great importance to the nature of the work detailed in this thesis, as thoroughly understanding the ways in which transmetallation can be optimised, can also simultaneously mean understanding how it can be avoided. Anhydrous non-basic conditions prevent formation of highly reactive oxopalladium(II) species necessary to perform transmetallation. The studies discussed in the chapter also state that an oxopalladium(II) species requires access to boron's unoccupied  $p_z$ -orbital to perform transmetallation. Boronic acid protecting groups operate by hindering access to boron's unoccupied  $p_z$ -orbital and are therefore able to preclude transmetallation.

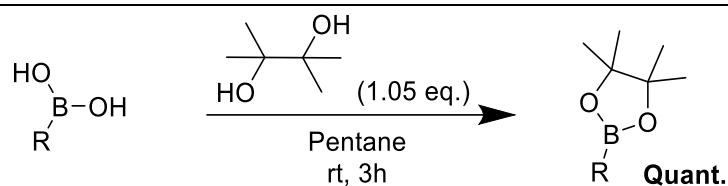
## 1.5. Boronic Acid Protecting Groups

Several boronic acid protecting groups diminish the rate of transmetallation, allowing transition metal catalysed reactions to be executed orthogonal to a boronic moiety.<sup>[47]</sup> The boronic acid protecting groups described in this chapter act to interfere with the empty  $p_z$ -orbital on boron. This hinders the formation of the key bridged Pd-O-B intermediate, thus precluding transmetallation. This interference can take the form of steric blocking, as observed in pinacol boronic acid esters (BPin), Direct coordination to a  $p_z$ -orbital by forming a charged  $sp^3$ -boronate species, as is the case with potassium trifluoroborate salts ( $BF_3K$ ) and *N*-methyl iminodiacetate protected boronic acids (BMIDA), or through conjugation of lone pairs, as in the diamidonaphthalene ancillary group (BDAN). Under standard Suzuki-Miyaura conditions, the key 4-membered transition state is destabilised creating a significant kinetic energy barrier to transmetallation (Scheme 19).



*Scheme 19: Boronic acid protecting groups slow transmetallation by reducing access to borons  $p_z$ -orbital.*

### 1.5.1. Boronic Pinacol Esters



*Scheme 20: Synthesis of Pinacol Boronic acid esters from Boronic acids*

---

The pinacol protecting group is a common ancillary for boronic moieties, which can easily be yielded *via* a condensation reaction with pinacol and a free boronic acid (Scheme 20).<sup>[48]</sup> Although there are many literature examples that employ boronic pinacol esters for cross-coupling reactions, the steric bulk and electron-donating effects of pinacol decrease the steric accessibility and Lewis acidity of the boron centre, slowing the rate of transmetallation. Lennox *et al.* suggest that in order for pinacol boronic esters to undergo transmetallation, the pinacol group must first be hydrolysed, releasing a free boronic acid *in situ*.<sup>[6]</sup>

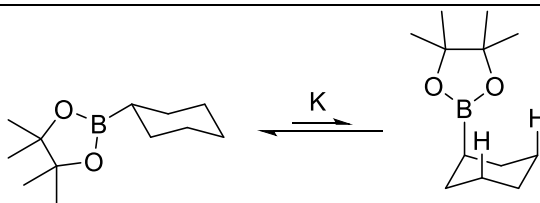
The steric argument for pinacol boronic acid esters has been disputed, however, by Fasano *et al.* who calculated the steric A-value for pinacol boronic acid esters.<sup>[49]</sup> The equilibrium constant between axial and equatorial conformations of cyclohexyl boronic acid esters was measured using NMR techniques. From the equilibrium constant the energy difference ( $\Delta G$ ) between the axial and equatorial conformations can be derived (Scheme 21). Fasano *et al.* found that the BPin has a surprisingly low A-value of 0.38 kcal/mol, whilst the analogous boronic ethylene glycol ester (BGly) reported a higher A-value of 0.73 kcal/mol; for reference a methyl group has a A-value of 1.7 kcal/mol.

Axial arrangements are disfavoured due to 1,3-diaxial interactions, for boronic esters the extent of these interactions is determined by the  $sp^2$  O-B-O motif, thus more electron-rich diols such as pinacol will cause an increase in the C-B bond length when coordinated to boron, reducing 1,3-diaxial interactions.<sup>[49]</sup> This study implies that pinacol may not destabilise the 4-



membered transmetallation transition state, but rather protects the boronic acid by lowering the Lewis acidity of boron.

---



$$A = -\Delta G = -RT\ln(K)$$

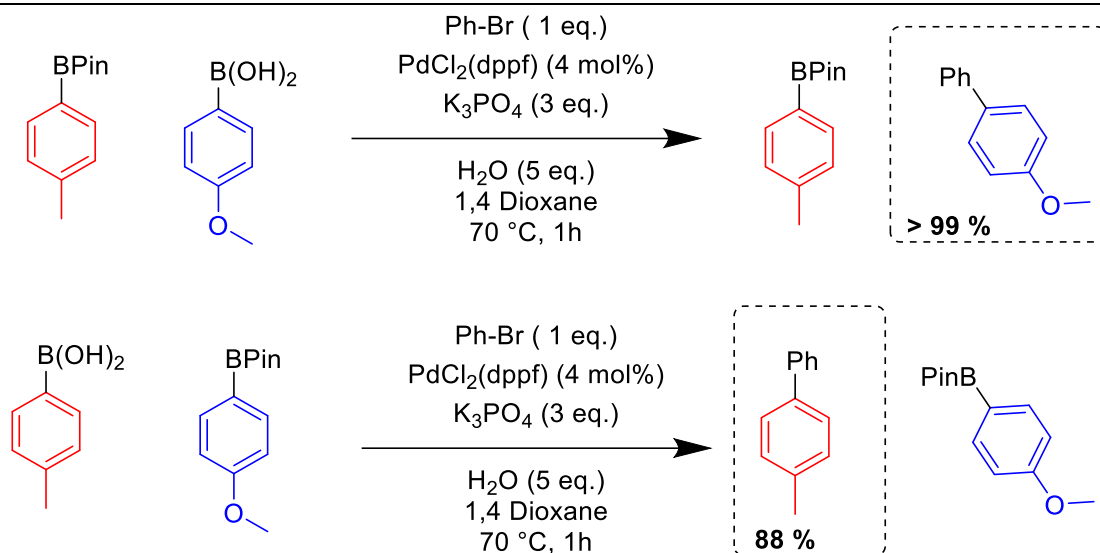
$$\text{Equatorial} : \text{Axial} = 74 : 26$$

*Scheme 21: The equilibrium between the equatorial and axial conformers was measured by Fasano et al. determining that the steric A-value for a pinacol boronic ester was 0.38.*

---

Kinetic studies have shown that the reaction of a phenyl hydroxopalladium(II) complex with 4-fluorophenyl boronic acid proceeds at -55 °C in under 2 minutes. However, the corresponding pinacol boronic acid ester reacts nearly 45 times slower, taking 1.5 hours at -55 °C. Other boronic acid esters tested, including catechol and neopentyl glycol analogues also react in under 2 minutes.<sup>[40]</sup>

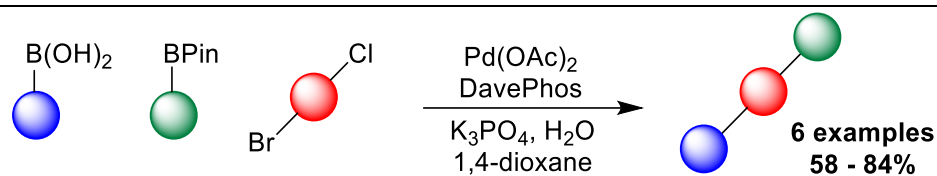
Fyfe *et al.* have taken advantage of the kinetic differences between free boronic acids and pinacol boronic acid esters to perform a series of chemo-selective Suzuki-Miyaura cross-couplings. When reacted independently, both  $B(OH)_2$  and  $B(\text{Pin})$  reagents are consumed at near identical rates. The rate determining step of the Suzuki-Miyaura catalytic cycle is oxidative addition to the organohalide reagent, and so the rate of boronic acid consumption is independent of the rate of transmetallation. Under competitive conditions, however, the boronic acid was found to outcompete the pinacol boronic ester for transmetallation, leaving the pinacol ester unreacted (Scheme 22). A substrate scope indicated that the preference for boronic acid under these conditions was largely unaffected by steric or electronic factors on either boron reagent.<sup>[50]</sup>



*Scheme 22: The kinetic rate difference for transmetallation can be exploited under competitive conditions, preferring a free boronic acid under Suzuki-Miyaura cross-coupling conditions.*

In these studies, it was found that selectivity was improved by inhibiting the inter-exchange of the pinacol protecting group. Inhibition was achieved by employing a relatively small quantity of water (5 equivalents) compared to standard Suzuki-Miyaura conditions where it is used as a co-solvent.<sup>[6]</sup> Performing the reaction with more than 20 equivalents of water was found to promote hydrolysis of the boronic acid pinacol ester and formation of a trihydroxyboronate, causing slow reactions with poor selectivity. Furthermore, at high equivalencies of water the reaction becomes biphasic, separating the water soluble boronate species from the palladium catalyst.

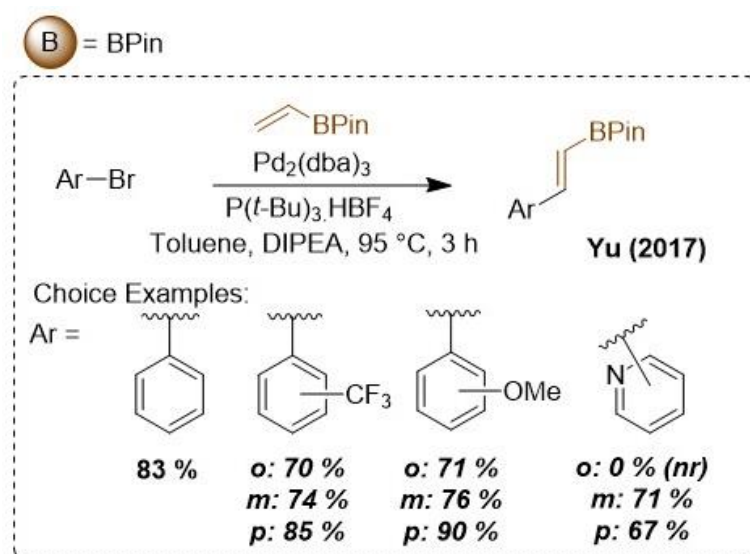
Fyfe *et al.* were able to showcase their chemo-selective cross-coupling performing 2 cross-couplings in a single synthetic step, with kinetic favourability for oxidative addition to an aryl bromide over an aryl chloride, and kinetic favourability for transmetallation to a free boronic acid over a pinacol boronic acid ester. Therefore, in a single pot, a dihaloarene underwent a chemo-selective oxidative addition (preferencing C-Br over C-Cl) followed by a chemo-selective transmetallation (preferencing C-B(OH)<sub>2</sub> over C-BPin) was achieved (Scheme 23).



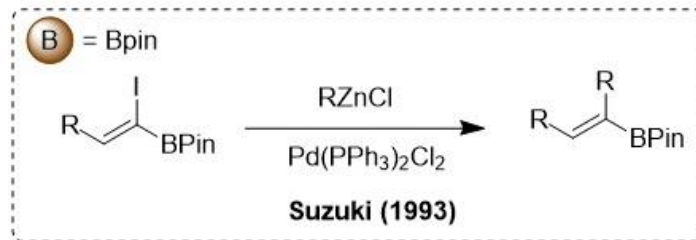
Scheme 23: Chemoselective cross-coupling of a dihaloarene with a boronic acid and boronic ester.

Whilst the kinetic transmetallation study by Fyfe *et al.* is an example of intermolecular competition, the following examples are of intramolecular competitions, where two different palladium cross-coupling processes are in competition. In the following cases the rate of the alternative transformation is sufficiently greater than the rate of transmetallation.

Vinyl boronic acid pinacol esters have been shown to be sufficiently averse to transmetallation under anhydrous conditions, allowing for Heck (Scheme 24) and Negishi couplings (Scheme 25) to be performed in the presence of a BPin moiety.<sup>[51]</sup>



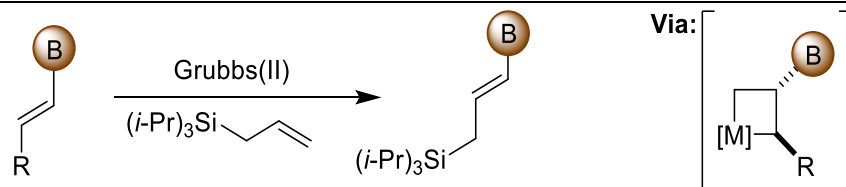
Scheme 24: Heck coupling reactions can perform orthogonally to vinylic pinacol boronic acid esters



*Scheme 25: Vinyl boronic acid esters have been shown to perform cross-coupling reactions whilst maintaining their C-B bond*

Ruthenium catalysed Grubb's olefin metathesis' can be achieved on vinyl pinacol boronic esters maintaining the boronic moiety (Scheme 26). Pinacol was found to improve the olefin metathesis' yield, compared with metathesis of an analogous vinyl boronic acid starting material. The poor yield afforded with free boronic acid starting materials was attributed to their high polarity and their desire to form boroxine trimers *in situ* (Table 1, Entry 1); this releases water, which Grubbs catalysts are sensitive to. Attempts starting with the boroxine trimer were not reported. The steric size of the hypothesised boroxine substrate may account for the high *E* selectivity (>20:1 *E:Z*) of the desired cross-coupling product.

Yields could be increased by employing a pinacol protected boronic acid starting material, at the expense of good *E/Z* selectivity (Table 1, Entry 2-3).<sup>[52]</sup> The issues arising from poor yield of boronic acids and poor *E/Z* selectivity for BPin are over-ridden by BMIDA which achieves the olefin metathesis in both high yield and high selectivity (Table 1, Entry 4). The MIDA-protecting group will be described in greater detail in Section 1.5.3.



Scheme 26: Ruthenium-catalysed olefin metathesis can be performed on vinyl boronic species with varying yields and stereoselectivities based on protecting group used

Table 1: Grubbs Olefin metathesis can also be performed on vinylic BPin compounds

	B	R	Product	Yield (%)	E:Z ratio
1	B(OH) <sub>2</sub>	Me	(i-Pr) <sub>3</sub> Si-CH=CH-B(OH) <sub>2</sub>	55	> 20 : 1
2	BPin	H	(i-Pr) <sub>3</sub> Si-CH=CH-BPin	86	7 : 1
3	BPin	Me	(i-Pr) <sub>3</sub> Si-CH=CH-BPin	99	10 : 1
4	BMIDA	H	(i-Pr) <sub>3</sub> Si-CH=CH-BMIDA	85	> 20 : 1

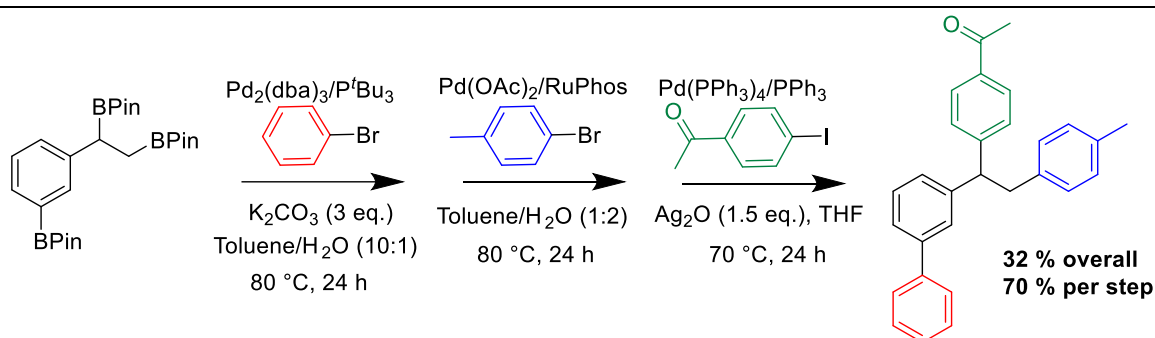
The rate of transmetallation of alkyl boronic acids/esters tends to be slower than the rate for *sp* and *sp*<sup>2</sup> analogues. In 2009, Crudden *et al.* disclosed that by introducing silver oxide as a base the transmetallation step may be accelerated.<sup>[53]</sup> It was found that in the absence of Ag<sub>2</sub>O, no reaction was observed, recovering the untouched boronic acid pinacol ester, yet reasonable yields were achieved when using the silver salt.

Ag<sub>2</sub>O has been reported, numerous times, to increase the rate of Suzuki cross-couplings with boronic esters bearing a  $\pi$ -system under anhydrous condition.<sup>[54–57]</sup> Uenishi *et al.* reported a SMCC by employing Ag<sub>2</sub>O in 5 minutes, whilst using KOH, under otherwise identical conditions, took 2 hours.<sup>[58]</sup> This indicates that in the absence of silver(I) oxide, benzylic pinacol boronic acid esters have a high kinetic barrier to transmetallation.

Rygun *et al.* proposed that the rate enhancement is afforded by  $\pi$ -coordination to the silver centre, with the oxygen coordinating to boron to form an intermediate boronate species. This suggestion, however, is in contradiction to observations discussed in Chapter 1.4, wherein Amatore *et al.* indicated that boronate formation inhibits transmetallation to a palladium(II) centre.<sup>[59]</sup>

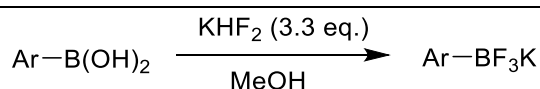
Interestingly, reactions of single enantiomers with stereogenic C-B centres retain their stereochemistry when performing silver(II) oxide mediated anhydrous Suzuki cross-couplings.<sup>[60]</sup> Inversion is observed using a Pd(OAc)<sub>2</sub>/PCy<sub>3</sub> catalyst system in the absence of Ag<sub>2</sub>O.<sup>[61]</sup>

The differing rates of transmetalation, dependent on the chemical environment of the carbon-boron bond and the reaction conditions employed, were utilised by Crudden *et al.* An iterative cross-coupling of a tri-borylated starting material was described, where three separate, chemo-selective SMCC reactions were performed (Scheme 27).<sup>[62]</sup>



*Scheme 27: Crudden et al. showed that the effect of a carbon environment on the rate of transmetalation could be utilised to perform three successive, highly selective, Suzuki-Miyaura cross-couplings on a tri-borylated starting material*

### 1.5.2. Trifluoroborate salts



*Scheme 28: Synthesis of BF<sub>3</sub>K Salts from Boronic acids*

Trifluoroborates, which primarily occur in the literature in the form of a potassium salt (BF<sub>3</sub>K), take advantage of the high bond dissociation energy of B-F bond. This allows them to strongly occupy the Lewis acidic, p<sub>z</sub>-orbital of boron yielding a quaternary boron centre. Formation of the salt can be achieved by treatment of a boronic acid with potassium hydrogen difluoride (KHF<sub>2</sub>) (Scheme 28),<sup>[63]</sup> and can be hydrolysed back to the boronic acid under

basic conditions.<sup>[64]</sup> Due to the high electronegativity of fluorine, the three coordinated fluorides pull electron density away from the boron centre, which acts to shorten and strengthen the C-B bond.<sup>[6,65]</sup>

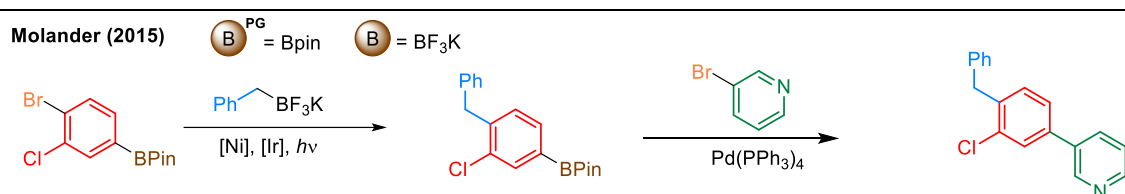
The utility of organotrifluoroborate salts is well explored, owing to a large body of work by the Molander group. These reactions with orthogonal reactivities include epoxidation with *m*CPBA<sup>[66]</sup>, lithium-iodine exchange with a subsequent trapping of an electrophile<sup>[67]</sup>, *cis*-dihydroxylation of alkenes with osmium tetroxide,<sup>[68]</sup> oxidation of alcohols using Swern, Dess-martin and Ley oxidation (TPAP/NMO) conditions<sup>[69]</sup>, Wittig and Horner-Wadsworth-Emmons reactions,<sup>[70]</sup> “click” of alkenes and azides,<sup>[71]</sup> and reductive amination.<sup>[72]</sup>

Of these, two examples utilise transition metal mediated chemistries, osmium tetroxide dihydroxylation and Ley-Griffith oxidation, both are excellent oxidising agents with good selectivity.<sup>[73]</sup> Ley-Griffith oxidation employs catalytic quantities of tetra-*n*-propylammonium perruthate (TPAP) in the presence of *N*-methyl morpholine *N*-oxide (NMO) as a secondary oxidant, (which regenerates the reduced TPAP allowing a catalytic loading of 5 mol%). These conditions promote oxidation of alcohols to ketones and aldehydes, with little over oxidation.<sup>[74]</sup> Due to solubility issues of BF<sub>3</sub>K salts in DCM, tetra-*n*-butyl ammonium salts were used instead, and subsequently maintained in the reaction. It should be noted that a control experiment using the free boronic acid was not reported, and no comment as to the stability of free boronic acids to Ley oxidation could be found in the literature. However, TPAP/NMO reaction conditions are mild, and many protecting groups remain unaffected, including acid-sensitive TMS ethers,<sup>[75]</sup> oxidant sensitive *para*-methoxy benzene (PMB),<sup>[76]</sup> and *p*-methoxybenzylidene acetates.<sup>[77]</sup>

The stability of organotrifluoroborate salts to a wide range of conditions, makes them an excellent form of protection for boronic acids for many organic methodologies. ArBF<sub>3</sub>K salts can undergo transmetallation to palladium under “anhydrous conditions”; Lennox and Lloyd-Jones note that many procedures require addition of a drop of water or do not thoroughly prevent ingress of adventitious water in the reaction.<sup>[35]</sup> It is believed that the

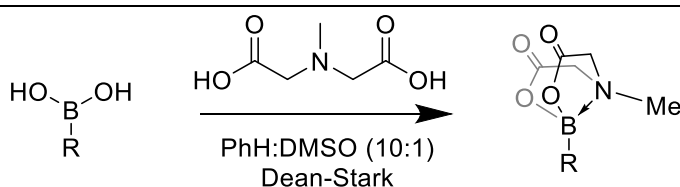
trace water hydrolyses  $\text{BF}_3\text{K}$  salts to release the boronic acid *in situ*, the fluorides released in the process may then promote transmetalation by formation of a palladium(II)-fluoride species.<sup>[78,79]</sup>

Photocatalytic cross-coupling reactions can be achieved by employing a nickel and iridium catalyst system to cleave benzylic  $\text{BF}_3\text{K}$  salts but maintain an aryl boronic acid derived moiety (Scheme 29). Aryl  $\text{B}(\text{OH})_2$ , BPin, BMIDA, and BDAN moieties were all maintained under the reaction conditions, but studies with aryl  $\text{BF}_3\text{K}$  salts were not reported.<sup>[80]</sup> These photocatalytic conditions induce radical pathways, and as C-B bonds have low bond dissociation energies they can be prone to homolytic cleavage. As benzylic radicals are more stable than aryl radicals, radical stability explains the reactions chemo-selectivity independently of the boronic acid derivatives employed. Therefore, it is unclear if the reactivity is unique to benzylic  $\text{BF}_3\text{K}$  salts or if it can be generalised to other benzylic boronic acid derivatives. Aryl  $\text{BF}_3\text{K}$  salts have previously been reported to cleave their C-B bonds under radical conditions.<sup>[20]</sup>



Scheme 29: Under nickel and iridium photocatalysed conditions, a benzyl  $\text{BF}_3\text{K}$  starting material can be coupled with a haloboronic acid pinacol ester, maintaining the BPin moiety in the product, ready for further elaboration.

### 1.5.3. MIDA boronates



Scheme 30: Dean-Stark condensation yields MIDA-boronates from free boronic acids



The *N*-methyl iminodiacetate (MIDA) protecting group, first described as a hydrolytically stable protecting group for boron by Mancilla *et al.* produces a tridentate co-ordination to boron: Two carboxylate groups form covalent bonds to boron, and the lone-pair of its tertiary amine forms a dative covalent bond with the empty  $p_z$ -orbital. MIDA-boronates can be easily synthesised *via* a Dean-Stark condensation reaction with MIDA (Scheme 30).<sup>[81]</sup>

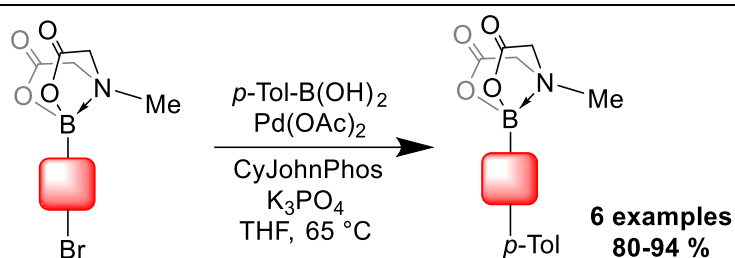
The tridentate chelation renders the MIDA-boronates quite hydrolytically stable. There are however two mechanisms for deprotection of MIDA-boronates, under neutral conditions the removal of MIDA is akin to a ligand displacement, with an excess of water out competing the MIDA for co-ordination to the boron, overcoming the chelation of the tridentate ligand, this mechanism is rate-limited by the B-N bond cleavage. Under treatment of aqueous base, a second deprotection mechanism, rate-determined by a nucleophilic attack of the MIDA-carbonyl carbon by hydroxide is three order of magnitude faster, and yields the deprotected boronic acid.<sup>[82]</sup>

Similar protecting systems such as *N*-methyl diethanolamine (MDEA), have been shown not to exhibit the same hydrolytic stability as the MIDA-protecting group.<sup>[83]</sup> This is due to a more labile B-N dative co-ordination for the MDEA-boronate. In MIDA-boronates the high stability of the B-N dative bond is attributed to (1) the electron withdrawing effect of MIDAs two carboxylates rendering the boron centre more electron deficient, reinforcing the B-N dative bond to compensate, and (2) the introduction of  $sp^2$  carbonyl carbons, which produce a higher degree of structural rigidity in the bicyclic system.<sup>[81]</sup>

This effect of the electron withdrawing carboxylate substituents can be observed by comparing the nucleophilicity of the C-B bond of BMIDA and BMDEA ancillary systems. The rate of reaction of MDEA-protected or MIDA-protected 2-boryl furan moieties is approximately four order of magnitude faster for the MDEA-boronate than for the BMIDA protecting group when reacting with an electrophilic benzhydrylium cation.<sup>[84]</sup> Therefore the hydrolytic resistance under non-basic conditions (B-N stability) and low

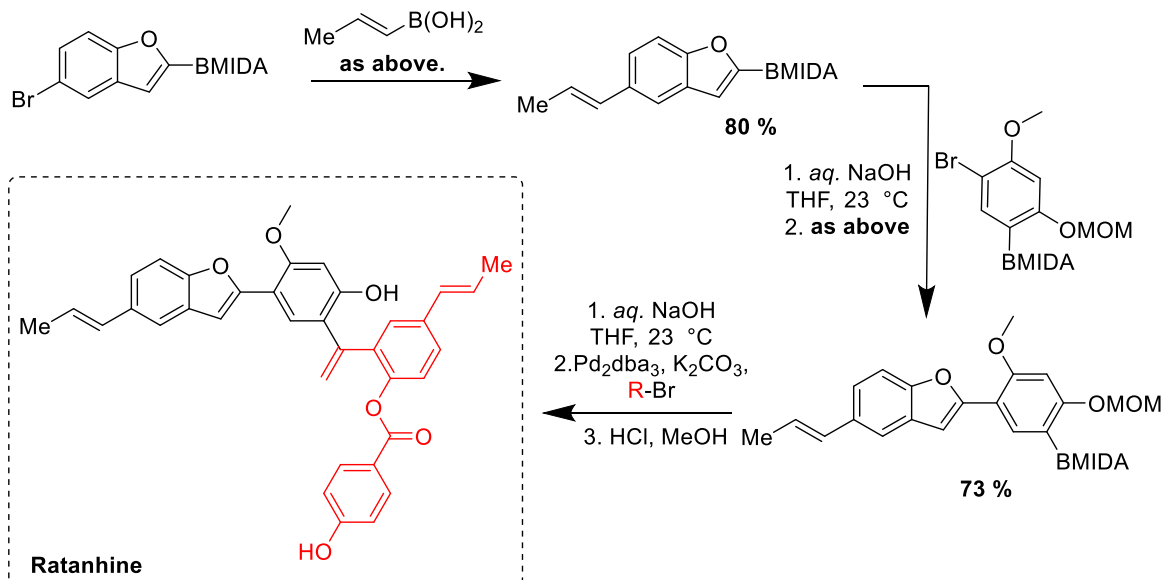
nucleophilicity (C-B stability), renders the MIDA protecting group an efficient protecting boronic acid protecting group.

Burke *et al.* were able to highlight the orthogonality of MIDA-boronates to transmetallation in a series of Suzuki-Miyaura cross-coupling reactions. Yielding a series of boronic acid products which maintained their original C-B bond with such an approach having a “theoretically limitless potential for iteration” (Scheme 31). Synthetic utility for this was highlighted *via* a series of Suzuki-Miyaura cross-coupling reactions to yield the natural product, ratanhine (Scheme 32).<sup>[85]</sup>



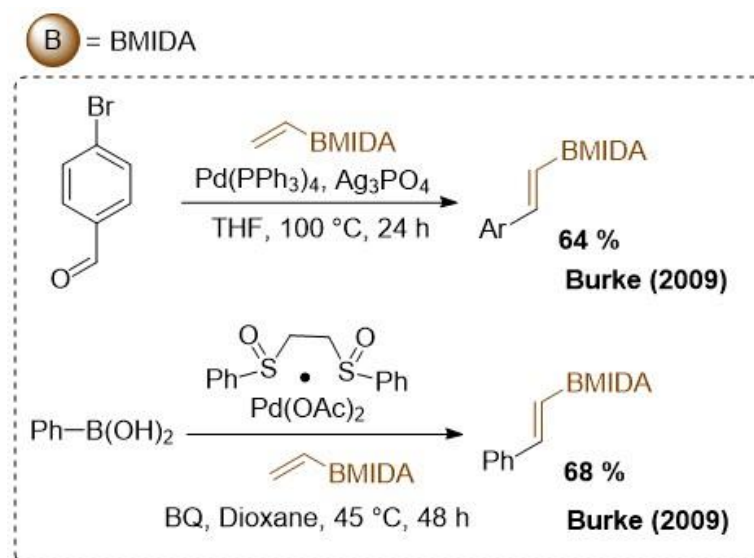
Scheme 31: MIDA-boronates are orthogonal to some Suzuki-Miyaura cross-coupling conditions.

#### Synthesis of Ratanhine



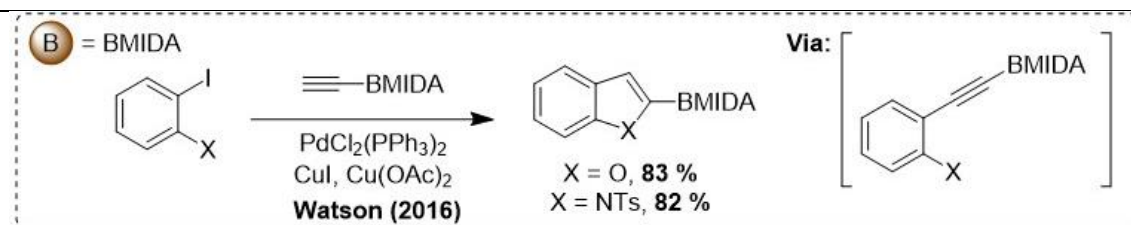
Scheme 32: Orthogonality of MIDA-boronates to Suzuki-Miyaura cross-coupling reactions was showcased, describing a novel synthetic route to Ratanhine

This approach can also be extended to vinylic MIDA-boronates for implementation in Heck cross-coupling reactions, using aryl halides and organoboronic acids as coupling partners (Scheme 33).<sup>[86]</sup>



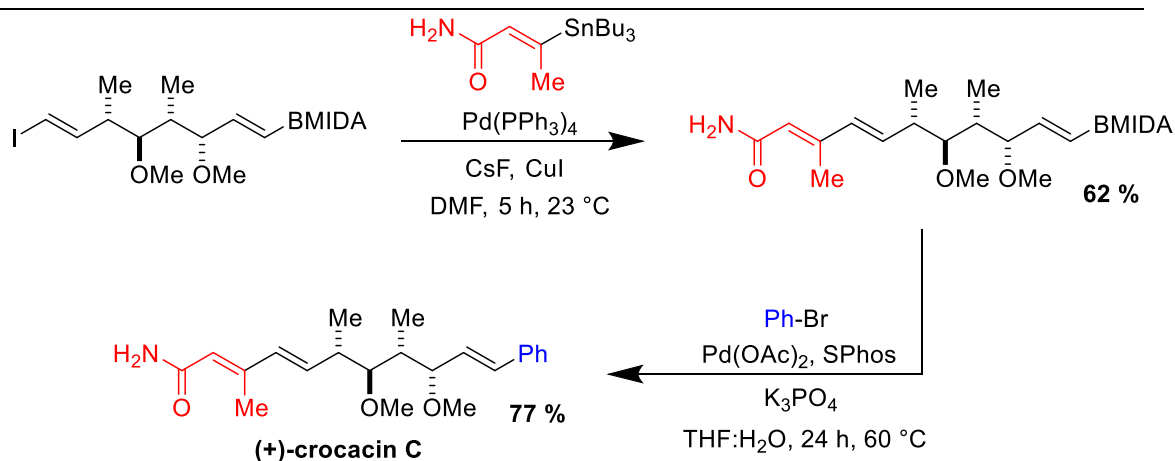
*Scheme 33: Heck and oxidative-Heck cross couplings have been performed in the presence of a vinyl BMIDA species*

Sonogashira reactions can also be realised with an orthogonal reactivity to C-B bonds. The Watson group described a two-step cascade reaction which operates orthogonally to a BMIDA allowing retention of a C-B bond primed for further derivatisation (Scheme 34).<sup>[87]</sup> This transformation can also be realised using gold catalysis, as described by the Toste group.<sup>[88]</sup>



*Scheme 34: Watson et al. described a cascade reaction wherein a Sonogashira reaction yields an aryl alkyne intermediate which undergoes cyclisation to produce a BMIDA containing product*

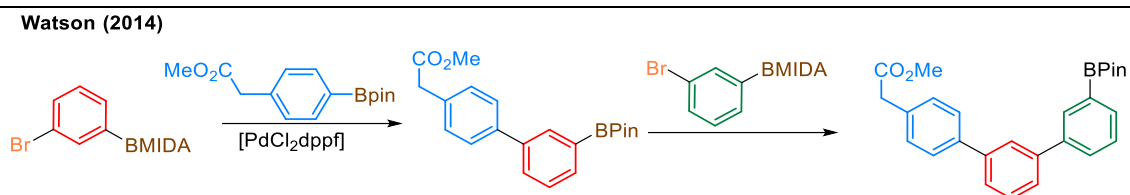
Use of the MIDA-boronate in a multi-step natural product synthesis has been described by Burke *et al.*, who utilised the protecting moiety for the synthesis of (+)-crocacin C. A nine-step synthesis from acrolein MIDA boronate, was shown to maintain the MIDA-boronate throughout. In the final step the MIDA-boronate is utilised in a SMCC, which, under aqueous conditions, releases the boronic acid *in situ* (Scheme 35). The synthetic route highlights the stability of MIDA-boronates and showcases its orthogonality to several metal catalysed reaction conditions including a Stille cross-coupling reaction.<sup>[89]</sup> Since, various other natural products have been produced utilising the MIDA-boronate orthogonality under Stille cross-coupling conditions.<sup>[90]</sup>



Scheme 35: Burke described a Stille coupling in a synthesis of (+)-crocacin C which maintains a BMIDA moiety throughout

Watson *et al.* further highlighted the iterative possibilities of MIDA-boronates, performing a formal homologation of halogenated aryl MIDA-boronates under Suzuki-Miyaura cross-coupling conditions with an aryl boronic acid pinacol ester.<sup>[91]</sup> It was shown that pinacol boronic esters and MIDA-boronates will, under aqueous conditions, exchange protecting groups.<sup>[92]</sup> By controlling this equilibria over the course of a Suzuki-Miyaura

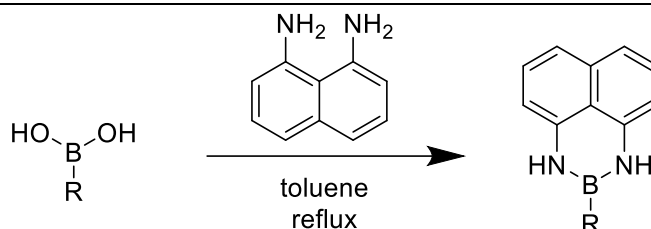
cross-coupling reaction, a product retaining a B(Pin) moiety can be obtained in high yields, allowing for further iterations in a single pot by adding a new coupling partner (Scheme 36).



Scheme 36: Watson's one-pot synthesis of multi-aryl compounds through iterative cross-couplings

Grubbs olefin metathesis can also be performed on vinyl MIDA-boronates, under similar conditions to those described in section 1.5.1 for vinyl pinacol boronic esters. Whereas pinacol boronic acid esters promoted good yields but at the expense of E/Z selectivity, the vinyl MIDA boronates are able to promote both a high yield (80 %) and excellent E/Z selectivity (<20:1 E:Z).<sup>[86]</sup>

#### 1.5.4. 1,8-Diaminonaphthalene Boronic Amides

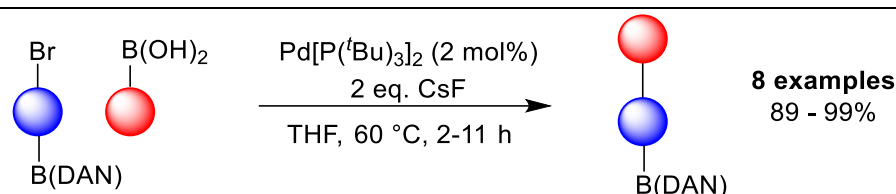


Scheme 37: Synthesis of 1,8-diaminonaphthalene boronic acid amides from a free boronic acid

1,8-Diaminonaphthalene (DAN) can be coordinated to boronic acids *via* condensation under Dean-Stark conditions to form DAN-boronic amides (Scheme 37).<sup>[93]</sup> B(DAN) moieties are often referred to in the literature as a DAN-boronate, despite not existing as a charged “-ate” species. DAN-boronic amides are highly hydrolytically stable under non-acidic conditions, as orbital overlap between the nitrogen lone-pairs and empty  $p_z$ -orbital at boron

minimises the Lewis acidic nature of the boron centre and thus precludes transmetallation. A significant amount of work has been done by the Suginome group to highlight the potential for orthogonal reactivities.

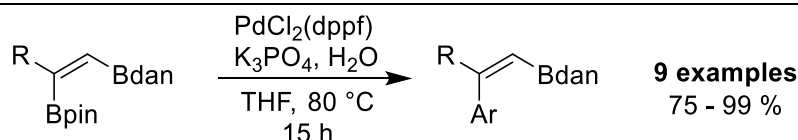
DAN-amides were shown to be inert to transmetallation relative to boronic acids (Scheme 38) with a chemo-selective SMCC performed on an organobromide substrate bearing a DAN-boronic amide moiety.<sup>[93]</sup> Fluoride-promoted transmetallation was chosen over a hydroxide base, to avoid hydrolysis of the DAN-boronic amide which would lead to transmetallation. Excellent yields of greater than 89% across 8 examples were observed.



*Scheme 38: A Suzuki-Miyaura cross-coupling with an aryl boronic acid, maintaining a 1,8-dinaphthalene boronic acid amide functionality*

---

The Suginome group later disclosed a pinacol boronic ester selective SMCC, this time using hydroxide to promote transmetallation, by addition of water and a phosphate base (Scheme 39).<sup>[94]</sup> Under these reaction conditions the hydrolysis rate for the DAN boronic amide was still suitably slow enough to afford a high chemo-selectivity. Nine examples were disclosed with a yield range of 75 – 99%.



*Scheme 39: Chemoselective Suzuki-Miyaura cross-coupling of a diborylated alkene, maintaining a 1,8-dinaphthalene boronic acid amide functionality*

---

DAN-derived protecting groups have been showcased in C-H functionalisation chemistry. They will be discussed in detail in Chapter 1.8.2.

## 1.6. C-H Functionalisation

### 1.6.1. Overview

Preceding sections have summarised the role of protecting groups and experimental conditions in achieving C-B bond orthogonality in the presence of a transition metal. The aim in doing this was to provide evidence to support a hypothesis that novel transition metal catalysed processes can be performed without interfering with a C-B bond. Furthermore, equally relevant to the experimental work outlined within this thesis, is an understanding of C-H functionalisation, which will be described in the following sections. A link will then be drawn as to how these methodologies can be applied to boronic acid containing substrates.

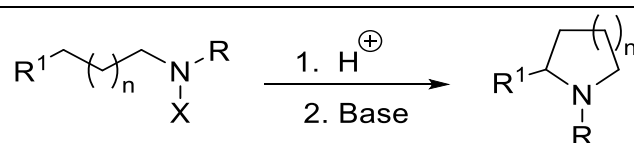
The relatively inert chemical nature of non-acidic C-H bonds has perpetuated their proliferation in organic molecules. Hydrocarbons are low-cost feedstocks, but step-economical and regio-selective elaboration of these cheap starting materials is challenging.<sup>[95]</sup>

The term “C-H activation” is commonly used yet imprecise. It typically refers to the reaction of transition metal complexes with unreactive C-H bonds of alkanes, arenes or alkyl chains to produce a metal-carbon intermediate. This is what differentiates it from processes such as Friedel-Crafts alkylation, which, despite cleaving a C-H bond, reacts with an aromatic  $\pi$ -system forming an arenium ion (Wheland intermediate), of which its stability is large dependent on electronic factors. C-H functionalisation refers to an overall catalytic cycle, with C-H activation/metallation constituting a process within that cycle.<sup>[96]</sup>

In the 1980s, there was a rapid increase in the number of metal salts and complexes able to perform oxidative addition at previously unreactive C-H bonds. The metal salts were first employed as stoichiometric reagents, but they directed development towards catalytic C-H functionalisation.<sup>[95,97]</sup> These processes are now achievable employing low, catalytic loadings metal

salts, enhancing the cost and atom economies of these chemical transformations.<sup>[98-101]</sup>

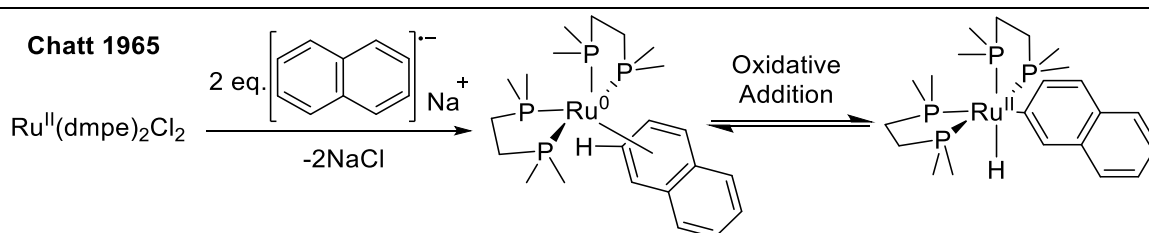
In lieu of a catalyst, harsh conditions are required. The Hofmann-Löffler-Freytag reaction (Scheme 40), for example, requires the generation of highly reactive nitrogen-based radicals under strongly acidic conditions; regio-selectivity is determined by transition state energies often affording a 5-membered cyclised product.<sup>[102]</sup> To achieve these types of transformations under milder conditions metal catalysts have been employed, offering a lower energy pathway.



*Scheme 40: General overview of the Hofmann-Löffler-Freytag Reaction*

---

C-H metallation under mild conditions was described in 1965 by Chatt *et al.*,<sup>[103]</sup> wherein insertion of a ruthenium(0) complex into a C-H bond of sodium naphthalenide yielded a naphthylated ruthenium(II) complex (Scheme 41).



*Scheme 41: Chatt's C-H metallation under ambient conditions.*

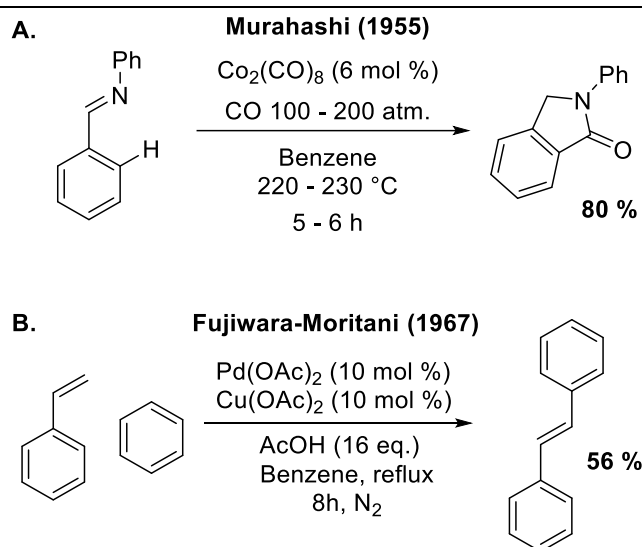
---

In 1955, an early example of metal catalysed C-H activation was described by Murahashi, who detailed a cobalt catalysed synthesis of phthalimidines from Schiff bases under a high pressure carbon monoxide atmosphere (Scheme 42, A).<sup>[104]</sup> Ligation of cobalt to an imine nitrogen, directed *ortho*-



selective carbonylation and a subsequent cyclisation was achieved in an 80 % yield.

Another notable example is the Fujiwara-Moritani reaction (Scheme 42, B),<sup>[105]</sup> which under Pd(OAc)<sub>2</sub> and Cu(OAc)<sub>2</sub> catalysed conditions, achieves olefination of benzene with styrene. This reaction predates cross-coupling work by Heck (for which he was later awarded a third share of the 2010 Nobel prize in chemistry). However, unlike the popular Heck reaction, the Fujiwara-Moritani reaction suffers from a limited substrate scope.



*Scheme 42: Early catalytic C-H activation systems were hindered by their undesirable reaction conditions*

---

This study was able to isolate the metalated species, and further work would be required to apply this to functionalisation with catalytic loadings of the metal complex. From the 1980s, this aim began to be addressed, owing to a dramatic increase in the number of metal salts and complexes that were found to initiate C-H activation.

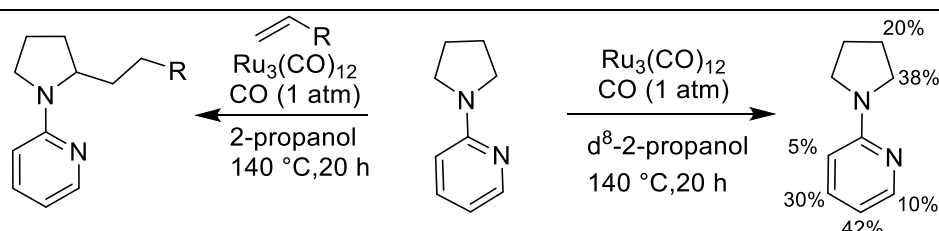
### 1.6.2. Mechanistic Insight

Treatment of pyridine under a D<sub>2</sub> atmosphere in the presence of various heterogeneous metal catalysts indicates that C-H metallation may be a facile process; a mixture of products from mono-deuteration to full isotopic

labelling of the pyridine( $C_5D_5N$ ) can be afforded.<sup>[106]</sup> The site-selectivity of deuteration occurs first at the 2/5-positions; pyridine co-ordination to the metal surface facilitates a high proximity between the 2/5 C-H bonds and the catalyst surface. A relay of metallation then occurs around the pyridine ring, with metallation occurring adjacent to an already metalated position.

In heterogenous catalysis the high local concentration of metal centres when in proximity to the catalyst surface, significantly expedites the formation of multi-metallic organic intermediates. Conversely, uniform dispersion of homogenous catalysts with often low catalytic loadings would slow the rate of a metallation relay pathway.

In homogenous catalysis, a deuteration study of 2-(1-pyrrolidiny)pyridine using a  $Ru_3(CO)_{12}$  catalyst in the presence of  $d^8$ -2-propanol facilitated deuterium incorporation to all positions. This indicates that C-H metallation can be both facile and nonselective using a homogeneous catalyst. However, high selectivity of coupling at the  $C(sp^3)$ -H adjacent to the pyrrolidine nitrogen atom, directed by co-ordination to proximal pyridine, was observed. The addition of alkenes under a carbon monoxide atmosphere yielded a mixture of mono and di-alkylated products (Scheme 43).<sup>[107]</sup>



*Scheme 43: High selectivity of  $\alpha$ -functionalisation despite metallation proceeding at all C-H bonds, indicated by deuteration studies.*

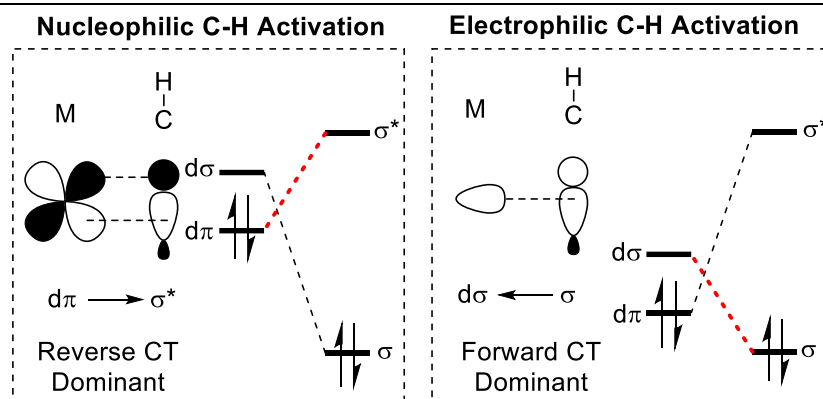
This implies that under certain catalytic conditions the metallation is facile and reversible, and not the rate determining step. Deuteration may occur as the solvent is the deuterium source rendering the isotopic exchange pseudo-zero order. Stabilisation of the organometallic intermediate afforded by co-ordination to the proximal pyridyl group is key to shift the C-H metallation

equilibria in favour of the organometallic intermediate thus promoting the desired site-selective C-H functionalisation.

Greater control of deuteration is possible: Crabtree's catalyst,  $[\text{Ir}(\text{COD})(\text{Cy}_3\text{P})(\text{Py})]\text{PF}_6$ , and derivatives, have found utility with excellent selectivity for hydrogen isotope exchange (HIE) directed by *N*-heterocycles,<sup>[108,109]</sup> with the heterocycle core itself remaining unlabelled.<sup>[110]</sup> The stability of the organometallic intermediate often dictates the degree of deuteration. Competition of 2 different directing groups on a single substrate using Kerr's catalyst,  $[\text{Ir}(\text{COD})(\text{IMes})(\text{PPh}_3)]\text{PF}_6$ , yields excellent selectivity dependent on the directing group. DFT studies were conducted to predict both the free energy of the intermediate complexes and the activation energies. Correlating this with experimental outcomes indicated that the HIE is under thermodynamic control, independent, to an extent, of the magnitude of the activation energy, although lowering the reaction temperature does afford kinetic control.<sup>[111]</sup>

There is a spectrum of mechanistic pathways by which C-H metallation can proceed. These range from a formal oxidative addition, to an isohypsic (non-redox) pathway, referred to as *ambiphilic metal ligand activation* (AMLA).<sup>[112]</sup>

These two extremes are determined by the direction of charge transfer (CT) between the frontier orbitals interacting in a metal-C-H bond coordination step (Scheme 44) which weakens the C-H bond: 1) From a filled  $d\pi$  orbital of the metal to the  $\sigma^*$  orbital of the coordinated C-H bond (reverse CT) 2) From the filled  $\sigma(\text{C-H})$  bond to an empty  $d\sigma$  orbital on the metal (forward CT). The directionality of charge transfer is determined by the relative energies of the relevant frontier orbitals, with orbital overlap improved when interacting orbitals are of similar energy.<sup>[113]</sup>



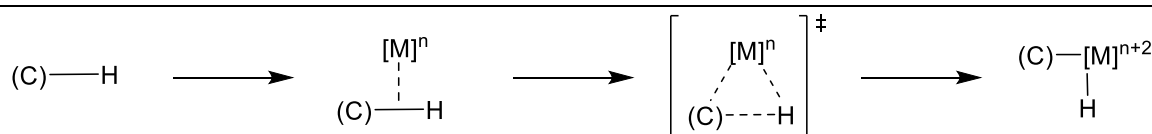
Scheme 44: Weak coordination of frontier orbitals of metal to the C-H bond facilitates C-H bond metallation

The mechanistic spectrum can be deconstructed into 3 broad classes, which will be discussed to give a general overview, these are:

- Oxidative Addition
- $\sigma$ -Bond metathesis
- Amphiphilic metal ligand activation (AMLA)

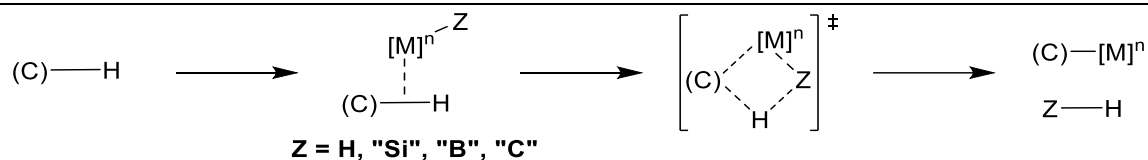
However, it should be kept in mind that there is interconnectivity between these classes, which can complicate mechanistic understanding.<sup>[114]</sup>

*Oxidative addition* – Common for electron rich, low valent complexes of late transition metals with high energy  $d\sigma$  and  $d\pi$  orbitals (e.g. Re, Fe, Ru, Os, Rh, Ir, Pt).<sup>[112]</sup> A nucleophilic C-H activation proceeds by coordination of the metal to a C-H bond, forming a three-membered transition state. The metal centre is oxidised, yielding a metal hydride bearing an organic fragment (Scheme 45).<sup>[115]</sup>



Scheme 45: General oxidative addition mechanism for C-H activation

*σ-Bond metathesis* - Proceeds via a kite-like  $[2\sigma + 2\sigma]$  cycloaddition transition state (Scheme 46), is preferred by metal compounds with a  $d^0$  metal count, such as early transition metals in high oxidation states, but shifts towards oxidative addition as d electron count is increased.<sup>[116]</sup>

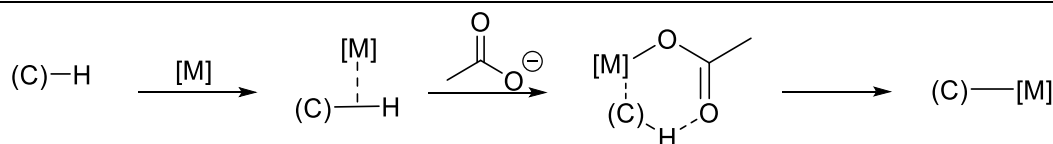


*Scheme 46: σ-Bond metathesis proceeds via a 4-member kite-like transition state.*

---

*Ambiphilic Metal-Ligand Activation (AMLA)* - Despite a general agreement of the mechanism for AMLA, the nomenclature remains disputed with the mechanism having various names across the literature. Alternative names include *concerted metallation deprotonation* (CMD), *internal electrophilic substitution* (IES) and *1,2-addition*.<sup>[112]</sup> Although IES and 1-2 addition are not often used in the literature. AMLA will be used exclusively herein.

Early proposals for an electrophilic activation mechanism at aromatic  $C(sp^2)$ -H bonds, proposed the formation of a Wheland intermediate, followed by heterolytic cleavage (deprotonation) using an intramolecular base bound to the metal. <sup>[117]</sup> However, density functional calculations suggest a cyclic six-membered transition state promoting a concerted formation of a carbon-metal bond *via* intramolecular deprotonation by a hetero-atom based ligand (Scheme 47).<sup>[118,119]</sup>



*Scheme 47: AMLA(6) - 6-membered transition state for C-H metallation*

---

AMLA is common for electron-poor, late transition metals in high oxidation states, (such as Pd(II), Pt(II), Rh(III), Ir(III) and Ru(II)), with low energy  $d\pi$

and  $d\sigma$  orbitals, experience a strong  $\sigma$ -donation from the C-H bond, a weaker  $\pi$ -back bonding interaction, mediating electrophilic activation.<sup>[112]</sup>

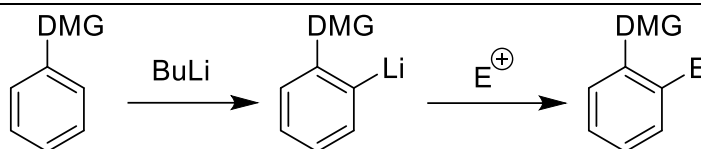
Oxidative addition to aryl bromides (C-Br  $\sim$ 67 kcal/mol) or iodides (C-I  $\sim$ 53 kcal/mol) is the initial step for catalytic processes such as Suzuki, Stille, and Heck couplings.<sup>[7,25]</sup> The process is highly exergonic, meaning the reverse reductive elimination is too thermodynamically disfavoured to occur easily.<sup>[120]</sup> However, reductive elimination to produce aryl halogens has been described in the literature, promoted by destabilisation of the organometallic intermediate. One example is the use of tris(*tert*-butyl)phosphine ( $P^tBu_3$ ) to both promote steric destabilisation of the organometallic intermediate formed *via* oxidative addition and therefore promote a reductive elimination to reform the C-X bond.<sup>[120-122]</sup>

C-H metallation is not an exergonic process.<sup>[96]</sup> The thermodynamic stability of C-H bonds is key factor in their ubiquity, and the strongest C-H bonds are the most desirable to functionalise. Evidence, however, shows that C-H metallation is facile under some conditions. Ligands can help control the metallation equilibrium by stabilising the organometallic intermediate.

## 1.7. Directed C-H Functionalisation

### 1.7.1. Directed *Ortho*-Functionalisation

Gilman & Bebb (1939) [123] and Wittig & Fuhrman [124] (1940) independently described formation of organolithium *ortho* to a Lewis basic moiety. This was later termed 'directed *ortho*-metallation' (DoM) (Scheme 48) by V. Sneikus.[125] DoM harnesses the Lewis acid-Lewis base pairings between a directed metallation group (DMG) and a strong organometallic base to yield proximity driven site-selective metallations. This aids in overcoming electronic and steric preferences, forming a highly reactive organometallic nucleophile *in situ*.<sup>[125]</sup>

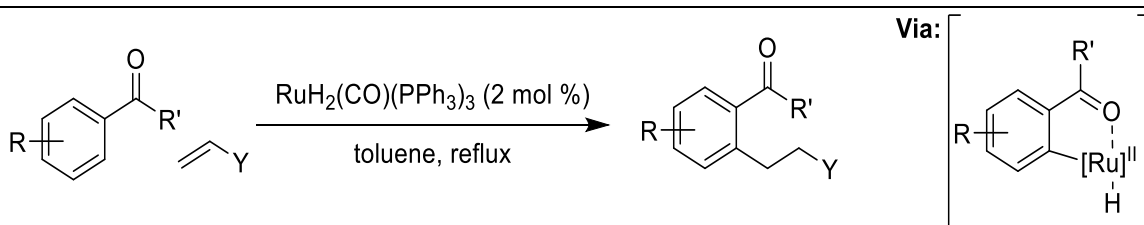


*Scheme 48: General overview of directed ortho metallation and subsequent functionalisation*

---

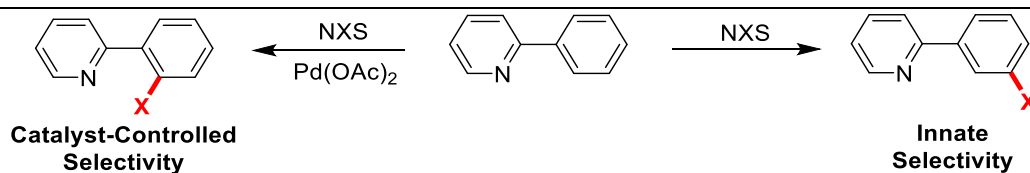
Despite their wide use, organolithium reagents must be added in stoichiometric amounts at low temperatures and have ultimately a poor substrate scope due to their high nucleophilicity.<sup>[126]</sup>

The Murai reaction uses a ruthenium catalyst to perform an aromatic olefination using a ketone attached to the substrate to direct oxidative addition at the *ortho* position (Scheme 49).<sup>[127]</sup> Here co-ordination to the ketone directs *ortho*-metallation allowing cross-coupling to a wide range of coupling partners.



*Scheme 49: The Murai reaction for olefination of arenes*

Directing groups can out-compete electronic site-selectivity. The Sanford group highlighted this with their *ortho*-halogenation of 2-phenylpyridine (Scheme 50). In the reaction, pyridine directs a palladium(II) catalyst to the *ortho* position of the phenyl, yielding an *ortho*-halogenated product over the electronically favoured *meta*-halogenated product. [128]

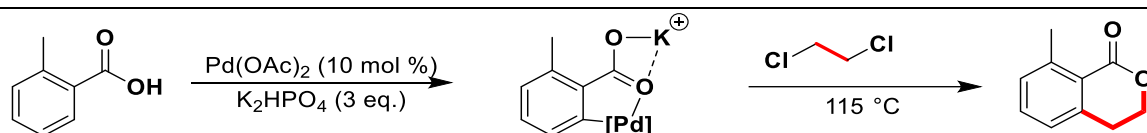


*Scheme 50: Mild palladium catalysed halogenation of arene C-H bonds vs. the innate selectivity of non-catalysed systems*

---

Since then, a wide range of methodologies for the C-H functionalisation of 2-phenylpyridine have been developed. The observations of these methodologies have persisted in later approaches. These chemistries highlight nuances and challenges that must be overcome to produce successful C-H functionalisation methods.

In 2009 the Yu group were able to harness carboxylic acids as a DMG, describing palladium(II) catalysed *ortho*-alkylation of benzoic acids with alkyl halides (Scheme 51). The described reactions incorporate potassium salts to occupy the  $\kappa^2$  binding site of the carboxylate, causing palladium to occupy the more weakly co-ordinating  $\kappa^1$  binding site, positioning it proximal to the *ortho*-C-H bond. [129]



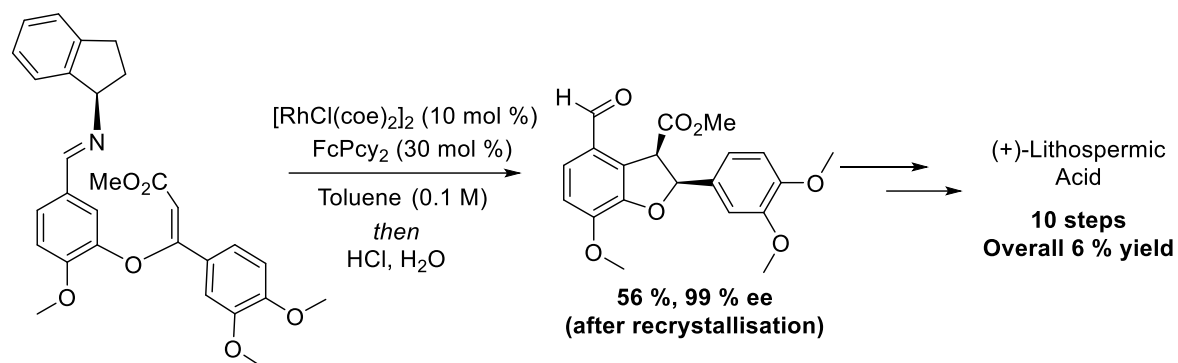
*Scheme 51: Ortho selective alkylation of benzoic acids*

---

Bergmann and Ellman performed an enantioselective synthesis (Scheme 42) using an imine to direct C-H insertion of rhodium to facilitate an intramolecular olefination (Scheme 52). [130] This was applied to their



synthesis of (+)-lithospermic acid in which the methodology was used to form the dihydrobenzofuran core.<sup>[131]</sup> Previous attempts by Jacobson *et al.* had only succeeded in producing the “racemic permethylated derivative of lithospermic acid”, heptamethyl lithospermate.<sup>[132]</sup>



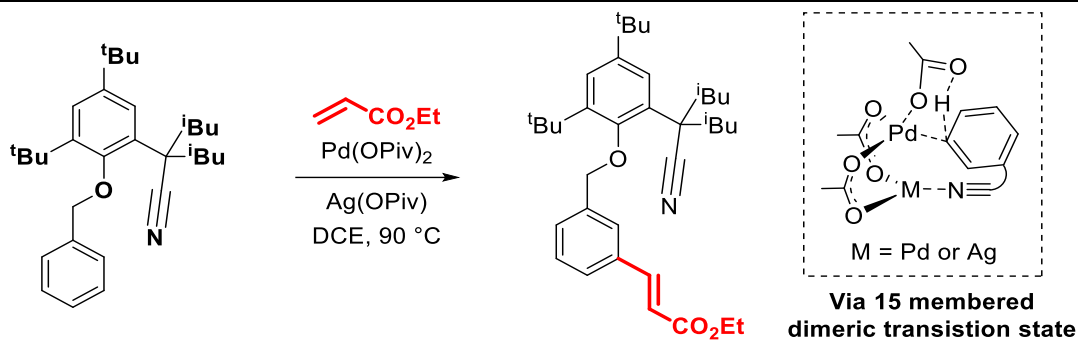
Scheme 52: Ellman and Bergmann's total synthesis of (+)-Lithospermic acid utilising C-H Functionalisation

### 1.7.2. Distal Directing Auxiliaries

Directing auxiliaries may be attached to a substrate to achieve functionalisation beyond the *ortho*-selective processes described in Chapter 1.7.1.

The Yu group published work using nitriles as an end-on ligation moiety in palladium catalysed *meta*-olefinations of arenes using a U-shaped template (Scheme 53).<sup>[133]</sup> Geminal *iso*-butyl groups on the auxiliary introduce Thorpe-Ingold effects, orientating the nitrile such that it can direct a metal to a target C-H bond.<sup>[134]</sup>

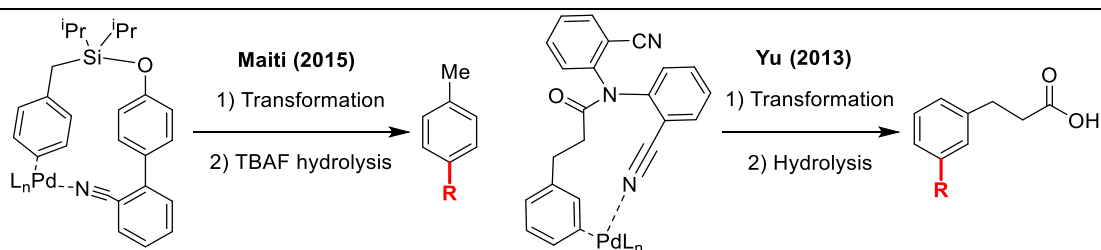
Nitriles act as weakly coordinating functionalities, as whilst stabilisation of a desired organometallic intermediate is key to push the C-H metallation equilibrium, excessive stabilisation can slow catalytic turnover.<sup>[135]</sup>



*Scheme 53: Nitrile directed meta-selective arene functionalisation forming a macrocyclic palladacycle intermediate*

A computational DFT study indicated that the expected monomeric intermediate should favour *ortho*-functionalisation rather than the observed *meta*-functionalisation. Modelling the reaction to proceed *via* a dimeric intermediate (Scheme 53) predicted the experimental outcome at a lower intermediate energy than the monomeric, *ortho*-directing intermediate.<sup>[136]</sup>

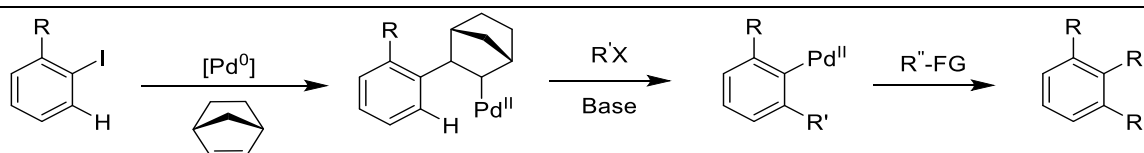
The Maiti group have successfully carried out olefination, acetoxylation and silylation of arenes at the *para*-position, utilising the Thorpe-Ingold effect and an end-on Nitrile coordination. The silyl directing group can then be removed by hydrolysis with TBAF to yield a *para* functionalised toluene (Scheme 54).<sup>[137,138]</sup> Another example of a detachable directing group is the *meta*-selective amide linked system that successfully performed arylations and methylations, and was shown to be removable post-transformation under hydrolysis conditions (Scheme 54).<sup>[139]</sup>



*Scheme 54: Examples of removable directing groups for arene functionalisation*

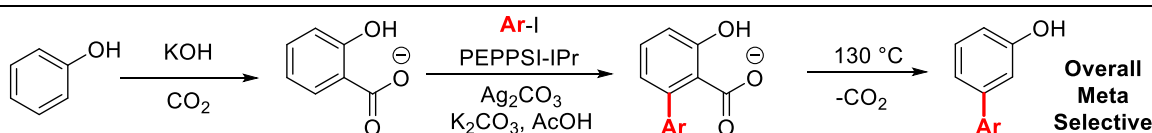
### 1.7.3. Traceless Directing Groups

Traceless directing group technologies are also prevalent in literature, using directing groups which are not present in the final product. The Catellani reaction (Scheme 55) utilises a non-heteroatom based traceless directing group using norbornene to direct *ortho* metallation and subsequent functionalisation. [140] Here norbornene facilitates both *ortho* and *ipso* functionalisation. [141] One such advancement utilises norbornene a transient mediator for *meta*-functionalisation applicable in enantioselective desymmetrisation of achiral benzylamines. [142,143]



Scheme 55: The Catellani reaction utilises norbornene for *ortho* C-H functionalisation

The Larrosa group achieved arylation of phenols using an *ortho*-carboxylated intermediate as a relay for an overall *meta*-selective functionalisation (Scheme 56) with subsequent decarboxylation. [144]

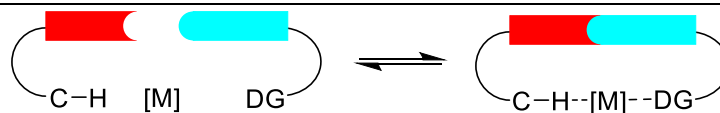


Scheme 56: The Traceless Directing Group Relay Strategy yielding an overall *meta* functionalisation of phenol

### 1.7.4. Transient Directing Groups

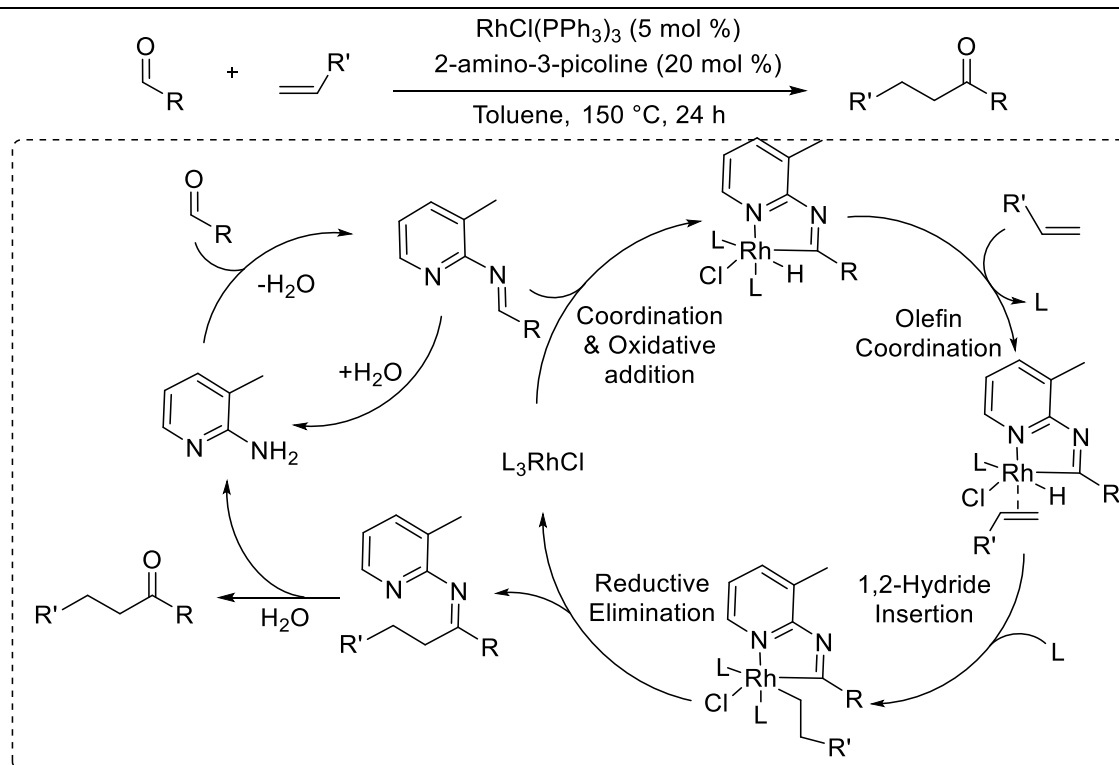
The drawback of many of the methodologies discussed is the requirement to preinstall directing groups stoichiometrically, adding additional steps to the synthesis. It is desirable to develop one-pot strategies that can utilise a plethora of substrate functionalities for site-selective transformations, without directing group insertion/removal being required.

The transient directing group strategy (TDG) employs a reversible interaction between a substrate and directing ligand (Scheme 57). As a result, the directing group performs as a catalyst and may be incorporated into a reaction in substoichiometric quantities.<sup>[145-149]</sup>



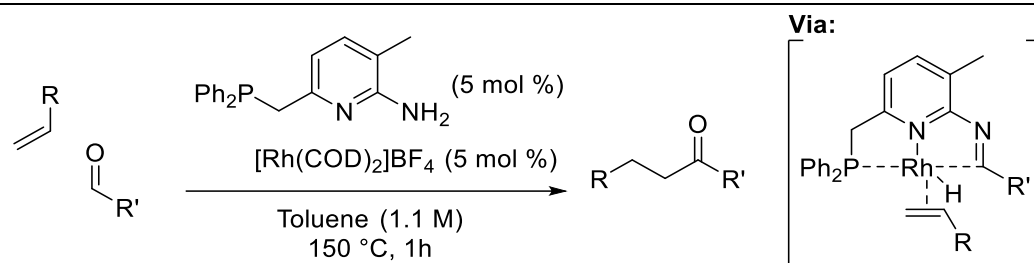
Scheme 57: General overview of the TDG strategy

An early example of the TDG approach was described by Jun *et al.* in 1997, in which 2-amino-3-picoline was used cooperatively alongside a rhodium catalyst (Wilkinson's catalyst) to perform a directed hydroacylation at the C(sp<sup>2</sup>)-H bond of various aldehydes to yield ketones. This was facilitated by the directing ability of the 2-iminopyridyl moiety formed *in-situ* (Scheme 58).<sup>[150,151]</sup>



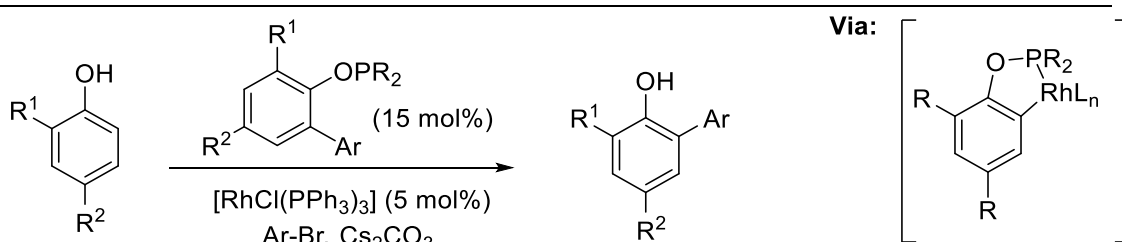
Scheme 58: Jun's pioneering work in the field of transient directing group technology

Breit *et al.* were able to improve upon Jun's work by adapting the TDG to bind to the metal in a bidentate fashion. The resulting decrease in lability allowed the complex to be added at 5 mol%, decreasing the required loading of the picoline derivative (Scheme 59).<sup>[152]</sup>



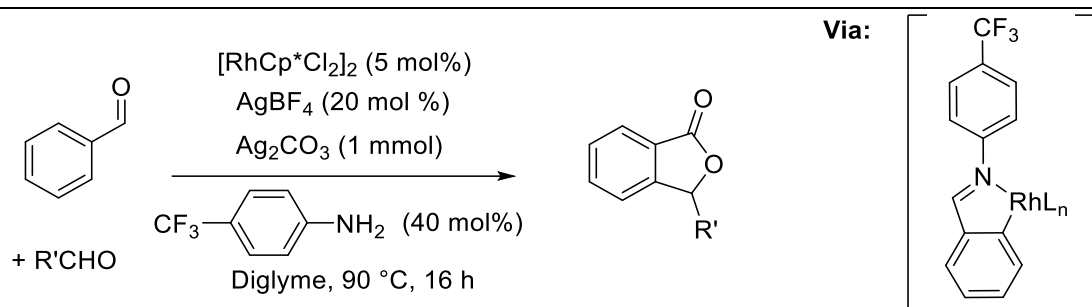
Scheme 59: Breit and Co-workers improvement on Jun's 1995 work

Some other notable pioneering examples include work by the Bedford group, who described the *ortho*-arylation of a 2-substituted phenol. They employed an aryl dialkylphosphinite TDG which interacts covalently with the phenol *via* transesterification, to direct *ortho*-metallation (Scheme 60).<sup>[153]</sup>



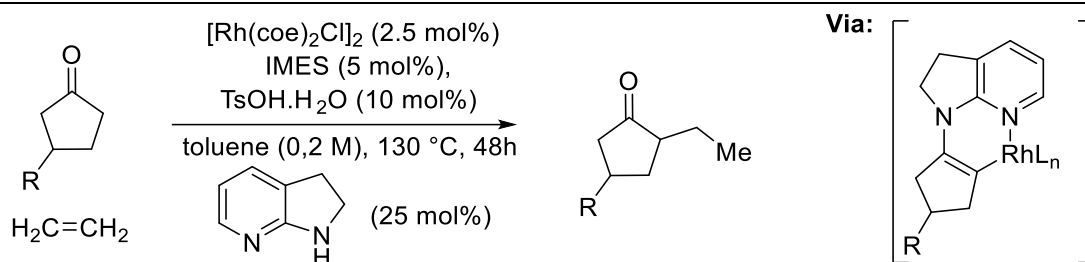
Scheme 60: Bedford's *ortho*-selective arylation of phenols using a phosphinite directing group.

The Seayad group published a rhodium catalysed homocoupling of aldehydes to form phthalides, using 4-trifluoromethylalanine to transiently form an imine directing group (Scheme 61).<sup>[154]</sup>



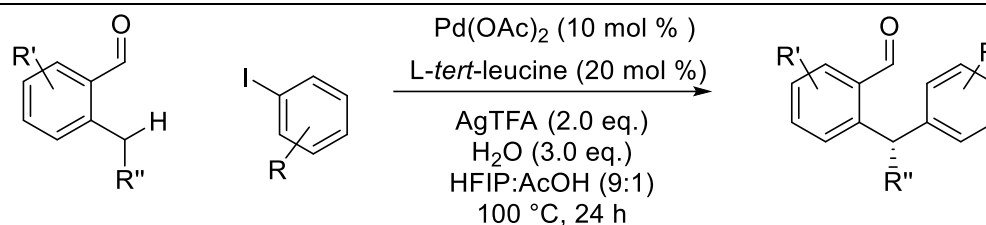
Scheme 61: Seyad's *ortho*-selective functionalisation of benzaldehydes using a transient imine linkage

Also, the Dong group performed an  $\alpha$ -alkylation of carbonyl compounds, via condensation of 7-azaindoline onto a ketone or aldehyde, to direct rhodium metallation to the proximal  $\alpha$ -C(sp<sup>3</sup>)-H centre, this strategy allowed the use of simple olefins as the alkylating agents over the more commonly used, yet expensive, haloalkane reagents (Scheme 62).<sup>[155]</sup>



Scheme 62: Dongs  $\alpha$ -selective functionalisation of ketones using a transient imine linkage.

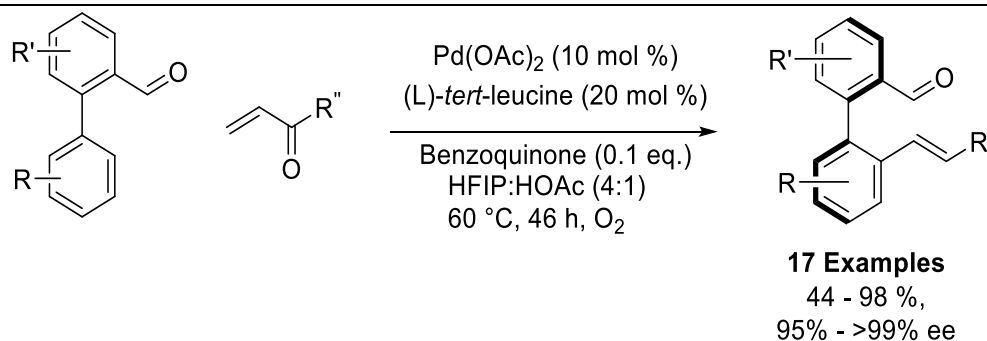
TDGs have also been applied in enantioselective synthesis. Yu *et al.* described the use of (*L*)-*tert*-leucine as a transient directing group for benzylic C(sp<sup>3</sup>)-H arylation of various *ortho*-substituted benzaldehydes, using a palladium(II) catalyst and an Ag(TFA) oxidant to achieve an enantiomeric ratio of greater than 95:5 across the substrate scope. In this case, the amine of the  $\alpha$ -amino acid undergoes a condensation reaction with the aldehyde, and the carboxylic acid acts to ligate the palladium catalyst (Scheme 63).<sup>[156]</sup>



*Scheme 63: An enantioselective TDG C(sp<sup>3</sup>)-H functionalisation*

---

Further use of transient directing groups in chiral synthesis is highlighted in work by the Shi group who used (L)-*tert*-Leucine to olefinate 2-naphthylbenzaldehydes in good yields between 65 – 95 % and high enantioselectivity of greater than 97 % ee across the substrate scope (Scheme 64).<sup>[157]</sup>



*Scheme 64: Example of TDG strategy utilised for atroposelective synthesis*

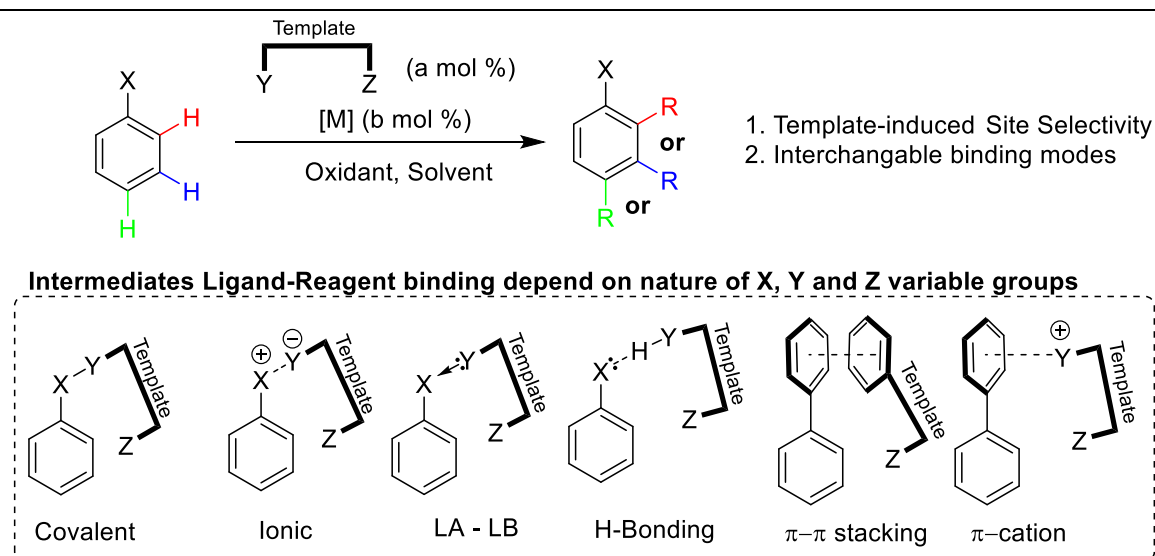
---

Most work in the field of transient directing groups has used covalent interactions in equilibrium to direct metallation to a desired C-H bond. However, this means that these reactions require a moiety on the reagent to accept covalent binding, which, in turn, require pre-installation. Thus, work in this field is now looking towards harnessing a myriad of non-covalent interactions to allow for a broader substrate scope.

### 1.7.5. Non-Covalently Bound Directing Groups

The substrate scope for covalent-TDG approaches is limited, as the chosen substrate must be able to undergo a transformation, such as an imine condensation, to form a strong yet reversible covalent bond. In the imine condensation example, this limits the substrates to aldehydes and ketones.

Non-covalent transient substrate-ligand interactions offer an opportunity to develop methodologies with an expansive substrate scope. Whilst imine condensation is limited to aldehydes and ketones, a broader range of substrate-ligand pairings can be proposed for ionic, Lewis Acid – Lewis Base (LA-LB), hydrogen-bonding,  $\pi$ - $\pi$  and  $\pi$ -cation interactions (Scheme 65); although weak, the strength of these interactions can be modulated and thus their transient behaviour can be exploited.



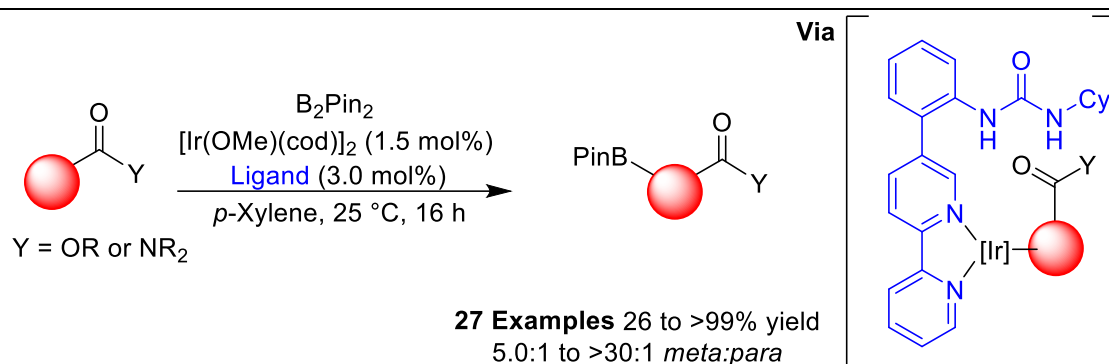
Scheme 65: Possible transient directing group interactions

Several examples of non-covalent substrate-ligand interactions have been described in the literature. Several examples of functionalisation of distal C-H bonds, with a catalytic loading of metal and ligand will be discussed, *vide infra*.

In 2015, the Kanai group utilised a urea substituted 2,2'-bipyridyl to perform a *meta*-selective iridium catalysed borylation (Scheme 66), with site-

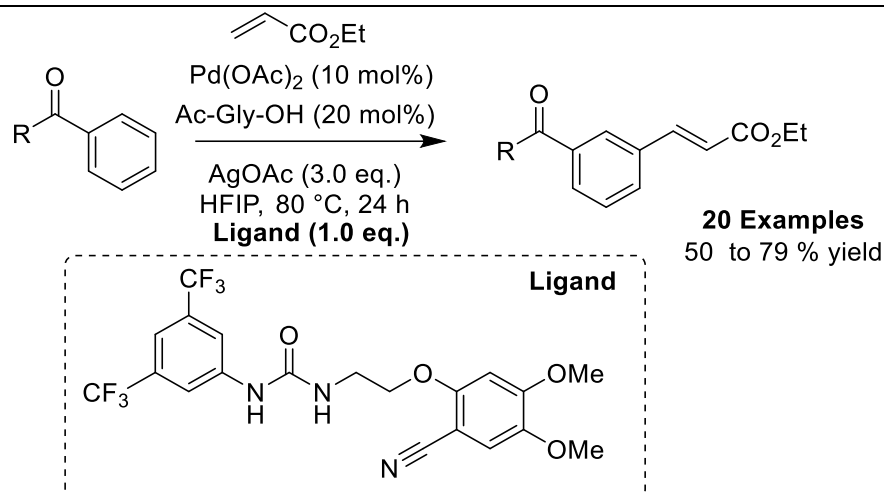


selectivity induced through hydrogen bonding interactions between the ligand and the substrate, a total of 27 examples were described between 26 and >99% yield, some examples exhibited selectivity issues with *para*-functionalisation sometimes being observed.<sup>[158]</sup>



*Scheme 66: A bifunctional template utilising hydrogen-bonding to stabilise an intermediate organoiridium complex preceding borylation*

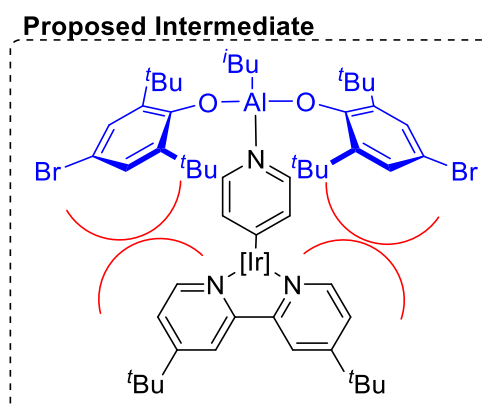
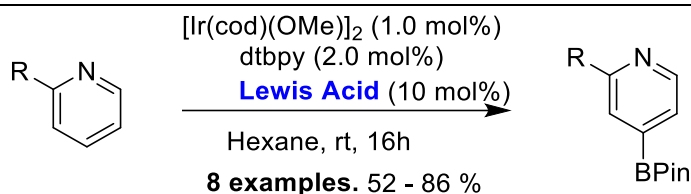
Hydrogen bonding has also been used to direct a *meta*-selective, palladium(II) catalysed C-H alkenylation of aromatic aldehydes, ketones, benzoate esters and benzamides (Scheme 67).<sup>[159]</sup> Poor control over site-selectivity was observed in some examples, with several examples yielding *ortho*-, *meta*- and *para*-functionalisation. This site-competition is likely due to the flexibility of the template, with two  $\text{sp}^3$ -carbons allowing for stabilisation of multiple C-H metallated intermediates.



Scheme 67: Meta-selective C-H alkenylations directed by a hydrogen bonding interaction between the substrate and a bifunctional ligand

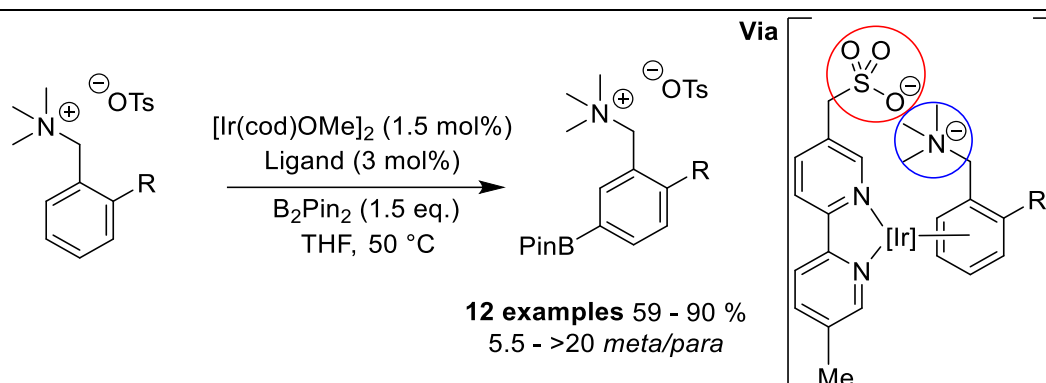
---

Steric interactions have also been shown to assist in directing C-H borylations with iridium catalysts. Co-ordination of pyridine to a sterically bulky aluminium reagent affords a large steric resistance to C-H borylation at the *ortho* and *meta* positions, affording *para*-selective functionalisation (Scheme 68).<sup>[160]</sup> This steric interference approach to iridium(I) C-H borylation is somewhat limited to mono-aryl systems, as it would be difficult to design a system which selectively blocks every undesired C-H site in a multi-aryl substrate.



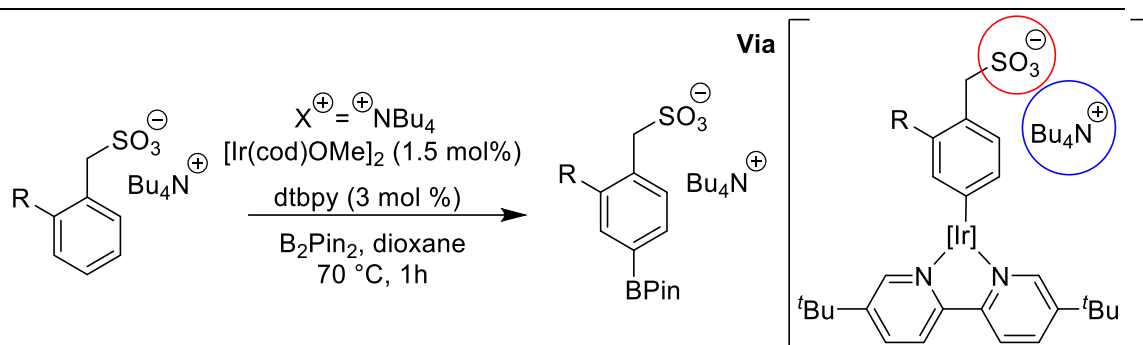
*Scheme 68: Steric Interactions assist in promoting C-H borylation para to the pyridine nitrogen*

The Phipps group described an iridium catalysed borylation, in this case employing a sulfonate substituted 2,2'-bipyridyl to harness ionic interactions with ammonium containing substrates (Scheme 69).<sup>[161]</sup> Using 1,2-disubstituted aryl substrates site-selectivity *meta* to the ammonium substituent was afforded (>5:1 *meta:para* across 12 examples); a control experiment, using dtbpy (4,4'-di-tert-butyl-2,2'-bipyridine) as the ligand, yields a 1:1 *meta:para* ratio. The control experiment shows that in the absence of the ionic interaction no preference over the two accessible C-H sites is afforded.



*Scheme 69: A bifunctional template utilising ionic bonding to stabilise an intermediate organoiridium complex preceding borylation*

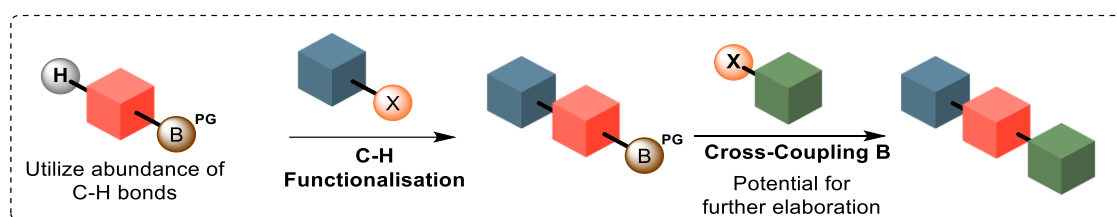
A continuation of this work combined ionic pairings with the steric hinderance strategy. By using a tetrabutyl ammonium benzyl sulfonate salt, the Phipps group were able to realise borylation *para* to a sulfonate of a 1,2-disubstituted arene (Scheme 70). The selectivity is likely realised *via* the ionic pairing of sulfonate and ammonium ions which sterically hinders C-H metallation *meta* to the sulfonate group.<sup>[162]</sup>



*Scheme 70: Ionic pairings can help create further steric constraints to iridium catalysed C-H borylations creating site-selectivity in 1,2-disubstituted arenes substrates*

## 1.8. C-H functionalisation Orthogonal to C-B Bonds

The use of transition metals for C-H functionalisation, adds difficulties when applied to organoboron-bearing reagents. They require the development of conditions which exhibit C-B bond orthogonality in parallel to the desired transformation, thus requiring a tight control of variables in order to counter an often-preferred transmetalation pathway. As will be highlighted in this section, methodologies which achieve this, exhibit an ability for iterative synthesis and rapid elaboration of substrates (Scheme 71).

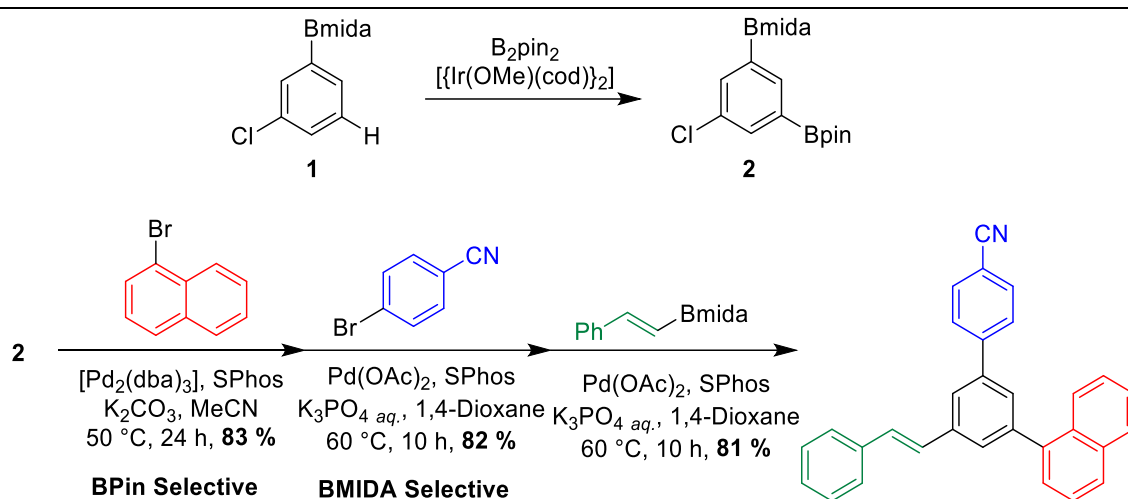


*Scheme 71: Overview of C-H functionalisation in presence of a C-B bond highlighting the potential for further elaboration*

### 1.8.1. Substrates with Boronic Moieties

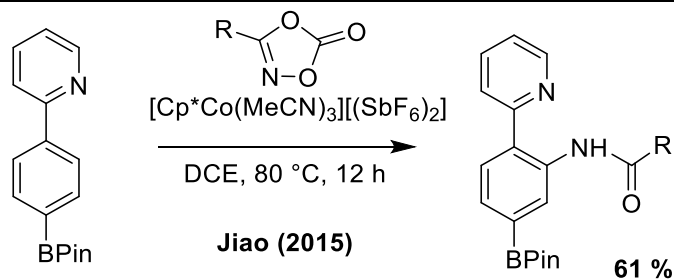
C-H borylations with iridium can be achieved in the presence of a C-B bond producing diboron products. Results published by Li *et al.* in 2014 disclosed borylation of an aryl MIDA-boronate substrate to install a pinacol boronic ester moiety, using  $[\text{Ir}(\text{cod})_2\text{OMe}]_2$  under anhydrous conditions (Scheme 72).<sup>[163]</sup> As with most iridium catalysed borylations, the borylation is directed to the least sterically hindered position.<sup>[164]</sup> This was achieved on 13 substrates including heteroaromatics and bromoaromatics, with a yield range of 84 - 94% (Scheme 72). The utility of this transformation was showcased on 3-chlorophenyl MIDA-boronate which was initially borylated under their iridium catalysed conditions in a 96 % yield. The authors then reported selective speciation of Bpin over BMIDA, in-line with findings by Burke *et al.*<sup>[89]</sup> to perform a chemoselective Suzuki-Miyaura cross-coupling with 1-bromonaphthalene in an 83 % yield. This was followed by a second cross-coupling, utilising the C-B(MIDA) moiety to couple with 4-bromobenzonitrile.

This was performed employing an aqueous base, as to deprotect the MIDA boronate *via* hydrolysis, and was achieved in a 82 % yield. Finally, a third cross-coupling utilised the C-Cl bond to install a styryl group in an 81 % yield. Producing a trisubstituted aromatic rapidly and with a high potential for variation of coupling partners.



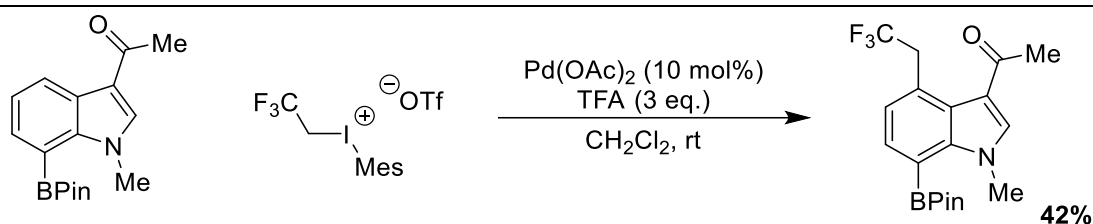
*Scheme 72: Meta-selective C-H borylation of BMIDA-substituted aromatics, with the utility highlighted through selective iterative synthesis to form a tri-substituted aromatic*

In 2015, Jiao *et al.* disclosed a cationic cobalt(III) catalysed C-H amidation of various substrates.<sup>[165]</sup> This included a 2-phenyl pyridine bearing a pinacol boronic ester moiety. When employing this substrate, a slight depreciation of yield was observed when compared to the rest of the substrate scope, 61 % for R = BPin, with the rest of the substrate scope yielding in range of 87 – 99 % (Scheme 73). Although not stated, this is likely a result of decomposition of the C-B bond, transmetalation between organoboron compounds and cobalt(I) complexes has previously been discussed in the literature.<sup>[166]</sup> It should be noted here that this methodology was not optimised with the orthogonality of C-B bonds as the primary objective, and thus it is likely that with further modification of conditions, the yield for this substrate could be improved.



*Scheme 73: Orthogonality of a BPin Moiety in directed C-H functionalisation of 2-Phenylpyridine derivatives*

Similarly, an aryl pinacol boronic acid ester was included in the substrate scope for a palladium(II) catalysed C-H fluoroalkylation of the C4-position of indoles in a 42% yield, indicating that palladium(II) catalysed C-H functionalisation can be achieved in the presence of a pinacol boronic acid ester (Scheme 74). [167]



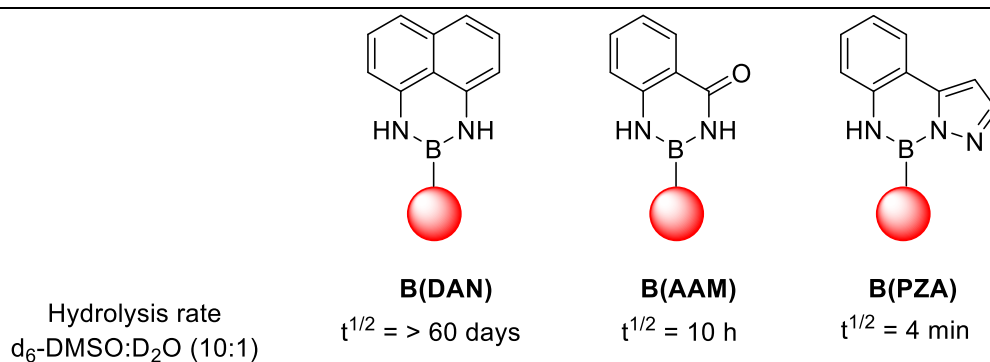
*Scheme 74: Fluoroalkylation of indoles can be achieved in the presence of a pinacol boronic acid ester*

### 1.8.2. Boron Tethered Directing Auxiliaries

Boronic acids may undergo condensation reactions to rapidly install directing auxiliaries. The auxiliaries described in this chapter are derived from protecting groups detailed in Chapter 1.5, as such, these directing groups play a secondary role as protecting groups against transmetalation.

The Suginome group have developed boron-tethered directing auxiliaries for site-selective C-H functionalisations. Two directing/protecting auxiliaries were developed based on the principles of 1,8-diaminonaphthalene protection of boronic acids (See Chapter 1.5.4). 2-pyrazol-5-ylalanine (PZA)

and anthanilamide (AAM) form boronic amides which can simultaneously direct C-H functionalisation and inhibit transmetallation (Scheme 75).



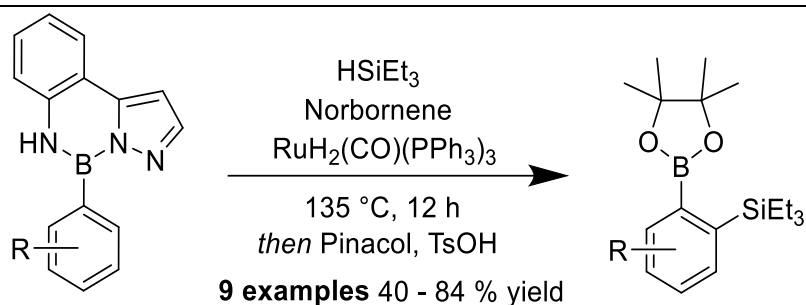
*Scheme 75: Structures of BDan inspired AAM and PZA directing auxiliaries with comparison of hydrolytic stability*

---

Although DAN-boronic amides exhibit a high hydrolytic stability, having a hydrolysis half-life of over 60 days in a 10:1 mixture of d<sub>6</sub>-DMSO:D<sub>2</sub>O, both B(AAM) ( $t^{1/2} = 10$  hours) and B(PZA) ( $t^{1/2} = 4$  minutes) are significantly less hydrolytically stable. Consequently, the auxiliaries are employed under anhydrous conditions, and work-ups may displace the auxiliaries with pinacol post-reaction under acidic conditions, to yield the corresponding pinacol boronic acid esters. Pinacol boronic acids are easier to purify as they are often stable to aqueous work-ups and column chromatography.<sup>[168]</sup> Acid is used in the pinacol work-up to protonate that boronic amide nitrogen's expediting esterification by pinacol.<sup>[6]</sup>

In 2009, Suginome *et al.* first disclosed PZA as an *ortho*-directing protecting-directing auxiliary for ruthenium catalysed C-H silylation of aryl boronic acids.<sup>[169]</sup> Installation and removal of PZA was reported to be efficient, with attachment achieved by reflux in toluene and removal with TsOH and pinacol to produce the pinacol ester product. The entire process of installation, transformation and removal was shown to be attainable in a single pot, and 9 synthetic examples were disclosed in yield range of 40 – 84 % (Scheme 76).



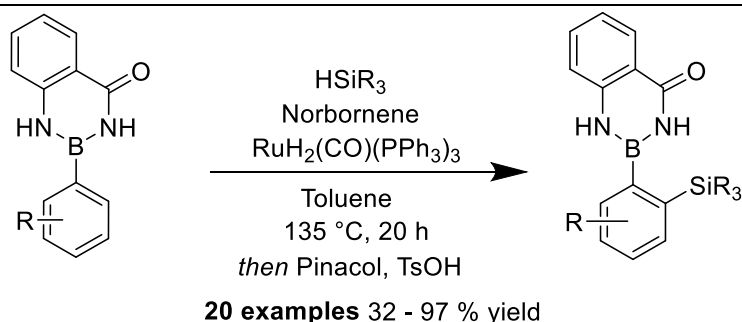


*Scheme 76: PZA directed ortho-selective C-H silylation of aryl boronic acids*

---

The authors noted that the reactions proceeded faster with more electron rich aromatics, and that the silylation was highly selective for the least sterically incumbered *ortho*-position, with almost no formation of double silylation products. This was attributed to steric factors, corroborated by *ortho*-tolylboronic acid yielding no *ortho'*-silylation.

Whilst *ortho*-tolyl PZA-boronic amides failed to achieve a desired silylation, the AAM-analogue produced the desired product in an albeit low 32 % yield. Across two papers disclosing AAM-directed *ortho*-C-H silylation,<sup>[168,170]</sup> a total of 20 examples were given, with a yield range of 32 – 97 %, with poor yields reported for more sterically bulky silylhydrides (Scheme 77).

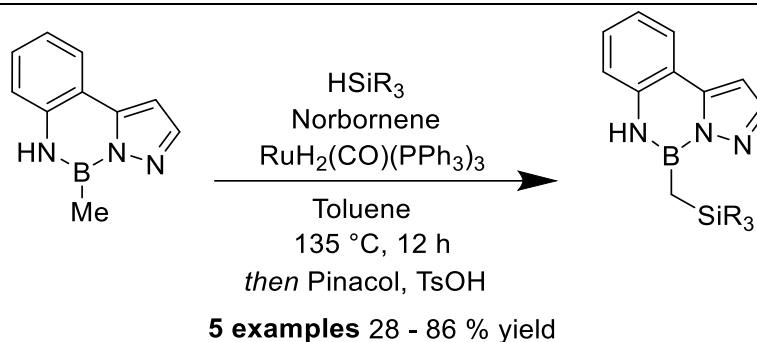


*Scheme 77: AAM directed ortho-selective C-H silylation of aryl boronic acids*

---

C-H silylation can also be realised at  $\alpha\text{-C}(\text{sp}^3)\text{-H}$  bonds of  $\text{MeB}(\text{PZA})$  with silyl hydrides, with the Suginome group producing 5 examples in a range of 27-97% (Scheme 78); the bulkiness of the silyl reagents was found to limit the yield.<sup>[171]</sup> Unfortunately, selectivity issues arose when extending the carbon

chain, with EtB(PZA) found to react slowly and yield both  $\alpha$  and  $\beta$  products in a 1:1 ratio, and when employing cyclohexyl-B(PZA) the reaction was slowed to such an extent that the PZA was functionalised instead. No report of C-B bond cleavage was reported.

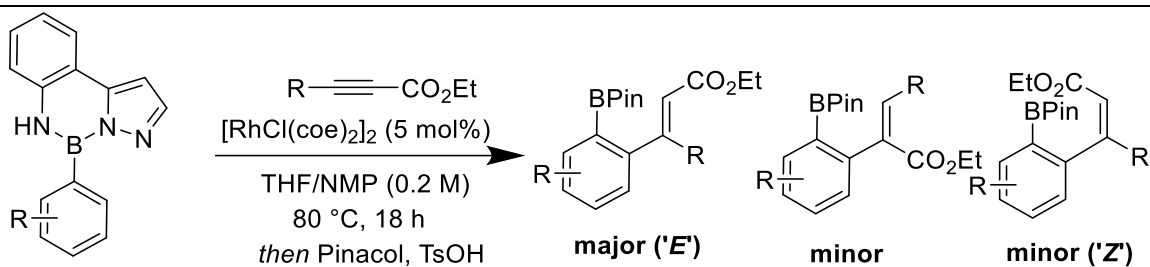


*Scheme 78:  $sp^3$  C-H functionalisation was described on MeBPZA, however, the yield was found to decrease using longer alkyl chain lengths.*

---

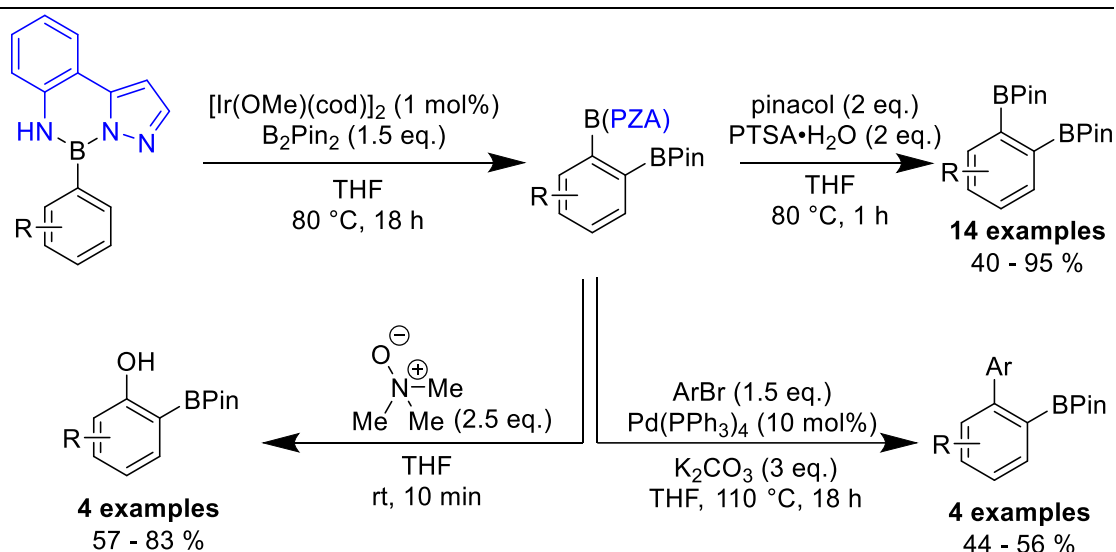
Rhodium catalysed *ortho*-C-H alkenylations coupling with a series of propynoic ethyl esters can be directed by BPZA,<sup>[172]</sup> whilst attempts to direct this functionalisation with MIDA, AAM, DAN and Pin protected boronic acid derivatives realised no desired reaction. Sixteen synthetic examples in a 0-84 % yield range were described, with the symmetrical alkyne diethyl acetylenedicarboxylate giving no desired product (Scheme 79).

There was reported to be a regioselective preference, which is likely afforded by a kinetic insertion of a rhodium hydride intermediate to the  $\beta$ -position of the alkyne with respect to the ester. This major:minor ratio was reported to lie between 74:26 and 93:7. The major product was then reported as a mixture of *E*- and *Z*-isomers, with the major *E*-isomer being preferred likely due to steric factors. This *E:Z* ratio was reported between 71:29 up to >99:1.



Scheme 79: Alkenylations directed by an aryl BPZA boronate

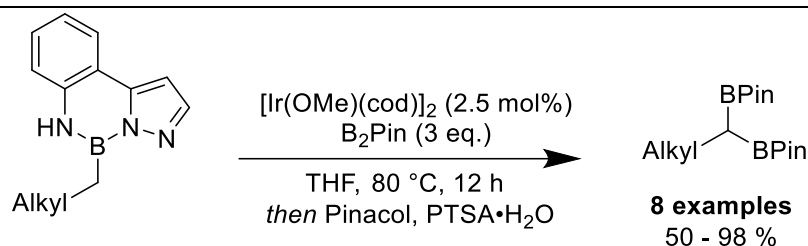
*Ortho*-selective iridium(I) catalysed aryl borylations may be directed by PZA; found to remain selective for *ortho*-selectivity.<sup>[173]</sup> A total of 14 examples in a yield range of 70 – 92% were discussed. In this case, good yields were still achieved on *ortho*-substituted substrates, overcoming the steric limitations of the C-H silylation and showing good tolerance to both electron rich and electron poor aromatics. To highlight synthetic value, kinetic speciation of B(PZA) over B(Pin) was showcased through Suzuki-Couplings and selective oxidation using tetramethyl ammonium N-oxide (Scheme 80).



Scheme 80: Iridium catalysed borylations ortho to BPZA with synthetic utility highlighted

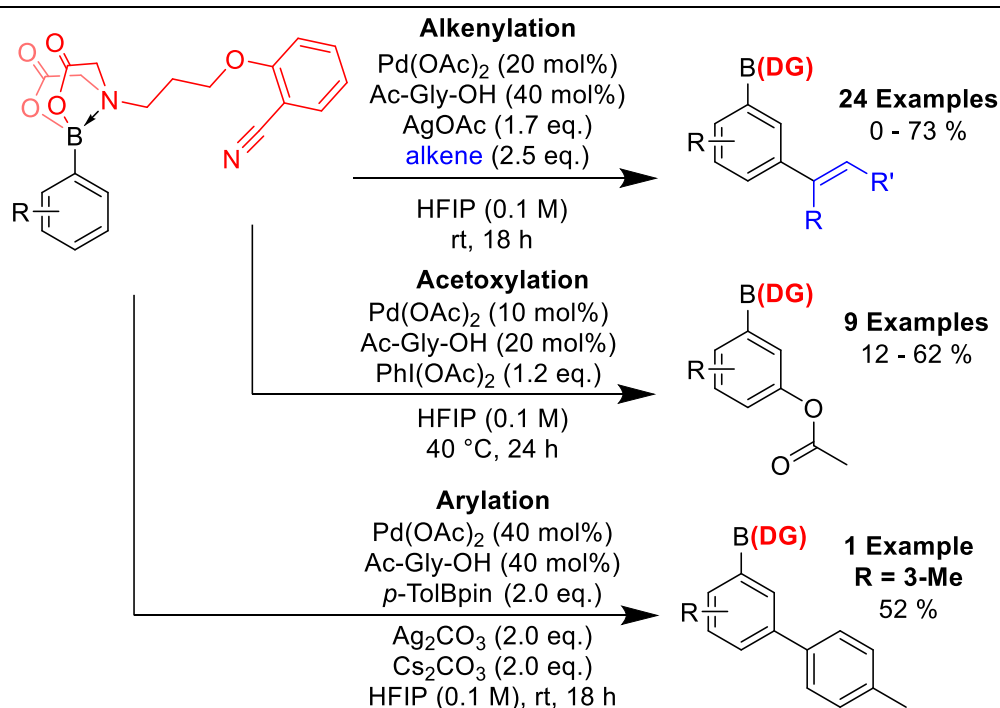
Fifteen examples of iridium(I) catalysed alkyl borylations in a yield range of 43 – 98 % were later disclosed. Di-, tri- and tetra-borylated products could also be realised by employing a pre-borylated iridium catalyst, with

[Ir(mes)(BPin)<sub>3</sub>] found to rapidly access multi-borylated products (Scheme 81).<sup>[174]</sup> Although  $\alpha$ -functionalisation was preferred, competition of  $\beta$ - and  $\gamma$ -hydrogens was observed, realising multi-borylated products.



Scheme 81: A series of multi-borylated products were produced via directed C-H Borylations using an iridium catalyst

MIDA-boronates have recently been shown to be suitable for derivatisation to promote directed C-H functionalisation. Williams *et al.* described a series of *meta*-selective C-H functionalisation's including acetoxylation (9 examples, 12 – 62 %), alkenylation (24 examples, 0 – 73 %) and arylation (1 example, 52 %), using a palladium(II) catalyst, facilitated by a directing auxiliary derived from the *N*-methyl iminodiacetate (MIDA) protecting group (Scheme 82).<sup>[175]</sup>

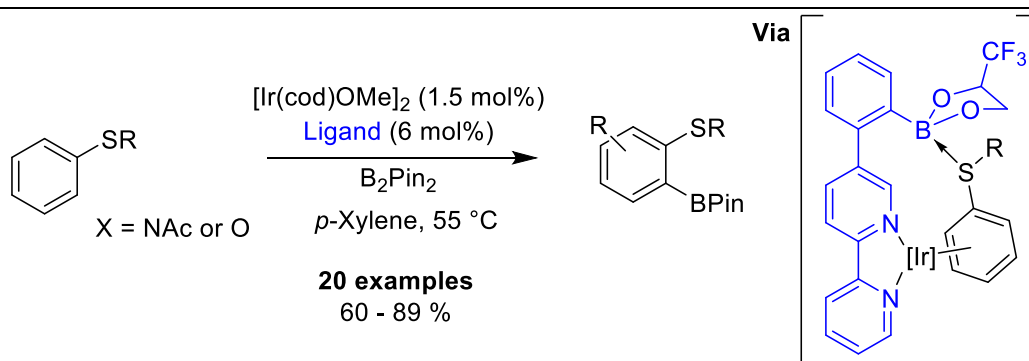


Scheme 82: Williams *et al.* described a MIDA-derived directing auxiliary for *meta*-selective C-H functionalisation

The MIDA protecting group suppresses B to M transmetallation, and by elaboration of the N-methyl group a nitrile-based template can be installed. As such, this will be referred to as *N*-templated iminodiacetate (TIDA). *Ips*o-substitution was a common side product in this reaction, realised *via* transmetallation to palladium; several screened TIDAs gave exclusively *ip*so-functionalisation. It was shown that electron-withdrawn substrates had improved yields, over electron-rich substrates. This can be attributed to tuning of electron density at boron, resulting in a strengthening or weakening of the B-N dative bond.

Competition between *meta* and *para* positions was observed, and when 2 *meta*-positions were available, difunctionalisation was common. This poor selectivity could likely be optimised by modifications to the directing template, aiming to limit undesired conformations which do not promote target site functionalisation; this may be achieved through introduction of sterically bulky substituents or increasing the number of  $sp^2$ -hybridised carbons, such as to destabilise intermediates that may mediate alternative-site functionalisation.

A final example uses Lewis acid – Lewis base pairings between aryl sulfides and boronic acid esters to direct C-H borylation with excellent selectivity (Scheme 83). Co-ordination of trifluoromethyl ethylene glycol to boron, reinforces the S-B interaction promoting the reaction, however when using tetra-(trifluoromethyl)ethylene, it was proposed that the S-B bond was excessively strong inhibiting catalytic turnover.<sup>[176]</sup>



Scheme 83: Lewis acid – Lewis base substrate-ligand interactions promoted an *ortho*-selective C-H borylation

## 1.9. Aims and Objectives

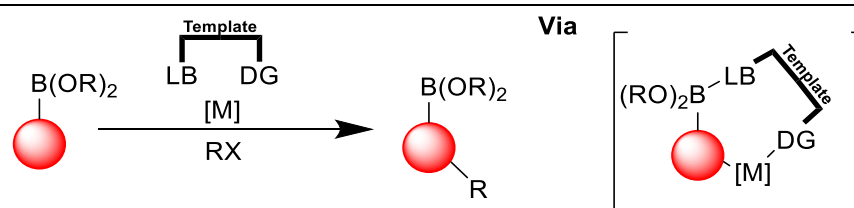
Early examples of site-selective C-H functionalisation were only able to access C-H bonds proximal to a directing functionality, limiting applicability (See Chapter 1.7.1). Then, directing auxiliaries which could reach beyond proximal C-H bonds (to *meta* and *para* positions for aryl substrates) were designed. These auxiliaries required installation and removal meaning poor atom- and step-economies (See Chapter 1.7.2). More recent examples overcome this with *in situ* transient linkage between a substrate and a bifunctional template, which then directs C-H functionalisation (See Chapter 1.7.4). By using a transient substrate-template binding, the template can be employed catalytically, therefore improving atom economies and allowing recycling of the templates for future reactions, minimising waste. Furthermore, under a transient directing group strategy, weaker non-covalent interactions between a substrate and ligand can be employed, allowing for a wider range of substrates to be used so long as they have the necessary functionalities to accommodate the chosen non-covalent interaction (See Chapter 1.7.5).

Boronic moieties are ubiquitous to organic chemistry; the Suzuki-Miyaura cross-coupling reaction has seen wide-spread adoption for efficient, high yielding, scalable and low hazard carbon-carbon bond forming reactions. Boronic moiety bearing compounds are often used as key intermediates in target-oriented synthesis but are recently finding utility in drug-targets (See Chapter 0).

Organoboronic moieties are often used only in a transitory manner, installed only as a means to install another functionality. However, the Lewis acid nature of boronic moieties, allow for rapid conversion to four-coordinate species. The Lewis acidity of 3-coordinate boron centres make these functionalities highly attractive for chemistries promoted by transient interactions.

This project aims to utilise transient Lewis acid-Lewis base interactions of a bifunctional template with boronic moieties for directed C-H functionalisation (Scheme 84). There was concern of using transition metal catalysts to perform C-H functionalisation whilst in the presence of a moiety susceptible to transmetallation, however the literature discussed throughout Chapter 1 highlights the feasibility of the project aim.

The rate of transmetallation can be slowed dramatically under anhydrous conditions, as the process requires either an oxygen-centred base or fluoride in order to perform transmetallation. Superstoichiometric quantities of oxygen-centred bases inhibit C-B bond cleavage in the presence of a transition metal, this is because 4-coordinate boronates cannot undergo transmetallation, so an excess of oxygen-centred bases will saturate the empty  $p_z$ -orbitals of boron moieties (See Chapter 1.4).



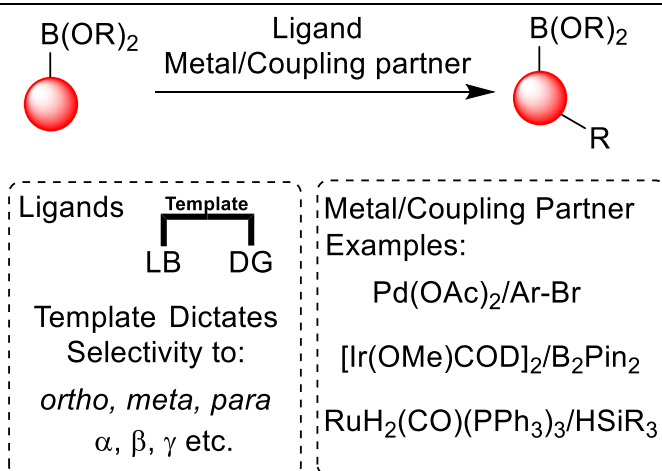
*Scheme 84: A transient directing group approach which utilises Lewis acid - Lewis base pairings.*

---

An ideal synthetic protocol would employ a low loading of metal and bifunctional template to achieve a desired functionalisation in high yields, excellent site-selectivity and perform reliably on scale. The bifunctional template would ideally be able to promote C-H functionalisation for a variety of different metals to produce a stabilised organometallic intermediate, such that the metal used is dictated by the cross-coupling partner. The ligands would remain unreacted in the reaction, meaning isolation from the product would allow the ligand to be reused in future transformations. The site-selectivity would only be determined by the template, this would mean that the site-selectivity can be modified by using a different template.

This ideal synthetic protocol would therefore be modular, for example if an *ortho*-selective borylation were required, an iridium catalyst can be employed in conjunction with an *ortho*-directing template and a diboron reagent. An analogous *para*-selective borylation could then be realised by changing to a *para*-selective template. If instead, the hypothetical chemist required *para*-selective arylation, the *para*-selective template can be used, with, for example, a palladium catalyst and an aryl iodide (Scheme 85). The ideal protocol need not be limited to aryl C-H functionalisation, as alkyl C-H bond functionalisation could also be realised using an appropriate template. Functionalisation of heterocycles bearing a boronic moiety would also be possible with an appropriate template.

The template ligands could bear a stereocentre which could induce enantioselective transformations on a substrate. Allowing for stereoselective, atroposelective synthesis of chiral products with high optical purity.



*Scheme 85: A modular synthetic protocol would allow a synthetic chemist to employ a metal/coupling partner pair with any site-selective ligand to direct site-selective C-H functionalisation of a range of organoboronic substrates*

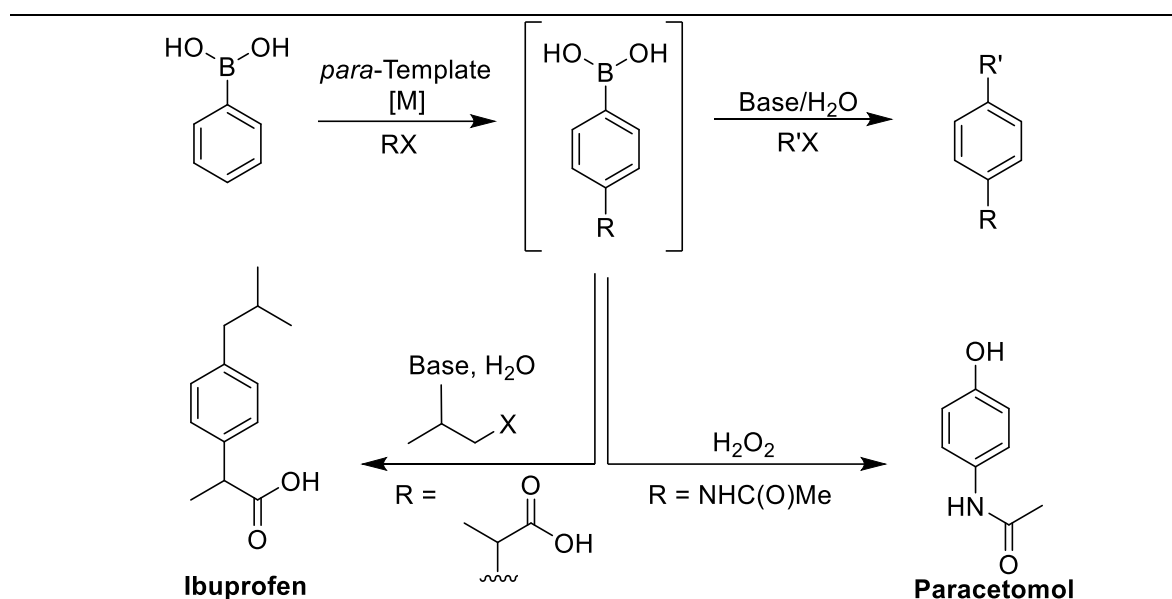
---

These reactions would utilise the boronic moiety to perform a desired transformation, and would be maintained in the starting material, generating products sporting multiple functionalities which can be further elaborated with a wide range of synthetic methodologies. Rather than installing boronic moieties only to replace them with other functionalities, this proposed



synthetic protocol would harness the chemical power of boron as a Lewis acid to dictate C-H functionalisation.

Single-pot synthesis of bifunctional arenes can be imagined, as boron-tethered templates direct an initial C-H functionalisation rapidly with one coupling partner, followed by addition of a second reagent to react at the C-B bond. This can be a second transition metal catalysed reaction reusing the metal catalyst from the first step in a second, mechanistically different, transformation (Scheme 86). A single pot synthesis of a compound such as ibuprofen could be imagined from phenyl boronic acid, wherein an initial *para*-selective alkylation is performed, followed by addition of a second coupling partner along with base and water to allow for a Suzuki-Miyaura cross-coupling. Alternatively, A single-pot synthesis of paracetamol could be performed from phenyl boronic acid by *para*-selective amidation followed by addition of hydrogen peroxide.



*Scheme 86: One-pot synthesis of a range of bifunctionalised arene can be proposed, with two examples of a one-pot synthesis of ibuprofen and paracetamol from phenyl boronic acid shown.*

With this stated, the feasibility of this approach needs to be assessed. There is literature precedent for C-B bond orthogonal C-H functionalisation (See Chapter 1.8) but the feasibility of performing C-H functionalisation using

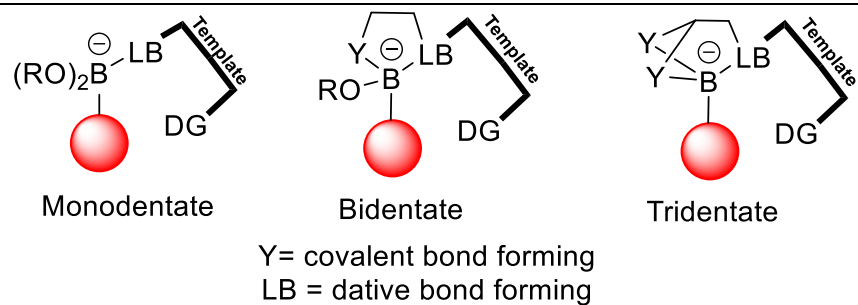
boronic acid derived moieties requires further examination. Therefore, the objectives which would allow development of the synthetically exciting protocols detailed above are outlined herein.

Firstly, the choice of Lewis base will be assessed, looking for the formation of substrate-ligand complexes bound by Lewis acid-Lewis base pairings. Substrate-ligand complexes will be detected and characterised using NMR techniques, which will allow for solvent phase assessment of substrate-ligand complexes that would be representative of their formation *in situ* under reaction conditions.

Quantification of the degree of complexation will be measured using qNMR techniques, using  $^{19}\text{F}$ -labelled substrates, as such a  $^{19}\text{F}\{^1\text{H}\}$  qNMR protocol will be refined to specifically study substrate-ligand complexes. Continuing to use a  $^{19}\text{F}\{^1\text{H}\}$  qNMR technique, the transient nature of substrate-ligand complexes will be studied, indicating which Lewis acid-Lewis base pairing would be most feasible for catalytic turnover of the ligands.

The ligand templates themselves will be produced on scale, and will be derived from literature precedent, studying examples of auxiliary directing groups (See Chapter 1.7.2) and modifying their covalent linkage to the substrate to design ligands with template skeletons previously shown to promote site-selective C-H functionalisation.

As a secondary objective a study of polydentate co-ordination to boron will also be performed, this will help to design ligands which bind more strongly to boron (Scheme 87). Polydentate ligands will create a chelate that likely will decrease the ability of a ligand to be transient, however studies to identify conditions which promote a controlled substrate-ligand dissociation can be performed.



*Scheme 87: Ligand can coordinate in multiple ways, with strong chelating ligands forming more tightly bound substrate-ligand complexes*

---

These ligand designs may also be derivatised, such that the sterics and electronics can be modified to promote catalytic turnover, enhance selectivity and improve yield. Later work may incorporate stereogenic centres onto the ligands, allowing development of enantioselective protocols. Substrate-ligand complexes will be screened for each ligand synthesised, and complexation of these to metal catalysts will also be studied.

A series of screening studies will then be performed, incorporating each ligand with a series of literature protocols shown to perform directed C-H functionalisation. These screening studies will be performed on small scale and analysed using GC-MS to rapidly assess the efficacy of a screened protocol without requirement of extensive workups such as column chromatography. Without the need of a work-up a wide range of different protocols can be screened in a short amount of time, creating a high-throughput screening approach. Each catalytic protocol found to achieve direct C-H functionalisation will then be optimised focusing on high site-selectivity and yield before a substrate scope is performed.

Once the feasibility studies have been performed, and hits have been generated from the reaction screenings, reaction optimisations will be performed to generate tractable protocols. Exemplification of the utility of these protocols will be done using the developed methodologies in target syntheses.

# Chapter 2

## Alkoxy Pinacol Boronates

## 2. Alkoxy Pinacol Boronates

### 2.1. Observing Transient Boron-Ligand Interactions

This project aims to develop a directed C-H functionalisation methodology which utilises Lewis Acid – Lewis Base pairings between the substrate and a bifunctional ligand, wherein the bifunctional ligand will consist of three parts; 1) Lewis basic functionality, for substrate-ligand interactions, 2) a template skeleton which will extend to assist in directing distal a metal to distal positions and 3) a directing group moiety which will coordinate to a metal and bring it to the position determined by the template.

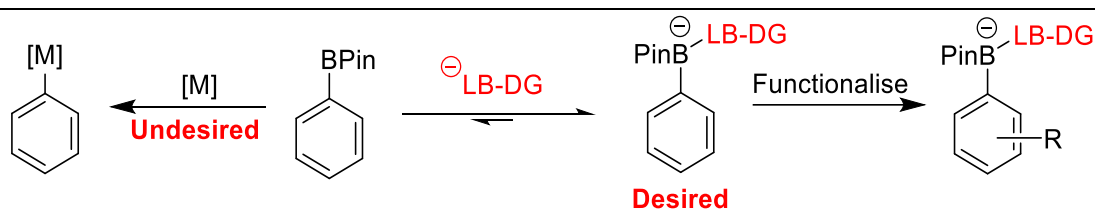
The excellent synthetic utility of boronic acids and their derivatives afforded by a broad range of functional group interconversions, make these substrates attractive for the development of novel C-H functionalisation methodologies. A successful C-H functionalisation of a boronic acid derivative utilising boron as a transient handle to direct site-selective functionalisation, which simultaneously maintains the boronic acid moiety, would facilitate a rapid access to a wide range of useful products in just two synthetic steps.

C-H functionalisation methodologies employ transition metal catalysts, and organoboron compounds have a propensity to undergo transmetallation to a metal centre, off-loading their organic component onto a metal centre, however examples throughout Chapter 1 highlighted the feasibility of achieving C-H functionalisation orthogonal to C-B bonds. Therefore, so long as the rate of transmetallation is minimised, a C-H functionalisation can become kinetically favoured.

As opposed to other protecting groups described in Chapter 1.3. pinacol boronic acids decrease the rate of transmetallation without formal occupation of borons  $p_z$ -orbital, thus boron can continue to perform as a Lewis acid.<sup>[177]</sup> Multiple examples of orthogonality towards transmetallation have been detailed in Chapter 1.5.1.

Amatore *et al.* showed that although a base is required to facilitate transmetalation, the rate of transmetalation is significantly slowed when a large concentration of base is employed.<sup>[59,178]</sup> A high concentration of base shifts the equilibrium between a boronic acid and a charged four-coordinate boronate species; this boronate species were found to be an off-cycle resting state in palladium catalysed Suzuki-Miyaura cross-couplings.

Applying the observation that boronate species are inert to classical transmetalation, it was proposed that by using a using a high concentration of a base a high equilibrium constant,  $K$ , for the equilibria between a neutral boronic acid and a Lewis acid – Lewis base paired boronate species could be maintained (Scheme 88). Then, by using a bifunctional Lewis basic template, it was proposed that the desired C-H functionalisation could be achieved at a greater rate than the undesired transmetalation.



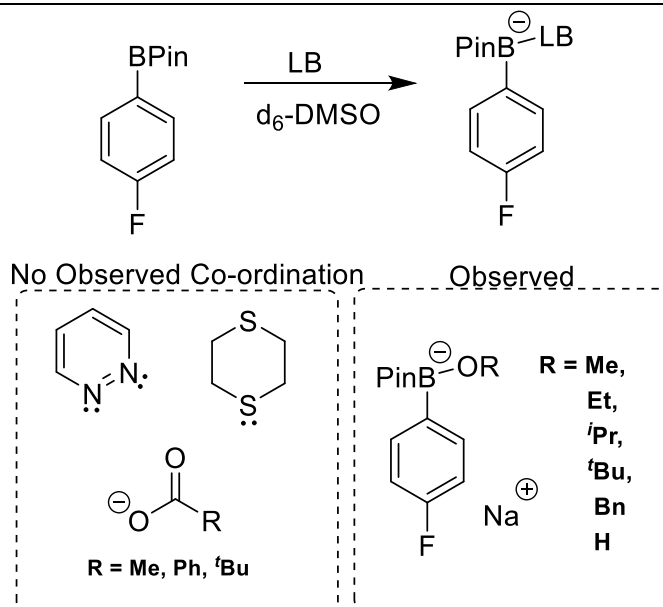
*Scheme 88: By promoting the in-situ formation of a desired pinacol boronate, it is hypothesised that the rate of transmetalation can be suppressed as to allow for directed C-H functionalisation.*

---

## 2.2. Detecting Lewis Base Co-ordination

Initial proof-of-concept studies were performed, first assessing the nature of boron-ligand coordination *via* addition of various Lewis bases, in the presence of base, to 4-fluorophenyl boronic acid pinacol ester; co-ordination was detected using NMR techniques. 4-Fluorophenylboronic acid pinacol ester was chosen as it allowed use of  $^{19}\text{F}\{^1\text{H}\}$  NMR spectroscopy, in parallel to  $^1\text{H}$  and  $^{11}\text{B}$  NMR spectroscopy. As the starting material contains only a single fluorine atom, each individual peak in the  $^{19}\text{F}\{^1\text{H}\}$  NMR spectra would correspond to a discrete chemical species, allowing for rapid assessment of a mixture.

A number of choice Lewis bases were selected, attempting to observe the co-ordination of pyridazine, 1,4-dithiane, several sodium carboxylates and various alcohols deprotonated *in situ* with sodium *tert*-butoxide. Except for alkoxides, upon dissolving the pinacol ester and each Lewis base in  $\text{d}^6\text{-DMSO}$ , no coordination was observed by NMR spectroscopy (Scheme 89).

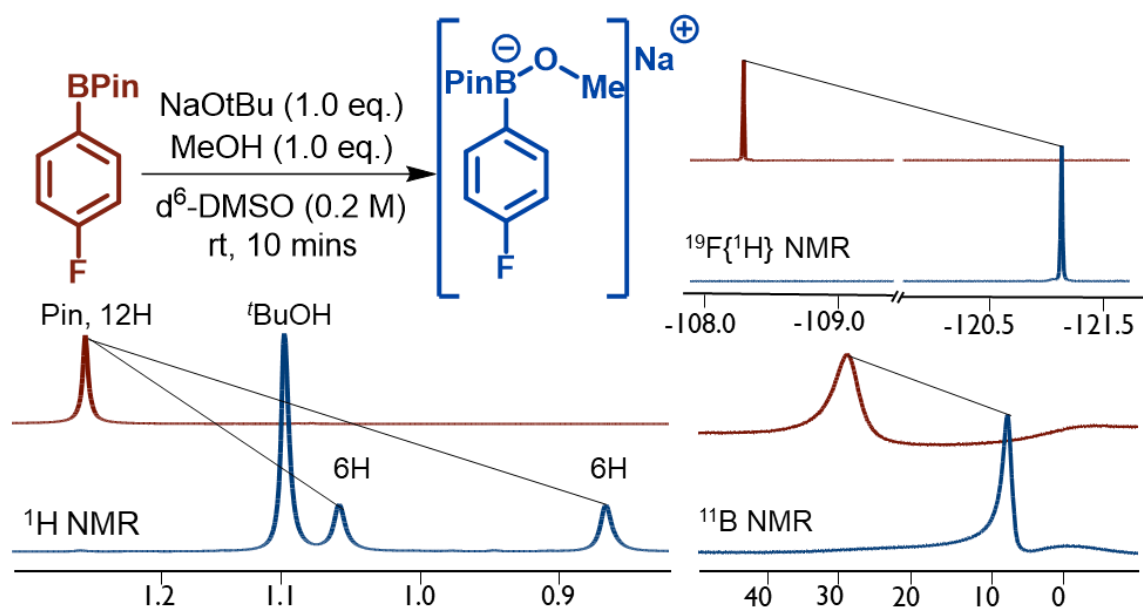


*Scheme 89: A variety of Lewis basic compounds were screened; however, no co-ordination was observed under observation by NMR spectroscopy, except for the co-ordination of alkoxides*

---

Upon treatment of the pinacol boronic acid ester with methanol in  $d_6$ -DMSO, no significant change in starting material peaks by  $^1\text{H}$ ,  $^{11}\text{B}$  and  $^{19}\text{F}\{^1\text{H}\}$  NMR were observed. However, upon *in situ* formation of the corresponding alkoxide by addition of sodium *tert*-butoxide, full conversion to the corresponding methoxy coordinated boronate ester was afforded. This was evidenced by an upfield shift of all  $^1\text{H}$  signals, with splitting of the twelve proton pinacol peak into two six proton peaks. These peaks are indicative of coordination to boron in  $^1\text{H}$  NMR because of the observed of desymmetrisation of the cyclic system afforded by restricted conformational rotation. This evidence was reaffirmed using  $^{11}\text{B}$  and  $^{19}\text{F}\{^1\text{H}\}$  NMR which also observed an upfield shift in peaks for both corresponding nuclei (Scheme 90).





*Scheme 90: Comparison of NMR spectra for the boronic acid ester starting material (Red) and the corresponding methoxy coordinated boronate (Blue). Reaction scheme shown indicates up-field shifts in  $^1\text{H}$ ,  $^{11}\text{B}$  and  $^{19}\text{F}\{^1\text{H}\}$  NMR spectra*

### 2.3. Quantitative NMR Methodologies

To further probe the nature of this and other alkoxy-bound pinacol boronates in a potentially transient environment, the observation of equilibrium states using quantitative NMR spectroscopy was attempted; however, there are several aspects that need to be considered before obtaining quantitative information from NMR spectroscopy.

$^1\text{H}$  NMR spectroscopy - As the chemical shift range in  $^1\text{H}$  NMR spectra is compressed into a relatively narrow band of up to 12 parts per million (ppm), signal overlapping is common. This may result in spectra that are difficult to elucidate information from, especially in spectra describing multiple discrete chemical species. [179] Hence,  $^1\text{H}$  NMR spectroscopy is not suitable for quantitative analysis of the target compound mixtures.

$^{11}\text{B}$  NMR spectroscopy – The large quadrupole moment of a  $^{11}\text{B}$  nuclei yields broad signals, resulting from a non-spherical charge distribution around its nuclei. This phenomenon is common in spin-active nuclei with a quantum number,  $I > 1/2$  (For  $^{11}\text{B}$ ,  $I = 3/2$ ).<sup>[180]</sup> Although quantitative  $^{11}\text{B}$  NMR spectroscopy methods have been developed,<sup>[181]</sup> due to the broad peaks in boron NMR spectra, it was assumed likely that peak overlap would occur in the target compound mixtures. It was therefore decided that  $^{11}\text{B}$  NMR spectroscopy was not suitable for quantitative NMR analysis for these studies.

$^{13}\text{C}$  NMR spectroscopy – With a low abundance of 1.1 %, many scans are required to reliably detect  $^{13}\text{C}$  nuclei. Furthermore, they exhibit long relaxation times, meaning a long delay is required to ensure a return to the ground state equilibrium before a second scan. These factors result in long acquisition times for experiments. Hence,  $^{13}\text{C}$  NMR spectroscopy is not suitable for quantitative NMR analysis of the target compound mixtures.

$^{19}\text{F}$  NMR spectroscopy - By using a  $^{19}\text{F}$  labelled substrate the issues associated with the other nuclei, *vide supra*, can be addressed. Fluorine exists almost exclusively with an atomic mass of 19 and has a spin quantum number,  $I = 1/2$ , it is also highly responsive to electronic environment changes, giving it a chemical shift range of more than 200 ppm, minimising signal overlap.<sup>[179]</sup> For these reasons,  $^{19}\text{F}$  NMR was deemed to be suitable for quantitative NMR spectroscopic analysis of the target compound mixtures.

However, there have been questions posed in the literature which have queried the validity of  $^{19}\text{F}$  and  $^{19}\text{F}\{^1\text{H}\}$  qNMR spectroscopies due to the electronic environment of the fluorine having a large influence on the relaxation/decay half-life of the nuclei. Attempts were therefore made to develop a quantitative  $^{19}\text{F}\{^1\text{H}\}$  NMR spectroscopy method, and then demonstrate its reliability for use in the characterisation of alkoxy pinacol boronate species.

### 2.3.1. Developing a $^{19}\text{F}\{^1\text{H}\}$ qNMR Spectroscopic Protocol

A proton decoupled,  $^{19}\text{F}\{^1\text{H}\}$ , experiment was used to acquire simplified and easily interpretable spectra of several alkoxy-boronates. These spectra are obtained using a pulse sequence wherein the sample is continuously radiated with a second radio signal with a broad bandwidth. The combination of field and radio frequency causes a rapid change in spin state for the hydrogen nuclei. This effectively prevents coupling to protons and sharp singlets are observed in the corresponding  $^{19}\text{F}\{^1\text{H}\}$  NMR spectra.<sup>[182]</sup>

$^{19}\text{F}$  qNMR spectroscopy has been shown to be a reliable source of quantitative information, with an accuracy and reliability comparable to  $^1\text{H}$  NMR spectra.<sup>[183]</sup> However, to obtain reliable quantitative data from  $^{19}\text{F}$  NMR spectra, the excitation bandwidth, number of scans and relaxation delay experimental parameters must be controlled.

Excitation Bandwidth - For qNMR spectroscopy, all resonances must be excited uniformly, therefore a broad excitation profile is required. This is not easily possible for  $^{19}\text{F}$  nuclei, as the spectral window is more than 200 ppm ( $\sim 100$  KHz). One simple solution is to centre the excitation half-way between the peaks of interest. However, where the peaks of interest are not in proximity multiple acquisitions may be required placing the centre of excitation at the peaks of interest. Alternative pulse sequences such as CHORUS developed by Power *et al.* affords a broad uniform excitation of more than 500ppm, but require longer acquisition time, where quantification maybe less accurate due to spin-spin relaxation. <sup>[184]</sup>

Number of Scans - The number of scans helps to improve the resolution of outputted spectra helping to reduce baseline noise, where a signal to noise integration ratio of  $>150:1$  obtains  $<1\%$  uncertainty in the measurement, thus the number of scans should aim to be at the minimum value that achieves this.<sup>[185]</sup> Conveniently, as fluorine exists almost exclusively as  $^{19}\text{F}$ , fewer scans are required to get a good signal to noise ratio, meaning shorter acquisition times.

Relaxation delay - The interval between scans, to allow time for the excited nuclei to return to their ground state before re-excitation, is the relaxation delay. If the relaxation delay is too short, information will be lost, as the absorbance intensity is decreased and thus the integration value, this is a result of failing to attain a ground state thermal equilibrium between scans. As the longitudinal relaxation,  $T_1$  is a constant in the exponential decay function:

$$M_z(t) = M_{z,eq} \left( 1 - e^{-\frac{t}{T_1}} \right)$$

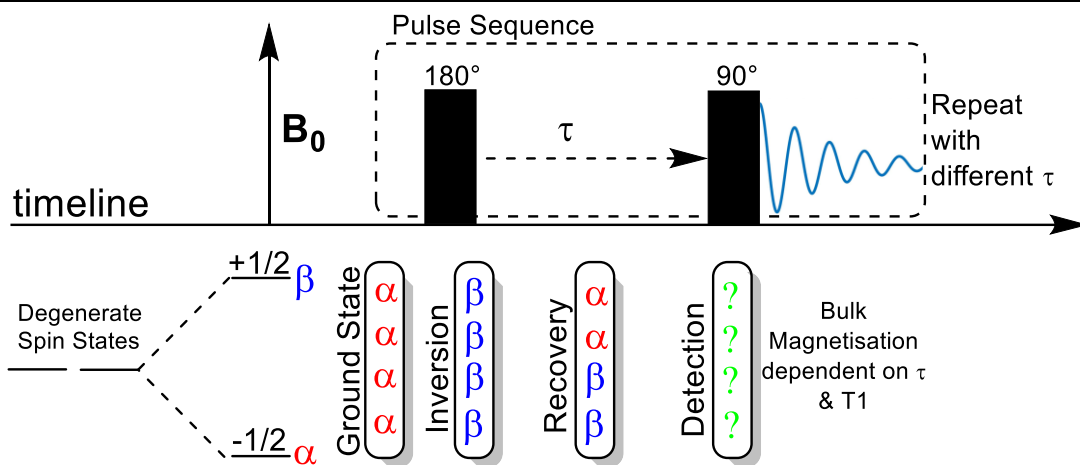
Where,  $M_z(t)$  is the total recovery of the nuclear spin magnetisation at time,  $t$ , towards the thermal equilibrium value,  $M_{z,eq}$ . meaning the contents of the brackets calculates the fraction of nuclei which have returned to their ground state. It is recommended to set the delay to five times the longitudinal relaxation,  $T_1$ , of the slowest relaxing nuclei; so when  $t = 5T_1$ , approximately 99.33% relaxation is afforded. [179]

$$1 - e^{-\frac{5T_1}{T_1}} = 1 - e^{-5} = 0.9933 \text{ or } 99.33 \%$$

Therefore, by obtaining a value for  $T_1$ , it is possible to ensure a minimal degree of error, whilst optimising total acquisition times across multiple scans.

### 2.3.2. Inversion Recovery Experiment

The Longitudinal relaxation constant,  $T_1$ , describes the rate by which an excited signal returns to thermal equilibrium. Upon application of a magnetic field,  $B_0$ , degenerate nuclear spin states are split in energy. In the case of fluorine, with a nuclear spin quantum number,  $I = 1/2$ , the spins are split into 2 energy levels, labelled  $\alpha$  and  $\beta$ .  $\alpha$  denotes the ground state energy level and  $\beta$  denotes the excited state. Upon a pulse excitation, the absorption of radio signals excites nuclear spins increasing the  $\beta$ -state population, the relaxation back to thermal equilibrium is then emission detected (Scheme 91).



*Scheme 91: An overview of the inversion recovery pulse sequence used to ascertain the  $T_1$  relaxation time*

The lifetime of excited nuclear spin states is long, on a scale of seconds to minutes, compared to the less than picosecond times for electrons. This property allows further manipulation of spin systems after their initial excitation.<sup>[186]</sup>

Inversion recovery is a multi-pulse technique that allows the determination of  $T_1$ . An initial pulse fully inverts the spin populations from  $\alpha$  to  $\beta$ , whilst a second pulse acts to detect the relaxation progress after a variable period,  $\tau$ .

If the number of  $\beta$  states exceeds the number of  $\alpha$  states then the signal is observed as a negative peak, this occurs after a short  $\tau$ , where little relaxation has occurred. Similarly, when  $\alpha > \beta$ , (>50 % relaxation) a positive peak is observed because of an almost fully relaxed system prior to the second pulse.

When  $\alpha = \beta$ , the absorbance is equal to the emission, resulting in a zero-intensity signal. The time taken for relaxation from the fully inverted system to reach this point is directly proportional to  $T_1$ .

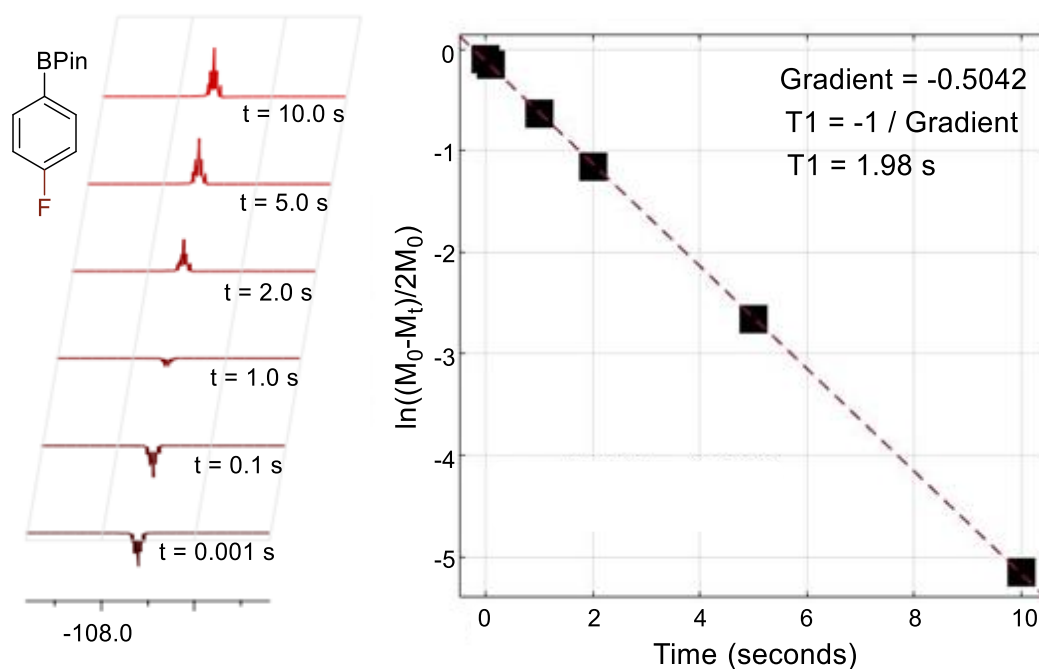
Spin Lattice relaxation is a first-order kinetic process that follows the regression:

$$M_{\tau} = M_0(1 - 2e^{-\frac{t}{T_1}})$$

Where  $M_0$  is the net magnetisation at thermal equilibrium for the fully relaxed system, and  $M_{\tau}$  is the net magnetisation after a delay of  $\tau$ . Practically, these parameters can be measured by comparing peak intensity in the acquired data. When  $\alpha = \beta$ ,  $M_{\tau} = 0$ . This equation can be rearranged such that:

$$\ln\left(\frac{M_0 - M_{\tau}}{2M_0}\right) = -\frac{\tau}{T_1}$$

Assigning the left-hand side of this equation to a logarithmic y-axis, and the right-hand side to the x-axis. The integration values can be plotted to give a linear regression wherein the gradient is the negative inverse of  $T_1$  (Scheme 92).



*Scheme 92: By plotting the integration values on a logarithmic scale vs. Time, the  $T_1$  relaxation time can be obtained*

This method is termed a “quick and dirty” way of deriving  $T_1$ . However, for the purpose of this study, only a rough estimate is required to give confidence in the sufficient relaxation (>99 %) of signals between scans.

We carried out an inversion recovery experiment for 4-fluorophenyl pinacol boronic acid ester. An initial guess of 15 seconds for full relaxation to thermal equilibrium was made, thus  $M_0$  was defined as the integration after this pulse delay,  $\tau$ .

It should be noted, however, that after calculating  $T_1$  the initial guess must be checked. If  $5T_{1calc.} > \tau(M_0)$  then the initial guess must be increased, and the experiment repeated until the condition is met.

Taking the integration values for each peak as a function of pulse delay,  $\tau$ , and plotting this as described above, a  $T_1$  value of 1.98 seconds was acquired.

As in this case  $5T_1 < 15$  seconds, we can confirm that the initial guess was valid giving confidence in this  $T_1$  value. Therefore, to gain quantitative information for this species a relaxation delay of 10 seconds ( $\sim 5T_1$ ) would be used.

### 2.3.3. Validation of the $^{19}\text{F}\{^1\text{H}\}$ qNMR Spectroscopic Protocol

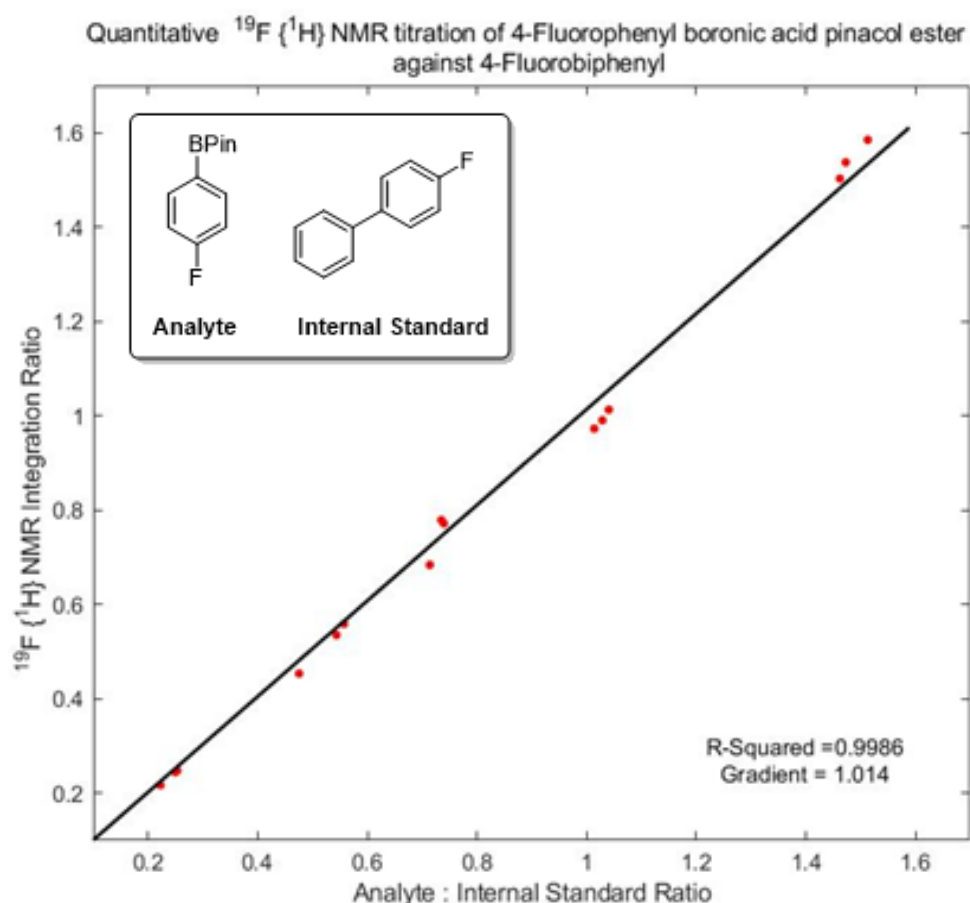
To next verify the validity of the  $^{19}\text{F}\{^1\text{H}\}$  qNMR protocol using the  $T_1$  relaxation time calculated, *supra vide*, an NMR titration using a solution of known concentration was performed. To achieve this, a 0.5 M solution for 4-fluorobiphenyl was produced, this internal standard was chosen as it has little functionality, minimising interference with the titre, it is a room-temperature solid, reducing any volatility problems, and as an aryl fluoride, the  $^{19}\text{F}$  NMR resonance occurs at a chemical shift of *ca.* -117 ppm which is suitably close to the materials of interest, meaning a uniform excitation of resonances can be assumed.

To 3 repetitions of this solution, 4-fluorophenyl pinacol boronic acid ester was added with the exact quantity measured by mass. 5 data points per

sample of 0.25, 0.5, 0.75, 1 and 1.5 equivalents, yielded a total of 15 data points.

The integration values were obtained from the resulting  $^{19}\text{F}\{^1\text{H}\}$ -NMR spectra obtained using a 10 second relaxation delay. Integration data was obtained at  $\pm 0.1$  ppm of the peak of interest; this was consistent across all the NMR spectra. The ratio of the boronic acid ester to the internal standard was then calculated.

These data were plotted against the equivalents of boronic acid added, to produce the resulting plot (Scheme 93), the linearity of the regression implies there is no interaction between the two compounds, and this is further evidenced by the consistency the chemical shifts of the peaks in the NMR independent of the ratio of analytes.

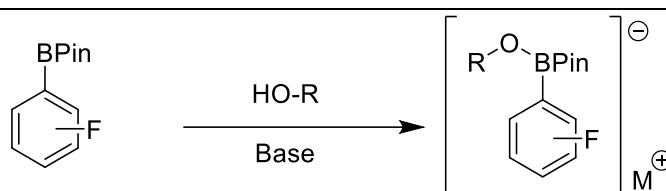


Scheme 93: High correlation of measure integration ratio vs. the experimental ratio indicates that  $^{19}\text{F}\{^1\text{H}\}$  NMR spectroscopy can be utilised as a quantitative technique.



The gradient of the regression for this plot is 1.0411, ideally, this value would be 1.0000, this would confirm that  $^{19}\text{F}\{^1\text{H}\}$  NMR spectroscopy is a valid method for quantitative analysis and that the relaxation delay ( $5T_1$ ) is of a suitable length for sufficient relaxation of the system.

## 2.4. NMR Characterisation



*Scheme 94: General structure of Alkoxy-Pinacol Boronates formed by in situ deprotonation of an alcohol in the presence of a fluoroaromatic boronic acid pinacol ester*

---

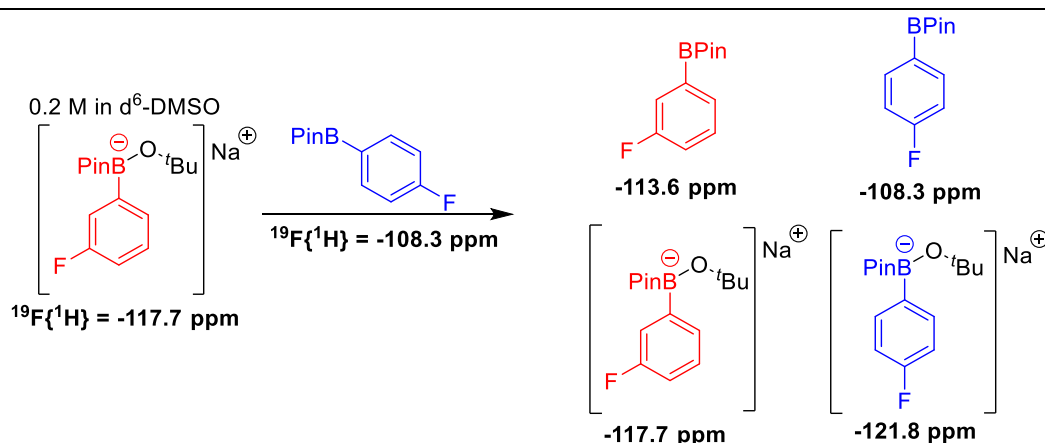
As discussed in Chapter 2.2, addition of methanol in the presence of sodium *tert*-butoxide and 4-fluorophenyl boronic acid pinacol ester affords the corresponding Lewis acid – Lewis base pairing (Scheme 94). Having developed a  $^{19}\text{F}\{^1\text{H}\}$  qNMR spectroscopic protocol, it would now be possible to quantify the formation of these adducts.

Use of sodium bicarbonate as a weaker base in the presence of methanol and phenyl boronic acid pinacol ester was attempted. Weak co-ordination of an alcohol to a Lewis acid such as boron would be expected to decrease the  $pK_a$  of an alcoholic proton allowing deprotonation by a weaker base. However, no phenyl methoxy pinacol boronate was observed. As such, we continued to use sodium *tert*-butoxide as this would produce an easily recognisable 9H-singlet peak corresponding to *tert*-butyl alcohol in the corresponding  $^1\text{H}$  NMR spectra.

The alkoxide binding to 4-fluorophenylboronic acid pinacol ester was possible with a single equivalent of sodium *tert*-butoxide when employing

accurate amounts from stock solutions, in the cases where less than one equivalent was added, conversion to the boronate was difficult to accurately characterise due to a broadening of the relevant peaks, this was hypothesised to be a result of a rapidly reversible interaction between the boron and alkoxide; broadening dependent on the degree of B-O co-ordination. When using sodium *tert*-butoxide in combination with water, ethanol, *iso*-propanol and *tert*-butanol, coordination to the boron centre of 4-fluorophenylboronic acid pinacol ester was observed.

To utilise alkoxides catalytically in a transient directing group role, some degree of fluxionality in the binding to boron reagents is necessary. Therefore, a simple qualitative experiment was devised to enable us to probe for reversible bind of alkoxides to organoboron compounds. We studied the reversibility of formation, by first producing a solution of the *tert*-butoxy bound boronate (addition of a single equivalent of sodium *tert*-butoxide to 3-fluorophenyl pinacol boronic acid ester in  $d^6$ -DMSO) to this 4-fluorophenyl pinacol boronic acid ester was added. By monitoring the  $^1\text{H}$  and  $^{19}\text{F}\{^1\text{H}\}$  NMR spectra, prior to and post competitor boronic acid ester addition, the interchange of the alkoxide between the 2 competing boronic acid esters was observed. Four discrete  $^{19}\text{F}\{^1\text{H}\}$  NMR peaks corresponding to the two boronic acid ester species and the two boronate species. Thus, the transient exchange of alkoxides between boron species was observed (Scheme 95).



Scheme 95: 4 discrete compounds were observed in the  $^{19}\text{F}\{^1\text{H}\}$  NMR corresponding to two boronate species and two boronic acid pinacol esters, indicating competition of two fluorine-labelled pinacol boronic acid esters.

## 2.5. Calculation of Dissociation Energies

Density Functional Theory (DFT) has found a range of applications for the understanding of intermolecular interactions, including Lewis acid – Lewis base pairings. Due to the advantage of low experimental cost and ease of calculations of *in silico*. experiments over laboratory methods, we opted to perform a short-study on the bond dissociation energies of a range of alkoxide-bound pinacol boronates. The thermodynamic favourability of the Lewis-acid Lewis-base adducts will be determined by the basicity of the alkoxide, a metric described by  $pK_a$ , and counterposing steric factors, which can be quantified with steric A-values, this study set out to ascertain which of these factors would be dominant.

### 2.5.1. DFT Overview

DFT is a theoretical model for the prediction of ground state electronic energies suitable for application in computational chemistry. DFT is based on a proof by Hohenberg and Kohn, wherein the energy of a system is a function of the ground-state electron density. This allows the energy of a system to be calculated from the overall electron density across a system.

In mathematics, a functional is a function which takes another function as its argument; mathematical notation dictates that a functional takes its argument in square brackets, whilst a function takes its argument in curved brackets. In DFT, the energy functional,  $E[\rho]$ , takes the electron density function,  $\rho(\vec{r})$ , as its argument, which is a function of the location of each electron,  $\vec{r}$ .<sup>[187]</sup>

Hohenberg and Kohn showed that the energy functional is minimal when the electron density is the actual ground-state density, as such, the energetic ground state can be found by calculating the energy of different “guesses” of electron density to approximate the ground state energy.

Kohn and Sham later set the foundation for DFT methods being implemented in computational chemistry; by introduction of orbitals to

approximate the electron density. The approximate density can be determined by summing the square moduli of a series of one-electron orbitals,  $\psi_i(\vec{r})$ :

$$\rho(\vec{r}) = \sum_i^N |\psi_i(\vec{r})|^2$$

Electrons are then filled into these orbital approximations and from this the electron density can be deduced. As the model is the summation of a series of single-electron orbitals, an orbital occupation can be either 0 or 1. Of course, electron spin allows two electrons to occupy a single orbital without breaking the Pauli exclusion principle; this will be accounted for by an exchange-correlation energy functional, *supra infra*.

Slater-type orbitals (STOs) are the general solution to the Schrödinger equation for one-electron systems, however, computationally these orbital functions are expensive to integrate, thus approximations of STOs are achieved by combining Gaussian-type orbitals (GTOs) to mimic an STO decay, these GTOs are, computationally, easier to integrate. A rule of thumb dictates that three times as many GTOs to STOs are required to achieve a given level of accuracy, this excess of GTOs is compensated by their relative ease of integration.

As electron density is a function of a series of approximate single-electron orbitals, the energy functional calculates energy under the assumption of non-interacting electrons. Naturally, electron interactions do occur, and so the true energy must be greater than the sum of the energies for non-interacting electrons. This discrepancy is accounted for within the energy functional as an exchange-correlation term,  $E_{xc}[\rho]$ .

The energy functional is thus divided into four functionals; the kinetic energy functional,  $T_s[\rho]$ , the nuclear-electron attraction,  $E_{ne}[\rho]$ , columbic interactions of electrons,  $J[\rho]$ , and the exchange-correlation energy,  $E_{xc}[\rho]$ . The sum of these four functionals forms the DFT energy functional:

$$E_{DFT}[\rho] = T_s[\rho] + E_{ne}[\rho] + J[\rho] + E_{xc}[\rho]$$

The exchange-correlation functional,  $E_{xc}[\rho]$ , accounts for the quantum effects arising in multi-electron systems. Exchange effects are the Pauli repulsions between electrons with the same quantum spin values, and correlation effects are the propensity for electrons of opposite spins to choose different orbitals. Furthermore, the coulombic electron interaction functional,  $J[\rho]$ , introduces an electron self-interaction term, which is compensated by the exchange-correlation functional.

If the exact exchange-correlation energy was known, DFT would provide the exact total energy, thus functional protocols which can more accurately calculate the exchange correlation of a system, can more accurately calculate the entire system energy. The difference between DFT methods is the form of the exchange correlation energy functional,  $E_{xc}[\rho]$ .

The Local Density Approximation (LDA) and Local Spin Density Approximation (LSDA) are two similar approaches to calculate the exchange-correlation energy. They assume that electron density locally can be treated as a uniform electron gas, this leads to significant errors with the exchange energy often underestimated by  $\sim 10\%$  and the electron correlation often overestimated by a factor of  $\sim 2$ ; bond energies are consequently overestimated.

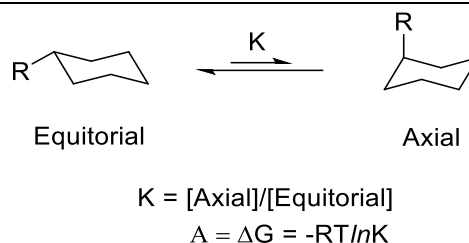
Any real electron system is non-homogenous, and variations in electron density would exist across a system. Generalised Gradient Approximation (GGA) methods improve the LSDA approach by considering a non-uniform electron gas. Although GGA does struggle to describe long-range effects, such as Van der Waals forces, however stronger electrostatic interactions such as hydrogen bonds are usually well described.

To combine the low computation cost of LSDA functionals with the greater accuracy of GGA functionals, hybrid functionals take different exchange and correlation functionals and uses weighting coefficients to closely fit experimentally known energies. Hybrid methods are therefore semi-empirical, relying on experimental data to improve accuracy.

B3LYP is an example of a hybrid functional; which, from 1990-2006, accounted for 80% of the total occurrences of density functionals in the literature.<sup>[188]</sup> The B3LYP exchange-correlation functional takes the form:

$$E_{xc}^{B3LYP} = E_x^{LSDA} + c_1 E_x^{B88} + c_2 E_c^{LYP} + (1 - c_2) E_c^{VWN} + c_3 [E_{ex.ex} - E_x^{LSDA}]$$

Where  $E_x^{LSDA}$  is the exchange functional (denoted by a sub-script  $x$ ) of local spin density approximation functional,  $E_x^{B88}$  is another exchange functional which acts as a correction to the LSDA exchange energy, this is followed by two correlation functionals,  $E_c^{LYP}$  and  $E_c^{VWN}$  and finally the difference between the exact exchange energy  $E_{ex.ex}$  and the LSDA exchange functional is added.<sup>[189]</sup> The weighting parameters in common use are  $c_1 = 0.72$ ,  $c_2 = 0.81$  and  $c_3 = 0.20$  based on fitting to heats of formation of small molecules.<sup>[190]</sup>



*Scheme 96: A-Value is determined by the equilibrium constant, K, for the equilibria between the equatorial and axial chair conformers*

---

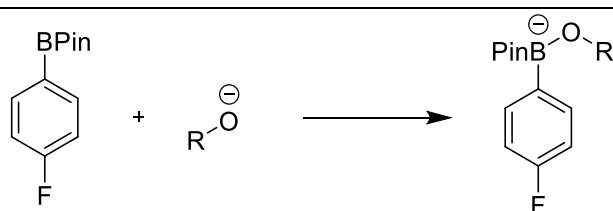
### 2.5.2. DFT Dissociation Energies

It was hypothesised that as a function of Lewis basicity the calculated bond energy of the boron-oxygen bond would increase; the magnitude of Lewis basicity can be described by the  $pK_a$  of the conjugate acid of each anion ( $pK_a-H$ ). It was also expected that steric interactions in the Lewis acid – Lewis base pair would decrease the bond energy; these values can be described using the steric A-values of each R-group. Comparison of the calculated bond energy against these two antagonistic factors, it is possible to ascertain whether steric or electronic factors are dominant in determining the strength of the B-O bond.

Steric A-values, or Winstein-Holness values, measure the free energy difference between the equatorial and axial conformation of a cyclohexyl ring based on ring substituents.<sup>[191]</sup> Bulkier groups will prefer an equatorial conformation, minimising steric 1,3-diaxial interaction. This steric bias towards an equatorial arrangement is less pronounced for smaller substituents.

By employing a low-cost method of B3LYP/6-31G\* a general trend of binding energies could be determined, although not necessarily accurate values. A total of three energy calculations were required for each binding energy: the Lewis basic anion, the 4-fluorophenyl boronic acid pinacol ester and the corresponding Lewis base – Lewis acid pairing. Then, the energy of heterolytic cleavage can be calculated from the difference between the sum of the energies of the unbound species and the energy of the bound species (Scheme 97 and Table 2).

Importantly, without accounting for solvent effects and counterion interactions, the calculated energies are likely to be vastly different from the true experimental value. However, the trends arising from these results are likely to be good qualitative indicators of the factors which control the strength of the investigated Lewis-acid Lewis Base adducts.



$$\text{Bond Energy (au)} = (E_A + E_B) - E_{AB}$$

*Scheme 97: Calculation of bond dissociation energies with DFT by calculating the difference in ground state energies between bound and unbound compounds*

---

Table 2: Calculated Bond dissociation energies by DFT compared against  $pK_a$ -H and Steric A-values

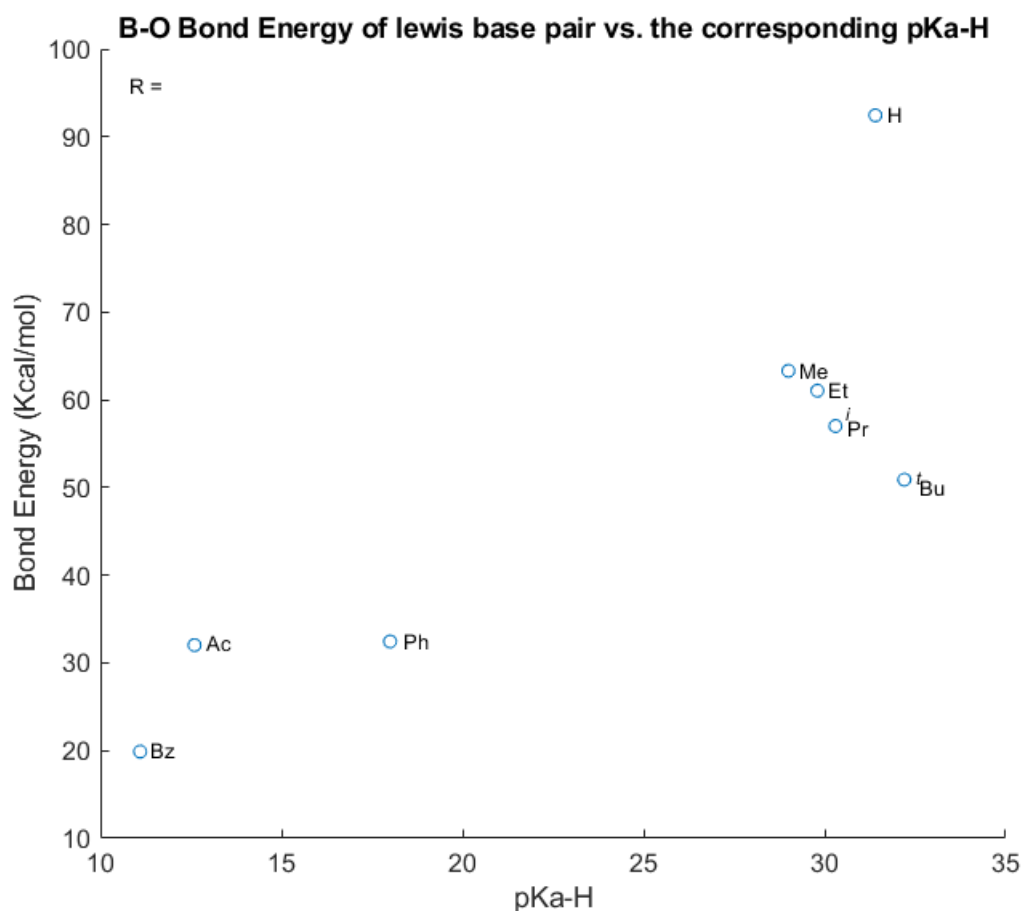
#	R	$pK_a$ -H in DMSO <sup>[192]</sup>	A-value	B3LYP/6-31G* (kcal/mol)	MP2/cc-pVDZ (kcal/mol)
1	H	31.4	0	92.45	89.32
2	Me	29.0	1.70	63.31	62.54
3	Et	29.9	1.75	61.04	61.01
4	<sup>i</sup> Pr	30.3	2.15	57.01	54.97
5	<sup>t</sup> Bu	32.2	>4	50.69	46.89
6	Ph	18.0	3.0	32.44	-
7	Ac	12.6	1.17	32.03	-
8	Bz	11.1		19.89	-

Hydroxide, entry 1, was found to bind strongest with a bond energy of 92.45 kcal/mol, indicating that there is a high energy pay-off from the formation of the B-O bond despite the formation of a charged boronate species, this is in line with earlier NMR observations, which showed that any residual water in the  $d^6$ -DMSO would produce hydroxide *in situ* and outcompete the alkoxide bases for co-ordination to the pinacol boronic esters, resulting in a hydroxy pinacol boronate ester, and a mixture of bound and unbound alkoxide. Entries 2-5 indicate an inverse relationship between  $pK_a$ -H and binding energy for alkoxides, this implies that for these alkoxides the steric factors outweigh base strength when determining the bond energy.

Calculations were also performed on a small set of Lewis bases that were not observed by NMR to co-ordinate to boron (entries 6-8). Acetate, benzoate and phenolate anions were each co-ordinated to boron *in silico*. and were found to have low calculated BDE's, indicating that low Lewis basicity (as indicated by the corresponding  $pK_a$ -H values) is a key factor in determining bond energies. The observation of low bond energies for carboxylate and phenoxide anions, suggests that the inability to observe these species by NMR techniques may be a result of a rapid transient interaction unobserved on the NMR timescale, or solvent effects which are not accounted for in this DFT study.

Representing this graphically it becomes easier to observe the expected general upward trend as a function of  $pK_a$ -H, with steric destabilising effects acting antagonistically to decrease the bond energies (Scheme 98).





*Scheme 98: Plot of Bond energies calculated using B3LYP/6-31G\* against the experimental pK<sub>a</sub>-H values for the alkoxides tested*

Using a MP2/cc-pVDZ *ab initio* method (entries 1-5) resulted in a general decrease in calculated bond energies, however the general trends of decreased steric size resulting in an increase BDE for the alkoxides was consistent in both computation methods. As such, further computational investigations would be required to test the accuracy of the quantitative data, however, the consistency of the trend across the computational methods employed provides evidence that qualitative trend observations can be drawn from the computationally cheaper B3LYP/6-31G\* method.

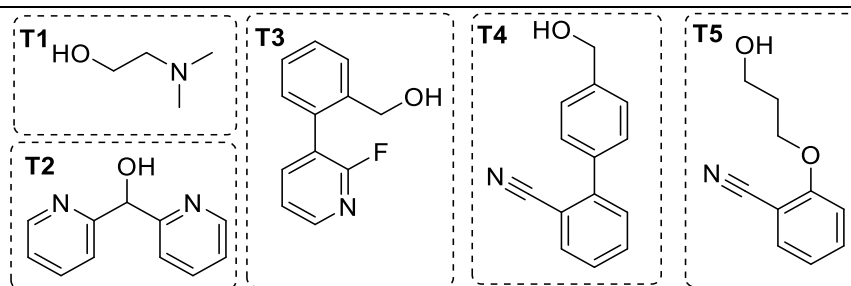
This trend can be useful in modulating ligands to control the lifetime of boronates to improve catalytic turnover. It also reaffirms that the reactions should be performed under anhydrous conditions, because under the basic

conditions of the reaction, hydroxide will be generated in the presence of water, allowing the reaction to potentially undergo transmetallation, or at least strongly bind to the boron, outcompeting co-ordination of a bifunctional alkoxide template.

## 2.6. Bifunctional Templates

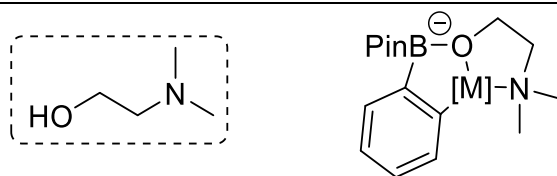
### 2.6.1. Proposed Bifunctional Templates

The novelty of the proposed transient directing group approach, a fluxional binding of an alkoxide to a boronic acid reagent, meant a broad range of screening templates could be tested. Even though this binding mode had not previously been reported in the literature, the choice of ligands was dictated by literature precedent. With no preference over *ortho*-, *meta*- or *para*- functionalisation, a set of 5 structurally different bifunctional templates were proposed (Scheme 99).



Scheme 99: Proposed Bifunctional templates

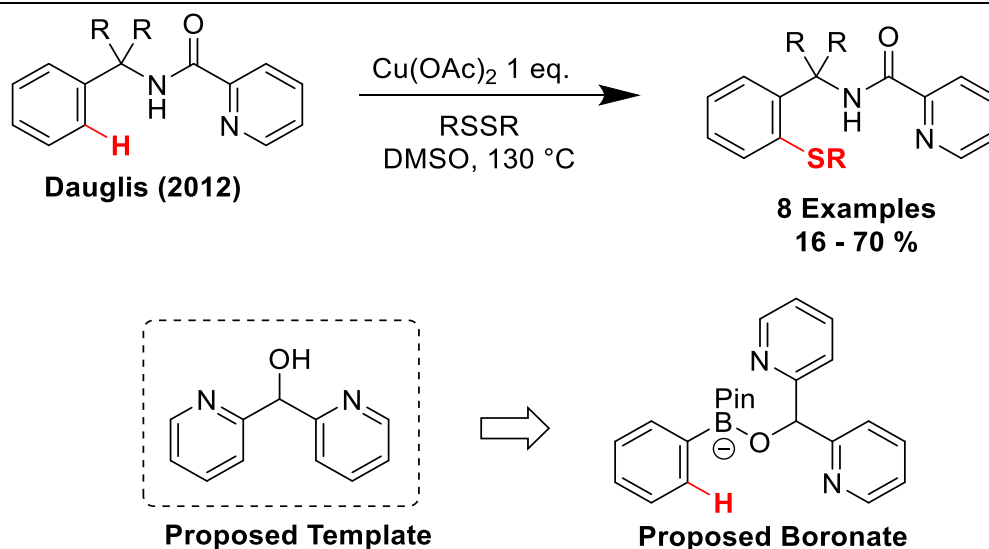
*N,N*-Dimethylethanolamine, was chosen due to its simplicity (Scheme 100). This design aims to perform directed C-H functionalisation at the *ortho*-position *via* a monodentate co-ordination to a metal at the amine, whilst the alcohol co-ordinates at boron, this oxygen may also act to stabilise an organometallic intermediate by a weak co-ordination to the metal centre, forming a 5,5-bicyclic intermediate. A potential pitfall is the propensity for a bidentate co-ordination to a metal, which would reduce the concentration of non-coordinated alkoxide *in situ*. There are no direct literature comparisons to indicate the feasibility of this ligand, however the low cost and simplicity renders this template an attractive candidate for this study. Whilst the other four templates require synthesis, their literature precedent for directed C-H functionalisation's at distal sites justify their use in this study.



**Proposed Intermediate**

*Scheme 100: Structure and proposed intermediate for N,N-dimethylethanolamine*

Dipyridyl methanol is based off the design of an *ortho*-selective template disclosed by Dauglis *et al.* to achieve copper(II) mediated sulfenylations.<sup>[193]</sup> The proposed ligand modified the literature to change an amide-linkage to a boronate species. To increase the chance of forming a desirable metallacycle two pyridyl moieties were incorporated (Scheme 101).

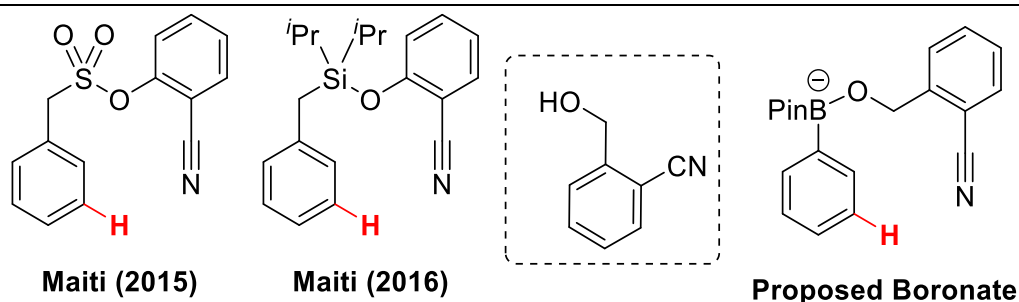


*Scheme 101: Structure, literature precedent and proposed intermediate for dipyridyl methanol,*

2-Cyanobenzyl alcohol is based off the design of two *meta*-selective templates disclosed by the Maiti group, they disclosed a sulfonate bound nitrile-based directing auxiliary to achieve *meta*-selective C-H alkenylations,<sup>[194]</sup> hydroxylations and acetoxylation,<sup>[195]</sup> later the sulfonate-linkage was exchanged for a silyl linkage and the new auxiliary was optimised

for alkenylations, the two *iso*-propyl groups on silicon act to induce Thorpe-Ingold effects which compress the C-Si-O bond angle, and reduce the degrees of rotational freedom by disfavouring the undesired rotational conformation which would direct the nitrile away from the substrate.<sup>[196]</sup>

2-Cyanobenzyl alcohol was proposed as an analogue for these systems, with the hypothesis that the pinacol auxiliary would replicate the Thorpe-Ingold effects for the silyl-liked literature precedent, assisting in creating a

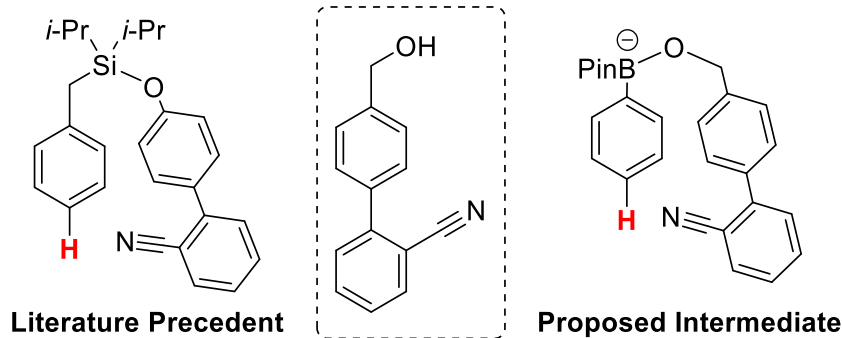


*Scheme 102: Structure, literature precedent and proposed intermediate for 2-cyanobenzyl alcohol*

---

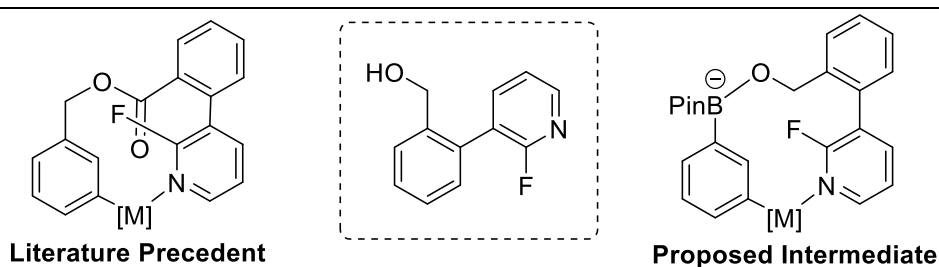
conformation bias towards the nitrile pointing at the substrate (Scheme 102).

4-(2-Cyanophenyl)benzyl alcohol was inspired by the work of the Maiti group who published multiple studies using this template design to achieve *para*-selective C-H functionalisation (Scheme 103). This auxiliary was previously discussed in Chapter 1.7.2. The silyl linkage is modified, similar to 2-cyanobenzylalcohol.



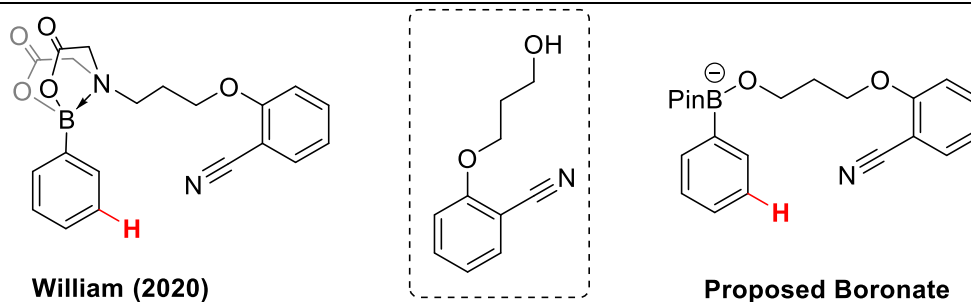
Scheme 103: Structure, literature precedent and proposed intermediate for 4-(2-cyanophenyl)benzyl alcohol

2-(2-Fluoro-3-pyridyl)benzyl alcohol inspired by work by Chu *et al.* utilises a strong  $\sigma$ -coordinating pyridine (relative to nitrile coordination) to help position a metal catalyst in an ideal position for *meta*-selective C-H functionalisation (Scheme 104). The fluorine performs two roles; firstly, it works to modulate the co-ordination of the pyridyl to a metal, enhancing turnover of the catalyst. Secondly, whilst the ground state of biphenyl is twisted about the central aryl-aryl bond by around  $44^\circ$  to minimise interaction between two *ortho*-hydrogens, the inclusion of a single fluorine atom increases this angle to  $50^\circ$ , this small change in ground state angle may be significant enough to stabilise a desired metallacycle.<sup>[197]</sup> Screening of a non-fluorinated template by Chu *et al.* resulted in no desired product, indicating that the effects of fluorine on the template are essential for the reaction.<sup>[198]</sup>



Scheme 104: Structure, literature precedent and proposed intermediate for 2-(2-fluoro-3-pyridyl)benzyl alcohol

Finally, *O*-(2-cyanophenyl)propandiol was inspired by the work of Williams *et al.* which utilised a MIDA-type linkage of an aryl boron substrate to the ligand,<sup>[175]</sup> wherein the MIDA-type linkage has been modified to an alcohol, without any change to the size of the desired metalacyclic intermediate (Scheme 105). Due to the increased flexibility of the template due to the high number  $sp^3$  carbons compared to the other target templates, the literature discusses poor selectivity over *meta*- and *para*- functionality. This issue however is a double-edged sword, poor selectivity is undesirable, however in the more rigid  $sp^2$  rich systems there is a potential for strain in the proposed metalacyclic intermediate, thus disfavouring a desired reaction pathway. By addition of flexibility afforded by the  $sp^3$  carbons, the template would be better able to adopt a metalacyclic intermediate with a



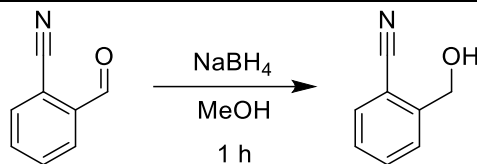
Scheme 105: Structure, literature precedent and proposed intermediate for *O*-(2-cyanophenyl)propandiol

---

conformation that minimises strain.

### 2.6.2. Synthesis of Bifunctional Templates

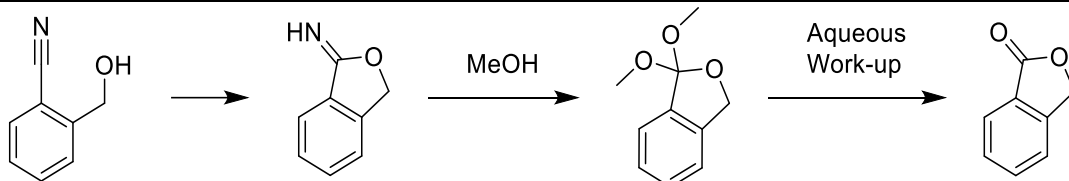
Synthesis of these templates was then performed, with the intent of producing each alcohol on large scale, in order to have a suitable amount for testing and eventually screening studies. *N,N*-dimethylethanolamine was purchased and used without further processing.



*Scheme 106: Synthesis of 2-cyanobenzyl alcohol by hydride reduction of 2-cyanobenzaldehyde*

---

The 2-cyanobenzyl alcohol template was synthesised simply by the reduction of 2-cyanobenzaldehyde with sodium borohydride in methanol (Scheme 106). This reaction produced the desired product in good yield (58 %), however we observed that the compound was not bench stable. Literature precedent indicates that decomposition occurs first cyclising to form a hydrolytically unstable iminoester which in methanol would produce an *ortho*-ester, this is hydrolysed to phthalide in an aqueous work-up,<sup>[199]</sup> and can be base-catalysed;<sup>[200]</sup> this degradation pathway accounts for the depleted yield of the aldehyde reduction (Scheme 107).

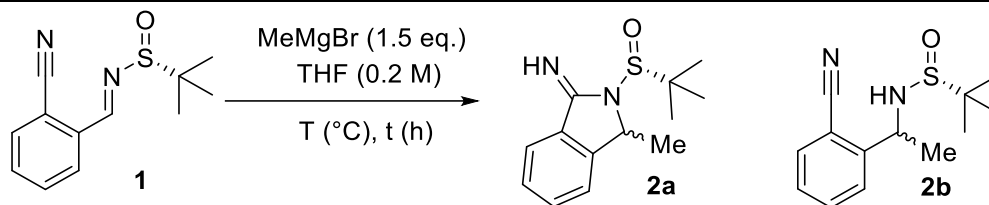


*Scheme 107: Cyclisation of 2-cyanobenzyl alcohol to phthalide*

---

This observation was in line with some early studies performed by the author, which are not covered in the scope of the thesis. A series of benzyl substituted 2-cyanobenzylamine derivatives were produced *via* addition of Grignard reagents to the corresponding Ellman sulfinimine resulting in high yields of an undesired cyclised amidine product (Scheme 108). It was found that by lowering the temperature and reaction time the selectivity for the desired sulfinamine product was improved (Table 3), and the product was found to be stable upon isolation.



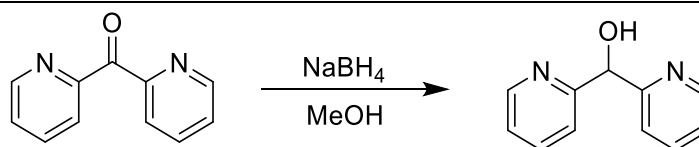


*Scheme 108: Grignard addition to a Ellman sulfinimine yielded a sulfinamine and an undesired cyclised amidine product*

Entry	t (min)	T (°C)	Scale (mmol)	2a (%)	2b (%)
1	120	0	0.21	84 (dr 1:1)	0
2	60	0	0.21	44	32
3	1	0	0.21	16	76
4	1	0	4.2	48	13
5	1	-20	0.21	7	64
6	2	-20	0.21	4	69 (dr 7:3)
7	5	-20	0.21	15	44
8	10	-20	0.21	10	52

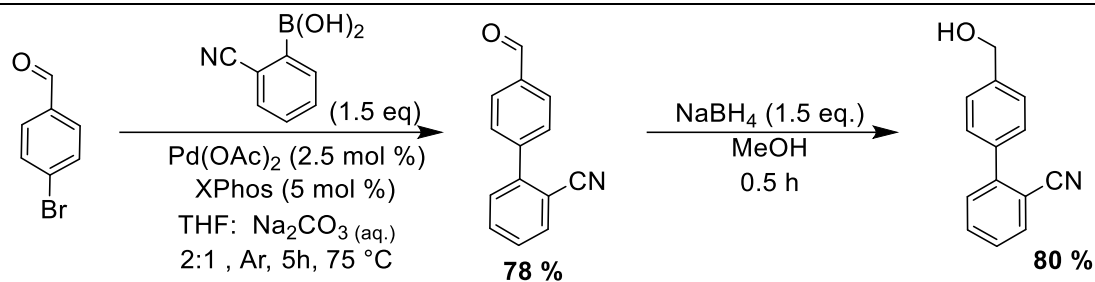
*Table 3: Optimisation of Grignard addition to Ellman Sulfinimine*

Benzylamines afforded, after removal of the Ellman auxiliary, were found not to be bench stable. As such it can be concluded that 2-cyanobenzyl alcohols and amines are not bench-stable due to the reactivity of O and N nucleophiles in proximity to an intramolecular nitrile electrophile. Due to this conclusion, 2-cyanobenzyl alcohol, was not used further in this study.



*Scheme 109: Reduction of dipyridyl methanol*

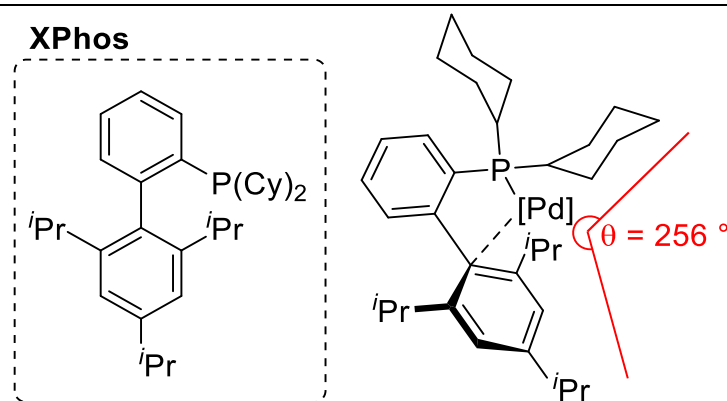
2,2'-Dipyridyl methanol – The desired alcohol was produced by reduction of 2,2'-dipyridylketone in the presence of sodium borohydride and a methanol solvent, the desired product was afforded in an 86 % yield (Scheme 109).



Scheme 110: Two-step synthesis of 4-(2-cyanophenyl)benzyl alcohol

4-(2-Cyanophenyl)benzyl alcohol - A Suzuki-coupling was performed to produce the initial aldehyde from 4-bromobenzaldehyde and 2-bromobenzonitrile catalysed by palladium(II) acetate with XPhos dissolved in THF and H<sub>2</sub>O using Na<sub>2</sub>CO<sub>3</sub> as a base, yielding the desired product. Upon scale-up a yield of 85% was achieved, producing 1.92 g of desired product (Scheme 110). As well as column chromatography, this compound was found also to be purifiable by recrystallisation from hot ethyl acetate, which could be washed with distilled water producing the desired product in high purity by <sup>1</sup>H NMR.

The Suzuki conditions chosen here, have been shown to be robust across a range of different couplings on scale,<sup>[201]</sup> allowing a single set of conditions to be used across the various Suzuki-Miyaura cross-couplings performed in this project, without having to optimise for each different cross-coupling reaction. XPhos has excellent utility in Suzuki-Miyaura cross-coupling reactions, due to its ability to improve the efficacy and rate of coupling.



Scheme 111: Structure of XPhos, with a proposed general palladium.XPhos complex indicating the large cone angle

This Buchwald ligand, is a phosphine based ligand with 2 cyclohexyl groups and a 4-(2,4,6-triisopropoxyphenyl)phenyl group (Scheme 111) and promotes turn-over of the desired catalytic cycle in multiple ways:

*Rapid palladium(II) reduction* – Palladium(II) salts are more bench-stable than palladium(0) salts, as such palladium(II) acetate is often employed and reduced *in situ*. XPhos acts as a reducing agent and is oxidised to XPhos oxide generating palladium(0),<sup>[202]</sup> as this consumes the ligand, XPhos is employed in a 2:1 ratio with respect to palladium(II).

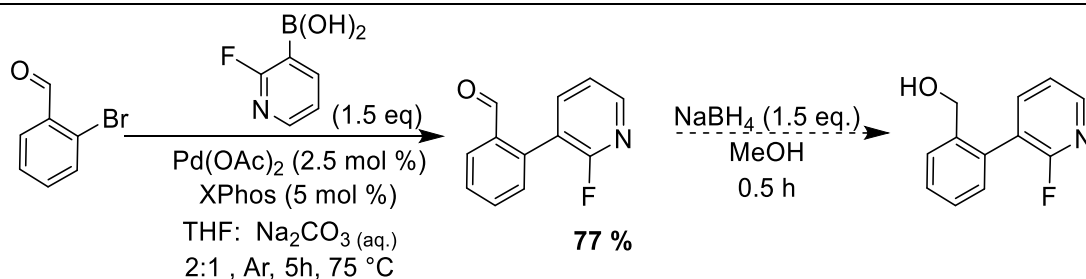
*Promoting Oxidative Addition* – XPhos has a high binding affinity to Pd(0), afforded by strong  $\pi$ -backbonding interactions enhanced by the two electron-rich cyclohexyl groups, and interactions between the metal centre and the biaryl  $\pi$ -system promoting a bidentate co-ordination.<sup>[203,204]</sup> The steric size of XPhos affords a cone angle of  $256^\circ$ ,<sup>[205]</sup> meaning the energy cost for further co-ordination around the tetrahedral centre is greatly increased. This renders the palladium(0) XPhos complex a high energy species, with a low formal d-electron count of 12, accelerating the rate of oxidative addition across a C-X bond; including C-Cl bonds which cannot be activated under classic conditions.<sup>[202,206,207]</sup>

*Promoting reductive elimination* - The large steric size of the XPhos ligand compresses the bond angle between the two organic substituents to be coupled, promoting reductive elimination, and regenerating the Pd(0).XPhos starting catalyst.<sup>[208]</sup>

*Destabilising off-cycle resting states* - Undesired off-cycle palladium species can be formed affecting turn-over number (TON) and turn-over frequency (TOF), this may be caused by metal co-ordination to starting materials, intermediates, additives or products. Due to the difficulty to displace XPhos, and it's large steric size, XPhos may destabilise these off-cycle palladium species helping to avoid catalyst deactivation, improving TON and TOF.<sup>[209]</sup>

The product was then reduced using sodium borohydride in methanol to yield 4-(2-cyanophenyl)-benzyl alcohol in a yield of 80 %. In the  $^1\text{H}$  NMR for

this product, coupling was observed between the benzylic hydrogens and the alcohol hydrogen, normally, alcohol peaks in  $^1\text{H}$  NMR tend to be very broad due to proton exchange with water, which is rapid on the NMR timescale. It is suspected that dimerisation of the product occurs by hydrogen-bonding interactions between the alcohol and nitrile of a second molecule.



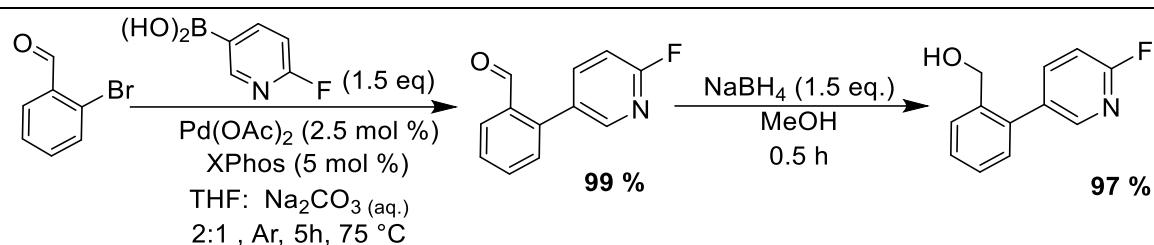
*Scheme 112: Two-step synthesis of 2-(2-fluoro-3-pyridyl)benzyl alcohol*

---

2-(2-Fluoro-3-pyridyl)benzyl alcohol - Synthesised using standard Suzuki-Miyuara conditions, *vide supra*. to cross-couple 2-fluoropyridine-3-boronic acid with 2-bromobenzaldehyde using literature conditions, producing the desired compound in a yield of 77% producing 0.84 g of desired product (Scheme 112).

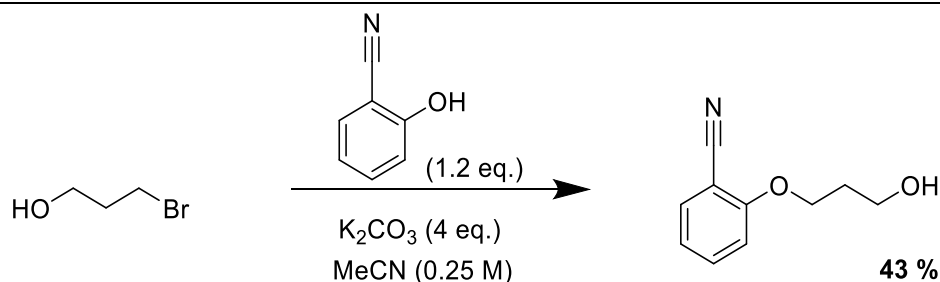
Upon reduction of the aldehyde however we did not observe the desired product, elucidation of the product of this reaction was difficult to confirm but a lack of  $^{19}\text{F}$  nuclear resonances in the  $^{19}\text{F}\{^1\text{H}\}$  NMR spectra indicated that an intramolecular  $\text{S}_{\text{N}}\text{Ar}$  had likely occurred, although further decomposition then produced a mixture of products.

One obvious modification is to use a non-fluorinated alternative, unfortunately however, the screening results disclosed by Chu *et al.* indicate that no desired C-H functionalisation was observed when employing a non-fluorinated template. However, the 4-fluoro isomer, was shown to promote C-H functionalisation albeit in a slightly lower yield. Hence, we modified our template accordingly.



Scheme 113: Two-step synthesis of 2-(4-fluoro-3-pyridyl)benzyl alcohol

The synthetic route used the same reaction conditions as used for the 2-fluoro isomer, with a Suzuki-Miyaura cross-coupling yielding the precursor aldehyde in a 99% yield and was scaled to 20 mmol. The reduction with sodium borohydride was successful this time, producing the desired alcohol in a 97% yield (Scheme 113).



Scheme 114: Williamson ether synthesis of O-(2-cyanophenyl)propandiol

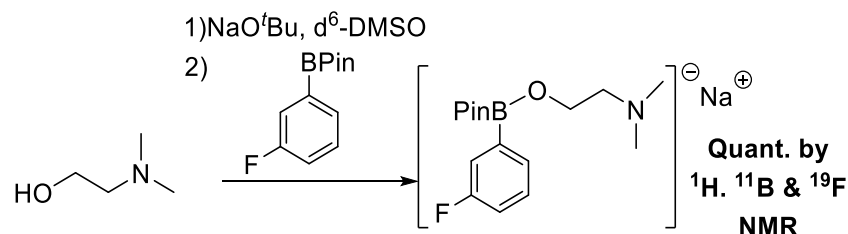
O-(2-Cyanophenyl)propandiol, – The final target ligand, based on the work by Spivey, Cordier *et al.* was synthesised by a Williamson ether synthesis using 3-bromopropanol and 2-hydroxybenzonitrile in the presence of  $K_2CO_3$  under reflux to produce the desired compound in a 43% yield on a 20 mmol scale (Scheme 114).

### 2.6.3. Substrate-Ligand Complexes

Having produced a set of bifunctional ligands which we expect will be able to facilitate C-H functionalisation, we moved forward to testing its

binding to 4-fluorophenyl boronic acid pinacol ester, this was performed under the same conditions detailed in section 2.1, wherein each alcohol was deprotonated *in situ* with sodium *tert*-butoxide in  $d^6$ -DMSO in the presence of 3-fluorophenyl boronic acid. We would then study the Lewis acid – Lewis base paired species using  $^1\text{H}$ ,  $^{11}\text{B}$  and  $^{19}\text{F}\{^1\text{H}\}$  NMR spectroscopy.  $^{11}\text{B}$  and  $^{19}\text{F}\{^1\text{H}\}$  NMR would indicate full complexation by the upfield shift observed between fluoroaromatic pinacol boronic acid esters ( $^{19}\text{F}\{^1\text{H}\}$   $\sim$ -110 ppm,  $^{11}\text{B}$   $\sim$ 25 ppm) and their corresponding alkoxide complexes ( $^{19}\text{F}\{^1\text{H}\}$   $\sim$ -120 ppm,  $^{11}\text{B}$   $\sim$ 10 ppm). An excess (3 equivalents) of each ligand with equal parts sodium *tert*-butoxide was added, this ensured co-ordination. This created some overlap in the  $^1\text{H}$  NMR which was difficult to deconvolute, however the upfield shift of the pinacol into two 6 hydrogen peaks was indicative of co-ordination and could be observed.

*N,N*-dimethyl ethanolamine – Quantitative conversion to the corresponding boronate was observed upon treatment of *N,N*-dimethyl ethanolamine with sodium *tert*-butoxide with an aryl pinacol boronic acid (Scheme 115).

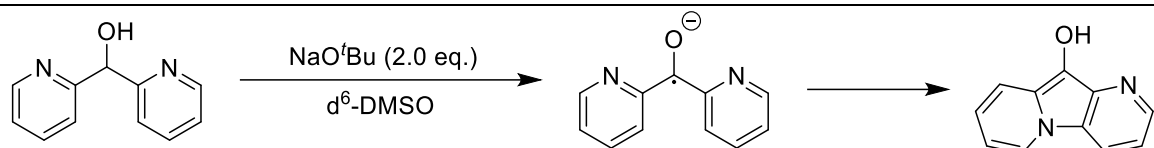


*Scheme 115: Substrate-ligand complex of dimethyl ethanolamine and an aryl pinacol boronic ester*

---

Dipyridyl methanol – When sodium *tert*-butoxide (3 equivalents) was added to a solution of 4-fluorophenyl boronic acid pinacol ester and dipyridyl methanol (3 equivalents) in  $d^6$ -DMSO, a deep blue precipitate was produced. It is possible to generate of ketyls in the presence of *tert*-butoxide in DMSO.<sup>[210,211]</sup> Ketyls are radical anions, which are often highly coloured. The colour eventually subsided after 24 hours, this may be the result of cyclisation as proposed by Elisie *et al.* during their laser flash photolysis studies of di-

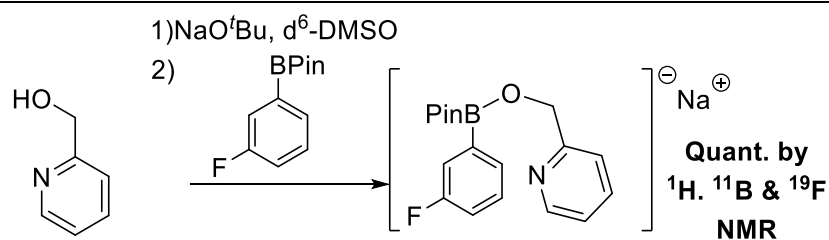
pyridyl ketones (Scheme 116).<sup>[212]</sup> No effort was made to study these species further, and dipyridyl methanol was not studied further in the body of this work.



*Scheme 116: Proposed ketyl anionic radical, generated in the presence of tert-butoxide*

---

Full coordination did proceed when using 2-pyridyl methanol, deprotonated *in situ* with sodium *tert*-butoxide (Scheme 117). Unfortunately, time constraints mean this simple molecule was not explored further, although future work may wish to study 2-pyridyl methanol as a potential template candidate.



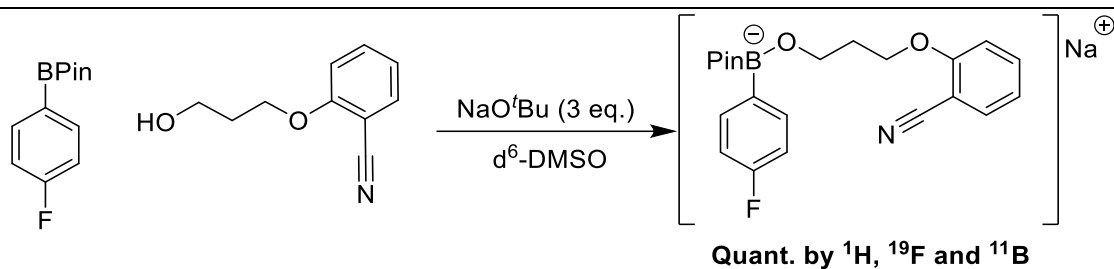
*Scheme 117: Substrate-ligand complex of 2-pyridyl methanol and an aryl pinacol boronic ester*

---

4-(2-cyanophenyl)benzyl alcohol - Quantitative coordination to the desired boronate, upon addition of 1 equivalent of the 4-(2-cyanophenyl)benzyl alcohol to an equivalent of both the boronic acid and sodium *tert*-butoxide (Scheme 118).







*Scheme 120: Substrate-ligand complex of O-(2-cyanophenyl)propanediol and an aryl pinacol boronic ester*

#### 2.6.4. Ligand-Substrate-Metal Ternary Complexation

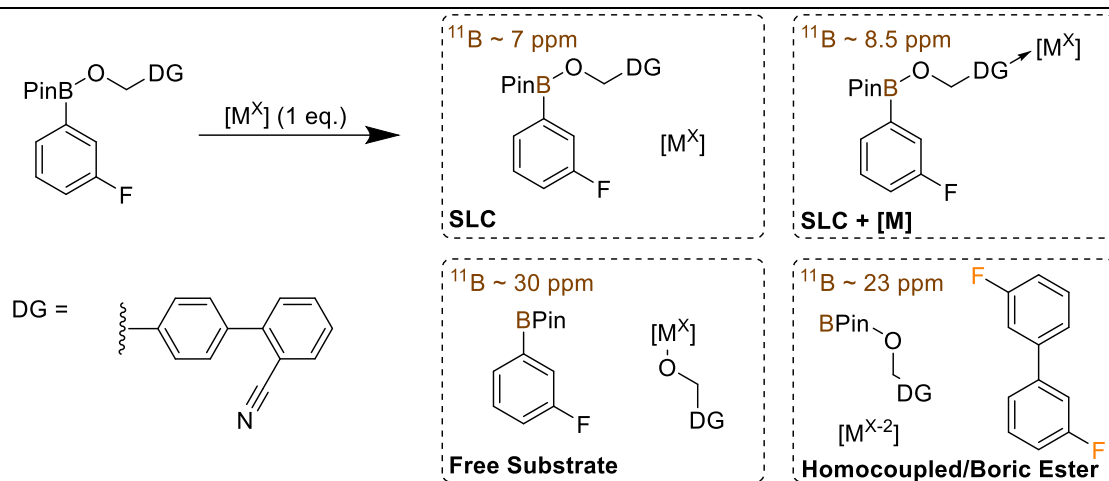
We next aimed to observe a ternary complex system, assessing the accessibility of a single metal-ligand-substrate bound species. Employing various metals in stoichiometric amounts, resulted in a mixture of intermediates.  $^{19}\text{F}\{^1\text{H}\}$  NMR spectra were found to contain numerous unique species that were difficult to identify, hypothesised to be due to the formation of organometallic complexes, arising from transmetallation. Further studies would need to be conducted to better observe these processes using  $^{19}\text{F}\{^1\text{H}\}$  NMR spectroscopy, which would be more desirable due to reasons detailed in chapter 2.3. It was found that these were best studied observing the  $^{11}\text{B}$  nuclei by NMR spectroscopy, for which four species were observed depending on the metal.

*Substrate Ligand Complex (SLC)* – The simplest possible case, in which the metal complex and directing group yield no interaction. In  $^{11}\text{B}$  NMR spectroscopy this would be observed as no change in chemical shift for the  $^{11}\text{B}$  nuclear resonance ( $^{11}\text{B}$  ~6.5 ppm) as previously characterised.

*Free Substrate* – Most likely arising from competition for ligation between the boron and metal centres, this competition may be in equilibrium. In  $^{11}\text{B}$  NMR spectroscopy this would be observed with a chemical shift for the  $^{11}\text{B}$  nuclear resonance ( $^{11}\text{B}$  ~30 ppm) as previously characterised.

*Homocoupled/Borate* – In Chapter 1.4, the mechanism of transmetallation of an organic fragment from boron to a metal was discussed. The "Free Substrate" system shown in Scheme 121 is primed for transmetallation, and thus transfer of the fluoro-aromatic onto the metal may occur, cleaving the carbon-boron bond producing a boric ester. Literature characterisation for boric esters tend to observe the boron nuclei of boric esters at around 20-25 ppm in  $^{11}\text{B}$  spectroscopy. A successive transmetallation would yield a metal-complex bearing two organic fragments, primed for a reductive elimination, yielding a homocoupled 3,3'-difluorobiphenyl, which could be observed by  $^{19}\text{F}\{^1\text{H}\}$  NMR spectroscopy.

*Ternary Complexation (SLC + [M])* - The desired intermediate, the boronate remains intact whilst the metal co-ordinates to the bifunctional template generating a complex of substrate linked to ligand linked to metal. Although these species have not been previously disclosed in the literature, it was hypothesised that these species would be observed in  $^{11}\text{B}$  NMR spectroscopy with a similar chemical shift to the substrate ligand complex. In these studies a second boronate species was observed upon addition of a some metal salts at  $\sim 8.5$  ppm in the  $^{11}\text{B}$  NMR spectra.



Scheme 121: Upon treatment of the substrate-ligand complex with metal salts, various species were observed

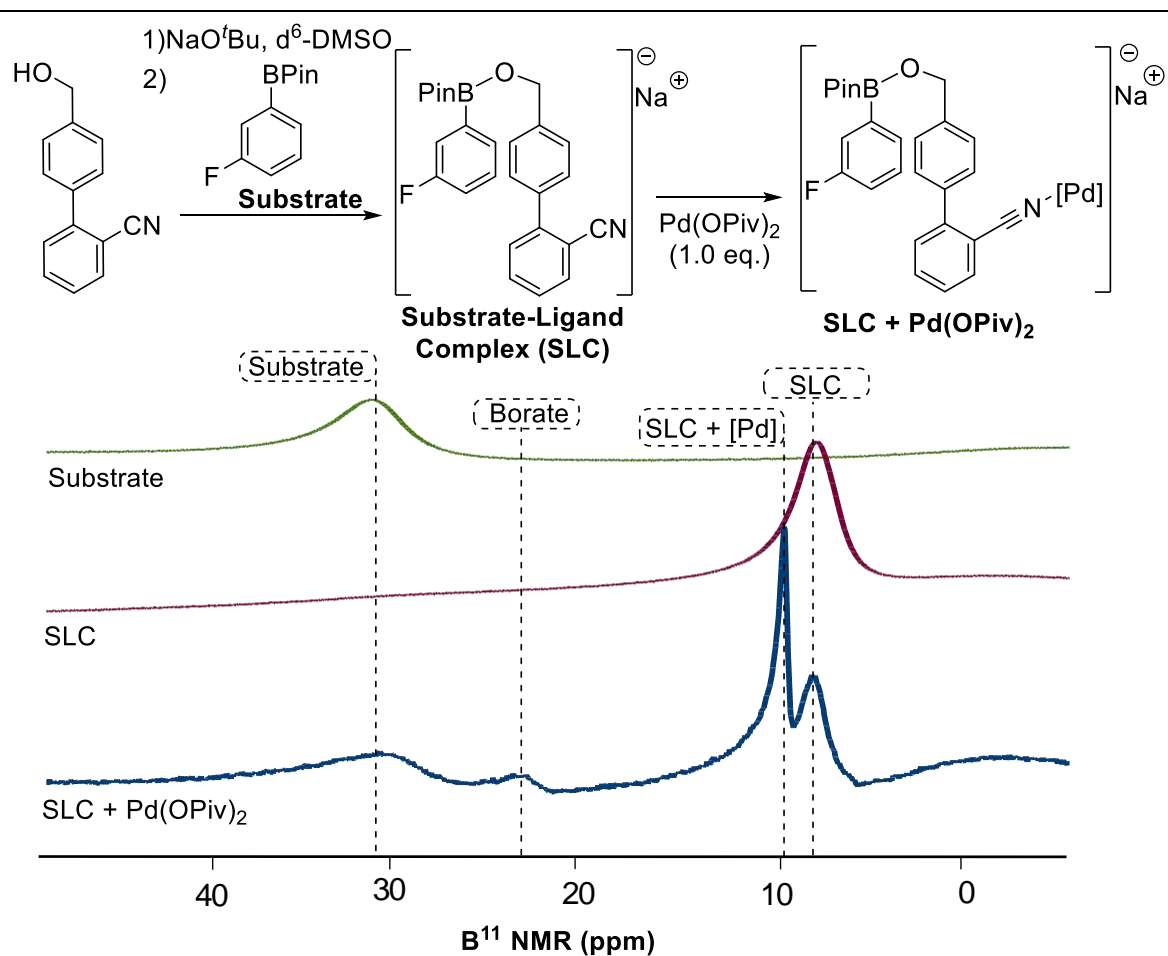
Table 4: A series of metal salts were added to a substrate-ligand complex, results are purely qualitative due to the unreliability of integrations in  $^{11}\text{B}$  NMR spectra

	[M]	SLC	Free Substrate	Boric Ester	SLC + [M]
1	$\text{Pd}(\text{OAc})_2$		trace		
2	$\text{Pd}(\text{OPiv})_2$			trace	
3	$[\text{Ir}(\text{OMe})(\text{Cod})]_2$			trace	
4	$[\text{Rh}(\text{C}_5\text{Me}_5)\text{Cl}_2]_2$			trace	
5	$[\text{Ru}(\text{p-cymene})\text{Cl}_2]_2$				
6	$\text{Cu}(\text{OAc})_2$	trace			
7	$\text{CuI}$			trace	

Most metal salts produced no observed ternary complex, with only copper(II) acetate and palladium(II) pivalate yielding a new boronate species (Table 4, Entries 2 and 6). We observed that upon treatment of the boronate with an equivalent of palladium(II) acetate (Table 4, Entry 1), a rapid colour change to black, indicative of a redox process precipitating a black reduced palladium species, and producing a biaryl *via* two subsequent transmetalations of the aryl group of boronic acid ester onto the metal followed by a reductive elimination. Indeed 3,3'-bifluorobiphenyl was confirmed by  $^{19}\text{F}$  NMR comparing against literature data ().

It was hypothesised that addition of palladium(II) pivalate as a more sterically hindered palladium complex may provide a window of opportunity to observe a ternary complex. In doing so a new species was observed.  $^{11}\text{B}$  NMR spectra gave an indication that a new boronate species was produced *in*

*situ* (Scheme 122); two peaks in the up-field region were detected, one corresponding to the substrate-ligand complex (6.8 ppm), and a second, which was found to be difficult to assign but was speculatively assigned as a ternary complex (8.6 ppm). The competition between the metal-centres and boron-centres for co-ordination with the alkoxide is indicated by the substrate resonance (28.9 ppm), and transmetallation is indicated by formation of pinacol alkoxy borate (22.3 ppm).



*Scheme 122: Potential formation of a ternary substrate-ligand-metal complex*

Unfortunately, despite the promise of this result, after half an hour, the boronate was no longer observed, as the pivalate salt proceeds down the same mechanistic pathway as the acetate. Further studies may have been carried out, to look at other metal complexes which may be less oxophilic and/or susceptible to transmetallation. Cleavage of the substrate-ligand complex was

observed with all metals, due to competition between boron and the metal centres for co-ordination with the alkoxides, therefore, to overcome this we proposed that adding an excess of alkoxide (3 equivalents) would allow a boronate to remain intact, therefore inhibiting transmetallation as indicated in studies by Amatore *et al.* Using an alkoxide may not be detrimental to the efficacy of the metal to perform C-H functionalisation as monodentate bases such as alkoxides or hydroxides could facilitate C-H functionalisation *via* a four-membered AMLA transition state.<sup>[213-215]</sup> Not all metals proceed *via* an AMLA mechanism, with oxidative addition available for metals such as Ru, Rh, Ir, and Pt. Although it is difficult to predict the active metal complex, as metal-ligand and ligand-complex interactions are transient, an equilibria between different complexes should allow a desired route to be accessible.

On the other hand, an excess of alkoxide may inhibit catalytic turnover, but this would depend on a range of factors, which would be difficult to identify without first obtaining a functioning system. Therefore, a large screening effort that covered a broad range of catalytic systems was proposed, further stoichiometric studies could then be performed to streamline reaction optimisation.

## 2.7. Screening Studies

Having performed brief stoichiometric studies, which indicated the formation of boronates for most of the bifunctional templates, and some indication of an albeit short-lived ternary complex formation, a screening system which would rapidly identify products of a potentially complex mixture was designed, to quickly assess the efficacy of a particular screening condition. The screening conditions were derived from literature conditions, we thought it necessary not to deviate significantly from literature precedent in this regard, however we did wish to cover a broad range of transformations and conditions, as such 37 conditions were selected for screening purposes. The resulting reaction mixtures from these literature conditions would then be analysed by gas chromatography – mass spectrometry (GC-MS)

### 2.7.1. High-throughput analysis by GC-MS

Gas Chromatography – Mass Spectrometry (GC-MS) combined two powerful microanalytical techniques. With a GC separating components of a mixture in time, whilst a mass spectrometer yields information to assist in the structural identification of each component, thus allowing for a rapid analysis of complex mixtures.<sup>[216]</sup>

The GC-MS equipment used for this study splits the gas from the column into two, with one batch proceeding towards a quadrupole mass spectrometer (MS) which will indicate the mass of each eluent. Whilst the second batch proceeds towards a flame ionisation detector (FID). Only some of the eluents reach the detector of the MS, due to either failed ionisation or loss against the side of the quadrupoles when the current is not yet at the right magnitude for the eluent to reach the detector. However, the FID can detect all species, at the expense of mass data, as such the FID is more sensitive to eluents, whilst the MS which normally gives some detection data in the form of total ion count (TIC) produces mass data that can be correlate with detection peaks in the FID.

The column conditions were optimised to balance two antagonistic factors:

1. Reasonable separation on the column to allow for discrete peaks for each eluent in a complex mixture; this requires a relatively slow elution as to allow reasonable interaction between the eluent and the stationary phase of the column
2. Reasonably short exposure to the stationary phase to minimise peak broadening resulting in poor detection by the MS; this requires a relatively rapid elution as to minimise the time in the column.

Furthermore, as there would be many samples to detect a short acquisition time of 20 minutes was chosen. As such the column conditions were modified to run all the starting materials through in under 10 minutes, allowing for effectively a 10 minute “blank run”, at an elevated temperature, between each acquisition to ensure any slow-moving products are both detected and removed from the column to avoid contaminating the next sample.

The choice of reaction conditions would be largely adapted from literature precedent, choosing robust reactions that had achieved chemically useful transformations. However, a decision needed to be made on the choice of starting material and the way the bifunctional templates were employed.

Our choice of starting material was phenyl boronic acid pinacol ester, this was chosen as it was the simplest aryl organoboron compound, with five hydrogens capable of performing a C-H functionalisation on. Future work would use different substituted aryl constituents, to explore electronic and steric effects, we opted to run the reaction on a small 0.1 mmol scale, using roughly 20 mg of phenyl boronic acid pinacol ester per reaction.

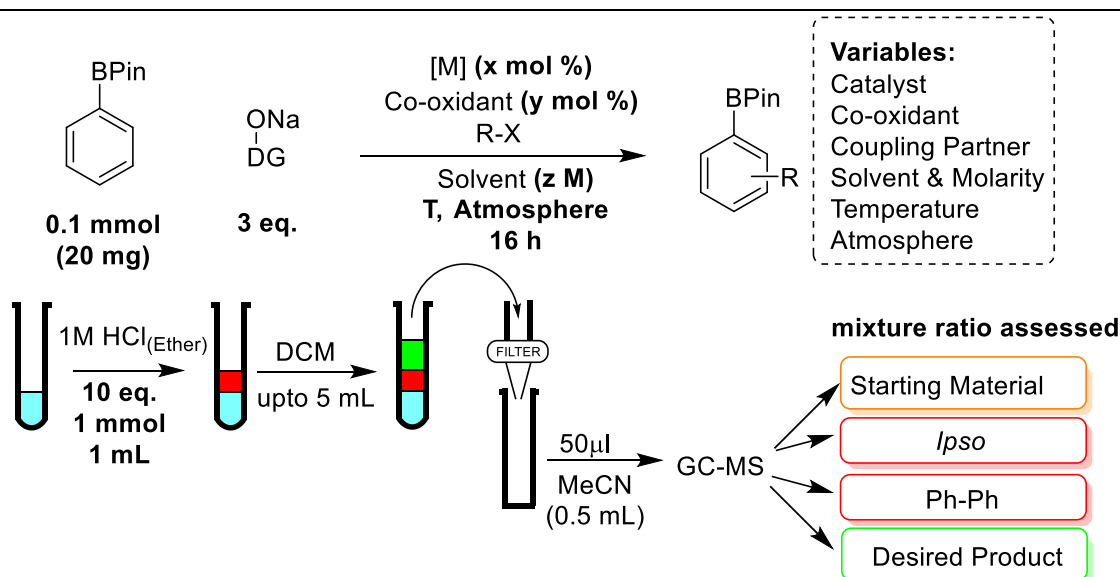
As discussed previously, by having a high concentration of alkoxide present in the reaction, the boronic acid ester will exist to a major extent as the boronate analogue, this in turn minimises the rate of transmetallation, avoiding a thermodynamic sink that results in an undesired *ipso*-substitution, breaking the C-B bond. Thus, whilst we could employ a more complicated system, wherein a dual alkoxide system is employed, such that the more expensive bifunctional template is used in sub-stoichiometric amounts whilst

a cheaper alkoxide such as isopropoxide (which as indicated by DFT calculations, in section 2.5, has a lesser bond dissociation energy than the primary alcohols) is employed to maintain a high concentration of boronate. We opted for a simpler approach, with the potential to return to the isopropoxide strategy in the future, we chose to employ 3 equivalents of each ligand using their deprotonated sodium alkoxide counterparts. By using the deprotonated templates, we were able to remove *tert*-butanol from the reaction mixtures, which, although it may have no adverse effects, means we have a tighter control over the variables. Further, by employing only the template alkoxide, and no cheap alkoxide, we would increase the concentration of template bound boronate species *in situ* and effectively increase the potential rate of the desired reaction. As these reactions, especially those employing a palladium catalyst, are competing with transmetallation, any approach which improves the rate of C-H functionalisation and minimises the rate of transmetallation should be considered.

The 37 reactions chosen covered literature conditions for acetoxylation, acylation, alkenylation, alkoxylation, alkylation, amidation, arylation, borylation, cyanation, halogenation and silylation. Across these reactions 8 different catalysts were employed with 14 different solvents, some reactions employed a co-oxidant such as silver or hypervalent iodine reagents, and reaction temperature was maintained from literature precedent. Further detail of these reactions will be discussed when exploring the results of these reaction.

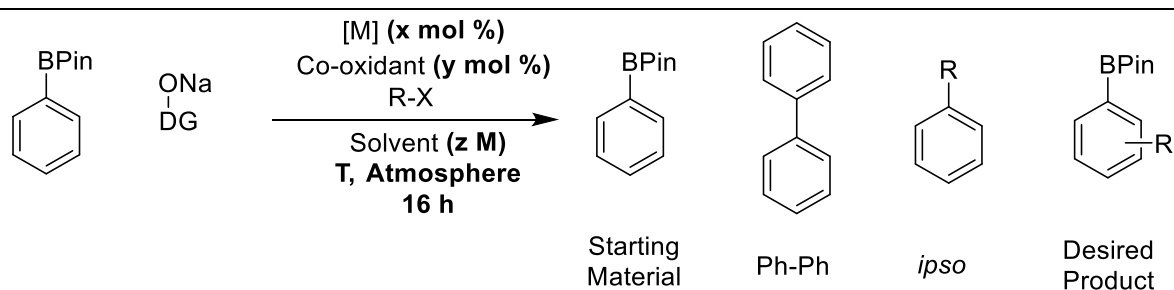
A simple and rapid work-up protocol was chosen. After 16 hours, 10 equivalents of 1M hydrochloric acid in DCM was added to protonate the alkoxides so that they could be detected by GC-MS and the solution was made up to 5 mL with DCM, such that each sample had a concentration *ca.* 0.02M. The acidified mixtures were filtered by gravity filtration through a wool plug and 100  $\mu$ L of this filtrate was added to 0.5 mL acetonitrile for GC-MS analysis (Scheme 123).





Scheme 123: Design of high-throughput ligand screening using GC-MS

Four starting material derived products were hypothesised to arise including retained starting material, *ipso* coupled product, biphenyl (derived from homocoupling of the starting material) and a desired C-H functionalised product (Scheme 124).



Scheme 124: Possible starting material derived products will be detected using GC-MS

During these studies several issues arose, which render the results only preliminary, with some ambiguity that needs further investigation: thus, only giving direction to future more direct studies. These issues are discussed here to give clarity to the way the data has been analysed.

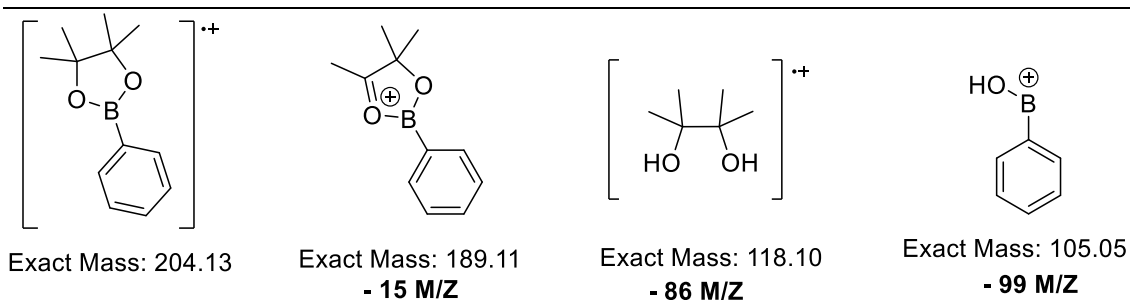
One key issue was that of a discrepancy in the limit of detection between the FID and MS, this led to some peaks in the FID spectra having no mass data associated with them, and therefore no structural information could be interpreted. Secondly, this study was designed without aim to quantify the components of the mixture, this is because to gather accurate quantitative data would require synthesis of desired products, potential by-products and then calibration against an internal standard would be required as to calculate the coefficient for corrected qualitative values. Rather than perform this comprehensively for every unique possible product, this study would instead inform which compounds should be calibrated for, based on reactions that give a successful result, quantitative data could then be collected for these reactions, and thus a protocol to rapidly analyses optimisation efforts could be realised.

As will be observed in the next chapter, no reaction yielded a desired product, this study however is not without merits, we observed the various expected by-products, namely yielded *via* transmetallation, producing cross-coupled products at the *ipso*-position, cleaving the C-B bond. The magnitude of these transformations across different reaction conditions is key to directing future work, the specifics of these results will be discussed in the next chapter. The manner by which the magnitude of starting material and ligand retention was assessed was by expressing the mixture as ratio of starting material and its corresponding by-products (*ipso*, biphenyl, product and other).

Use of libraries of known compounds and fragmentation patterns in the mass spectra allowed for rapid identification of compounds, or where the compound could not be identified, gave reasonable confidence as to functionalities present, determined from fragmentation patterns, and thus allowed us to determine whether the product was derived from substrate, ligand or reagents.

Under the GC-MS conditions designed for this experiment, the starting material, phenyl boronic acid pinacol ester, eluted at around ~4.6minutes and had a unique MS fragmentation pattern which we could use to determine if

other products maintained a BPin moiety. The nominal mass molecular ion peak was observed as a radical cation with a M/Z of 204, fragments were then observed at M/Z 189, 118 and 105, these were attributed to the fragments given in Scheme 125. One issue we noted was that the limit of detection for the FID was lower than the limit of detection for the mass spectrometer, this meant that several species detected by FID, no corresponding mass data could be observed for these species. The mass-spec was performed using electron ionisation (EI), with chemical ionisation (CI) unavailable at the time of this study.



*Scheme 125: Proposed fragments matching the masses observe in the GC-MS*

---

## 2.7.2. Screening Results

Table 5 and Table 6 detail the screening reactions performed, and an overview of the resulting mixture analysed by GC-MS is presented also in these tables. In all cases, no desired product was observed, the full chromatograph was searched for the principle mass ion peak and the expected fragmentation of a pinacol boronic ester.

The presence of 4 species was tracked including product, starting material, biphenyl and formation of a phenyl-coupling partner species referred to as *ipso*. In cases where the corresponding *ipso* coupling product is biphenyl, an arbitrary choice was made to refer to this as *ipso*, as phenyl boronic acid pinacol ester was chosen it is impossible to distinguish homocoupling from cross-coupling. Future work may consider using a fluorine labelled starting material, to be able to distinguish homocoupling from cross-coupling but also to allow further data collection by  $^{19}\text{F}$  NMR spectroscopy.

Only starting material (SM) or SM-derived products are presented, expressing their quantity as a percentage of the total SM-derived components, determined by the integrated peak area for each component of the crude mixture in the FID-chromatograph. It should be noted that this data is qualitative in nature, as the components detected have not been calibrated for quantitative analysis by GC-MS.

Drawing conclusions from this data was difficult due to ambiguities. For example, where high retention of starting material is observed this could be because orthogonality of the C-B bond is promoted by formation of a boronate. Alternatively, high retention of starting material may be due to poisoning of the catalyst under the reaction conditions, therefore no reaction proceeds as there is no active catalyst.

All reactions: PhBPIn (1.0 eq.), sodium 4-(2-cyanophenyl)benzyl alkoxide (3.0 eq.)									Starting Material Derived (%)					
#	R	Cat. (mol%)	Coupling Partner (Eq.)	Additive(s) (Eq.)	Solvent (M)	Atmos.	T (°C)	Ref.	SM	<i>ipso</i>	P	Ph-Ph		
1	Acetoxylation	Pd(OAc) <sub>2</sub> (10)	PhI(OAc) <sub>2</sub> (2)	Cu(OAc) <sub>2</sub> (1)	MeCN (0.15)	O <sub>2</sub>	130	[217]	100	0	0	0		
2					MeCN (0.15)	Air	100	[218]	42	0	0	58		
3					HFIP (0.15)	Air	50	[175]	100	0	0	0		
4	Acylation	Pd(OAc) <sub>2</sub> (10)	PhCOH (1.5)		Xylene (0.15)	Air	120	[219]	0	46	0	54		
5	Alkenylation	Pd(MeCN) <sub>2</sub> Cl <sub>2</sub> (10)	Ethyl Acrylate (2)	AgOAc (2)	HFIP (0.15)	Air	90	[223]	47	53	0	0		
6					DCE (0.15)	O <sub>2</sub>	120	[222]	53	43	0	4		
7					HFIP (0.15)	Air	80	[137]	17	83	0	0		
8					DCE/TFE (0.15)	Air	80	[137]	32	62	0	6		
9					HFIP (0.15)	Air	90	[223]	3	97	0	0		
10					HFIP (0.15)	O <sub>2</sub>	80	[224]	0	100	0	0		
11					HFIP (0.15)	Air	75	[225]	70	30	0	0		
12					DCE (0.15)	Air	90	[133]	92	8	0	0		
13					<sup>t</sup> BuOMe (0.15)	Air	90	[133]	40	60	0	0		
14					Alkoxylation	Pd(OAc) <sub>2</sub> (5)	PhI(OAc) <sub>2</sub> (1.5)	PhCOOH (0.4)	EtOH (0.15)	O <sub>2</sub>	150	[226]	34	0
15	EtOH (0.15)	Air	100	[218]					35	0	0	65		
16	<sup>i</sup> PrOH (0.15)	Air	100	[218]					86	0	0	14		
17	Alkylation	Pd(OAc) <sub>2</sub> (10)	3-Butene-2-ol (3)	AgOAc (3)	HFIP (0.15)	Air	90	[227]	88	0	0	12		
18					Norbornene (1.5)	AgOAc (3)	DCE (0.15)	Air	95	[142]	100	0	0	0
19					<sup>t</sup> BuCOOH (2)	PhI(OAc) <sub>2</sub> (2)	DCE (0.15)	Air	50	[228]	100	0	0	0
20	Amidation	Pd(OAc) <sub>2</sub> (5)	H <sub>2</sub> NCOCH <sub>3</sub> (3)	PhI(OAc) <sub>2</sub> /MgO (2)	H <sub>2</sub> NCOCF <sub>3</sub> (3)	K <sub>2</sub> S <sub>2</sub> O <sub>8</sub> (5)	DCE (0.15)	Air	80	[229]	100	0	0	
21					H <sub>2</sub> NCOCH <sub>3</sub> (3)	PhI(OAc) <sub>2</sub> /MgO (2)	Toluene (0.15)	Air	80	[229]	65	0	0	35
22					PhI(OAc) <sub>2</sub> /MgO (2)	Acetamide (0.15)	Air	80	[229]	49	0	0	51	
23	Arylation	Pd(OAc) <sub>2</sub> (10)	PhI (3)	AgOAc (2)	[Ph <sub>2</sub> ]BF <sub>4</sub> (1.5)		Benzene (0.15)	Air	100	[230]	97	3	0	
24					PhTMS (2)	AgF·BQ (2:1)	Dioxane (0.15)	Air	100	[231]	7	93	0	
25					PhI (3)	AgOAc (2)	HFIP (0.3)	Air	130	[232]	5	95	0	
26					PhI (3)	AgOAc (2)	HFIP (0.3)	Air	130	[232]	100	0	0	
27	Borylation	[Ir(OMe)(cod)] <sub>2</sub> (1.5)	B <sub>2</sub> Pin <sub>2</sub> (2)		THF(0.15)		Air	80	[173]	100	0	0		
28					Dioxane(0.15)	Air	70	[162]	100	0	0	0		
29	Cyanation	Pd(OAc) <sub>2</sub> (5)	K <sub>3</sub> Fe(CN) <sub>6</sub> (2)	CuBr <sub>2</sub> (1)	DMF (0.15)	Air	130	[233]	100	0	0	0		
30	Halogenation	Pd(OAc) <sub>2</sub> (5)	NCS (1.5)		MeCN (0.15)		Air	100	[128]	100	0	0		
31					NBS (1.5)	MeCN (0.15)	Air	100	[128]	100	0	0	0	
32					NIS (1.5)	MeCN(0.15)	Air	100	[128]	100	0	0	0	
33					I <sub>2</sub> /PhI(OAc) <sub>2</sub> (1.5)	MeCN(0.15)	Air	100	[128]	100	0	0	0	
34	Silylation	Pd(OPiv) <sub>2</sub> (10)	(Me <sub>3</sub> Si) <sub>2</sub> (5)	Ag <sub>2</sub> CO <sub>3</sub> (3)	HFIP (0.15)	O <sub>2</sub>	50	[234]	74	0	0	26		

Table 5: Conditions and results for the high-throughput screening study using the 4-(2-cyanophenyl)benzylalkoxide ligand, (*ipso* refers to coupling at the C-B Bond)

All reactions: PhBPIn (1.0 eq.), Na(DMAE)(3.0 eq.)									Starting Material Derived (%)					
#	R	Cat. (mol%)	Coupling Partner (Eq.)	Additive(s) (Eq.)	Solvent (M)	Atmos.	T (°C)	Ref.	SM	<i>ipso</i>	P	Ph-Ph		
1	Acetoxylation	Pd(OAc) <sub>2</sub> (10)	Cu(OAc) <sub>2</sub> (1)		MeCN (0.15)	O <sub>2</sub>	130	[217]	100	0	0	0		
2			PhI(OAc) <sub>2</sub> (2)		MeCN (0.15)	Air	100	[218]	71	0	0	29		
3					HFIP (0.15)	Air	50	[175]	94	0	0	6		
4	Acylation	Pd(OAc) <sub>2</sub> (10)	PhCOH (1.5)		Xylene (0.15)	Air	120	[219]	57	0	0	43		
5	Alkenylation	[RhCp*Cl <sub>2</sub> ] (5)	Diphenyl acetylene (1.3)	AgOAc:NaOAc (2.5:5)	DCE (0.15)	N <sub>2</sub>	110	[220]	Unable to interpret					
6				Cu(OAc) <sub>2</sub> (2)	DMF (0.15)	N <sub>2</sub>	120	[221]	Unable to interpret					
7				Ethyl Acrylate (4)	Cu(OAc) <sub>2</sub> (2)	DMF (0.15)	N <sub>2</sub>	100	[221]	0	100	0	0	
8						DCE (0.15)	O <sub>2</sub>	120	[222]	10	85	0	5	
9				Pd(MeCN) <sub>2</sub> Cl <sub>2</sub> (10)	Ethyl Acrylate (2)	AgOAc (2)	HFIP (0.15)	Air	90	[223]	79	21	0	0
10							HFIP (0.15)	Air	80	[137]	27	73	0	0
11						AgOAc (3)	DCE/TFE (0.15)	Air	80	[137]	0	91	0	9
12						Ag <sub>2</sub> CO <sub>3</sub> (2)	HFIP (0.15)	Air	90	[223]	62	25	0	13
13						Cu(OAc) <sub>2</sub> (2)	HFIP (0.15)	O <sub>2</sub>	80	[224]	0	100	0	0
14						Ag <sub>2</sub> CO <sub>3</sub> (2)	HFIP (0.15)	Air	75	[225]	88	12	0	0
15				Pd(OPiv) <sub>2</sub> (10)	Ethyl Acrylate (2)		DCE (0.15)	Air	90	[133]	92	8	0	0
16				AgOPiv (3)	<sup>t</sup> BuOMe (0.15)	Air	90	[133]	32	62	0	6		
17	Alkoxylation	Pd(OAc) <sub>2</sub> (5)	Cu(OAc) <sub>2</sub> (20)	PhCOOH (0.4)	EtOH (0.15)	O <sub>2</sub>	150	[226]						
18				PhI(OAc) <sub>2</sub> (1.5)		EtOH (0.15)	Air	100	[218]	67	0	0	33	
19						<sup>t</sup> PrOH (0.15)	Air	100	[218]	89	0	0	11	
20	Alkylation	Pd(OAc) <sub>2</sub> (10)	3-Butene-2-ol (3)	AgOAc (3)	HFIP (0.15)	Air	90	[227]	Overlapped		0	0		
21			Norbornene (1.5)	AgOAc (3)	DCE (0.15)	Air	95	[142]	99	1	0	12		
22			<sup>t</sup> BuCOOH (2)	PhI(OAc) <sub>2</sub> (2)	DCE (0.15)	Air	50	[228]	88	0	0	12		
23	Amidation	Pd(OAc) <sub>2</sub> (5)	H <sub>2</sub> NCOCF <sub>3</sub> (3)	K <sub>2</sub> S <sub>2</sub> O <sub>8</sub> (5)	DCE (0.15)	Air	80	[229]	100	0	0	0		
24			H <sub>2</sub> NCOCH <sub>3</sub> (3)	PhI(OAc) <sub>2</sub> /MgO (2)	Toluene (0.15)	Air	80	[229]	94	0	0	6		
25					PhI(OAc) <sub>2</sub> /MgO (2)	Acetamide (0.15)	Air	80	[229]	90	0	0	10	
26	Arylation	Pd(OAc) <sub>2</sub> (10)	[Ph <sub>2</sub> I]BF <sub>4</sub> (1.5)		Benzene (0.15)	Air	100	[230]	79	21	0			
27			PhTMS (2)	AgF:BQ (2:1)	Dioxane (0.15)	Air	100	[231]	87	13	0			
28			PhI (3)	AgOAc (2)	HFIP (0.3)	Air	130	[232]	0	100	0			
29		Pd(PPh <sub>3</sub> ) <sub>2</sub> Cl <sub>2</sub> (10)	PhI (3)	AgOAc (2)	HFIP (0.3)	Air	130	[232]	0	100	0			
30	Borylation	[Ir(OMe)(cod)] <sub>2</sub> (1.5)	B <sub>2</sub> Pin <sub>2</sub> (2)		THF(0.15)	Air	80	[173]	100	0	0	0		
31					Dioxane(0.15)	Air	70	[162]	100	0	0	0		
32	Cyanation	Pd(OAc) <sub>2</sub> (5)	K <sub>3</sub> Fe(CN) <sub>6</sub> (2)	CuBr <sub>2</sub> (1)	DMF (0.15)	Air	130	[233]	88	9	0	3		
33	Halogenation	Pd(OAc) <sub>2</sub> (5)	NCS (1.5)		MeCN (0.15)	Air	100	[128]	100	0	0	0		
34			NBS (1.5)		MeCN (0.15)	Air	100	[128]	100	0	0	0		
35			NIS (1.5)		MeCN(0.15)	Air	100	[128]	98	2	0	0		
36			I <sub>2</sub> /PhI(OAc) <sub>2</sub> (1.5)		MeCN(0.15)	Air	100	[128]	100	0	0	0		
37	Silylation	Pd(OPiv) <sub>2</sub> (10)	(Me <sub>3</sub> Si) <sub>2</sub> (5)	Ag <sub>2</sub> CO <sub>3</sub> (3)	HFIP (0.15)	O <sub>2</sub>	50	[234]	33	0	0	67		

Table 6: Conditions and results for the high-throughput screening study using the dimethylaminoethoxide ligand (*ipso* refers to coupling at the C-B Bond)

The large breadth of conditions employed in this study resorted to a “hit or miss” approach. According to the aims of this study, all examples resulted in a “miss”. However, information may still be gleaned from these results, with some conditions better able to retain the starting material, thus indicating conditions which may preclude transmetallation. Without further studies, it is difficult to glean whether the cause of orthogonality of the starting material to reaction conditions. There is the possibility that the hypothesis that an excess of ligand forms the boronate *in situ*, which was hypothesised to slow transmetallation, or simply the reaction conditions cause poisoning of the catalyst and thus no reaction occurs. Attempts to glean information from the data presented in Table 5 and Table 6 are herein detailed.

**Possible precipitation of metal halides** - Table 5, entry 2 details an attempted acetoxylation with diacetoxy iodobenzene, the resulting mixture comprises of the starting material (42%) and biphenyl (58%). Table 5, entry 36, differs by addition of I<sub>2</sub> for iodination, in this case starting material retention is observed. This indicated formation of an insoluble palladium iodide complex thus poisoning the catalyst. Formation of insoluble palladium halides can be extended to entries 32-35 in Table 5, and entries 32 -36 in Table 6.

For palladium-catalysed reaction with no halide-source, *ipso*-substituted and homocoupled products were observed, arising from transmetallation. Oxidants seem to have an effect on boronic ester orthogonality, with entries 20-26 in Table 5 maintaining starting material (49 - 100%) and entries 21-26 in Table 6 also affording some orthogonality (79 - 100%).

**DCE improves retention of starting material** - Reactions employing DCE tend to have an improved retention of starting material. Entries 7 and 8 in Table 5 differ by solvent used, using DMF and DCE respectively. Entry 7 has 6% starting material whilst DCE improves to 53 %. In Table 6, entry 7 no starting material is retained using DMF as the solvent, whilst in DCE (Table 6, entry 8) the starting material makes up 10%. Entry 8 was however performed under an oxygen atmosphere at a slightly elevated temperature (120 °C) to entry 7 (Nitrogen, 100 °C) therefore confirmation of this conclusion would require further investigation.

A similar pattern is observed between entries 10 and 11 in Table 5. Using HFIP observes 17% starting material is observed, whilst a 1:1 DCE:TFE mixture

improves to 32 %. This observation is, however, not consistent with entries 10 and 11 in Table 6.

Finally, entries 15 and 16 in Table 5, differ by solvent. with *tert*-butyl methyl ether retaining 40% starting material whilst DCE retained 98%. This observation is consistent with entries 15 and 16 in Table 6, giving 32% starting material in *tert*-butyl methyl ether and 92% in DCE.

***Sterically bulky ligands promote orthogonality*** - Entries 12 and 14 in Table 5 differ only by catalyst employed, using palladium(II) acetate and palladium(II) pivalate respectively. *Ips*o-substitution accounts for 94% when using Pd(OAc)<sub>2</sub>, whilst only 30% *is*po-substitution is observed when using a more sterically bulky analogue of the acetate ligands. This observation is consistent with Entries 12 and 14 in Table 6. This result is similar to the observations made during the ternary complexation studies detailed in section 2.6.4, wherein application of palladium(II) acetate rapidly caused homocoupling. When employing palladium(II) pivalate the homocoupling was sufficiently slow to observe a ternary complex. The steric size of the pivalate ligands aids in destabilising the key intermediates of transmetallation (see section 1.4 for further detail)

***Coupling partners influence orthogonality*** - Entries 6 and 7 in Table 5 are both rhodium catalysed alkenylation protocols differing only by the choice of coupling partner, diphenyl acetylene and ethyl acrylate respectively. Table 5, entry 6 retains starting material, whilst Table 5, entry 7 observed 84% of the *ip*so-alkenylated product. Corroboration of this is with result from was not possible due to overlap of product peaks. One suggestion to explain these observations is the co-ordination of the two coupling partners to the rhodium centre significantly influence its reactivity.

***Low influence of temperature on orthogonality*** - Suzuki-Miyaura cross coupling reaction normally require heating in order to proceed, this may lead to the conclusion that transmetallation is slow significantly at low temperature. However orthogonality was observed at 130 °C, for entries 32 in both Table 5 and Table 6, as well as entries 3 and 4 in Table 5.

***Other observations*** - Iridium catalysed borylation conditions (entries 30 and 31, Table 5) resulted in full retention of starting materials. Reactions employing



acetonitrile (MeCN) also gave a high proportion of starting material, in a range of 42-100% for entries 1-2 and 33-36 in Table 5. MeCN is mainly used in reaction using halogen source.

Other observations may be drawn however further studies are required to determine their validity. Unfortunately, catalytic systems with monodentate coordination of bifunctional alkoxide templates to pinacol boronic esters were difficult to study. Boronate formation was shown to be transient indicating that catalytic loadings of a directing ligand were feasible. However, ternary complexation studies indicated that there was a competition between boron and metals for alkoxide coordination. In the case of forming palladium alkoxides, this resulted in rapid cleavage of a C-B bond *via* transmetallation with a boronic ester. As a strategy to suppress transmetallation an excess of alkoxide ligand was added, as to saturate the system with alkoxy pinacol boronates, which cannot undergo transmetallation. This strategy likely slowed transmetallation, albeit not to such an extent that the desired C-H functionalisation was more facile. To address these issues, a second study was developed, using polydentate co-ordination.

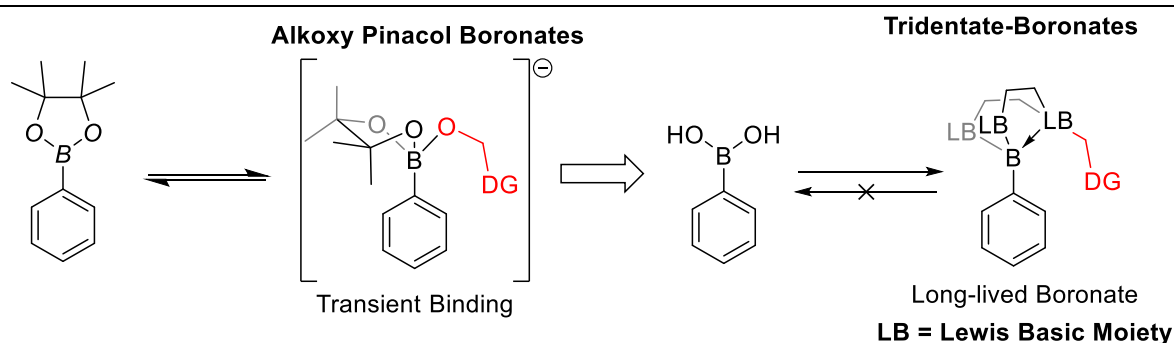
# Chapter 3

## TIDA-boronates in C-H functionalisation

### 3. TIDA-boronates for C-H Functionalisation

#### 3.1. Polydentate Ligand-Substrate Binding

Polydentate boron ligand dissociates from boron slowly owing to formation of a chelate. The strong co-ordinate of a polydentate ligand would simplify the catalytic cycle, forming a non-transient substrate-ligand complex (Scheme 126). A more permanent substrate-ligand complex would simplify testing of template feasibility, as with monodentate co-ordination the bifunctional templates must both direct C-H functionalisation and favour co-ordination to a boron moiety.

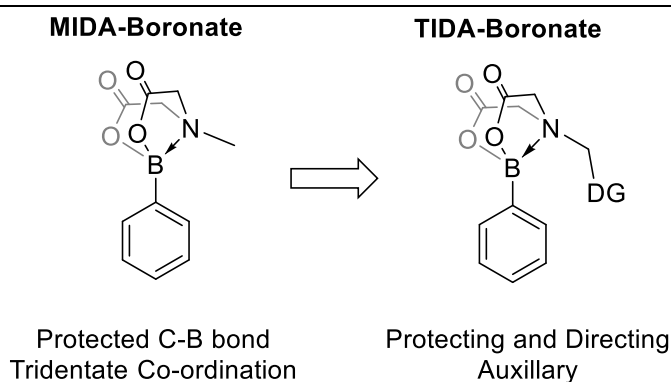


*Scheme 126: Polydentate co-ordination to boron will slow dissociation of substrate-ligand complexes, in comparison to more transient monodentate ligands.*

The *N*-methyl iminodiacetate boronic acid (BMIDA) protecting group is well established, and has been shown to maintain a boronic moiety under transition metal catalysed chemistries (See Chapter 1.5.3). MIDA-boronate's resistance to transmetalation is attributed to formation of a stable four-coordinate boronate species, blocking access to boron's  $p_z$ -orbital which is necessary to perform transmetalation.

Modifications to the bifunctional alcohol ligands as discussed in Chapter 2, were made to adopt a MIDA-like coordination mode. The *N*-methyl group of MIDA-boronates was chosen as a point for installation of the templates, as its presence is not pertinent to the functionality of the protecting group; rather it is a simple way of removing the acidic hydrogen that exists on the secondary amine analogue.<sup>[81]</sup>

These directing auxiliaries will be referred to as *N*-template iminodiacetate protecting/directing groups or TIDA-boronates (Scheme 127).

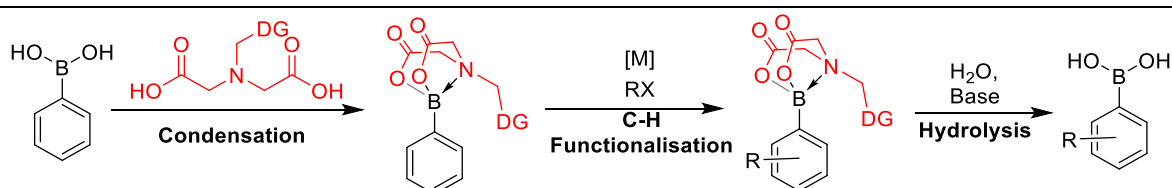


*Scheme 127: Proposed modification to the MIDA protecting group to incorporate a directing group*

---

The ability of a MIDA-boronate to be maintained under C-H functionalisation conditions was, at the time this research was conducted, not verified. Therefore, initial studies would focus on the feasibility of TIDA-boronates by testing the stability of MIDA-boronates under C-H functionalisation conditions (See Chapter 3.2).

Once the stability was tested and suitable conditions found, a series of TIDA-boronates could be synthesised, installed, and screened for C-H functionalisation (Scheme 128). Initial studies towards these objectives were performed (See Chapter 3.3).

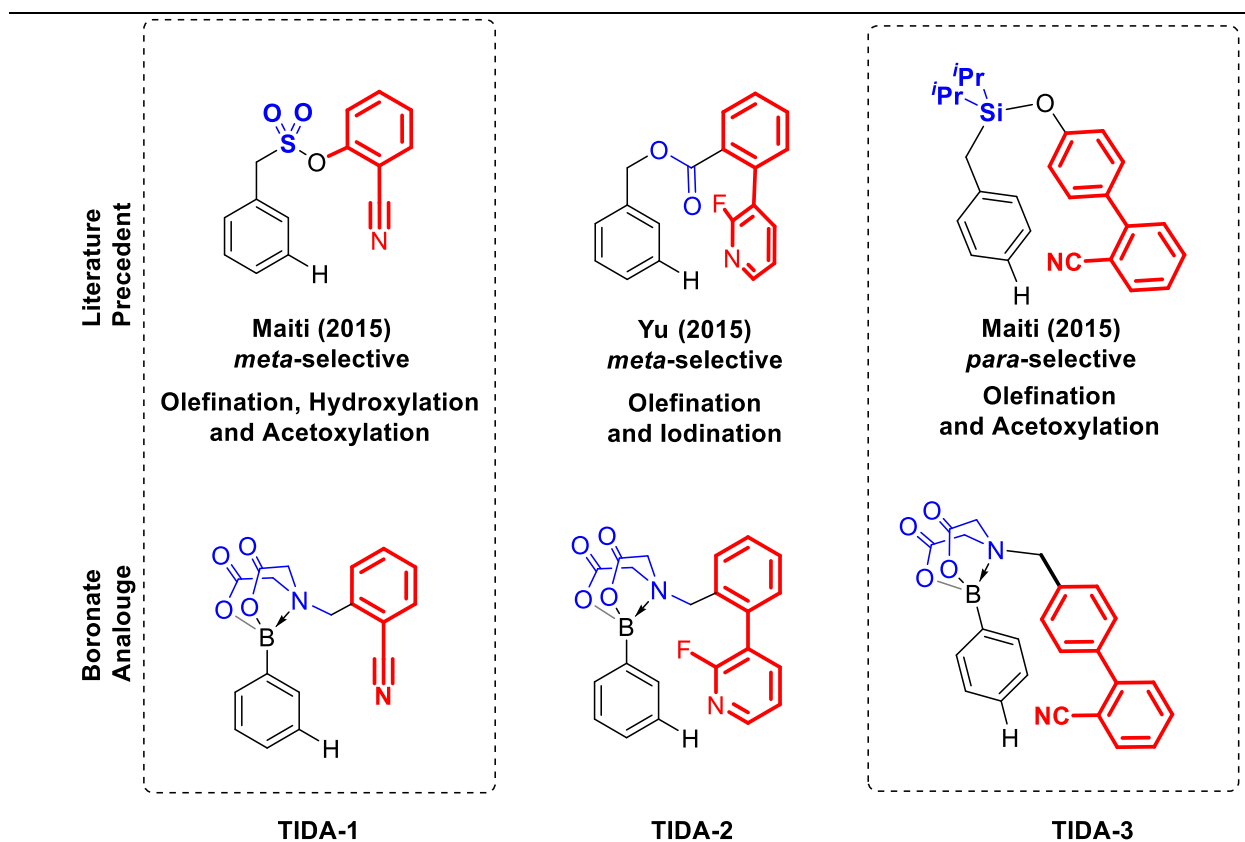


*Scheme 128: Proposed route for the functionalisation of organoboronic acids, requiring additional installation and removal of a directing auxiliary.*

---

With regards to the design of the TIDA-ligands, three preliminary TIDA-boronates were selected (Scheme 129). *Ortho*-directed C-H functionalisation on aryl boronic acids had already been described by Suginome *et al.* (See Chapter 1.8.2) using B(PZA)- and B(AAM)-directing auxiliaries to achieve silylation [168,170],

alkenylation<sup>[94]</sup> and borylation<sup>[173,174]</sup>. Therefore, the TIDA-ligands chosen focus on site-selectivity at the distal *meta*- and *para*-positions.



Scheme 129: Proposed auxiliaries for directed C-H functionalisation of TIDA-boronates

Whilst this project was ongoing and making progress towards achieving the defined research objectives, Williams *et al.* published their work of using a TIDA-boronate to perform a distal C-H functionalisation.<sup>[175]</sup> These results were used to inspire a directing group screened in Chapter 2.7.

The work published by Williams *et al.* highlighted that flexible,  $sp^3$ -carbon rich, templates, were effective at achieving C-H functionalisation but often at the cost of site-selectivity, affording a mixture of *meta*- and *para*-functionalised products. The TIDA-boronate utilised by Williams *et al.* has a flexible alkyl chain which allows energy minimising conformations of the desired metalacyclic intermediate to be adopted, however this comes at the cost of losing site-selectivity, as the flexibility allows favourable metallacycles to form at multiple C-H sites.

The TIDA-boronates proposed in this work, have more rigid, sp<sup>2</sup>-carbon rich, templates, therefore a higher degree of site-selectivity may be afforded, although potentially at the cost of yield, which can later be optimised.

TIDA-1 – Inspired by the work of Bera *et al.* wherein they described directed *meta*-selective C-H olefination, hydroxylation and acetoxylation of aryl C(sp<sup>2</sup>)-H bonds using an sulfonate ester linked directing auxiliary. [194] TIDA-1 adapts the sulfonate ester linkage to a TIDA-boronate linkage, without significant modification to the template backbone, thus targeting *meta*-selective C-H functionalisation of aryl boronic acids.

TIDA-2 – Inspired by the work of Maji *et al.* wherein a *para*-selective C-H silylation<sup>[138]</sup> and alkenylations<sup>[235]</sup> produces a series of *para*-functionalised phenol products after removal of the silyl-linked directing auxiliary. TIDA-2 modifies the silyl linkage to the tridentate linkage proposed above, targeting *para*-selective C-H functionalisation of aryl boronic acids.

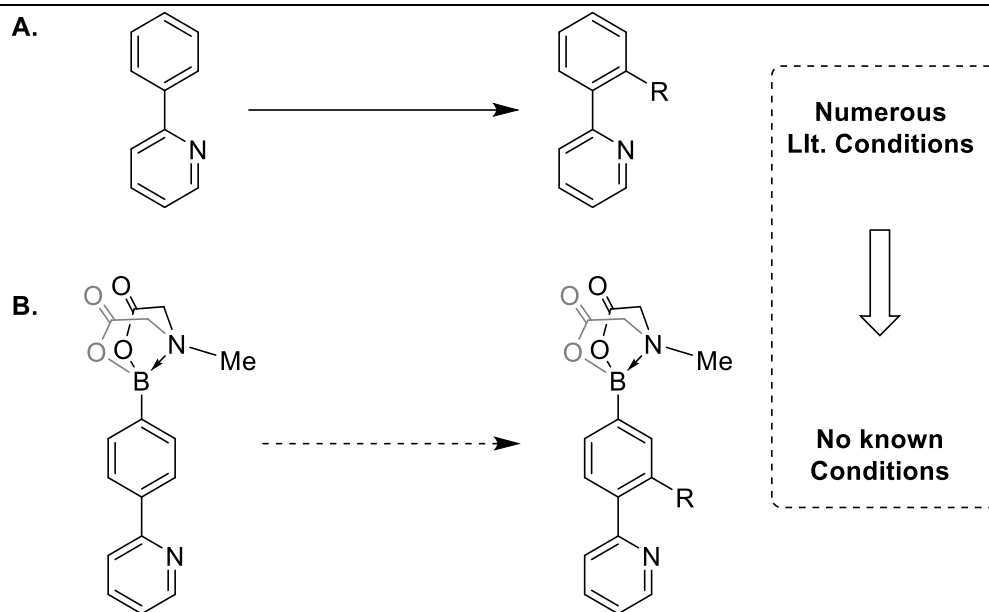
TIDA-3 – The final target TIDA auxiliary is inspired by the work of Yu *et al.* for *meta*-selective C-H alkenylation and iodination tethered *via* an ester linkage, to produce functionalised benzyl alcohols after auxiliary removal *via* hydrolysis.<sup>[198]</sup> TIDA-3 modifies the ester linkage to the tridentate MIDA-derived linkage proposed above, targeting *meta*-selective C-H functionalisation of aryl boronic acids.

In section 2.6, 2-(2-Fluoro-3-pyridinyl)benzyl alcohol, was found to undergo an intramolecular cyclisation *via* an S<sub>N</sub>Ar, wherein a nucleophilic attack by an alkoxide at 2-fluoropyridyl moiety results in an undesired product. The template was changed to change a 4-fluoro isomer, however this was also found to be unsuitable due to reactivity in the presence of sodium *tert*-butoxide. As tertiary amines are less nucleophilic than alkoxides, we decided to pursue TIDA-2, rather than a 4-fluoro isomer, as this was shown by literature precedent to be better at promoting *meta*-selective C-H functionalisation, with the 2-fluoro isomer producing a 79 % yield of the desired product whilst the 4-fluoro isomer yielded only 43 % under identical conditions. [198]

### 3.2. BMIDA Orthogonality in C-H Functionalisation

The stability of MIDA-boronates under various reaction conditions has been described in various publications in the literature, improving the utility of this protecting moiety (see also Chapter 1.5.3). However, only a small pool of literature exists describing C-BMIDA orthogonal metal catalysed functionalisations (see section 1.8). Thus, prior to developing a series of TIDA-boronates, a proof-of-concept study was devised to ascertain the stability of the C-B bond in substrates containing a BMIDA moiety under C-H functionalising conditions. This was achieved by installing a MIDA-boronate onto a substrate primed for directed metallation, which already had a plethora of C-H functionalisation synthetic methodologies described in the literature.

2-Phenylpyridine was selected as a benchmark substrate. The functionalisation of 2-phenylpyridine was first described by Sanford in 2006.<sup>[128]</sup> The rigidity of the biaryl, coupled with the propensity for a metal to co-ordinate to the pyridyl, helps to bring a metal into proximity with an *ortho*-C(sp<sup>2</sup>)-H bond thus promoting C-H metallation. 2-phenylpyridine is an excellent benchmark substrate for many C-H functionalisation proof-of-concept studies and thus numerous differing methodologies have been developed to achieve a range of functionalisations (Scheme 130, A). These conditions, utilise a wide range of catalysts, co-catalysts, oxidants, solvents, temperatures and coupling partners. This allowed us to assess the stability of the BMIDA moiety under a range of conditions, aiding the design of future methodologies.



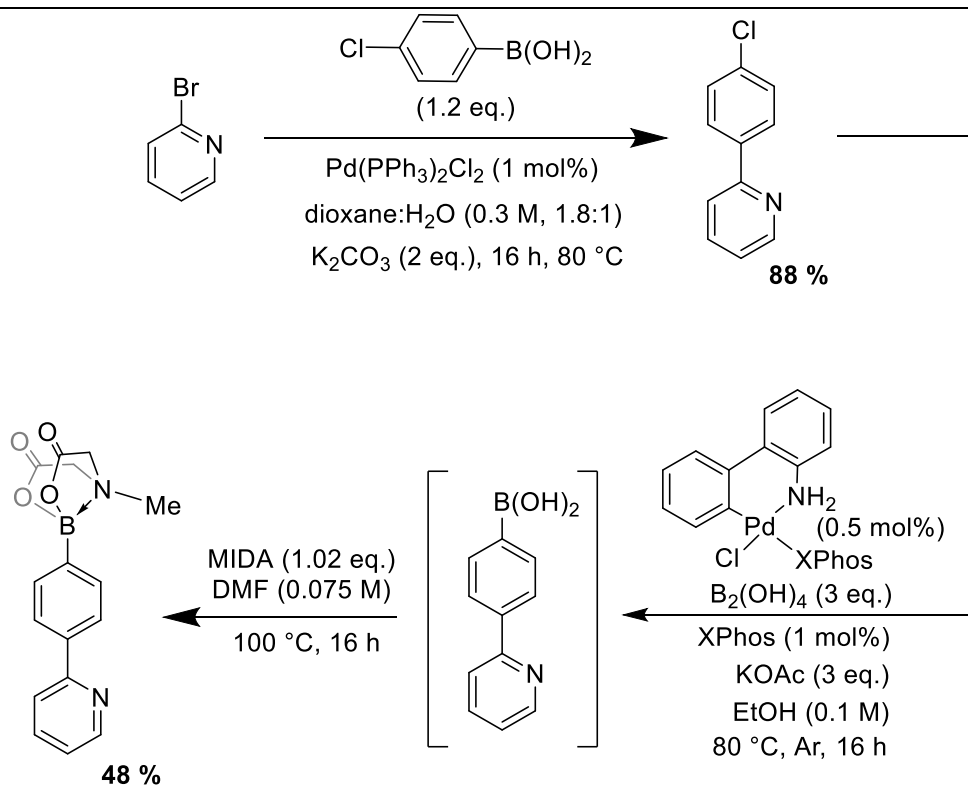
*Scheme 130: The efficiency of C-H functionalisation of 2-phenylpyridines in the presence of a BMIDA moiety is largely unknown.*

---

4-(2-Pyridyl)phenyl MIDA-boronate was chosen as the substrate for these studies (Scheme 130, B), opting for *para*-substituted phenyl to ensure the MIDA boronate was distal to the C-H functionalisation, preventing any undesired side reactions as a result of directed metallation into the C-B bond.



### 3.2.1. Starting Material Synthesis



Scheme 131: Overall synthetic route for the synthesis of a MIDA-boronate containing derivative of 2-phenylpyridine

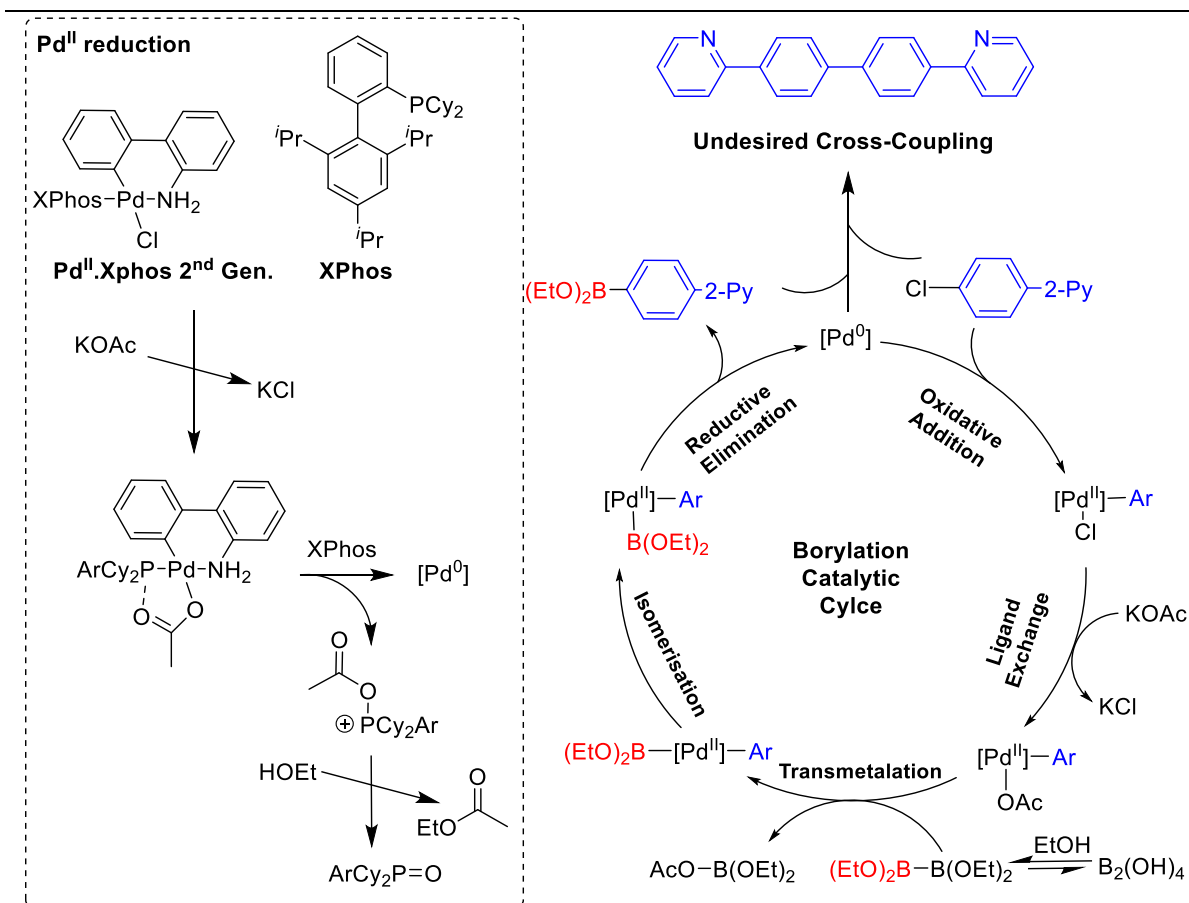
A three step route to synthesise 4-(2-pyridyl)phenyl MIDA-boronate was performed (Scheme 131). The first step coupled 2-bromopyridine and 4-chlorophenyl boronic acid by a Suzuki cross-coupling (using a methodology previously described in the literature) to produce 2-(4-chlorophenyl)pyridine in an 88 % yield.<sup>[236]</sup> The general Suzuki cross-coupling conditions used multiple times in section 2.6.2 were not employed, due to the use of XPhos, which can promote oxidative addition across a C-Cl bond due to the generation of an electron-deficient phosphine coordinated palladium(0) intermediate.<sup>[237]</sup> The resulting 2-(4-chlorophenyl)pyridine, was partially purified *via* an acid-base extraction to removing non-protonatable by-products, further purification was achieved by silica gel chromatography.

Borylation of the C-Cl bond was performed using a synthetic methodology first described by Molander *et al.* employing tetrahydroxydiboron as

a borylating agent in the presence of the second generation palladium.XPhos precatalyst and potassium acetate in ethanol.<sup>[28]</sup>

The second generation palladium.XPhos precatalyst, first disclosed by Kinzel *et al.*, is a palladium(II) complex of *ortho*-palladated 2-phenyl aniline and XPhos, and is able to rapidly reduce to palladium(0), and then rapidly perform oxidative addition across a C-Cl bond.<sup>[238]</sup> These properties of the precatalyst are important to the success of the reaction, rapid reduction to palladium(0), mediated by XPhos and the acetate base, prevents undesired decomposition of tetrahydroxydiboron resulting from exposure to palladium(II). XPhos also promotes oxidative addition across C-Cl bonds, as the sterically bulky nature of the Buchwald ligand, makes the palladium(0) centre electron-deficient. <sup>[202,239]</sup>

The potassium acetate promotes reduction of the palladium(II) precatalyst in conjunction with XPhos, and also activates the diboron coupling partner. In ethanol, the tetrahydroxydiboron undergoes transesterification to the triethoxy analogue. Molander *et al.* speculate that the acetate then co-ordinates to the diboron reagent to produce a boronate intermediate which then undergoes transmetallation. However in-line with the findings of Amatore *et al.* detailed in Chapter 1.4,<sup>[178]</sup> and a computational mechanistic study on the transmetallation of diboron compounds,<sup>[240]</sup> the transmetallation likely occurs by interaction of an acetate-coordinated organopalladium(II) intermediate with tetraethoxydiboron (Scheme 132).



Scheme 132: Proposed catalytic cycle for borylation conditions described by Molander *et al.*

The potential pitfall of this reaction is for C-H palladation to occur at the *ortho* position directed by co-ordination to the pyridyl ring. Although Molander *et al.* reported their borylation methodology to be robust in the presence of heteroaromatics such as pyridines, indoles and benzoxazoles, there was no report on the efficacy of the methodology when the heteroaromatic is primed to direct C-H metallation, which may result in additional undesired by-products.

The reaction resulted in the formation of the desired boronic acid and 2-phenylpyridine, as identified in the  $^1\text{H}$  NMR spectra of the crude material, with the potential tetraaryl by-product described in Scheme 132 not observed. The undesired pathway resulting in the formation of 2-phenylpyridine is unclear; it may be either a result of protodeborylation of the product, or a result of slow transmetalation of the diboron compound leading to hydrodehalogenation.

Furthermore, this step proved to be capricious, with the ratio of desired product to 2-phenylpyridine varying between synthesis attempts due to variables

that could not be identified. The solids were dried under reduced pressure prior to use, ethanol was dried and stored over 4Å molecular sieves, efforts were made to fully purge the reaction vessel with an argon atmosphere using Schlenk techniques, a heating block was preheated to 80 °C to allow reaction temperature to be achieved rapidly, and order of addition was kept consistent across multiple runs. However, the ratios of these two products varied between identical reaction, as observed in the crude <sup>1</sup>H NMR. As this methodology was not central to the aim of the project, it was not considered appropriate to spend time identifying and optimising extraneous variables. Since 2-(4-chlorophenyl)pyridine is low cost and rapid to produce the reaction was performed several times on scale without further optimisation.

Silica-gel chromatography was attempted on the boronic acid product, however the high polarity of the product resulted in significant tailing on the column while using a DCM:MeOH:TEA (9:1:0.1) elution system. Further studies could have been attempted to design an efficient purification protocol for the aryl boronic acid, however, as the identity of the two major components of the crude mixture were known (the desired product and 2-phenylpyridine), the reaction was subsequently telescoped and the synthesis of the MIDA-boronate performed without further purification. as 2-phenylpyridine would not likely interfere with the MIDA condensation,

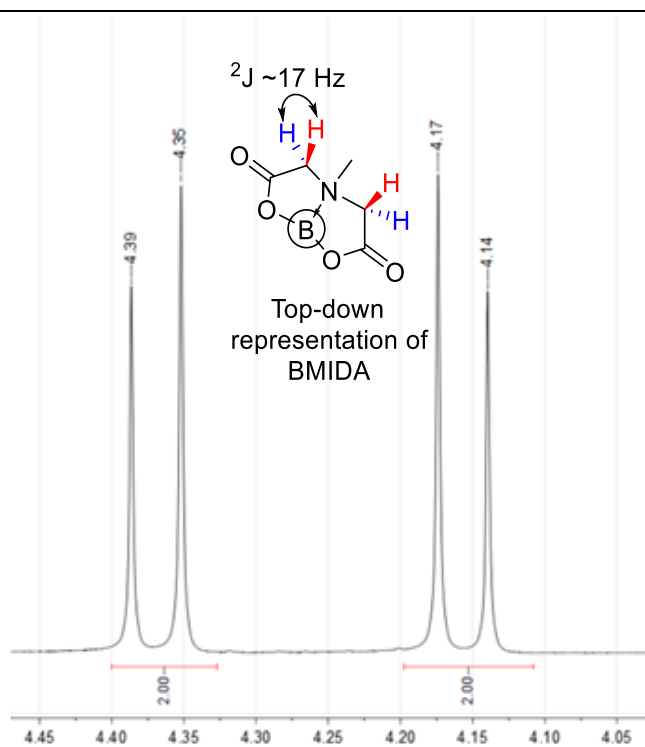
The condensation was performed in DMF, which was removed post reaction *in vacuo* (aqueous work-up was avoid due to uncertainty over the MIDA-boronate stability). On a small scale this proved straightforward, but on larger scales the removal of DMF *in vacuo* was difficult. However it was found that adding silica to the solution accelerated the evaporation of DMF, yielding a dry load of the reaction mixture on silica, ready for purification by silica gel chromatography.

The subsequent purification by column chromatography was non-standard; it entailed two different column mobile phases with an initial run with one solvent system and then a change to a different solvent system. We observed, in line with existing literature,<sup>[241]</sup> a zero-value R<sub>f</sub> for the MIDA compound in solvent systems which did not contain polar aprotic solvents such a THF and MeCN. In the presence of THF however, we observed elution of the MIDA compound. We used this to our advantage, by flushing the column to release the 2-phenylpyridine and other non-

MIDA containing by-products in hexane:ether:TEA (8:2:0.1), the solvent was then flushed with an acetone:THF:TEA (2:8:0.1) mixture to elute the desired compound with an  $R_f$  of 0.4, leading to isolation of the desired product in a 48% yield.

The synthesis of the desired 4-(2-pyridinyl)phenyl boronic acid MIDA ester was therefore achieved in an overall 31 % yield; although this yield is relatively low, by performing the reaction multiple times, 1.5 g of material was isolated.

The  $^1\text{H}$  NMR of the final MIDA-boronate product shows a pair of roofed doublets between 4.16 to 4.37 ppm. Each doublet has a coupling of 17.2 Hz corresponding to a  $^2\text{J}$  coupling between the geminal protons on the MIDA-boronate. These peaks are indicative of the presence of the bicyclic BMIDA moiety, as, due to the fixed ring system, the protons become diastereotopic.



*Scheme 133: NMR and visual representation of the splitting pattern observed for the  $\alpha$ -protons of the MIDA protecting group*

---

### 3.2.2. Design of Screening Studies

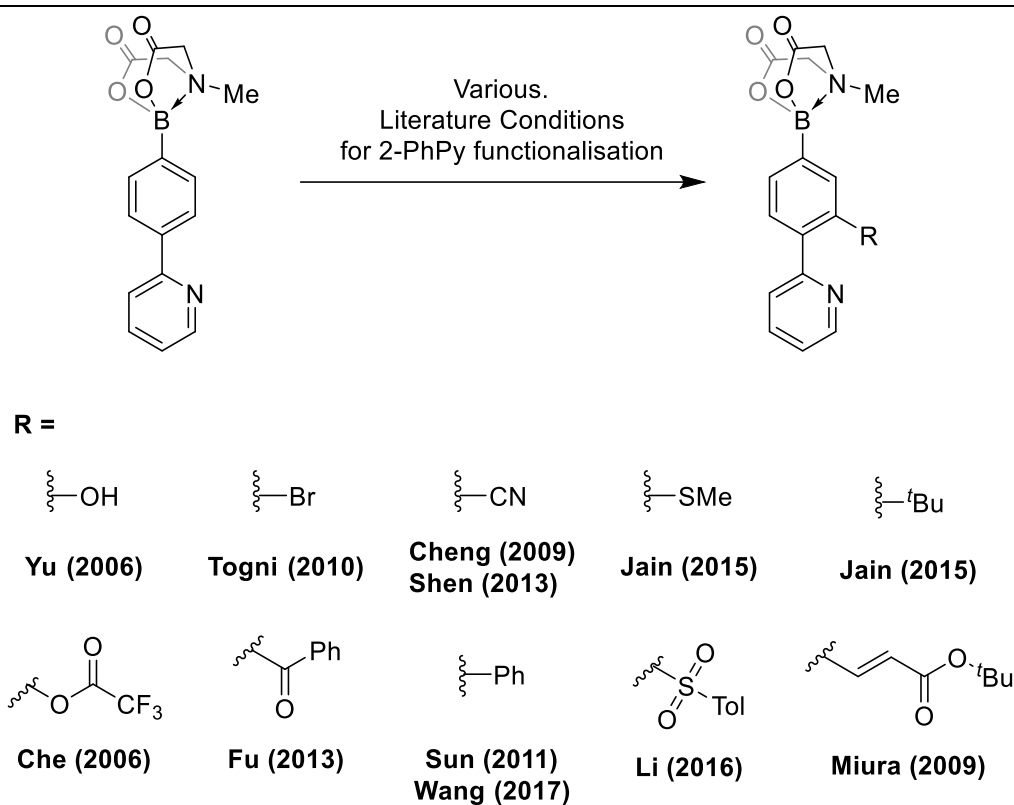
Having established a method by which we can assess the formation of products in a complex mixture by observing the key  $^1\text{H}$  NMR chemical shifts of the diastereotopic protons, we set out to subject the 2-pyridinyl MIDA-boronate,

to a series of C-H functionalisation conditions, previously disclosed in the literature. This initial study would give a broad-strokes understanding of which reaction conditions maintain the MIDA-boronate, and which conditions promote undesired reactions, such as homo-coupling or *ipso*-coupling.

These reactions (detailed in Table 3) cover a range of conditions, including high temperatures, high stoichiometric metal loadings and low catalyst loadings and a broad selection of solvents. From any successful screening results, optimisation of those conditions would then be performed to gauge the effects of different variables on the orthogonality of the MIDA-boronate more accurately.

*Table 7: Initial screening conditions selected for determining the orthogonality of a MIDA moiety under C-H functionalisation conditions*

	Cat. (mol%)	Coupling Partner (eq.)	Additive (eq.)	Solvent (M)	T (°C)	Ref.
1				DMSO (1.28)	Air	[242]
2		Cu(OAc) <sub>2</sub> (1)	H <sub>2</sub> O (1)	MeCN (0.15)	O <sub>2</sub>	[217]
3	Cu(OAc) <sub>2</sub> (30)	(Me <sub>3</sub> Si) <sub>2</sub>	TMEDA(0.3), H <sub>2</sub> O(1)	MeCN (0.27)	O <sub>2</sub>	[243]
4	[(RhCp*Cl <sub>2</sub> ) <sub>2</sub> ] (1)	Styrene (1)	Cu(OAc) <sub>2</sub> (1)	DMF (0.33 M)	N <sub>2</sub>	[244]
5	[(RhCp*Cl <sub>2</sub> ) <sub>2</sub> ] (5)	TolSO <sub>2</sub> Na (1.6)	PhI(OH)OTs (1.6)	Acetone (0.1)	Air	[245]
6	Pd(OAc) <sub>2</sub> (5)	CF <sub>3</sub> C(=O)NH <sub>2</sub> (1.5)	K <sub>2</sub> S <sub>2</sub> O <sub>8</sub> (5), MgO (2)	DCE (0.15)	Air	[229]
7		PhCOOH (4)	TFAA (20)	<i>neat</i>	Air	[246]
8		PhI (1.5)	TFA (8)	AcOH/Anisole 1:1 (0.32)	O <sub>2</sub>	[247]
9	Pd(OAc) <sub>2</sub> (10)	PhSi(OMe) <sub>3</sub> (2)	AgF (2), BQ (1)	1,4-Dioxane (0.25)	N <sub>2</sub>	[231]
10		PivOH (2)	PhI(OAc) <sub>2</sub> (2)	<i>neat</i>	Air	[228]
11	Pd(OAc) <sub>2</sub> (18)	NBS (1.1)		MeCN (1.7)	Air	[248]
12	Pd(OAc) <sub>2</sub> (5)	K <sub>3</sub> Fe(CN) <sub>6</sub> (0.2)	CuBr <sub>2</sub> (1)	DMF (0.2 M)	Air	[233]

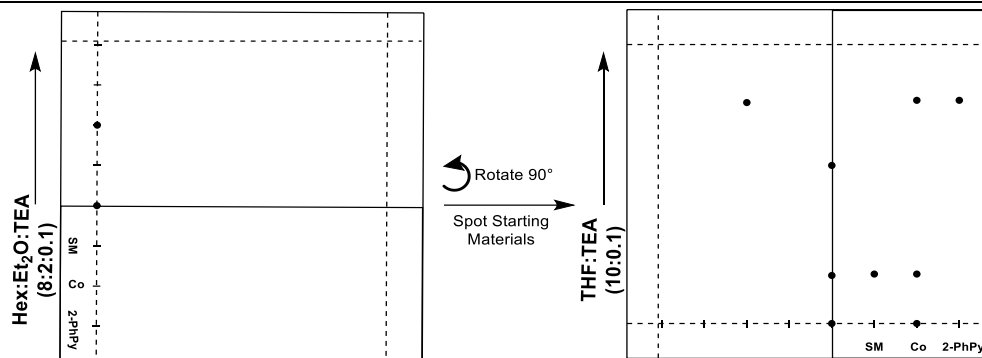


*Scheme 134: Screening approach with each of the 12 target products given, along with literature basis for each transformation*

---

Each reaction was set-up as per the literature preparation, with identical reaction conditions, altering only the starting material. The work-up was altered from the literature, with all reactions filtered through celite with DCM washings and purified by column chromatography.

To assess the number of species in a crude mixture, a 2D-TLC was used, which took advantage of the zero-value retention factor for MIDA -boronates in the absence of a polar mobile phase solvent such as THF. On a square TLC plate a spot of the crude mixture was eluted first in the absence of THF (hexane:ether:TEA - 8:2:0.1), then with THF as the mobile phase (Scheme 135). Spotting of starting materials was done prior to eluting with a THF mobile phase, allowing a rapid qualitative indication of the identity of spots (Scheme 135). As MIDA compounds only move in a THF mobile phase, this 2D approach allowed separation of MIDA-containing compounds from non-MIDA containing compounds helping to simplify interpretation of the TLCs.



*Scheme 135: Example 2D-TLC for rapid interpretation of number and type of species in a complex mixture*

This 2D-TLC also emulates the work-up using a short silica gel plug; first a diethyl ether flush elutes non-MIDA bearing components of a crude mixture. Then distilled THF releases MIDA-containing products.

An internal standard, 2,4,6-trimethoxybenzene, was added to the crude residues and  $^1\text{H}$  NMR spectra were obtained; allowing yields to be calculated. This overall approach allowed us to assess the success of these procedures quantitatively.

This approach was decided upon as attempts to observe the starting material by GC-MS analysis resulted in significant tailing of the FID-chromatogram, due to the high polarity of MIDA-bearing compounds. This rendered the GC-MS analysis unable to characterise a complex mixture of MIDA-boronates as peak overlap made analysis difficult. One alternative option would have been to perform a transesterification by addition of pinacol post-reaction. However, as this study had the aim of showcasing MIDA-boronate orthogonality under C-H functionalisation methodologies, it was decided to retain a MIDA-boronate in the product.

### 3.2.3. Screening Results

Nine of the ten reactions resulted in no observed desired product (Table 8, Entries 1-10 and 12), indicating that there are a variety of conditions in which the MIDA moiety is not an efficient protecting group.



	Cat. (mol%)	Coupling Partner (eq.)	Additive (eq.)	Solvent (M)	SM	P	2-PhPy	Other
1		Cu(OAc) <sub>2</sub> (1)	H <sub>2</sub> O (1)	MeCN ( )	0	0	63	
2	Cu(OAc) <sub>2</sub> (30)	(Me <sub>3</sub> Si) <sub>2</sub>	TMEDA(0.3), H <sub>2</sub> O (1)	MeCN (0.27)	0	0	72	
3	[[RhCp*Cl <sub>2</sub> ] <sub>2</sub> ] (1)	<i>tert</i> -butyl acrylate	Cu(OAc) <sub>2</sub> (1)	DMF (0.33)	0	0	0	Complex Mix
4	[[RhCp*Cl <sub>2</sub> ] <sub>2</sub> ] (5)	TolSO <sub>2</sub> Na (1.6)	PhI(OH)OTs (1.6)	Acetone (0.1)	25	0	0	Complex Mix
5	Pd(OAc) <sub>2</sub> (5)	CF <sub>3</sub> C(=O)NH <sub>2</sub>	K <sub>2</sub> S <sub>2</sub> O <sub>8</sub> (5), MgO (2)	DCE (0.15)	45	0	0	Complex Mix
6	Pd(OAc) <sub>2</sub>	PhI (1.5)	TFA (8)	AcOH/Anisole 1:1 (0.32)	50	0	0	<i>Ips</i> o (7 %)
7		PhSi(OMe <sub>3</sub> ) (2)	AgF (2), BQ (1)	1,4-Dioxane (0.25)	16	0	0	Complex Mix
8		PivOH (2)	PhI(OAc) <sub>2</sub> (2)		68	0	0	
9	Pd(OAc) <sub>2</sub> (18)	NBS (1.1)		MeCN (1.7)	0	16	Trace	Di- (3 %)
10	Pd(OAc) <sub>2</sub> (5)	K <sub>3</sub> Fe(CN) <sub>6</sub> (0.2)	CuBr <sub>2</sub> (1)	DMF (0.2 M)	17	0	0	Complex Mix

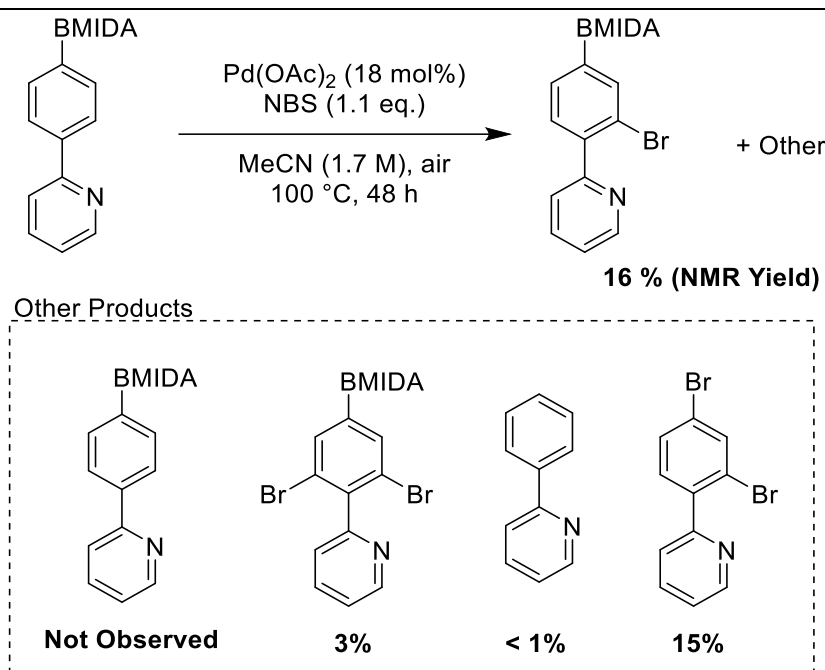
Table 8: Results of MIDA-boronate orthogonality screening study

Employing copper salts resulted in a high proportion of the deborylated 2-phenylpyridine (Entries 1-2), no 2-phenylpyridine was observed in a Rh(II) catalysed functionalisations (Entry 3-4), although both formed a complex mixture that was difficult to elucidate any information from.

Although entries 5-8 and 10 were unsuccessful, the palladium(II) catalysed processes often returned the MIDA-boronate starting material, suggesting some degree of orthogonality. But complex mixtures and poor mass balances from these reactions made it difficult to identify the by-products. Where mass balance is low, it was speculated that *ortho*-metallation may yield a homo-coupled product, dimerising the starting material and/or the desired product, such palladium(II) catalysed dimerisation has been previously disclosed in the literature.<sup>[249-252]</sup>

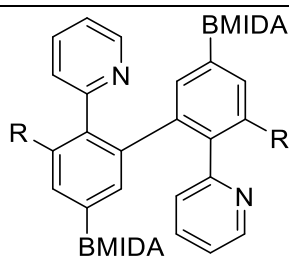
MIDA-boronates are known to have some solubility issues, only dissolving in polar aprotic solvents such as acetonitrile or THF, only two reactions employ acetonitrile. It was expected that the high reaction temperatures would allow the MIDA-boronate to dissolve, however if this were not the case, or if only partial dissolution would occur. Partial dissolution would limit the rate of functionalisation and potentially encourage undesirable side reactions to occur.

A palladium acetate catalysed bromination in acetonitrile yielded the desired *ortho*-brominated product (entry 9), albeit in a low 16 % yield. The C-H *ortho*-bromination of 2-phenylpyridine was first described by Sanford *et al.* in 2006, [128] the conditions used originate from an optimisation of this chemistry by Togni *et al.*[248] The desired transformation for the bromination of our BMIDA-containing phenyl pyridine is described in Scheme 136. Full consumption of the starting material was observed and the ratio of desired product and by-products were quantified by NMR spectroscopy using 1,3,5-trimethoxybenzene as an internal standard.



*Scheme 136: Desired bromination of BMIDA containing 2-PhenylPyridine following conditions disclosed by Togni et al.*

The desired product, was observed in a 15% yield, along with the dibrominated product (3%). Alongside these we were able to observe 2 deborylation products: 2-phenylpyridine, was observed albeit in trace amounts (<1 %), we also observed a dibrominated product, in a 15 % yield. It should also be noted that we were only able to isolate a total mass balance of 34 %, thus other products are formed, but unfortunately not isolated. It is possible that this may be a result of homocoupled products, as these will have a high polarity and would likely streak and move slowly on a column causing fractions to have too low a concentration for detection ().



**R = H or Coupled Product**

*Scheme 137: Suspected highly polar family of by-products accounting for low mass balance*

Although the success of the bromination indicated, as a proof-of-concept, that C-H functionalisation can be achieved in the presence of a BMIDA moiety, some optimisation was required to minimise the cleavage of the C-B bond which still showed some issues with orthogonality, and try to ascertain an explanation on the drop in yield from 72 % for 2-phenylpyridine (from the conditions used by Togni *et al.*<sup>[248]</sup>) to 16 % when a MIDA-boronate is present on the molecule.

Based on a range of reaction conditions discussed by Sanford *et al.* we set out to expose the starting material to a series reaction conditions altering only a single variable at a time, to ascertain the effects of different variables on MIDA-boronate orthogonality more accurately.

*Table 9: Series of C-H functionalisation conditions used to explore the successful C-H bromination reaction*

Entry	Cat. (mol%)	RX (eq.)	Solvent (M)	T (°C)	Time (h)	% Yield
1	Pd(OAc) <sub>2</sub> (18)	NBS (1.2)	MeCN (1.7)	100	18	16 <sup>a</sup>
2	Pd(OAc) <sub>2</sub> (5)	NBS (1.2)	MeCN (0.15)	100	18	<b>40<sup>b</sup></b>
3			AcOH (0.15)	100	18	11 <sup>a</sup>
4		NCS (1.2)	MeCN (0.15)	100	18	<b>56<sup>a</sup>/16<sup>c</sup></b>
5		NIS (1.2)	MeCN (0.15)	100	18	Complex Mix
6		PhI(OAc) <sub>2</sub> (1.2)	MeCN (0.15)	100	18	Complex Mix
7		Ph <sub>2</sub> IBF <sub>4</sub> (1.2)	MeCN (0.15)	100	18	Complex Mix

a = NMR yield. b = calculated from mixture SM:P of 1:8.3. c = calculated from mixture SM:P of 1:1.3 on separate run

A low catalytic loading of palladium(II) acetate and a reaction concentration 0.15 M in acetonitrile resulted in a 40% yield of the desired product (entry 2), improving the yield from entry 1. Under these conditions only unreacted starting material and desired product were observed, indicating that lower catalytic loading was necessary to reduce defunctionalisation and *ipso*-substitution. Efforts

to purify the MIDA-compound were unsuccessful due to co-elution of the product with the starting material.

Acetic acid had also been shown to be a suitable solvent for this reaction, yielding the desired product in an 11% yield by  $^1\text{H}$  NMR spectroscopy.

Entries 5-8 aimed to observe whether other coupling can be achieved under the same conditions changing only the coupling partner. Altering the halogenation reagent to *N*-chlorosuccinimide (entry 5) produced an *ortho*-chlorinated product in a 56%. This product is less susceptible to oxidative addition, perhaps explaining the increased yield over *ortho*-bromination, where oxidative addition may occur in the presence of palladium(0) this hypothesis is supported by entry 6, where no desired product was observed when employing NIS.

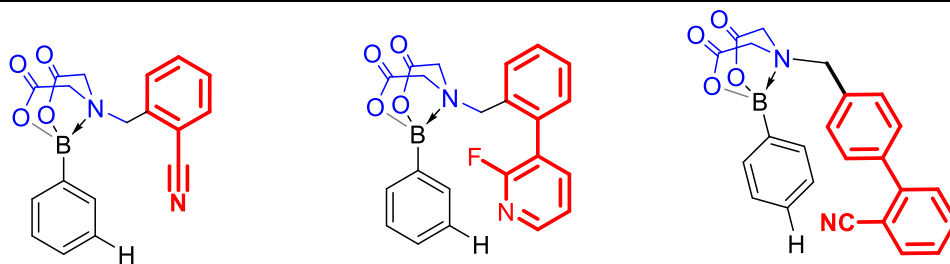
Acetoxylation was also attempted (entry 7), swapping the halogenating reagent for diacetoxy iodobenzene. The hypervalent iodine(III) reagent is able to perform as a co-oxidant and an acetylating agent. However a mixture of products were produced in this reaction, of which the individual products were difficult to elucidate. A complex mixture was also observed with an attempted arylation using a biaryl iodonium salt (entry 8).

Attempts to isolate both the chlorinated and brominated products were made, unfortunately MIDA-compounds tended to co-elute with one another, thus yields were calculated from mass of the mixture and the ratio components within that mixture. Displacement of MIDA-boronates with pinacol may be done to allow easier purification.

Further optimisations were not performed, these studies indicated that palladium-catalysed C-H functionalisation can be performed in the presence of a MIDA-boronate. It is probable that full solubilisation of MIDA-boronates is key to achieving C-H functionalisation, this does limit the choice of solvents but several C-H functionalisation methods in acetonitrile have been described in the literature.

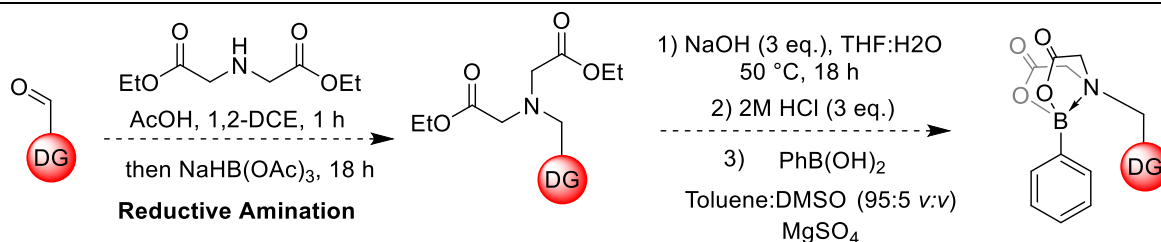
With the feasibility of TIDA-orthogonality showcased, the synthesis of TIDA-boronates was performed.

### 3.3. Synthesis of TIDA-Boronates



Scheme 138: TIDA-boronate synthetic targets

A generalised approach was proposed for the synthesis of each TIDA-boronate target (Scheme 138), starting with the relevant benzaldehyde derivatives as starting materials. A reductive amination would then be performed on each benzaldehyde to install diethyl iminodiacetate, which would then, after saponification, undergo a condensation reaction with phenyl boronic acid to produce the desired set of TIDA-boronates (Scheme 139).



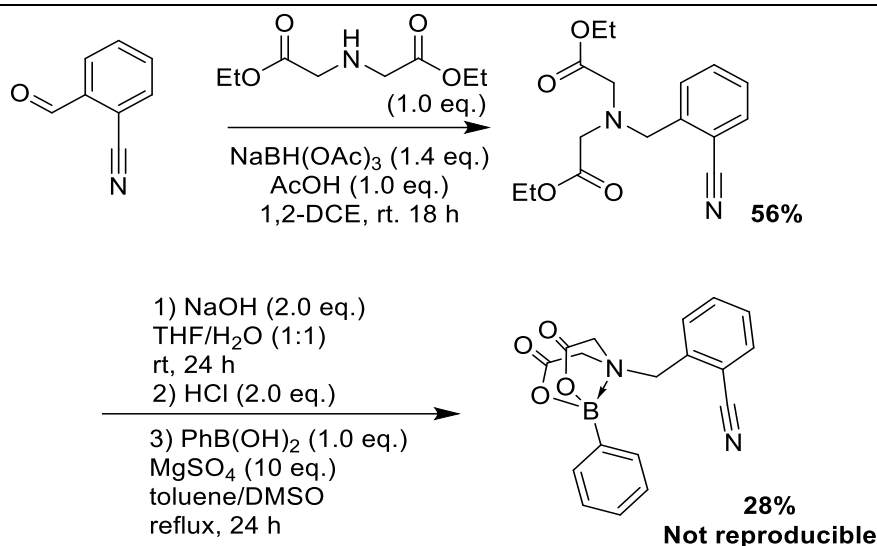
Scheme 139: Proposed route for synthesis of a series of TIDA-Boronates

For 2-Cyanobenzaldehyde was purchased and used without further purification, whilst 4-(2-cyanophenyl)benzaldehyde and 2-(2-fluoro-3-pyridyl)benzaldehyde were synthesised *via* the Suzuki-Miyaura cross-coupling previously described in Section 2.6.2.

For each aldehyde starting material, a reductive elimination was performed with diethyl iminodiacetate and sodium triacetoxyborohydride in the presence of acetic acid in dry 1,2-DCE.

***N*-(2-cyanobenzyl)iminodiacetate** – The reductive amination and condensation to yield the TIDA-boronate was reported by Chi-Kin Wong, a previous member of

the Storr group, it was then reported that the condensation was successful describing a 28 % yield. Some efforts to reproduce these results were unsuccessful, facing similar difficulties in isolation for the TIDA-boronates which are discussed for the 4-(2-cyanophenyl)benzyl iminodiacetate product.



*Scheme 140: Synthesis of TIDA-X reported by Chi-Kin Wong, a previous member of the Storr Lab.*

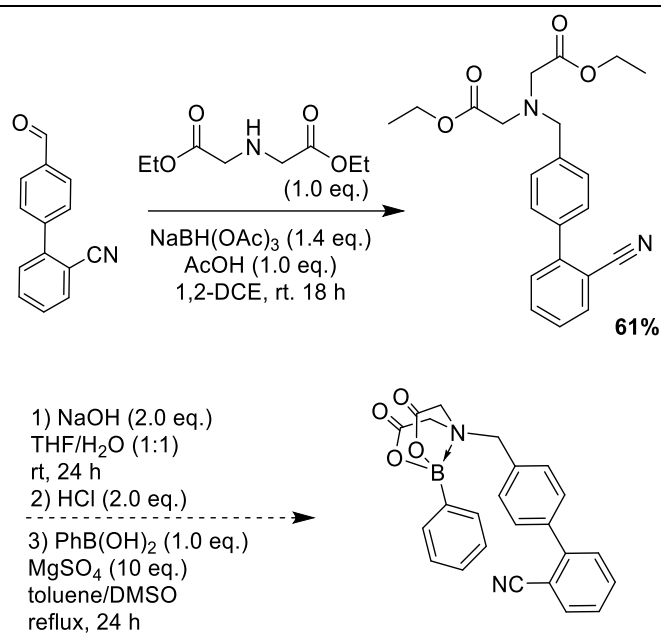
---

**N-4-(2-cyanophenyl)benzyl iminodiacetate** - The reductive amination to produce the TIDA-boronate was straightforward and could be achieved on scale with a good yield (Scheme 141). However, when attempting to perform the subsequent hydrolysis and condensation step to produce the desired TIDA-boronate, a series of attempted syntheses were unsuccessful. The hydrolysis of the esters was performed overnight at an elevated temperature to ensure maximum conversion to the desired diacetate product. The acid work-up then formed the corresponding HCl salt of the TIDA-compound (water was removed *in vacuo*).

The resulting salt was dissolved in toluene and DMSO (the salt was not soluble in toluene alone), 10 equivalents of dried magnesium sulfate were used to remove water from the reaction by formation of the hydrate of magnesium sulfate. This was refluxed overnight and then the solvent was removed *in vacuo*.

It was found that DMSO was problematic in the synthesis of these compounds, drying *in vacuo* was not possible, blowing down overnight with argon was not

successful, an aqueous work-up was attempted but the compound likely decomposed due to poor hydrolytic stability.



Scheme 141: Synthesis of TIDA-X targeting para-selective C-H functionalisation

Thus, column chromatography was attempted by dry loading the residue onto a silica. The column was first flushed with ether to remove any non-TIDA organic components of the crude residue, then flushed with a THF mobile phase to elute the TIDA-boronate. Upon removal of solvent *in vacuo*, a viscous oil was realised. Based on literature precedent, it was expected that the TIDA compound would be a solid, a complex mixture was observed by <sup>1</sup>H NMR spectroscopy, with broad peaks indicating a transient coordination.

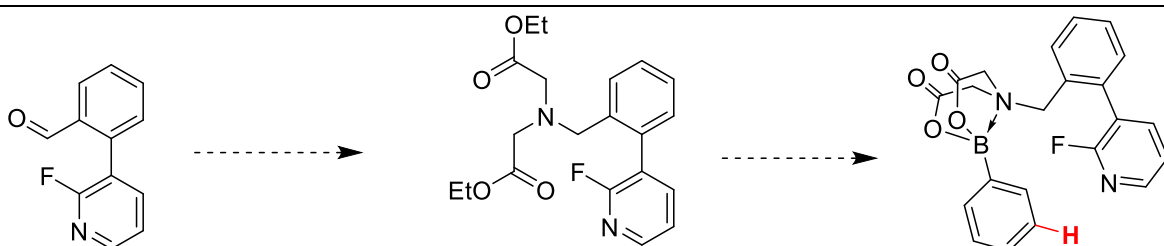
On a separate attempt at formation, a trituration work-up was also attempted, wherein a minimal amount of acetone was added to help dissolve the crude residue, then, an excess of diethyl ether was added as an anti-solvent. A solid white precipitate was observed, however upon attempts to collect the solid by vacuum filtration, once exposed to air, the solid turned to an oil, and was not recovered from the filtrate. Broad peaks were observed in the <sup>1</sup>H NMR spectra, again indicating a transient interaction of the TIDA-ligand with the boronic acid.

This observation led us to believe that the TIDA-boronate was not hydrolytically stable, although this would make the compound difficult to use in the project, we set out to test this hypothesis. We reattempted the synthesis under an argon atmosphere; solvent was then removed *in vacuo* and the vessel backfilled

with argon. Upon retrying the trituration under an argon atmosphere, a solid white precipitate was again observed; the diethyl ether was then removed by canular filtration using a positive argon pressure. However, once the solvent was fully removed the compound again began to convert to an oil. Broad peaks were again observed in the  $^1\text{H}$  NMR spectra, again indicating a transient interaction of the TIDA-ligand with the boronic acid.

Evidence for the formation of this product has since been reported.<sup>[253]</sup> The TIDA-boronate was produced in an 88 % yield from the diacid ammonium salt, by microwave radiation in acetonitrile to 130 °C for 30 minutes. The product was then isolated by column chromatography, flushing with diethyl ether to remove non-TIDA components of a reaction mixture and releasing the TIDA-boronate using acetonitrile. This led to the conclusion that DMSO was problematic in the synthesis of the desired TIDA-boronate. Potentially a co-crystallisation of the TIDA-boronate with DMSO occurs upon addition of diethyl ether, and the DMSO co-elutes on a column resulting in oiling upon removal of the solvent. An approach, such as the high temperature microwave reaction described in the literature, avoiding the use of DMSO, should be used to produce these compounds in the future. Unfortunately, time-constraints meant this compound was not explored further in this project.

**N-2-(2-Fluoro-3-pyridinyl)benzyl iminodiacetate** - Unfortunately the reductive amination of 2-(2-fluoro-3-pyridyl)benzaldehyde did not result in the desired product instead producing a complex mixture that was ultimately difficult to elucidate information from. The presence of acid may have catalysed an intramolecular  $\text{S}_{\text{N}}\text{Ar}$  *via* protonation of the pyridyl ring enhancing the electrophilicity of the 2-fluoropyridyl moiety thus promoting an undesired over-reaction, a complex mixture was eventually realised with no resonances observed in the  $^{19}\text{F}$  NMR spectra after work-up. Thus, a second route was proposed to avoid the need for the acidic reductive amination step.

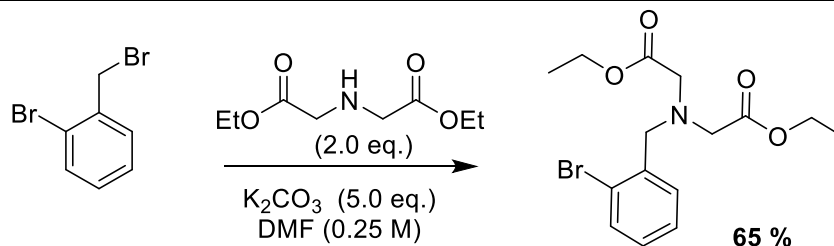


*Scheme 142: Initial Route for synthesis of TIDA-X targeting meta-selective C-H functionalisation using a pyridyl directing group*

---



An  $S_N2$  displacement of the  $C(sp^3)$ -Br of 2-bromobenzyl bromide was performed by heating the benzyl bromide in DMF for 18 hours at 70 °C in the presence of 3 equivalents of potassium carbonate and two equivalents of diethyliminodiacetate. The reaction successfully afforded the desired product, in a 63 % yield (Scheme 143).

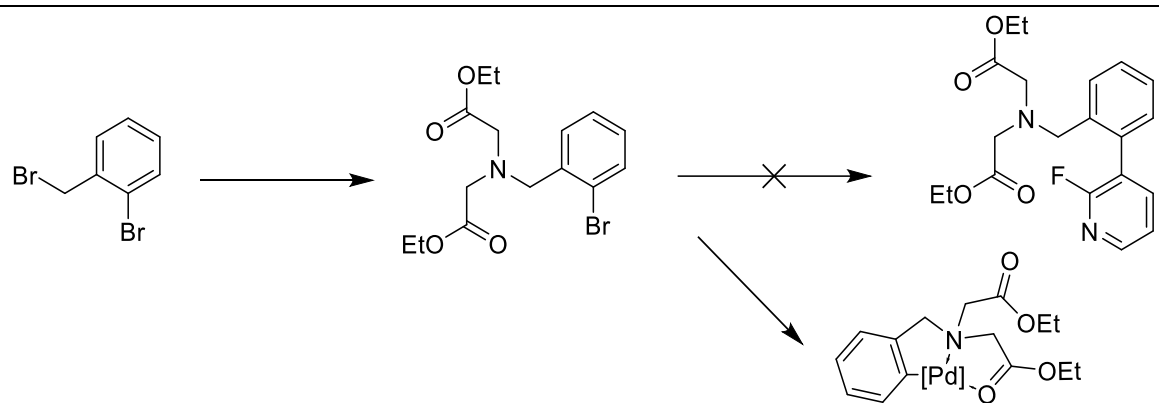


*Scheme 143:  $S_N2$  displacement of a benzyl bromide with diethyl iminodiacetate affords the desired *N,N*-bis(ethoxycarbonylmethyl)-2-bromo-benzylamine*

---

We next attempted a Suzuki-Miyaura cross-coupling reaction on the brominated TIDA-precursor, attempting to couple with 2-fluoro-3-pyridyl boronic acid. The conditions, based on those described in Chapter 2, was catalysed by 5 mol% of palladium(II) acetate and 10 mol% of XPhos in a 2:1 mixture of THF and a saturated aqueous solution of sodium hydrogen carbonate. The reaction was heated to 80 °C overnight. Unfortunately, analysis of the reaction TLC and crude NMR indicated retention of the starting material, with the aryl boronic acid removed in the basic aqueous work-up and thus not detected in the crude NMR (Scheme 144).

Although not detected, we hypothesise that the organometallic intermediate arising from the oxidative addition of a palladium(0) complex across the C-Br bond was stabilised by the diethyl iminodiacetate moiety forming a stable organometallic intermediate preventing turnover of the catalytic reaction, similar intermediates have been previously isolated in the literature.<sup>[254-256]</sup>



*Scheme 144: Unsuccessful alternative route for the synthesis of TIDA-X*

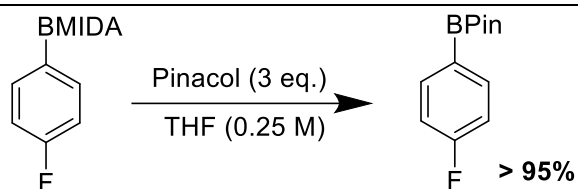
---

Further attempts at synthesis were not performed due to time constraints, although using the 4-fluoro analogue, as was done in Chapter 2.6, may be suitable for future investigations.

Unfortunately, without successful isolation of the desired TIDA-boronates, screening for efficiency in C-H functionalisation was not possible.

As these TIDA compounds were found to be difficult to purify, obtaining isolated yields from screening reactions may be problematic. One strategy to overcome this is to add an excess of pinacol in the work-up, converting the highly polar TIDA-group to a non-polar pinacol boronic ester which is stable to aqueous work-up and can be isolated rapidly by column chromatography. MIDA-boronates were found to tail significantly under gas chromatography, however pinacol boronic esters give sharper peaks in the gas chromatograph. Therefore, by converting to the corresponding pinacol boronic acid ester, future screening reactions will be able to be subjected to analysis by GC-MS, allowing for a high-throughput analysis approach, as per the GC-MS screening detailed in Chapter 2.7.

To ascertain if such a work-up strategy could be employed with the TIDA-compounds produced, a simple study was performed. 3 equivalents of pinacol were added to 4-fluorophenyl MIDA-boronate and dissolved in THF. This solution was then heated to 90 °C for 1-hour whereafter it was dried *in vacuo*. Upon addition of chloroform, a white precipitate was produced corresponding to *N*-MIDA iminodiacetic acid, and the solute contained 4-fluorophenyl pinacol boronic acid ester, afforded in a >95% isolated yield (Scheme 145).



*Scheme 145: Displacement of tridentate MIDA-ligands can be achieved by addition of an excess of pinacol*

---

# Chapter 4

## Conclusions

## 4. Conclusions

### 4.1. Summary

Organoboronic acids have excellent synthetic utility, able to undergo a series of functional group interconversions. As organoboronic species are reactive to a wide range of reaction conditions, they are often employed in multi-step syntheses as a transitory functionality, installed as a means to undergo a chemical reaction. Transitory or sacrificial use of functionalities is neither step- nor atom-economical, and boronic moieties have the potential to improve the efficiency of chemical reactions.

Boronic moieties, bear an unoccupied  $p_z$ -orbital allowing them to rapidly and reversibly switch from a 3-coordinate neutral species to a 4-coordinate anionic species. The field of directed C-H functionalisation is currently exploring different transient interactions to realise a desired transformation, and this project aimed to design a Lewis acid – Lewis base pairing strategy between a organoboronic substrate and a directing ligand bearing a Lewis basic moiety.

The orthogonality of C-B bonds in transition metal catalysed methodologies was discussed in Chapter 1. The need to preclude transmetallation was shown to be possible, with two strategies proposed: 1) Anhydrous reaction conditions; transmetallation required hydroxide to proceed, however this strategy requires extensive drying of reagents as even small quantities of water can promote transmetallation; 2) Blocking access to borons  $p_z$ -orbital; transmetallation requires access to the  $p_z$ -orbital in order to form a M-O-B bridge intermediate primed for transmetallation.

This aim of this project was not fully realised, however a body of information as to the feasibility of this aim has been disclosed. A pipeline for designing, synthesising and screening bespoke ligands for directed C-H functionalisation of boronic esters has been developed. The pipeline initiates at deriving ligand designs from literature precedent, synthesising the ligands on scale, testing for transient coordination to a boronic substrate before performing high-throughput screening analysed by GC-MS.

Lewis basic alkoxides were chosen due to their ability to rapidly form boronate species *in situ*, with a series of fluorinated aryl alkoxy pinacol boronates characterised using NMR techniques. The alkoxy pinacol boronates were shown to form rapidly and transiently, this behaviour was deemed to be ideal for a transient directing group approach (See Chapter 1.7.4).

A  $^{19}\text{F}\{^1\text{H}\}$  qNMR methodology was developed to allow for quantitative analysis of these boronate species. This method was not actually utilised within the work disclosed in this thesis, boronates were found to form quantitatively in the presence of at least 1 equivalent of alkoxide. Where less than an equivalent of alkoxide base was added, there was a significant broadening of fluorine resonance peaks, indicating a rapid ligand exchange between free boronic species and the corresponding boronates. Decreasing the NMR acquisition temperature may have resolved this broadening, unfortunately  $d^6$ -DMSO was found to be the best solvent for studying alkoxy pinacol boronates, and due to a relatively high melting point, DMSO is not suitable for low temperature NMR acquisitions. Future rate or equilibrium studies may utilise the NMR protocol, this may be especially helpful for optimisation.

DFT studies were performed which indicated that the bond dissociation energy is inversely proportional to the  $\text{p}K_{\text{a-H}}$  of each alkoxide, with adverse steric interaction between the alkoxide and pinacol moiety outweighing the desirable binding affinity as described by  $\text{p}K_{\text{a}}$ . This data indicated that less sterically bulky alkoxides would outcompete more sterically bulky alkoxides. Hydroxide was found to greatly outcompete alkoxides both in the DFT studies and observed experimentally by NMR techniques when running a study without sufficient removal of water prior. This was especially an issue with  $d^6$ -DMSO which is hygroscopic and thus required drying over molecular sieves before use, and lead to alkoxy-boronate NMR samples left open to the air converting to the hydroxy-boronate over time. This information indicated that anhydrous reaction conditions were necessary.

Five alkoxide templates were devised based on literature precedent. Of these 3 were successfully synthesised, one was used as purchased and a fifth was found not to be bench stable. Treatment of these with base resulted in one undergoing a  $\text{S}_{\text{N}}\text{Ar}$  reaction thus making it inappropriate for further use. Therefore, studies continued

with 3 ligands: Dimethyl ethanolamine, 2-pyridyl methanol and 4-(2-cyanophenyl)benzyl alcohol. Co-ordination to an aryl boronic acid under basic conditions was performed, with the resulting substrate-ligand complexes characterised by  $^{19}\text{F}$ ,  $^1\text{H}$  and  $^{11}\text{B}$  NMR.

There were difficulties in identifying a metal-ligand-substrate ternary complex using stoichiometric studies. Addition of palladium pivalate to the substrate-ligand complex, of 4-(2-cyanophenyl)benzyl alcohol, seemed to form a new boronate species, but attempts to elucidate more information were unsuccessful due to transmetallation of boronic ester substrate. A hypothesis was made, that the undesired transmetallation was expedited by the high concentration of metal salt. Therefore, studies should use loadings of metal more representative of the reactions that would be performed. To do this, and hopefully find a principal protocol which could be optimised, a C-H functionalisation screening study was performed, using GC-MS to rapidly analyse reaction mixtures.

A series of literature derived screening conditions were chosen, to cover a range of catalysts, coupling partners, additives, solvents, atmospheres, and temperatures, to attempt to identify conditions that not only gave rise to a desired C-H functionalisation, but also the types of conditions that lead to a yield of undesired by-products, namely *ipso*-substitution products arising from the undesired transmetallation pathway. We chose to analyse the mixtures by GC-MS analysis as this allowed for rapid analysis of complex mixtures.

Across 74 screening reactions, a reasonable amount of evidence was collected to suggest that alkoxy pinacol boronates are unlikely to be a suitable Lewis acid - Lewis base pairing for a transient directing group strategy for C-H functionalisation. No screening reaction yielded any detectable quantity of desired product, with different conditions varying as to the degree of transmetallation.

A large proportion of the screening resulted in an undesired *ipso*-substitution. The overriding issue with the alkoxide-bound pinacol boronates approach is the competition between the metal catalyst and boron for complexation.

To strengthen the ligand-substrate complex, the mode of connection was changed from a monodentate coordination to a tridentate coordination. MIDA-boronates had excellent utility as protecting groups for boronic acids, and their *N*-

methyl group was a suitable handle for installation of a directing moiety; the synthesis of a selection selection of N-templated iminodiacetate (TIDA) protecting-directing groups was attempted.

The TIDA-boronates would permanently occupy of the boron centres empty  $p_z$  by the dative covalent binding with the amine lone pair, combined with the electron withdrawing properties of the two co-ordinated carboxylate moieties results in a protection of the C-B bond, dramatically slowing the rate of transmetalation. As such, at the cost of a transient co-ordination mode, we proceeded to begin development of an auxiliary directed C-H functionalisation with the perspective of taking findings of this approach and being able to apply this to a more transient system later.

As an initial proof-of-concept study, the MIDA moiety was shown to perform orthogonally in 2 C-H functionalisation methodologies performed on a 2-phenylpyridine bearing a BMIDA-moiety. The successful reactions were disclosed without optimisation. Chlorination with NCS and  $\text{Pd}(\text{OAc})_2$  was afforded in a yield 56% yield, and bromination with NBS and  $\text{Pd}(\text{OAc})_2$  was afforded in 40% NMR yield. These compounds were unfortunately difficult to purify, transesterification with pinacol is a possible and may allow for an easier purification by column chromatography.

Attempts to then synthesise target TIDA-boronates were ultimately unsuccessful and were eventually found to be a result of solvent related issues. DMSO was used for the synthesis of the compounds and was ultimately difficult to remove. Future syntheses of these compounds may wish to use other protocols detailed in the literature, including microwave irradiation to 130 °C in MeCN.<sup>[253]</sup>

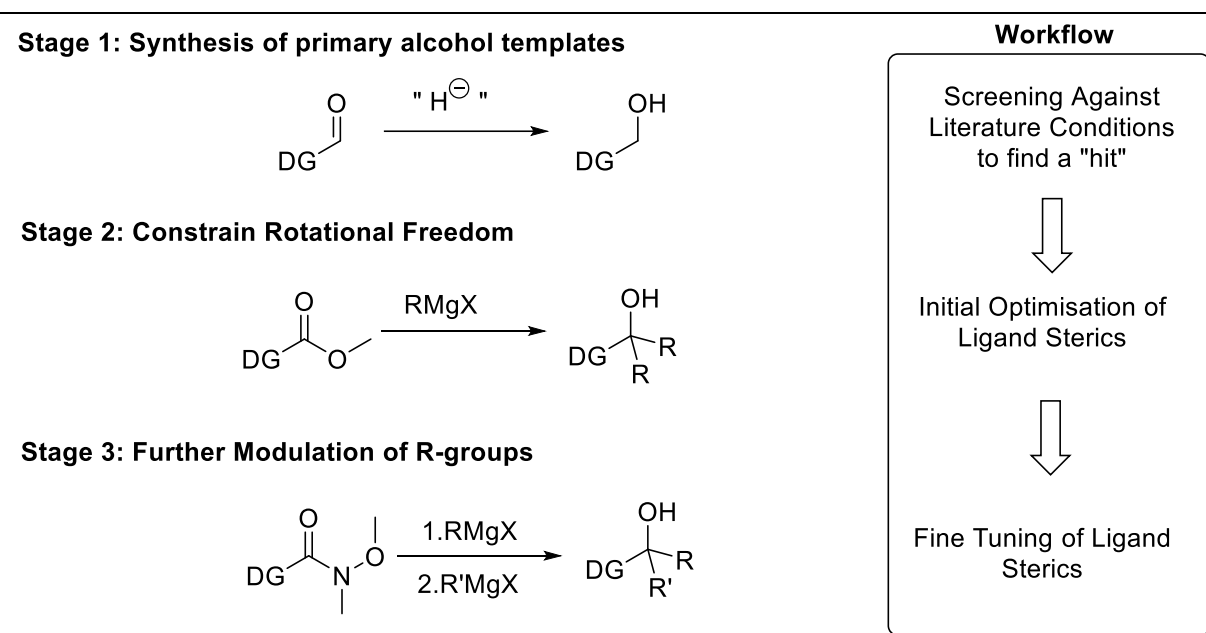
## 4.2. Future Work

There are indications that C-H functionalisation of pinacol boronic acid esters using alkoxide ligands is feasible, however further investigations are required to realise a desired transformation. A wide variety of ligands could be proposed however, it is difficult to determine which deviation from literature precedent (ligand structure, substrate or co-ordination mode) renders the conditions unable



to fulfil a desired reaction; studies which isolate these deviations should therefore be performed. In the next chapter, Chapter 3, the co-ordination mode is modified such that the ligand structure can be probed, whilst reinforcing both the substrate C-B bond stability and the stability of the ligand-substrate interaction, opting for a tridentate co-ordination, using MIDA derived templates.

Studies however could be performed on the co-ordination mode, whilst fixing both ligand structure and the substrate. The ligands proposed and synthesised have potential for modification, which may enhance both the steric and electronic favourability of forming pinacol alkoxy boronates *in situ*. A simple point of elaboration is the benzylic position of the appropriate ligands, where a variety of different R-variable groups may be installed by Grignard addition to a benzoate ester, further modification may then be realised by successive Grignard additions to a Weinreb amide, as to fine-tune (Scheme 146).

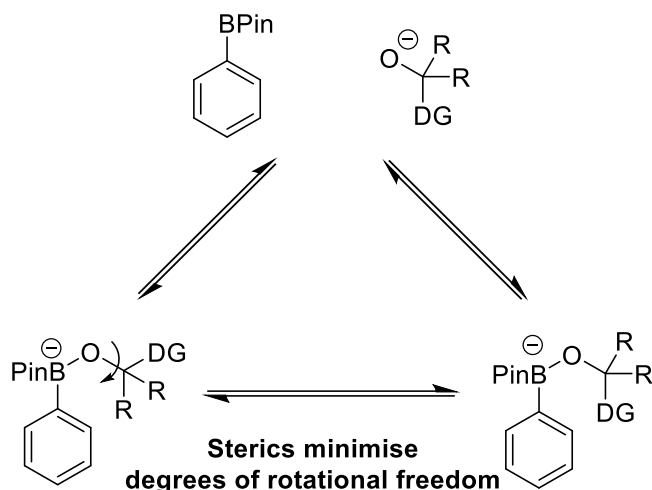


Scheme 146: General Workflow for Synthesis of Bifunctional ligands to screen

Through modulation of R-groups the steric and electronic properties of the corresponding boronates could be controlled to decrease the ground state energy of the desired rotational conformer, by promoting a desirable rotational conformation and modulating the B-O bond strength (Scheme 147).

---

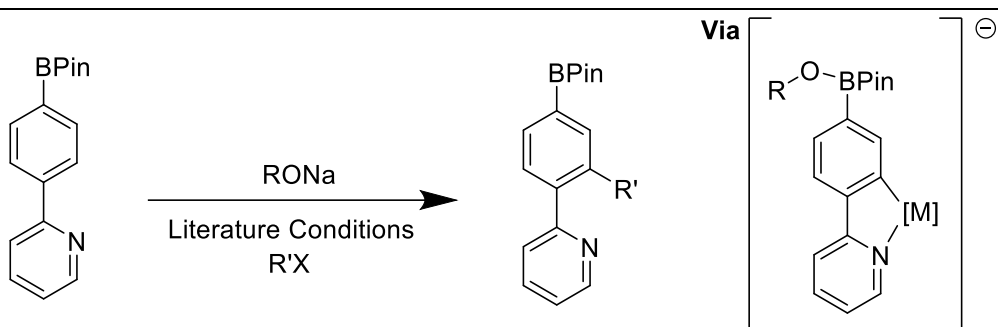
Dissociation affected by B-O bond strength  
dependent on both sterics and electronics



Scheme 147: Importance of variable R-groups in success of Ligand designs

---

This approach does however require an initial successful ligand to modify, else determining the suitability of each derivative becomes difficult to impossible. It may be that the use of alkoxides, creates relatively harsh conditions which inhibit the desired C-H functionalisation. The efficacy of C-H functionalisation in the presence of pinacol alkoxy boronate could therefore be studied using a benchmark substrate such as 2-phenylpyridine (Scheme 148); a similar study for MIDA-boronates was performed in Chapter 3.2.



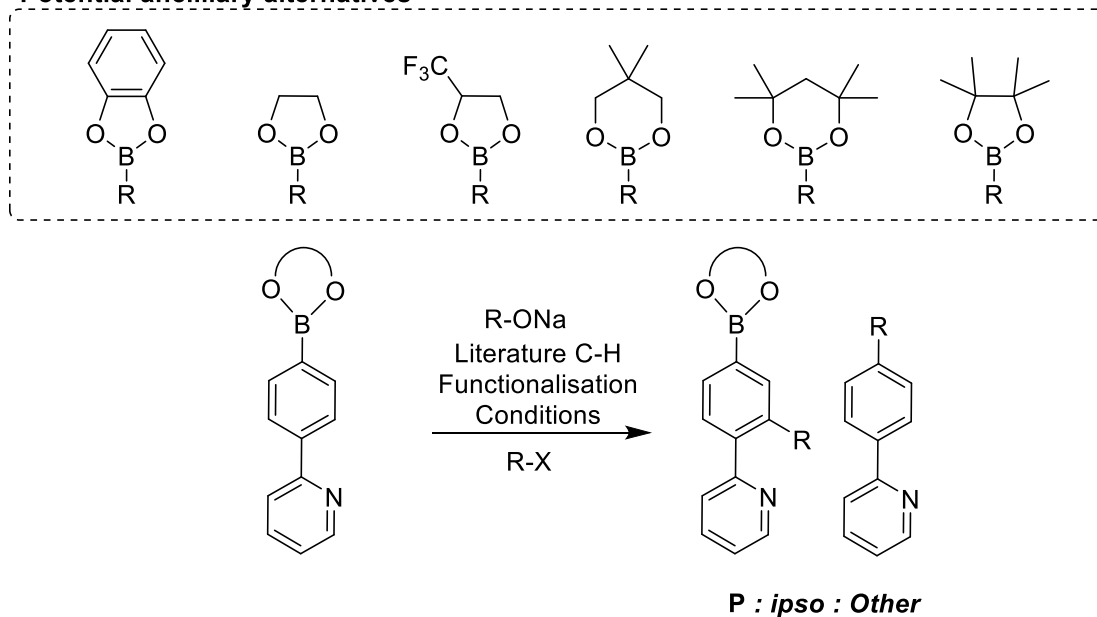
Scheme 148: Screening C-H functionalisation in the presence of a pinacol alkoxy boronate to indicate if the choice of co-ordination mode is feasible.

---

Substrate modifications would also be a suitable avenue for further investigation, the wide use of aryl pinacol boronic esters led to an investigative

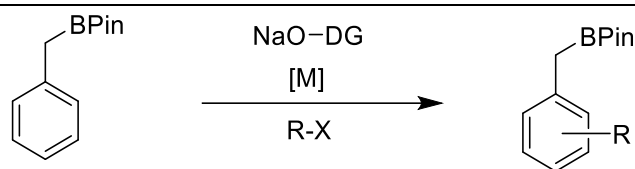
focus on these substrates. Modifications could be made to the choice of ancillary group, as various diols exist in the literature that may be more suitable for enhancing transmetallation orthogonality, utilising electronic and steric factors to reinforce the strength of an intermediate alkoxy-pinacol boronate and further destabilise the transmetallation transition state (Scheme 149). These studies can be performed on a benchmark substrate such as a 2-phenylpyridine derivative, further derivatisation of these diols can then be performed to improve the reaction yield if required.

Potential ancillary alternatives



*Scheme 149: Variation of Protecting groups on Boron may be studied to enhance C-B orthogonality*

If aryl C-B bonds are found to be unsuitable for this approach it may also be of interest to investigate the efficacy of C-H functionalisation in the presence of a C(sp<sup>3</sup>)-boronate. Transmetallation of C(sp<sup>3</sup>)-B bonds is slower than C(sp<sup>2</sup>)-B bonds, however where transmetallation does occur, a  $\beta$ -hydride elimination may rapidly occur. To avoid this potential pitfall, benzylic boronic acid esters may be investigated, literature precedent shows that under some Suzuki-Miyaura cross-coupling conditions these substrates are unreactive (Scheme 150).<sup>[62]</sup> The feasibility of this approach may also be tested using a suitable derivative of 2-phenylpyridine.



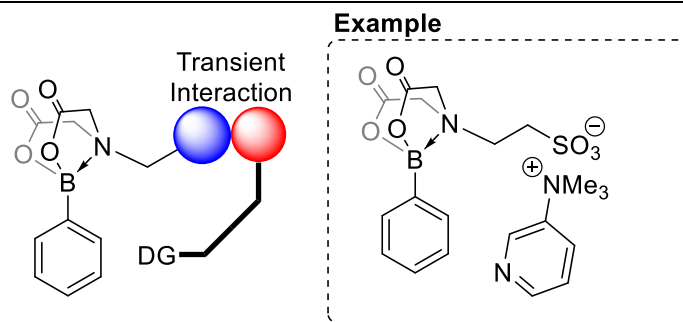
*Scheme 150: Changing to a C(sp<sub>3</sub>)-B substrate which transmetalate slower than C(sp<sub>2</sub>)-B bonds*

---

Alkoxide co-ordination was chosen because boronate species have been shown to be inert to transmetalation, furthermore more weakly co-ordinating functionalities that may be proposed such as carboxylates and thioethers were found in initial NMR studies not to produce observable co-ordination on the NMR timeframe. This suggested that ligands supporting these tethering-functionalities would likely fail to inhibit transmetalation, however, saturation of pinacol boronic acid esters with a Lewis base to yield boronates is only one approach to realising transmetalation orthogonal reactivities. If a suitable catalyst system, or C-B protecting group can be found that creates a significant barrier to transmetalation then saturation of boronic acid esters to their corresponding boronates would become less necessary, and weaker co-ordinating functionalities such as carboxylates and thioethers may be explored.

Monodentate ligands may be found to be unsuitable for directed C-H functionalisation, hence a small amount of work was done to explore TIDA-boronates. These initially can be developed as directing auxiliaries, but there is a literature indication that these may be developed into transient directing groups. Fyfe *et al.* showed that a BPin and BMIDA moieties slowly exchange protecting ligand. Thus, a reaction system could be designed in which a TIDA-auxiliary is employed in catalytic quantities.

Furthermore, the TIDA-boronate may not need to be a directing group bearing auxiliary, but rather a simpler system able to accept different modes of co-ordination. For example, a sulfonate group may be added in order to allow for ionic interactions between the TIDA-boronate and a range of *ortho*-, *meta*- and *para*-selective ammonium-bearing ligands (Scheme 151). This ionic binding has been disclosed by the Phipps group.<sup>[161,257]</sup>



*Scheme 151: Transient linkage may be moved from the boron centre to a functionality on the TIDA-boronate, potentially allowing ionic interactions between a substrate and ligand to be utilised*

---

## 5. References

- [1] D. R. Lide (ed.), in *CRC Handbook of Chemistry and Physics*, **2017**, pp. 14–17.
- [2] T. Türkbay, B. Laratte, A. Çolak, S. Çoruh, B. Elevli, *Sustainability (Switzerland)* **2022**, *14*, DOI 10.3390/su14031787.
- [3] A. Briocche, *Minerals Yearbook (Volume I.-- Metals and Minerals)*, USGS, **2018**.
- [4] E. Steponaitis, A. Andrews, D. McGee, J. Quade, Y. Te Hsieh, W. S. Broecker, B. N. Shuman, S. J. Burns, H. Cheng, *Quat Sci Rev* **2015**, *127*, 174–185.
- [5] J. Carter, *Inorg Chem* **1968**, *7*, 1945–1964.
- [6] A. J. J. Lennox, G. C. Lloyd-Jones, *Chem. Soc. Rev.* **2014**, *43*, 412–443.
- [7] C. C. C. Johansson Seechurn, M. O. Kitching, T. J. Colacot, V. Snieckus, *Angewandte Chemie - International Edition* **2012**, *51*, 5062–5085.
- [8] A. B. Pagett, G. C. Lloyd-jones, J. B. Building, D. B. Rd, **2020**, *100*.
- [9] A. Meudt, S. Nerdinger, B. Lehnemann, *Chim Oggi* **2004**, *22*.
- [10] A. Taheri Kal Koshvandi, M. M. Heravi, T. Momeni, *Appl Organomet Chem* **2018**, *32*, DOI 10.1002/aoc.4210.
- [11] X. F. Wu, P. Anbarasan, H. Neumann, M. Beller, *Angewandte Chemie - International Edition* **2010**, *49*, 9047–9050.
- [12] H. Doucet, **2013**, 2013–2030.
- [13] S. R. Chemler, D. Trauner, S. J. Danishefsky, *Angew. Chem. Int. Ed* **2001**, *40*, 4544–4568.
- [14] Y. P. Budiman, S. A. Westcott, U. Radius, T. B. Marder, *Adv Synth Catal* **2021**, adsc.202001291.
- [15] J. Plescia, N. Moitessier, *Eur J Med Chem* **2020**, *195*, 112270.
- [16] D. S. Matteson, *Journal of Organic Chemistry* **2013**, *78*, 10009–10023.
- [17] P. S. Baran, T. J. Maimone, J. M. Richter, *Nature* **2007**, *446*, 404–408.
- [18] M. V. Rangaishenvi, H. C. Brown, B. Singaram, *Journal of Organic Chemistry* **1991**, *56*, 3286–3294.
- [19] P. Ranjan, S. Pillitteri, G. Coppola, M. Oliva, E. V. Van der Eycken, U. K. Sharma, *ACS Catal* **2021**, *11*, 10862–10870.
- [20] I. B. Seiple, S. Su, R. A. Rodriguez, R. Gianatassio, Y. Fujiwara, A. L. Sobel, P. S. Baran, *J Am Chem Soc* **2010**, *132*, 13194–13196.
- [21] R. S. J. Proctor, R. J. Phipps, *Angewandte Chemie - International Edition* **2019**, *58*, 13666–13699.
- [22] A. S. Ivanov, A. A. Zhalnina, S. V. Shishkov, *Tetrahedron* **2009**, *65*, 7105–7108.
- [23] A. Kwong, J. D. Firth, T. J. Farmer, P. O'Brien, *Tetrahedron* **2021**, *81*, 131899.
- [24] D. S. Matteson, *ACS Symposium Series* **2016**, *1236*, 173–208.
- [25] D. Deb. Darwent, *Bond Dissociation Energies of Simple Molecules*, National Bureau Of Standards, Washington, **1970**.
- [26] S. A. Iqbal, J. Pahl, K. Yuan, M. J. Ingleson, *Chem Soc Rev* **2020**, *49*, 4564–4591.
- [27] S. A. Iqbal, J. Cid, R. J. Procter, M. Uzelac, K. Yuan, M. J. Ingleson, *Angewandte Chemie - International Edition* **2019**, *58*, 15381–15385.
- [28] G. A. Molander, S. L. J. Trice, S. M. Kennedy, S. D. Dreher, M. T. Tudge, *J Am Chem Soc* **2012**, *134*, 11667–11673.
- [29] J. S. Wright, P. J. H. Scott, P. G. Steel, *Angewandte Chemie - International Edition* **2021**, *60*, 2796–2821.
- [30] J. F. Hartwig, *Acc Chem Res* **2012**, *45*, 864–873.
- [31] M. E. D. Hillman, *J Am Chem Soc* **1962**, *84*, 4715–4720.
- [32] A. Fawcett, T. Biberger, V. K. Aggarwal, *Nat Chem* **2019**, *11*, 117–122.
- [33] M. Busch, M. D. Wodrich, C. Corminboeuf, *ACS Catal* **2017**, *7*, 5643–5653.

- [34] C. Amatore, A. Jutand, G. Le Duc, *Chemistry - A European Journal* **2011**, *17*, 2492–2503.
- [35] A. J. J. Lennox, G. C. Lloyd-Jones, *Angewandte Chemie International Edition* **2013**, *52*, 7362–7370.
- [36] J. Q. Chen, J. H. Li, Z. B. Dong, *Adv Synth Catal* **2020**, *362*, 3311–3331.
- [37] H. G. Cheng, H. Chen, Y. Liu, Q. Zhou, *Asian J Org Chem* **2018**, *7*, 490–508.
- [38] N. Miyaura, K. Yamada, A. Suzuki, *Tetrahedron Lett* **1979**, 3437–3440.
- [39] F. Firooznia, C. Gude, K. Chan, Y. Satoh, *Tetrahedron Lett* **1998**, *39*, 3985–3988.
- [40] B. P. Carrow, J. F. Hartwig, *J Am Chem Soc* **2011**, *133*, 2116–2119.
- [41] C. Sicre, A. A. C. Braga, F. Maseras, M. M. Cid, *Tetrahedron* **2008**, *64*, 7437–7443.
- [42] C. Amatore, A. Jutand, G. le Duc, *Chemistry - A European Journal* **2011**, *17*, 2492–2503.
- [43] I. Pantcheva, Y. Nishihara, K. Osakada, *Organometallics* **2005**, *24*, 3815–3817.
- [44] P. Zhao, C. D. Incarvito, J. F. Hartwig, *J Am Chem Soc* **2007**, *129*, 1876–1877.
- [45] A. A. Thomas, S. E. Denmark, *Science (1979)* **2016**, *352*, 329–332.
- [46] J. F. McGarrity, J. Prodoliet, *Journal of Organic Chemistry* **1984**, *49*, 4465–4470.
- [47] J. P. G. Rygus, C. M. Crudden, *J Am Chem Soc* **2017**, *139*, 18124–18137.
- [48] G. J. Lovinger, M. D. Aparece, J. P. Morken, *J Am Chem Soc* **2017**, *139*, 3153–3160.
- [49] V. Fasano, A. W. McFord, C. P. Butts, B. S. L. Collins, N. Fey, R. W. Alder, V. K. Aggarwal, *Angewandte Chemie - International Edition* **2020**, *59*, 22403–22407.
- [50] J. W. B. Fyfe, N. J. Fazakerley, A. J. B. Watson, *Angewandte Chemie International Edition* **2017**, *56*, 1249–1253.
- [51] N. Miyaura, A. Suzuki, *Chem Rev* **1995**, *95*, 2457–2483.
- [52] C. Morrill, R. H. Grubbs, *Journal of Organic Chemistry* **2003**, *68*, 6031–6034.
- [53] D. Imao, B. W. Glasspoole, V. S. Laberge, C. M. Crudden, *J Am Chem Soc* **2009**, *131*, 5024–5025.
- [54] G. Zou, Y. K. Reddy, J. R. Falck, **2001**, *42*, 7213–7215.
- [55] J. Chen, A. Cammers-Goodwin, *Tetrahedron Lett* **2003**, *44*, 1503–1506.
- [56] S. Napier, S. M. Marcuccio, H. Tye, M. Whittaker, *Tetrahedron Lett* **2008**, *49*, 6314–6315.
- [57] Y. Q. Mu, R. A. Gibbs, *Tetrahedron Lett* **1995**, *36*, 5669–5672.
- [58] J. Uenishi, J. M. Beau, R. W. Armstrong, Y. Kishi, *J Am Chem Soc* **1987**, *109*, 4756–4758.
- [59] C. Amatore, G. Le Duc, A. Jutand, *Chemistry - A European Journal* **2013**, *19*, 10082–10093.
- [60] S. C. Matthew, B. W. Glasspoole, P. Eisenberger, C. M. Crudden, *J Am Chem Soc* **2014**, *136*, 5828–5831.
- [61] Y. Lou, P. Cao, T. Jia, Y. Zhang, M. Wang, J. Liao, *Angewandte Chemie - International Edition* **2015**, *54*, 12134–12138.
- [62] C. M. Crudden, C. Ziebenhaus, J. P. G. Rygus, K. Ghazati, P. J. Unsworth, M. Nambo, S. Voth, M. Hutchinson, V. S. Laberge, Y. Maekawa, D. Imao, *Nat Commun* **2016**, 1–7.
- [63] S. Darses, G. Michaud, J. P. Genêt, *European J Org Chem* **1999**, 1875–1883.
- [64] A. J. J. Lennox, G. C. Lloyd-Jones, *J Am Chem Soc* **2012**, *134*, 7431–7441.
- [65] G. Berionni, B. Maji, P. Knochel, H. Mayr, *Chem Sci* **2012**, *3*, 878–882.
- [66] G. A. Molander, M. Ribagorda, *J Am Chem Soc* **2003**, *125*, 11148–11149.
- [67] G. A. Molander, N. M. Ellis, *J Org Chem* **2006**, *71*, 7491–7493.

- [68] G. A. Molander, R. Figueroa, *Org Lett* **2006**, *8*, 75–78.
- [69] G. A. Molander, D. E. Petrillo, *J Am Chem Soc* **2006**, *128*, 9634–9635.
- [70] G. A. Molander, R. Figueroa, *J Org Chem* **2006**, *71*, 6135–6140.
- [71] G. A. Molander, J. Ham, *Org Lett* **2006**, *8*, 2767–2770.
- [72] G. A. Molander, D. J. Cooper, *J Org Chem* **2008**, *73*, 3885–3891.
- [73] G. Tojo, M. Fernández, *Oxidation of Alcohols to Aldehydes and Ketones*, Springer, Boston, MA, **2006**.
- [74] W. P. Griffith, S. V. Ley, G. P. Whitcombe, A. D. White, *J Chem Soc Chem Commun* **1987**, 1625.
- [75] G. Matsuo, N. Hori, H. Matsukura, T. Nakata, *Tetrahedron Lett* **2000**, *41*, 7677–7680.
- [76] J. Aiguade, J. Hao, C. J. Forsyth, *Org Lett* **2001**, *3*, 979–982.
- [77] R. W. Hoffmann, G. Mas, T. Brandl, *European J Org Chem* **2002**, 3455–3464.
- [78] B. Schmidt, S. Krehl, A. Kelling, U. Schilde, *Journal of Organic Chemistry* **2012**, *77*, 2360–2367.
- [79] L. Grimaud, A. Jutand, *Synthesis (Germany)* **2017**, *49*, 1182–1189.
- [80] Y. Yamashita, J. C. Tellis, G. A. Molander, *Proceedings of the National Academy of Sciences* **2015**, *112*, 12026–12029.
- [81] T. Mancilla, R. Contreras, B. Wrackmeyer, *J Organomet Chem* **1986**, *307*, 1–6.
- [82] J. A. Gonzalez, O. M. Ogba, G. F. Morehouse, N. Rosson, K. N. Houk, A. G. Leach, P. H. Y. Cheong, M. D. Burke, G. C. Lloyd-Jones, *Nat Chem* **2016**, *8*, 1067–1075.
- [83] R. Contreras, C. García, T. Mancilla, B. Wrackmeyer, *J Organomet Chem* **1983**, *246*, 213–217.
- [84] G. Berionni, B. Maji, P. Knochel, H. Mayr, **2012**, 878–882.
- [85] E. P. Gillis, M. D. Burke, *J Am Chem Soc* **2007**, *129*, 6716–6717.
- [86] B. E. Uno, E. P. Gillis, M. D. Burke, *Tetrahedron* **2009**, *65*, 3130–3138.
- [87] C. P. Seath, K. L. Wilson, A. Campbell, J. M. Mowat, A. J. B. Watson, *Chemical Communications* **2016**, *52*, 8703–8706.
- [88] J. M. W. Chan, G. W. Amarante, F. D. Toste, *Tetrahedron* **2011**, *67*, 4306–4312.
- [89] E. P. Gillis, M. D. Burke, *J Am Chem Soc* **2008**, *130*, 14084–14085.
- [90] S. J. Lee, T. M. Anderson, M. D. Burke, *Angewandte Chemie - International Edition* **2010**, *49*, 8860–8863.
- [91] J. W. B. Fyfe, C. P. Seath, A. J. B. Watson, *Angewandte Chemie - International Edition* **2014**, *53*, 12077–12080.
- [92] J. W. B. Fyfe, A. J. B. Watson, *Synlett* **2015**, *26*, 1139–1144.
- [93] H. Noguchi, K. Hojo, M. Suginome, *J Am Chem Soc* **2007**, *129*, 758–759.
- [94] N. Iwadate, M. Suginome, *J Am Chem Soc* **2010**, *132*, 2548–2549.
- [95] R. G. Bergman, *Nature* **2007**, *446*, 391–393.
- [96] J. F. Hartwig, *Organotransition Metal Chemistry: From Bonding to Catalysis*, University Science Books, Sausalito, **2010**.
- [97] T. Gensch, M. N. Hopkinson, F. Glorius, J. Wencel-Delord, *Chem Soc Rev* **2016**, *45*, 2900–2936.
- [98] E. J. E. Caro-Diaz, M. Urbano, D. J. Buzard, R. M. Jones, *Bioorg Med Chem Lett* **2016**, *26*, 5378–5383.
- [99] K. Chen, X. Lei, *Curr Opin Green Sustain Chem* **2018**, *11*, 9–14.
- [100] T. Brückl, R. D. Baxter, Y. Ishihara, P. S. Baran, *Acc Chem Res* **2012**, *45*, 826–839.
- [101] W. R. Gutekunst, P. S. Baran, *Journal of Organic Chemistry* **2014**, *79*, 2430–2452.
- [102] A. W. Hofmann, *Berichte der deutschen chemischen Gesellschaft* **1883**, *16*, 558–560.
- [103] J. Chatt, J. M. Davidson, *J. Chem. Soc.* **1965**, 843–855.



- [104] S. Murahashi, *J Am Chem Soc* **1955**, *77*, 6403–6404.
- [105] I. Moritani and Y. Fujiwara, *Tetrahedron Lett* **1967**, 1119–1122.
- [106] R. B. Moyes, P. B. Wells, *J Catal* **1971**, *21*, 86–92.
- [107] N. Chatani, T. Asaumi, S. Yorimitsu, T. Ikeda, F. Kakiuchi, S. Murai, *J Am Chem Soc* **2001**, *123*, 10935–10941.
- [108] D. Hesk, P. R. Das, B. Evans, *J Labelled Comp Radiopharm* **1995**, *36*, 497–502.
- [109] J. A. Brown, S. Irvine, A. R. Kennedy, W. J. Kerr, S. Andersson, G. N. Nilsson, *Chemical Communications* **2008**, 1115.
- [110] H. Yang, C. Zarate, W. N. Palmer, N. Rivera, D. Hesk, P. J. Chirik, *ACS Catal* **2018**, *8*, 10210–10218.
- [111] M. Valero, T. Kruissink, J. Blass, R. Weck, S. Güssregen, A. T. Plowright, V. Derdau, *Angewandte Chemie - International Edition* **2020**, *59*, 5626–5631.
- [112] F. Roudesly, J. Oble, G. Poli, *J Mol Catal A Chem* **2017**, *426*, 275–296.
- [113] D. H. Ess, W. A. Goddard, R. A. Periana, *Organometallics* **2010**, *29*, 6459–6472.
- [114] P. E. M. Siegbahn, M. R. A. Blomberg, *Dalton Transactions* **2009**, 5832.
- [115] P. O. Stoutland, R. G. Bergman, *J Am Chem Soc* **1985**, *107*, 4581–4582.
- [116] R. Waterman, *Organometallics* **2013**, *32*, 7249–7263.
- [117] M. A. Martínez-Aguirre, A. K. Yatsimirsky, *Journal of Organic Chemistry* **2015**, *80*, 4985–4993.
- [118] D. L. Davies, S. M. A. Donald, S. A. Macgregor, *J Am Chem Soc* **2005**, *127*, 13754–13755.
- [119] S. I. Gorelsky, D. Lapointe, K. Fagnou, E. Lilly, A. Zeneca, **2008**, 10848–10849.
- [120] D. J. Jones, M. Lautens, G. P. McGlacken, *Nat Catal* **2019**, *2*, 843–851.
- [121] A. H. Roy, J. F. Hartwig, *J Am Chem Soc* **2001**, *123*, 1232–1233.
- [122] S. G. Newman, M. Lautens, *J Am Chem Soc* **2010**, *132*, 11416–11417.
- [123] H. Gilman, W. Langham, *J Am Chem Soc* **1939**, *61*, 106–109.
- [124] G. Wittig, G. Pieper, G. Fuhrmann, *Berichte der deutschen chemischen Gesellschaft (A and B Series)* **1940**, *73*, 1193–1197.
- [125] V. Snieckus, *Chem Rev* **1990**, *90*, 879–933.
- [126] U. Wietelmann, J. Klett, *Z Anorg Allg Chem* **2018**, *644*, 194–204.
- [127] S. Murai, F. Kakiuchi, S. Sekine, Y. Tanaka, A. Kamatani, M. Sonoda, N. Chatani, *Nature* **1993**, *366*, 529–531.
- [128] D. Kalyani, A. R. Dick, W. Q. Anani, M. S. Sanford, *Org Lett* **2006**, *8*, 2523–2526.
- [129] Y. H. Zhang, B. F. Shi, J. Q. Yu, *Angewandte Chemie - International Edition* **2009**, *48*, 6097–6100.
- [130] R. K. Thalji, J. A. Ellman, R. G. Bergman, *J Am Chem Soc* **2004**, *126*, 7192–7193.
- [131] S. J. O'Malley, K. L. Tan, A. Watzke, R. G. Bergman, J. A. Ellman, *J Am Chem Soc* **2005**, *127*, 13496–13497.
- [132] R. M. Jacobson, R. A. Raths, *J Org Chem* **1979**, *44*, 4013–4014.
- [133] D. Leow, G. Li, T. S. Mei, J. Q. Yu, *Nature* **2012**, *486*, 518–522.
- [134] R. M. Beesley, C. K. Ingold, J. F. Thorpe, *J. Chem. Soc., Trans.* **1915**, *107*, 1080–1106.
- [135] K. M. Engle, T. S. Mei, M. Wasa, J. Q. Yu, *Acc Chem Res* **2012**, *45*, 788–802.
- [136] Y.-F. Yang, G.-J. Cheng, P. Liu, D. Leow, T.-Y. Sun, P. Chen, X. Zhang, J.-Q. Yu, Y.-D. Wu, K. N. Houk, *J Am Chem Soc* **2014**, *136*, 344–355.
- [137] S. Bag, T. Patra, A. Modak, A. Deb, S. Maity, U. Dutta, A. Dey, R. Kancherla, A. Maji, A. Hazra, M. Bera, D. Maiti, *J Am Chem Soc* **2015**, *137*, 11888–11891.
- [138] A. Maji, S. Guin, S. Feng, A. Dahiya, V. K. Singh, P. Liu, D. Maiti, *Angewandte Chemie International Edition* **2017**, *56*, 14903–14907.
- [139] L. Wan, N. Dastbaravardeh, G. Li, J. Q. Yu, *J Am Chem Soc* **2013**, *135*, 18056–18059.

- [140] M. Catellani, F. Frignani, A. Rangoni, *Angewandte Chemie International Edition in English* **1997**, *36*, 119–122.
- [141] J. Ye, M. Lautens, *Nat Chem* **2015**, *7*, 863–870.
- [142] X.-C. Wang, W. Gong, L.-Z. Fang, R.-Y. Zhu, S. Li, K. M. Engle, J. Q. Yu, *Nature* **2015**, *519*, 334–338.
- [143] H. Shi, A. N. Herron, Y. Shao, Q. Shao, J. Yu, *Nature* **2018**, 1–6.
- [144] J. Luo, S. Preciado, I. Larrosa, *J Am Chem Soc* **2014**, *136*, 4109–4112.
- [145] L. Ping, D. S. Chung, J. Bouffard, S. Lee, L. Ping, D. S. Chung, *Chem Soc Rev* **2017**, *46*, 4299–4328.
- [146] Q. Zhao, T. Poisson, X. Pannecoucke, T. Besset, *Synthesis (Stuttg)* **2017**, DOI 10.1055/s-0036-1590878.
- [147] P. Gandeepan, L. Ackermann, *Chem* **2017**, 1–24.
- [148] H. Sun, N. Guimond, Y. Huang, *Org. Biomol. Chem.* **2016**, *14*, 8389–8397.
- [149] S. St John-Campbell, J. A. Bull, *Org Biomol Chem* **2018**, DOI 10.1039/C8OB00926K.
- [150] C. H. Jun, H. Lee, J. B. Hong, *Journal of Organic Chemistry* **1997**, *62*, 1200–1201.
- [151] Y. J. Park, J. Park, C. Jun, *Acc Chem Res* **2008**, *41*, 222–234.
- [152] N. R. Vautravers, D. D. Regent, B. Breit, *Chemical Communications* **2011**, *47*, 6635.
- [153] R. B. Bedford, S. J. Coles, M. B. Hursthouse, M. E. Limmert, *Angewandte Chemie International Edition* **2003**, *42*, 112–114.
- [154] P. W. Tan, N. A. B. Juwaini, J. Seayad, *Org Lett* **2013**, *15*, 5166–5169.
- [155] F. Mo, G. Dong, *Science (1979)* **2014**, *345*, 68–72.
- [156] F.-L. Zhang, K. Hong, T.-J. Li, H. Park, J.-Q. Yu, *Science (1979)* **2016**, *351*, 252–256.
- [157] Q. J. Yao, S. Zhang, B. B. Zhan, B. F. Shi, *Angewandte Chemie - International Edition* **2017**, *56*, 6617–6621.
- [158] Y. Kuninobu, H. Ida, M. Nishi, M. Kanai, *Nat Chem* **2015**, *7*, 712–717.
- [159] G. Li, Y. Yan, P. Zhang, X. Xu, Z. Jin, *ACS Catal* **2021**, *11*, 10460–10466.
- [160] L. Yang, K. Semba, Y. Nakao, *Angewandte Chemie - International Edition* **2017**, *56*, DOI 10.1002/anie.201701238.
- [161] H. J. Davis, M. T. Mihai, R. J. Phipps, *J Am Chem Soc* **2016**, *138*, 12759–12762.
- [162] M. T. Mihai, B. D. Williams, R. J. Phipps, *J Am Chem Soc* **2019**, *141*, 15477–15482.
- [163] L. Xu, S. Ding, P. Li, *Angewandte Chemie - International Edition* **2014**, *53*, 1822–1826.
- [164] J. Y. Cho, M. K. Tse, D. Holmes, R. E. Maleczka, M. R. Smith, *Science (1979)* **2002**, *295*, 305–308.
- [165] Y. Liang, Y. F. Liang, C. Tang, Y. Yuan, N. Jiao, *Chemistry - A European Journal* **2015**, *21*, 16395–16399.
- [166] J. M. Neely, M. J. Bezdek, P. J. Chirik, *ACS Cent Sci* **2016**, *2*, 935–942.
- [167] A. J. Borah, Z. Shi, *Chemical Communications* **2017**, *53*, 3945–3948.
- [168] H. Ihara, M. Koyanagi, M. Suginome, *Org Lett* **2011**, *13*, 2662–2665.
- [169] H. Ihara, M. Suginome, *J Am Chem Soc* **2009**, *131*, 7502–7503.
- [170] M. Koyanagi, N. Eichenauer, H. Ihara, T. Yamamoto, M. Suginome, *Chem Lett* **2013**, *42*, 541–543.
- [171] H. Ihara, A. Ueda, M. Suginome, *Chem Lett* **2011**, *40*, 916–918.
- [172] T. Yamamoto, A. Ishibashi, M. Suginome, *Chem Lett* **2017**, *46*, 1169–1172.
- [173] T. Yamamoto, A. Ishibashi, M. Suginome, *Org Lett* **2017**, *19*, 886–889.
- [174] T. Yamamoto, A. Ishibashi, M. Suginome, *Org Lett* **2019**, *21*, 6235–6240.

- [175] A. F. Williams, A. J. P. White, A. C. Spivey, C. J. Cordier, *Chem Sci* **2020**, *11*, 3301–3306.
- [176] H. L. Li, Y. Kuninobu, M. Kanai, *Angewandte Chemie - International Edition* **2017**, *56*, 1495–1499.
- [177] D. Leonori, V. K. Aggarwal, *Angewandte Chemie International Edition* **2015**, *54*, 1082–1096.
- [178] C. Amatore, A. Jutand, G. Le Duc, *Chemistry - A European Journal* **2011**, *17*, 2492–2503.
- [179] A. O. Mattes, D. Russell, E. Tishchenko, Y. Liu, R. H. Cichewicz, S. J. Robinson, *Concepts in Magnetic Resonance Part A* **2016**, *45A*, e21422.
- [180] C. E. Houscroft, A. G. Sharpe, *Inorganic Chemistry: Third Edition*, Pearson Education Limited, London, **2008**.
- [181] L. M. Aguilera-Sáez, J. R. Belmonte-Sánchez, R. Romero-González, J. L. Martínez Vidal, F. J. Arrebola, A. Garrido Frenich, I. Fernández, *Analyst* **2018**, *143*, 4707–4714.
- [182] R. J. Ouellette, J. D. Rawn, in *Organic Chemistry*, Elsevier, **2018**, pp. 427–461.
- [183] F. Bloch, *Phys. Rev.* **1946**, *70*, 460–474.
- [184] J. E. Power, M. Foroozandeh, R. W. Adams, M. Nilsson, S. R. Coombes, A. R. Phillips, G. A. Morris, *Chemical Communications* **2016**, *52*, 2916–2919.
- [185] F. Malz, H. Jancke, *J Pharm Biomed Anal* **2005**, *38*, 813–823.
- [186] T. D. W. Claridge, *High-Resolution NMR Techniques in Organic Chemistry*, Elsevier Science Ltd, Oxford, **1999**.
- [187] F. Finocchi, *Density Functional Theory for Beginners*, **2011**.
- [188] I. Y. Zhang, J. Wu, X. Xu, *Chemical Communications* **2010**, *46*, 3057–3070.
- [189] O. Salomon, M. Reiher, B. A. Hess, *Journal of Chemical Physics* **2002**, *117*, 4729–4737.
- [190] P. J. Stephen, F. J. Devlin, C. F. Chabalowski, M. J. Frisch, *J Phys Chem* **1994**, *98*, 11623–11627.
- [191] S. Winstein, N. J. Holness, *J Am Chem Soc* **1955**, *77*, 5562–5578.
- [192] B. Olmstead, J. H. ; Steiner, *Acid-Base Equilibria*, Pergamon Press, **1980**.
- [193] L. D. Tran, I. Popov, O. Daugulis, *J Am Chem Soc* **2012**, *134*, 18237–18240.
- [194] M. Bera, A. Maji, S. K. Sahoo, D. Maiti, *Angewandte Chemie International Edition* **2015**, *54*, 8515–8519.
- [195] A. Maji, B. Bhaskararao, S. Singha, R. B. Sunoj, D. Maiti, *Chem Sci* **2016**, *7*, 3147–3153.
- [196] T. Patra, R. Watile, S. Agasti, T. Naveen, D. Maiti, *Chemical Communications* **2016**, *52*, 2027–2030.
- [197] R. Ruzziconi, S. Spizzichino, A. Mazzanti, L. Lunazzi, M. Schlosser, *Org Biomol Chem* **2010**, *8*, 4463–4471.
- [198] L. Chu, M. Shang, K. Tanaka, Q. Chen, N. Pissarnitski, E. Streckfuss, J. Q. Yu, *ACS Cent Sci* **2015**, *1*, 394–399.
- [199] B. Markus, C. -H Kwon, *J Pharm Sci* **1994**, *83*, 1729–1734.
- [200] F. Mayer, W. Schäfer, J. Rosenbach, *Arch Pharm (Weinheim)* **1929**, *267*, 571–584.
- [201] A. Alhaj Zen, J. W. Aylott, W. C. Chan, *Tetrahedron Lett* **2014**, *55*, 5521–5524.
- [202] S. Wagschal, L. A. Perego, A. Simon, A. Franco-Espejo, C. Tocqueville, J. Albaneze-Walker, A. Jutand, L. Grimaud, *Chemistry - A European Journal* **2019**, *25*, 6980–6987.
- [203] J. Yin, M. P. Rainka, X. X. Zhang, S. L. Buchwald, *J Am Chem Soc* **2002**, *124*, 1162–1163.
- [204] S. D. Walker, T. E. Barder, J. R. Martinelli, S. L. Buchwald, *Angewandte Chemie* **2004**, *116*, 1907–1912.

- [205] H. Clavier, S. P. Nolan, *Chemical Communications* **2010**, 46, 841–861.
- [206] S. Borjian, M. C. Baird, *Organometallics* **2014**, 33, 3936–3940.
- [207] U. Christmann, R. Vilar, *Angewandte Chemie - International Edition* **2005**, 44, 366–374.
- [208] P. R. Melvin, A. Nova, D. Balcells, N. Hazari, M. Tilset, *Organometallics* **2017**, 36, 3664–3675.
- [209] S. D. McCann, E. C. Reichert, P. L. Arrechea, S. L. Buchwald, *J Am Chem Soc* **2020**, 142, 15027–15037.
- [210] G. A. Russell, E. G. Janzen, *J Am Chem Soc* **1962**, 84, 4153–4154.
- [211] E. C. Ashby, J. N. Argyropoulos, *J Org Chem* **1986**, 51, 3593–3597.
- [212] F. Elisei, G. Favaro, A. Romani, *Chem Phys* **1990**, 144, 107–115.
- [213] R. A. Alharis, C. L. McMullin, D. L. Davies, K. Singh, S. A. Macgregor, *Faraday Discuss* **2019**, 220, 386–403.
- [214] Y. Boutadla, D. L. Davies, S. A. Macgregor, A. I. Poblador-Bahamonde, *Dalton Transactions* **2009**, 5820.
- [215] D. H. Ess, S. M. Bischof, J. Oxgaard, R. A. Periana, W. A. Goddard, *Organometallics* **2008**, 27, 6440–6445.
- [216] D. Sparkford, Z. E. Penton, F. G. Kitson, *Gas Chromatography and Mass Spectrometry: A Practical Guide (Second Edition)*, Elsevier, **2011**.
- [217] X. Chen, X.-S. Hao, C. E. Goodhue, J.-Q. Yu, *J Am Chem Soc* **2006**, 128, 6790–6791.
- [218] A. R. Dick, K. L. Hull, M. S. Sanford, *J Am Chem Soc* **2004**, 126, 2300–2301.
- [219] X. Jia, S. Zhang, W. Wang, F. Luo, J. Cheng, *Org Lett* **2009**, 11, 3120–3123.
- [220] S. Wu, Z. Wang, Y. Bao, C. Chen, K. Liu, B. Zhu, *Chemical Communications* **2020**, 56, 4408–4411.
- [221] J. Chen, G. Song, C. L. Pan, X. Li, *Org Lett* **2010**, 12, 5426–5429.
- [222] H.-J. Xu, Y. Lu, M. E. Farmer, H.-W. Wang, D. Zhao, Y.-S. Kang, W.-Y. Sun, J.-Q. Yu, *J Am Chem Soc* **2017**, 139, 2200–2203.
- [223] M. Bera, A. Modak, T. Patra, A. Maji, D. Maiti, *Org Lett* **2014**, 16, 5760–5763.
- [224] S. Li, L. Cai, H. Ji, L. Yang, G. Li, *Nat Commun* **2016**, 7, 10443.
- [225] E. Casali, P. Kalra, M. Brochetta, T. Borsari, A. Gandini, T. Patra, G. Zanoni, D. Maiti, *Chemical Communications* **2020**, 56, 7281–7284.
- [226] W. Lu, H. Xu, Z. Shen, *Org Biomol Chem* **2017**, 15, 1261–1267.
- [227] R. Jayarajan, J. Das, S. Bag, R. Chowdhury, D. Maiti, *Angewandte Chemie International Edition* **2018**, 57, 7659–7663.
- [228] C. Premi, A. Dixit, N. Jain, *Org Lett* **2015**, 17, 2598–2601.
- [229] H.-Y. Thu, W.-Y. Yu, C.-M. Che, *J Am Chem Soc* **2006**, 128, 9048–9049.
- [230] D. Kalyani, N. R. Deprez, L. V. Desai, M. S. Sanford, *J Am Chem Soc* **2005**, 127, 7330–7331.
- [231] W. Li, Z. Yin, X. Jiang, P. Sun, *J Org Chem* **2011**, 76, 8543–8548.
- [232] J. Xu, Y. Liu, Y. Wang, Y. Li, X. Xu, Z. Jin, *Org Lett* **2017**, 19, 1562–1565.
- [233] X. Jia, D. Yang, W. Wang, F. Luo, J. Cheng, *Journal of Organic Chemistry* **2009**, 74, 9470–9474.
- [234] M. Bera, S. Agasti, R. Chowdhury, R. Mondal, D. Pal, D. Maiti, *Angewandte Chemie International Edition* **2017**, 56, 5272–5276.
- [235] T. Patra, S. Bag, R. Kancherla, A. Mondal, A. Dey, S. Pimparkar, S. Agasti, A. Modak, D. Maiti, *Angewandte Chemie - International Edition* **2016**, DOI 10.1002/anie.201601999.
- [236] S. Wübbolt, M. Oestreich, *Angewandte Chemie - International Edition* **2015**, 54, 15876–15879.
- [237] K. Billingsley, S. L. Buchwald, *J Am Chem Soc* **2007**, 129, 3358–3366.
- [238] T. Kinzel, Y. Zhang, S. L. Buchwald, *J Am Chem Soc* **2010**, 132, 14073–14075.

- [239] J. M. Fox, X. Huang, A. Chieffi, S. L. Buchwald, *J Am Chem Soc* **2000**, *122*, 1360–1370.
- [240] M. Sumimoto, N. Iwane, T. Takahama, S. Sakaki, *J Am Chem Soc* **2004**, *126*, 10457–10471.
- [241] J. Li, S. G. Ballmer, E. P. Gillis, S. Fujii, M. J. Schmidt, A. M. E. Palazzolo, J. W. Lehmann, G. F. Morehouse, M. D. Burke, **2015**, *347*, 1221–1226.
- [242] P. Sharma, S. Rohilla, N. Jain, *J Org Chem* **2015**, *80*, 4116–4122.
- [243] X. Kou, M. Zhao, X. Qiao, Y. Zhu, X. Tong, Z. Shen, *Chemistry - A European Journal* **2013**, *19*, 16880–16886.
- [244] N. Umeda, K. Hirano, T. Satoh, M. Miura, *Journal of Organic Chemistry* **2009**, *74*, 7094–7099.
- [245] F. Wang, X. Yu, Z. Qi, X. Li, *Chemistry - A European Journal* **2016**, *22*, 511–516.
- [246] J. Lu, H. Zhang, X. Chen, H. Liu, Y. Jiang, H. Fu, *Adv Synth Catal* **2013**, *355*, 529–536.
- [247] L. Su, D.-D. Guo, B. Li, S.-H. Guo, G.-F. Pan, Y.-R. Gao, Y.-Q. Wang, *ChemCatChem* **2017**, *9*, 2001–2008.
- [248] K. Niedermann, J. M. Welch, R. Koller, J. Cvengroš, N. Santschi, P. Battaglia, A. Togni, *Tetrahedron* **2010**, *66*, 5753–5761.
- [249] T. Itahara, *Journal of Organic Chemistry* **1985**, *50*, 5272–5275.
- [250] M. Takahashi, K. Masui, H. Sekiguchi, N. Kobayashi, A. Mori, M. Funahashi, N. Tamaoki, *J Am Chem Soc* **2006**, *128*, 10930–10933.
- [251] K. Masui, H. Ikegami, A. Mori, *J Am Chem Soc* **2004**, *126*, 5074–5075.
- [252] A. I. McKay, W. A. O. Altalhi, L. E. McInnes, M. L. Czyz, A. J. Canty, P. S. Donnelly, R. A. J. O'Hair, *Journal of Organic Chemistry* **2020**, *85*, 2680–2687.
- [253] A. Williams, Directed, Meta-Selective C – H Functionalisation of Aryl Boronic Acid MIDA Esters, Imperial College London, **2020**.
- [254] J. Vicente, I. Saura-Llamas, J. Cuadrado, M. C. Ramírez de Arellano, *Organometallics* **2003**, *22*, 5513–5517.
- [255] N. Barr, S. F. Dyke, *PALLADIUM ASSISTED ORGANIC REACTIONS III \*. THE PREPARATION OF DI-p-CHLOROBIS-(NJV-DIALKYL BENZYLAMINE-2,C,N)DIPALLADIUM(II) COMPLEXES*, Elsevier Sequoia S.A, **1983**.
- [256] A. R. Petrov, K. A. Rufanov, K. Harms, J. Sundermeyer, *J Organomet Chem* **2009**, *694*, 1212–1218.
- [257] H. J. Davis, R. J. Phipps, *Chem. Sci.* **2017**, *8*, 864–877.

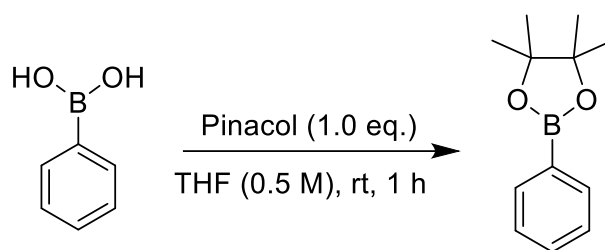
## 6. Appendix

### General Experimental Procedures

THF was freshly distilled under argon from the sodium anion of benzophenone, all other solvents and reagents were purchased and used as supplied. TLCs were performed on Merck silica gel 60 F254 and visualised by UV lamp. Nuclear Magnetic Resonance (NMR) spectra were recorded on 500 or 400 MHz Bruker NMR spectrometers in CDCl<sub>3</sub> at 300 K. For proton NMR spectroscopy, samples were prepared using ca. 10 mg of compound dissolved in 0.5 mL of deuterated solvent and for carbon NMR spectroscopy using ca. 30 mg of compound dissolved in 0.7 mL of deuterated solvent. All spectra were referenced to the residual solvent peaks; CHCl<sub>3</sub> ( $\delta$  = 7.26 ppm) for <sup>1</sup>H NMR spectra and the CDCl<sub>3</sub> solvent peak ( $\delta$  = 77.16 ppm) for <sup>13</sup>C{<sup>1</sup>H} NMR spectra, *d*<sub>6-x</sub>-DMSO ( $\delta$  = 2.50 ppm) for <sup>1</sup>H NMR spectra and the *d*<sub>6</sub>-DMSO solvent peak ( $\delta$  = 39.52 ppm) for <sup>13</sup>C{<sup>1</sup>H} NMR spectra, *d*<sub>3-x</sub>-MeCN ( $\delta$  = 1.94 ppm) for <sup>1</sup>H NMR spectra and the CD<sub>3</sub>CN solvent peak ( $\delta$  = 118.26 ppm) for <sup>13</sup>C{<sup>1</sup>H} NMR spectra. NMR chemical shifts ( $\delta$ ) are reported in ppm; coupling constants (*J*) are reported in Hz; splitting patterns are assigned s = singlet, d = doublet, t = triplet, q = quartet, p = pentet, br = broad signal. Infrared spectral data were recorded using a Bruker ATR-FTIR spectrometer, only indicative peaks were assigned with expected functionality assigned. High resolution mass spectrometry (HRMS) was measured for novel compounds using electrospray ionisation or electron impact ionisation (EI) using a 1  $\mu$ g/mL solution of compound in acetonitrile.

## 4,4,5,5-tetramethyl-2-phenyl-1,3,2-dioxaborolane

*European J. Org. Chem.* **2020**, *26*, 423–427.

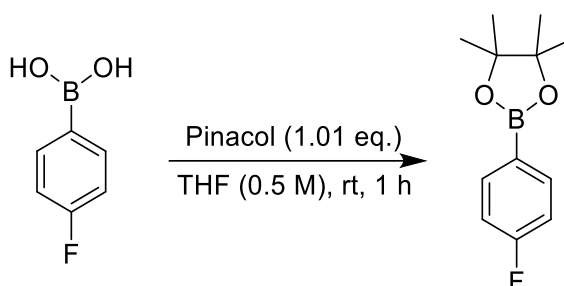


A solution of phenyl boronic acid (3.60 g, 29.5 mmol) and pinacol (3.49 g, 29.5 mmol, 1.0 eq.) in THF (59 mL, 0.5 M) was stirred under ambient conditions for 1 hour. The resulting solution was dried in vacuo and the remaining residue was purified by column chromatography yielding the title product (5.88 g, 97 %) as a crystalline white solid.

M.P. = 28 – 29 °C.  $R_f$  (20 % EtOAc/PE) 0.8.  $^1\text{H}$  NMR (500 MHz,  $\text{CDCl}_3$ )  $\delta$  7.80 (dd,  $J = 8.1, 1.4$  Hz, 2H), 7.45 (tt,  $J = 7.4, 1.7$  Hz, 1H), 7.37 (t,  $J = 7.4$  Hz, 2H), 1.35 (s, 12H).  $^{11}\text{B}$  NMR (128 MHz,  $\text{CDCl}_3$ )  $\delta$  30.6.  $^{13}\text{C}\{^1\text{H}\}$  NMR (126 MHz,  $\text{CDCl}_3$ )  $\delta$  134.9, 131.4, 127.9, 83.9, 25.0. 5 of 6 expected resonance observed, likely due to boron coupling to the already slowly relaxing quaternary carbon compounded by quadrupolar broadening affecting peak width. ATR-FTIR ( $\text{cm}^{-1}$ ) 2979 (C-H Stretch)

## 2-(4-Fluorophenyl)-4,4,5,5-tetramethyl-1,3,2-dioxaborolane

*European J. Org. Chem.* **2020**, *26*, 423–427.



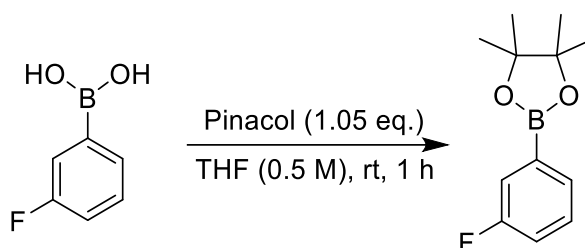
A solution of 4-fluorobenzene boronate pinacol ester (10.01 g, 71.4 mmol) and Pinacol (8.41 g, 71.4 mmol, 1.0 eq.) in THF (140 mL, 0.5 M) was stirred under ambient conditions for 1 hour. The reaction was dried *in vacuo* and the residue was purified by column chromatography (EtOAc/PE) yielding the desired product (15.86 g, 64.3 mmol, 90 %) as a pale-yellow oil.

$R_f$  (10% EtOAc/PE) 0.7.  $^1\text{H}$  NMR (500 MHz,  $\text{CDCl}_3$ )  $\delta$  7.84 – 7.78 (m, 2H), 7.09 – 7.02 (m, 2H), 1.35 (s, 12H).  $^1\text{H}$  NMR (376 MHz,  $\text{DMSO-}d_6$ )  $\delta$  7.76 – 7.66 (m, 2H), 7.20 (dd,  $J = 10.1, 7.9$  Hz, 2H), 1.28 (s, 12H).  $^{19}\text{F}\{^1\text{H}\}$  NMR (471 MHz,  $\text{CDCl}_3$ )  $\delta$  -108.4.  $^{19}\text{F}\{^1\text{H}\}$  NMR (471 MHz,  $d_6$ -DMSO)  $\delta$  -108.3.  $^{11}\text{B}$  NMR (128 MHz,  $\text{CDCl}_3$ )  $\delta$  30.5.  $^{11}\text{B}$  NMR (128 MHz,  $\text{DMSO-}d_6$ )  $\delta$  30.9.  $^{13}\text{C}\{^1\text{H}\}$  NMR (126 MHz,  $\text{CDCl}_3$ )  $\delta$  165.25 (d,  $J = 250.7$  Hz), 137.12 (d,  $J = 8.2$  Hz), 114.98 (d,  $J = 20.2$  Hz), 84.04 (s), 25.00 (s). 5 of 6 expected resonance observed, likely due to boron coupling to the already slowly relaxing quaternary carbon, compounded by quadrupolar broadening affecting peak width. ATR-FTIR ( $\text{cm}^{-1}$ ) 2980 (C-H stretch)



## 2-(3-Fluorophenyl)-4,4,5,5-tetramethyl-1,3,2-dioxaborolane

*J. Am. Chem. Soc.* **2021**, 13266–13273.

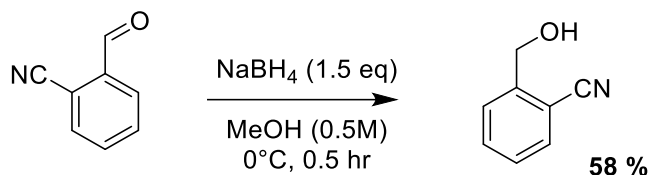


A solution of 4-fluorobenzene boronate pinacol ester (2.0 g, 14.2 mmol) and pinacol (1.75 g, 14.8 mmol, 1.05 eq.) in THF (30 mL, 0.5 M) was stirred under ambient conditions for 1 hour. The reaction was dried *in vacuo* and the residue was purified by column chromatography (EtOAc/PE) yielding the desired product (2.54 g, 11.4 mmol, 80 %) as a pale-yellow oil.

R<sub>f</sub> (10% EtOAc/PE) 0.7. <sup>1</sup>H NMR (400 MHz, CDCl<sub>3</sub>) δ 7.57 (dd, *J* = 7.3, 1.0 Hz, 1H), 7.48 (ddd, *J* = 9.3, 2.8, 1.0 Hz, 1H), 7.34 (ddd, *J* = 8.3, 7.3, 5.5 Hz, 1H), 7.14 (dddd, *J* = 9.3, 8.3, 2.8, 1.0 Hz, 1H), 1.35 (s, 12H). <sup>1</sup>H NMR (500 MHz, *d*<sub>6</sub>-DMSO) δ 7.51 (d, *J* = 7.3 Hz, 1H), 7.46 – 7.32 (m, 2H), 7.28 (td, *J* = 9.0, 8.6, 3.2 Hz, 1H), 1.26 (t, *J* = 2.1 Hz, 12H). <sup>19</sup>F{<sup>1</sup>H} NMR (471 MHz, CDCl<sub>3</sub>) δ -114.2. <sup>19</sup>F NMR (471 MHz, *d*<sub>6</sub>-DMSO) δ -113.6 ppm. <sup>11</sup>B NMR (128 MHz, CDCl<sub>3</sub>) 30.6. <sup>11</sup>B NMR (128 MHz, *d*<sub>6</sub>-DMSO) δ 30.7. <sup>13</sup>C{<sup>1</sup>H} NMR (101 MHz, CDCl<sub>3</sub>) δ 162.66 (d, *J* = 246.4 Hz), 130.43 (d, *J* = 2.9 Hz), 129.61 (d, *J* = 7.2 Hz), 121.11 (d, *J* = 19.1 Hz), 118.30 (d, *J* = 21.0 Hz), 84.23, 25.00. ATR-FTIR (cm<sup>-1</sup>) 2978 (C-H stretch)

2-(hydroxymethyl)benzonitrile

*Org. Lett* **2021**, 23, 6014–6018.

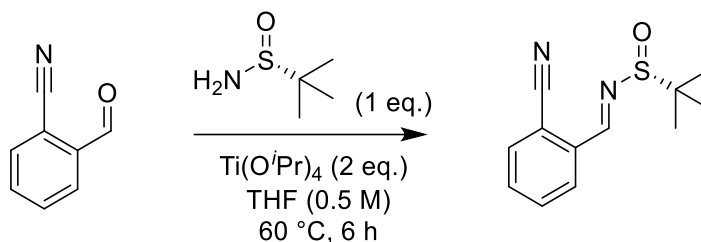


To a solution of 2-cyanobenzaldehyde (503 mg, 3.84 mmol) in methanol (20 mL) at 0 °C, sodium borohydride (239 mg, 1.6 eq., 6.32 mmol) was added portion-wise, followed by stirring at 0 °C for 10 minutes. The reaction was then allowed to return to room temperature over 20 minutes. Water (20 mL) was added, and the product was extracted with DCM (3 X 20 mL). The combined organic extracts were dried over magnesium sulphate, filtered and dried *in vacuo*. The resulting residue was purified by silica-gel chromatography (60 % to 80 % EtOAc/PE) yielding the title product (293 mg, 2.2 mmol, 58 %) as an off-white solid.

<sup>1</sup>H NMR (500 MHz, CDCl<sub>3</sub>) δ 7.87 (d, J = 7.5 Hz, 1H), 7.56 (t, J = 7.5 Hz, 1H), 7.47 (t, J = 7.5 Hz, 1H), 7.40 (d, J = 7.5 Hz, 1H), 5.31 (s, 2H). *Due to rapid decomposition of the product, it was not possible to perform full analysis of this compound.*

**(R)-N-(2-Cyanobenzylidene)-2-methylpropane-2-sulfinamide**

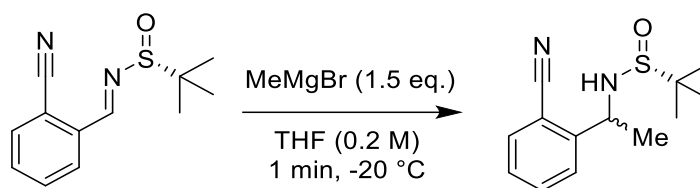
*European J. Org. Chem.*, 2014, 24, 5265–5272.



A solution of 2-cyanobenzaldehyde (5.04 g, 38.4 mmol, 1 eq.), (*R*)-*tert*-butanesulfinamide (4.65 g, 38.4 mmol, 1 eq.) and in titanium(IV) isopropoxide (21.8 g, 76.8 mmol, 2 eq.) in THF (77 ml, 0.5 M) was stirred at 60 °C for 6 hours under an atmosphere of argon. At ambient temperature the reaction was quenched with brine (100 ml), the filtrate was collected by suction filtration through a celite plug. The filtrate was washed with EtOAc (3 X 20 mL) and brine (1 X 20 mL) and the organic layer was dried *in vacuo*. The product was purified by column chromatography on silica gel (EtOAc/Petroleum Ether) to yield the desired product (7.47 g, 90 %) as an off-white solid.

M.P. = 75-78 °C.  $R_f$  = 0.3 (20 % EtOAc/PE).  $^1\text{H}$  NMR (400 MHz,  $\text{CDCl}_3$ )  $\delta$  8.80 (s, 1H), 7.97 (dd,  $J$  = 7.7, 1.2 Hz, 1H), 7.82 (dd,  $J$  = 7.7, 1.2 Hz, 1H) 7.73 (td,  $J$  = 7.7, 1.3 Hz, 1H), 7.63 (td, 7.7, 1.3 Hz, 1H), 1.32 (s, 9H) ppm.  $^{13}\text{C}\{^1\text{H}\}$  NMR (126 MHz,  $\text{CDCl}_3$ )  $\delta$  159.5, 135.6, 134.8, 133.1, 132.2, 131.0, 117.2, 112.5, 58.6, 22.7. ATR-FTIR ( $\text{cm}^{-1}$ ) 2924, 2226, 1086, 772. HRMS calculated for  $\text{C}_{17}\text{H}_{15}\text{N}_2\text{OS}$  [ $\text{M} + \text{H}^+$ ] 235.0905; found 235.0904

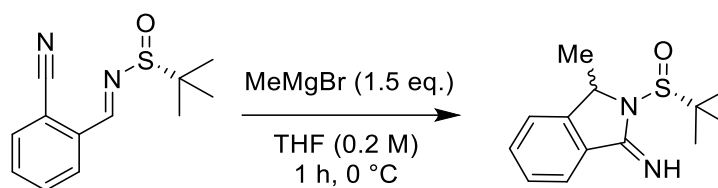
**(R)-N-(1-(2-Cyanophenyl)ethyl)-2-methylpropane-2-sulfinamide**



Methyl magnesium bromide (0.26 ml, 0.64 mmol, 2.5 M in diethyl ether, 1.5 eq.) was added to a solution of (R)-N-(2-Cyanobenzylidene)-2-methylpropane-2-sulfinamide (100 mg, 0.43 mmol) in THF (2.15 ml, 0.2 M) at -20 °C under an argon atmosphere. After 1 minute the reaction was quenched with saturated aqueous NaHCO<sub>3</sub> (5 mL) and washed with ethyl acetate (3 X 5 mL) and Brine (1 X 5 mL brine), the organic layer was dried *in vacuo* and the residue was purified by column chromatography on silica gel (EtOAc/Petroleum Ether) to yield the desired product (82 mg, 76 %) as a yellow solid.

M.P. 65 - 71 ° C. R<sub>f</sub> (60 % EtOAc/PE) 0.2. <sup>1</sup>H NMR as mixture of diastereoisomers where A:B is 7:3 (400 MHz, CDCl<sub>3</sub>) δ 7.69 (apparent dtd, J = 7.7, 1.4, 0.5 Hz, H<sub>A</sub> + H<sub>B</sub> = 1H), 7.66 - 7.51 (m, H<sub>A</sub> + H<sub>B</sub> = 2H), 7.40 (tt, J = 7.6, 1.6 Hz, H<sub>A</sub> + H<sub>B</sub> = 1H), 4.97 - 4.86 (m, H<sub>A</sub> + H<sub>B</sub> = 1H), 3.73 (s, H<sub>B</sub> = 1H), 3.52 (s, H<sub>A</sub> = 1H), 1.69 (d, J = 6.8 Hz, H<sub>A</sub> = 3H), 1.64 (d, J = 6.7 Hz, H<sub>B</sub> = 3H), 1.27 (s, H<sub>B</sub> = 9H), 1.25 (s, H<sub>A</sub> = 9H). <sup>13</sup>C{<sup>1</sup>H} NMR as a mixture of diastereoisomers (126 MHz, CDCl<sub>3</sub>) δ 147.8, 147.4, 133.9, 133.7, 133.4, 133.2, 128.1, 127.9, 127.4, 117.8, 111.3, 111.0, 56.2, 56.2, 53.9, 53.7, 29.8, 24.1, 23.0, 22.7, 22.6. 21 of a possible 22 carbon resonances observed. ATR-FTIR (cm<sup>-1</sup>) 2926 (C-H Stretch) 2225 (C≡N Stretch). HRMS calculated for C<sub>13</sub>H<sub>19</sub>N<sub>2</sub>OS [M + H<sup>+</sup>] 251.1218; found 251.1216.

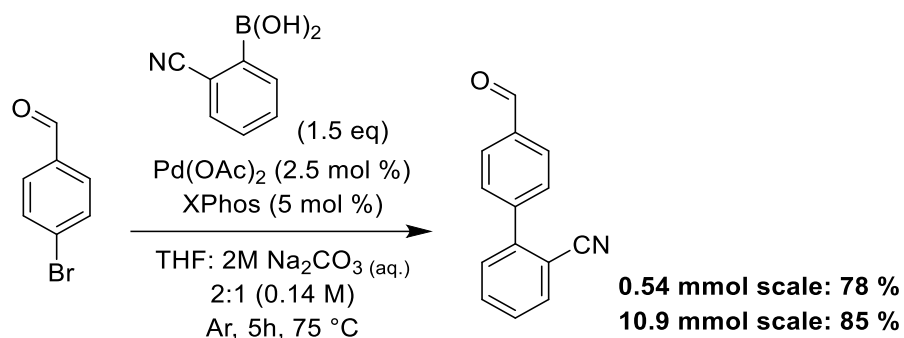
### (R)-2-(*tert*-Butylsulfinyl)-3-methylisoindoline-1-imine



To a solution of (R)-N-(2-Cyanobenzylidene)-2-methylpropane-2-sulfonamide (1.0 g, 4.3 mmol) in THF (8.6 mL, 0.5 M) at 0 °C under a nitrogen atmosphere, Methyl magnesium bromide (2.5 M in diethyl ether, 2.6 mL, 6.4 mmol, 1.5 eq.) was added. The reaction was stirred for 1 hour and quenched with saturated aqueous NaHCO<sub>3</sub> (10 mL), the resulting suspension was filtered, and the filtrate was washed with EtOAc (3 X 50 mL), the combined organic layers were washed with Brine (50 mL) and dried over MgSO<sub>4</sub>, filtered and then dried *in vacuo*. The product was purified by silica gel chromatography yielding the title product (0.52 g, 49 %) as a yellow solid.

M.P. 81 – 86 °C. R<sub>f</sub> (60 % EtOAc/PE) 0.3. <sup>1</sup>H NMR reported as a 1:1 mixture of diastereoisomers (400 MHz, CDCl<sub>3</sub>) δ 8.22 (broad s, H<sub>A</sub> = 1), 8.09 (broad s, H<sub>B</sub> = 1), 7.80 (apparent dt, *J* = 7.5, 1.2 Hz, H<sub>A</sub> + H<sub>B</sub> = 1H), 7.54 (apparent td, *J* = 7.5, 1.2 Hz, H<sub>A</sub> + H<sub>B</sub> = 1H), 7.47 – 7.38 (m, H<sub>A</sub> + H<sub>B</sub> = 2H), 4.81 (apparent dq, *J* = 13.2, 6.7 Hz, H<sub>A</sub> + H<sub>B</sub> = 1H), 1.48 (apparent dd, *J* = 6.7, 1.7 Hz, H<sub>A</sub> + H<sub>B</sub> = 3H), 1.30 (apparent d, 0.5 Hz, H<sub>A</sub> + H<sub>B</sub> = 9H). <sup>13</sup>C{<sup>1</sup>H} NMR as a mixture of diastereoisomers (126 MHz, CDCl<sub>3</sub>) δ 163.0, 162.8, 146.3, 156.1, 134.3, 131.5, 131.5, 128.1, 128.1, 123.4, 122.0, 57.9, 57.2, 56.8, 24.4, 22.5, 22.4, 20.7, 20.5 (19 of a possible 22 carbon resonances observed). ATR-FTIR (cm<sup>-1</sup>) 3184, 2924, 1624, 1025. HRMS calculated for C<sub>13</sub>H<sub>19</sub>N<sub>2</sub>OS [M + H<sup>+</sup>] 251.1218; found 251.1215.

### 4-(2-Cyanophenyl)benzaldehyde

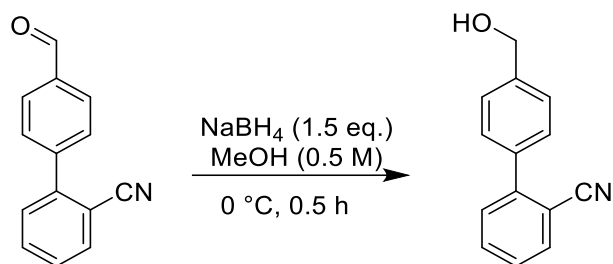


To an oven dried 250 mL round bottom flask was added 4-bromobenzaldehyde (2.00 g, 10.9 mmol, 1 eq.), 2-cyanophenylboronic acid (2.40 g, 16.4 mmol, 1.5 eq.), XPhos (0.26 g, 0.55 mmol, 5.0 mol%) and palladium(II) acetate (65.3 mg, 0.29 mmol, 2.7 mol%). The reaction vessel was flushed with Ar with gentle stirring for 5 minutes at 20 °C. Distilled THF (52 mL) and *aq.* Na<sub>2</sub>CO<sub>3</sub> (26 mL, 2M, degassed) were added simultaneously washing solids from the sides of the flask. Argon was bubbled through the resulting solution for 5 minutes at 20 °C before being transferred to a hotplate preheated to 75 °C for vigorous stirring. After 5 hours the reaction was equilibrated to room temperature over 30 minutes, distilled water (40 mL) and brine (10 mL) was then added to the reaction mixture and the product was extracted with EtOAc (3 X 50 mL). The combined organic extracts were dried over MgSO<sub>4</sub>, filtered and then dried *in vacuo*. The resulting residue was purified by silica-gel chromatography yielding the title compound (1.92 g, 9.29 mmol, 85 %) as a yellow powder.

M.P. 164 -167 °C. <sup>1</sup>H NMR (400 MHz, CDCl<sub>3</sub>) δ 10.10 (s, 1H), 8.02 (d, *J* = 8.3 Hz, 2H), 7.81 (dd, *J* = 7.7, 0.9 Hz, 1H), 7.74 (d, *J* = 8.3 Hz, 2H), 7.70 (td, *J* = 7.7, 1.4 Hz, 1H), 7.58 – 7.49 (m, 2H). <sup>13</sup>C NMR (101 MHz, CDCl<sub>3</sub>) δ 191.68, 144.03, 143.93, 136.22, 133.94, 133.05, 130.06, 129.57, 128.52, 118.22, 111.35. ATR-FTIR (cm<sup>-1</sup>) 2853 (C-H), 2222 (C≡N), 1659 (C=O) HRMS calculated for C<sub>14</sub>H<sub>10</sub>NO [M + H<sup>+</sup>] 208.0757; found 208.0757.

## 4-(2-Cyanophenyl)benzylalcohol

*Org. Lett.* **2001**, 3, 10, 1435–1437

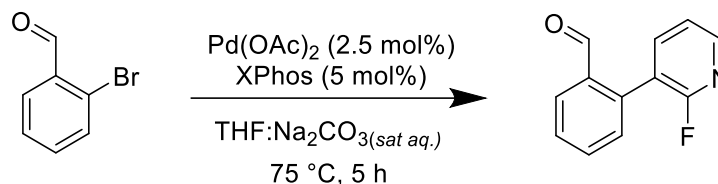


To a solution of 4-(2-cyanophenyl)-benzaldehyde (2.8 g, 13.5 mmol) in methanol (54 mL, 0.25 M) at 0 °C, Sodium borohydride (0.77 g, 1.5 eq., 20.3 mmol) was added portion-wise, followed by stirring at 0 °C for 10 minutes. The reaction was then allowed to return to room temperature over 20 minutes. Water (5 mL) was added, and the product was extracted with DCM (3 X 10 mL). The combined organic extracts were dried over magnesium sulphate, filtered, and dried *in vacuo*. The resulting residue was purified by silica-gel chromatography (40 % EtOAc/PE) yielding the title product (1.43 g, 6.9 mmol, 51 %) as a white solid.

M.P. 120 – 123 °C. R<sub>f</sub> (40 % EtOAc/PE) 0.3. <sup>1</sup>H NMR (500 MHz, CDCl<sub>3</sub>) δ 7.77 (dd, *J* = 7.7, 1.0 Hz, 1H), 7.65 (td, *J* = 7.7, 1.4 Hz, 1H), 7.57 (*Ar*-d, *J* = 7.7 Hz, 2 H) 7.55-7.49 (m, 3H), &.45 (td, *J* = 7.6, 1.2 Hz, 1H), 4.78 (d, *J* = 5.8 Hz, 2H), 1.73 (t, *J* = 5.9 Hz, 1H). <sup>13</sup>C NMR (101 MHz, CDCl<sub>3</sub>) δ 145.34, 141.60, 137.65, 133.90, 132.98, 130.18, 129.13, 127.73, 127.39, 119.01, 111.81, 65.10. ATR-FTIR (cm<sup>-1</sup>) 3220 (O-H Stretch), 2928 (C-H Stretch), 2223 (C≡N Stretch).

## 2-(2-Fluoropyridin-3-yl)benzaldehyde

*J. Med. Chem.* **2018**, 61, 22, 10310–10332



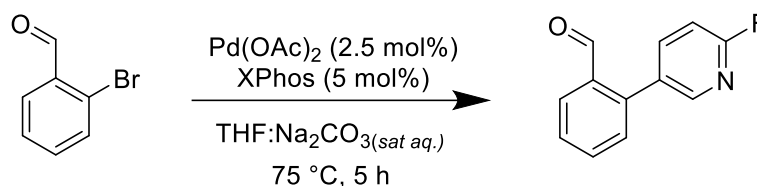
To an oven dried 250 mL round-bottom flask was added 2-bromobenzaldehyde (1.0 g, 0.63 mL, 5.4 mmol, 1.0 eq.), 2-fluoro-3-pyridine boronic acid (1.15 g mg, 8.2 mmol, 1.5 eq.), XPhos (130.0 mg, 0.3 mmol, 5 mol%), Pd(OAc)<sub>2</sub> (32.0 mg, 0.2 mmol, 2.5 mol%). The reaction vessel was purged with Ar with gentle stirring for 5 minutes at 20 °C. Anhydrous THF (26.0 mL) and Na<sub>2</sub>CO<sub>3</sub>(aq.) (13.0 mL, 2M, degassed) were added simultaneously washing solids from the sides of the flask. Argon was bubbled through the resulting solution for 5 minutes at 20 °C before being transferred to a hotplate preheated to 75 °C for vigorous stirring. After 5 hours the reaction was equilibrated to room temperature over 30 minutes, distilled water (40 mL) and brine (10 mL) was then added to the reaction mixture and the product was extracted with EtOAc (3 X 100 mL). The combined organic extracts were dried over MgSO<sub>4</sub>, filtered, and then dried *in vacuo*. The resulting residue was purified by column chromatography yielding the title compound (0.84 g, 4.2 mmol, 77%) as a pale-yellow solid.

M.P. 81-83 °C. <sup>1</sup>H NMR (500 MHz, CDCl<sub>3</sub>) δ 9.95 (d, *J* = 1.5 Hz, 1H) 8.32 (ddd, *J* = 4.9, 1.9, 1.2 Hz, 1H), 8.04 (dd, *J* = 7.7, 1.2 Hz, 1H), 7.77 (ddd, *J* = 9.4, 7.3, 2.0 Hz, 1H), 7.70 (td, *J* = 7.5 Hz, 1.4 Hz, 1H), 7.63 – 7.59 (m, 1H), 7.40 (d, *J* = 7.6 Hz, 1H), 7.34 (ddd, *J* = 7.2, 4.9, 1.8 Hz). <sup>19</sup>F NMR (471 MHz, CDCl<sub>3</sub>) δ -69.1, <sup>13</sup>C NMR (101 MHz, CDCl<sub>3</sub>) δ 190.81, 160.33 (d, *J* = 238.6 Hz), 147.75 (d, *J* = 14.5 Hz), 141.97 (d, *J* = 4.0 Hz), 136.34, 133.91, 131.41, 129.39 (d, *J* = 31.4 Hz), 121.59 (d, *J* = 4.5 Hz), 121.01 (d, *J* = 31.3 Hz). ATR-FTIR (cm<sup>-1</sup>) 2927 (C-H stretch), 1697 (C=O stretch). HRMS calculated for C<sub>12</sub>H<sub>9</sub>FNO [M + H<sup>+</sup>] 202.0663; found 202.0660.



## 2-(4-Fluoropyridin-3-yl)benzaldehyde

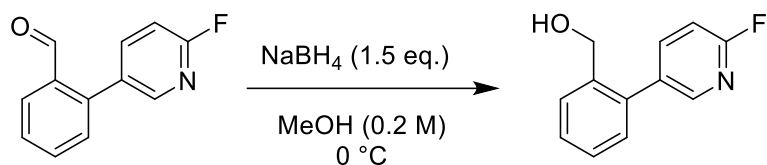
*J. Med. Chem.* **2018**, 61, 22, 10310–10332



To an oven dried 500 mL round-bottom flask was added 2-bromobenzaldehyde (3.7 g, 20.0 mmol, 1.0 eq.), 4-fluoro-3-pyridine boronic acid (4.23 g, 30.0 mmol, 1.5 eq.), XPhos (0.95 g, 2.0 mmol, 5 mol%), Pd(OAc)<sub>2</sub> (0.22 g, 1.0 mmol, 2.5 mol%). The reaction vessel was purged with Ar with gentle stirring for 5 minutes at 20 °C. Anhydrous THF (95 mL) and Na<sub>2</sub>CO<sub>3(aq.)</sub> (48 mL, 2M, degassed) were added simultaneously washing solids from the sides of the flask. Argon was bubbled through the resulting solution for 5 minutes at 20 °C before being transferred to a hotplate preheated to 75 °C for vigorous stirring. After 16 hours the reaction was equilibrated to room temperature over 30 minutes, distilled water (100 mL) and brine (20 mL) was then added to the reaction mixture and the product was extracted with EtOAc (3 X 150 mL). The combined organic extracts were dried over MgSO<sub>4</sub>, filtered, and then dried *in vacuo*. The resulting residue was purified by column chromatography yielding the title compound (3.99 g, 19.8 mmol, 99%) as a pale-yellow solid.

M.P. 60 – 64 °C. R<sub>f</sub> (30 % EtOAc/PE) 0.3. <sup>1</sup>H NMR (400 MHz, CDCl<sub>3</sub>) δ 9.96 (s, 1H), 8.23 (d, *J* = 2.6 Hz, 1H), 8.03 (dd, *J* = 7.7, 1.5 Hz, 1H), 7.81 (ddd, *J* = 8.4, 7.7, 2.6 Hz, 1H), 7.68 (td, *J* = 7.5, 1.5 Hz, 1H), 7.57 (tt, *J* = 7.5, 1.0 Hz, 1H), 7.39 (dd, *J* = 7.6, 1.3 Hz, 1H), 7.05 (ddd, *J* = 8.3, 3.0, 0.7 Hz, 1H) ppm. <sup>19</sup>F{<sup>1</sup>H} NMR (471 MHz, CDCl<sub>3</sub>) δ -68.49 ppm. <sup>13</sup>C{<sup>1</sup>H} NMR (126 MHz, CDCl<sub>3</sub>) δ 191.12, 163.51 (d, *J* = 241.0 Hz), 147.95 (d, *J* = 15.0 Hz), 142.43 (d, *J* = 8.1 Hz), 140.38, 134.08, 133.94, 131.88 (d, *J* = 4.7 Hz), 131.21, 129.20, 129.00, 109.35 (d, *J* = 37.7 Hz) ppm. ATR-FTIR (cm<sup>-1</sup>) 3065, 2864, 1690 (C=O stretch)

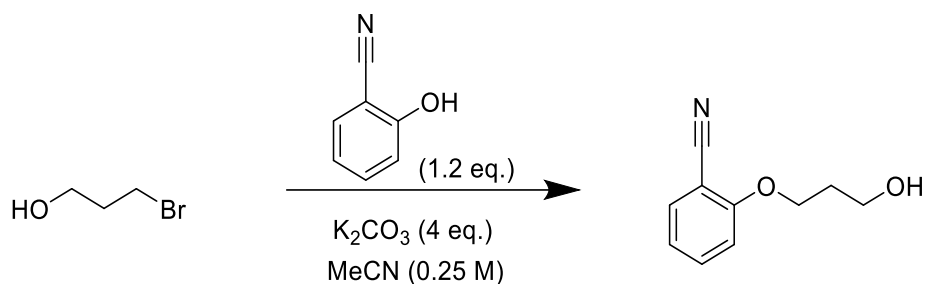
### 2-(4-fluoropyridin-3-yl)benzyl alcohol



To a solution of 2-(4-fluoropyridin-3-yl)benzaldehyde (50.0 mg, 0.25 mmol) in methanol (1.25 mL, 0.25 M) at 0 °C, Sodium borohydride (14.0 mg, 2.0 eq., 0.5 mmol) was added portion-wise, followed by stirring at 0 °C for 10 minutes. The reaction was then allowed to return to room temperature over 20 minutes. A saturated aqueous solution of NaHCO<sub>3</sub> (5 mL) was added, and the product was extracted with DCM (3 X 10 mL). The combined organic extracts were dried over magnesium sulphate, filtered, and dried *in vacuo*. The resulting residue was found to be >95% by <sup>1</sup>H NMR and was used without further purification (49.4 mg, 0.24 mmol, 97%) as a colourless oil.

<sup>1</sup>H NMR (500 MHz, CDCl<sub>3</sub>) δ 8.24 (d, *J* = 2.5 Hz, 1H), 7.89 (ddd, *J* = 8.3, 7.5, 2.5 Hz, 1H), 7.58 (dd, *J* = 7.5, 1.5 Hz, 1H), 7.45 (td, *J* = 7.5, 1.5 Hz, 1H), 7.40 (td, *J* = 7.5, 1.5 Hz, 1H), 7.27 (dd, *J* = 7.5, 1.5 Hz, 1H), 7.00 (ddd, *J* = 8.3, 3.0, 0.7 Hz, 1H), 4.57 (d, *J* = 2.0 Hz, 2H). <sup>19</sup>F{<sup>1</sup>H} NMR (471 MHz, CDCl<sub>3</sub>) δ -70.2. <sup>13</sup>C{<sup>1</sup>H} NMR (126 MHz, CDCl<sub>3</sub>) δ 162.97 (d, *J* = 239.8 Hz), 147.42 (d, *J* = 14.5 Hz), 142.01 (d, *J* = 8.0 Hz), 138.21, 136.66, 134.23 (d, *J* = 4.8 Hz), 130.28, 129.18, 128.76, 128.22, 108.94 (d, *J* = 37.2 Hz), 62.97. ATR-FTIR (cm<sup>-1</sup>) 3330 (O-H stretch).

## 2-(3-Hydroxypropoxy)benzonitrile

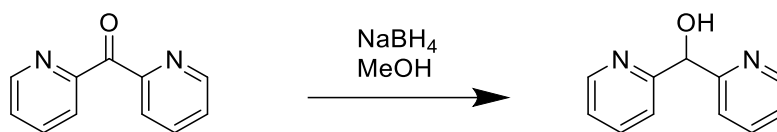


2-Hydroxybenzonitrile (2.9 g, 24.0 mmol, 1.2 eq.), and potassium carbonate (11.1 g, 80.0 mmol, 4 eq.) were dissolved in acetonitrile (80 mL, 0.25 M) with stirring, 3-bromopropan-1-ol (1.8 mL, 2.8 g, 20 mmol, 1 eq.) was added and the reaction was heated to 90 °C for 16 hours. After cooling to ambient temperature, water (40 mL) was added and the reaction acidified with 6M HCl<sub>(aq.)</sub>, the product was then extracted with DCM (3 X 50 mL), the combined organic extracts were dried over MgSO<sub>4</sub>, filtered, and dried *in vacuo*. The resulting residue was purified by column chromatography yielding the title compound (1.50 g, 8.5 mmol, 43%) as a yellow oil.

<sup>1</sup>H NMR (500 MHz, CDCl<sub>3</sub>) δ 7.58 – 7.47 (m, 2H), 7.03 – 6.95 (m, 2H), 5.29 (s, 1H), 4.23 (t, *J* = 5.9 Hz, 2H, C<sup>10</sup>), 3.91 (t, *J* = 5.9 Hz, 2H), 2.10 (p, *J* = 5.9 Hz, 2H). <sup>13</sup>C{<sup>1</sup>H} NMR (126 MHz, CDCl<sub>3</sub>) δ 160.63, 134.38, 133.69, 120.87, 116.49, 112.27, 102.07, 66.11, 59.45, 31.70. ATR-FTIR (cm<sup>-1</sup>) 3407 (O-H stretch), 2951 (C-H Stretch), 2885 (C-H stretch), 2227 (C≡N stretch). HRMS calculated for C<sub>10</sub>H<sub>12</sub>NO<sub>2</sub> [M + H<sup>+</sup>] 178.0863; found 178.0868.

## Bis(pyridin-2-yl)methanol

Chem. Eur. J. 2018, 24, 9269 –9273

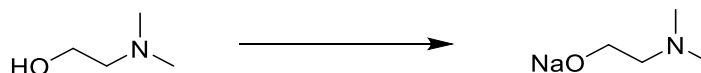


To a solution of 2,2-dipyridyl methanol (2.5 g, 1.0 eq., 13.6 mmol) in methanol (136 mL, 0.1 M) at 0 °C, Sodium borohydride (0.77 g, 1.5 eq., 20.4 mmol) was added portion-wise, followed by stirring at 0 °C for 10 minutes. The reaction was then allowed to return to room temperature over 20 minutes. Water (50 mL) was added, and the product was extracted with DCM (3 X 20 mL). The combined organic extracts were dried over magnesium sulphate, filtered, and dried *in vacuo*. The remaining residue was purified by column chromatography yielding the title compound (2.17 g, 11.7 mmol, 86%) as a white solid.

M.P. 35 -38 °C. R<sub>f</sub> (90% EtOAc/PE) 0.3. <sup>1</sup>H NMR (400 MHz, CDCl<sub>3</sub>) δ 8.52 (d, *J* = 4.9 Hz, 2H), 7.62 (td, *J* = 7.7, 1.8 Hz, 2H), 7.51 (d, *J* = 7.9 Hz, 2H), 7.16 (ddd, *J* = 7.5, 4.9, 1.3 Hz, 2H), 5.88 (s, 1H). <sup>13</sup>C{<sup>1</sup>H} NMR (101 MHz, CDCl<sub>3</sub>) δ 160.88, 148.31, 136.98, 122.69, 121.26, 75.33. ATR-IR (cm<sup>-1</sup>) 3252 (O-H).

### sodium *N,N*-dimethylaminoethoxide

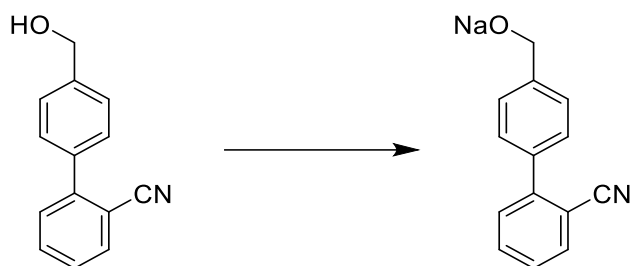
J. Chem. Soc. Perkin Trans. 1 **1998**, 1685–1690.



A 60 % dispersion of sodium hydride in mineral oil (0.45 g, X mmol) was washed three times with hexane (50 mL) by canular filtration under argon. The resulting solid was suspended in hexane (40 mL) and *N,N*-dimethyl ethanolamine (1.00 g, 1.14 mL, X mmol) was added. The mixture was stirred under argon for 5 hours, the solvent was then removed and the solid collected with cold hexane washings yielding the title compound (0.57 g, 5.14 mmol, 40 %) as a white solid.

M.P. > 300 °C. <sup>1</sup>H NMR (400 MHz, DMSO-*d*<sub>6</sub>) δ 3.86 (t, *J* = 6.3 Hz, 2H), 2.63 (t, *J* = 3.8 Hz, 2H), 2.50 (s, 6H). <sup>13</sup>C NMR (101 MHz, DMSO) δ 63.36, 59.77, 46.13. ATR-FTIR (cm<sup>-1</sup>) *No major peaks*

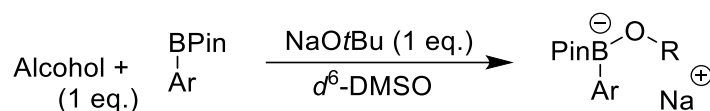
## Sodium 4-(2-Cyanophenyl)benzyloxide



4-(2-cyanophenyl)benzaldehyde 314 mg, 1.5 mmol, 1.0 eq.) was dissolved in hexane (6 mL), to this a 60% mineral oil dispersion of sodium hydride (36 mg, 1.5 mmol, 1.0 eq.) was added, the reaction was stirred for 1 hour, the solvent was removed *in vacuo* and the solid collected with cold hexane washings yielding the title compound (340 mg, 1.47 mmol, 98 %) as a white solid.

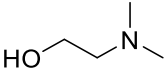
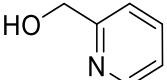
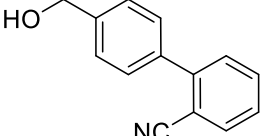
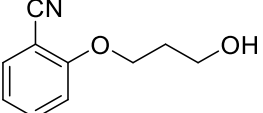
M.P. 109-112 °C. <sup>1</sup>H NMR (400 MHz, *d*<sub>6</sub>-DMSO) δ 7.94 (dd, *J* = 7.7, 1.3 Hz, 1H), 7.79 (td, *J* = 7.7, 1.3 Hz, 1H), 7.65 – 7.51 (m, 4H), 7.47 (d, *J* = 8.4 Hz, 2H), 4.57 (s, 2H). <sup>13</sup>C NMR (101 MHz, *d*<sub>6</sub>-DMSO) δ 145.02, 143.70, 136.65, 134.30, 133.99, 130.54, 128.92, 128.53, 127.17, 119.09, 110.61, 62.92. ATR-FTIR (cm<sup>-1</sup>) 2357, 2238 (C≡N stretch)

## Observation of alkoxy pinacol boronate complexes

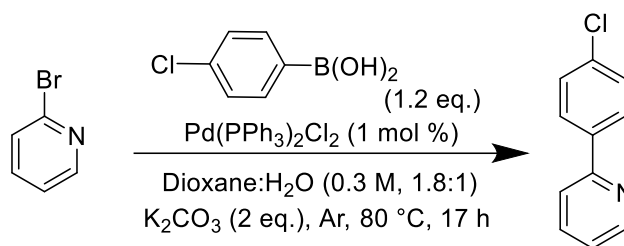


$d^6$ -DMSO was dried and stored over 4Å molecular sieves. A solution of the boronic ester was made up in  $d^6$ -DMSO (0.5 M), a second solution of the alcohol was made up in  $d^6$ -DMSO (0.5 M). Sodium *tert*-butoxide (10 mg, 0.10 mmol, 1 eq.) was weighed directly into an NMR vial, the alcohol (0.10 mmol, 0.2 mL of a 0.5 M solution, 1.0 eq.) was added from stock solution and the mixture sonicated for 5 minutes. The boronic ester (0.10 mmol, 0.2 mL of a 0.5 M solution, 1.0 eq.) was then added and the mixture sonicated again for 5 minutes. The sample was then studied by  $^{19}\text{F}\{^1\text{H}\}$  (setting relaxation delay to 10 seconds to permit quantitative analysis),  $^1\text{H}$  and  $^{11}\text{B}$  NMR spectroscopy.

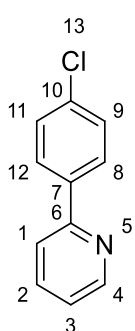
Co-ordination was best characterised from  $^{19}\text{F}\{^1\text{H}\}$  and  $^{11}\text{B}$  NMR spectra with difficulty in characterising with  $^1\text{H}$  NMR spectra due to peak overlap.

Alcohol	3-F-PhBPIn		4-F-PhBPIn	
	$^{11}\text{B}$ (ppm)	$^{19}\text{F}$ (ppm)	$^{11}\text{B}$ (ppm)	$^{19}\text{F}$ (ppm)
<b>No Alcohol/No Base</b>	30.7	-113.6	30.9	-108.3
H <sub>2</sub> O			6.0	-121.0
MeOH			6.9	-121.0
EtOH			6.9	-121.2
<i>i</i> PrOH			7.1	-120.8
<i>t</i> BuOH	6.8	-117.7	6.5	-120.8
	6.4	-117.4	6.6	-121.0
			7.0	-120.8
	7.3	-117.2		
	6.6	-117.3	6.6	-120.8

## 2-(4-Chlorophenyl)-pyridine



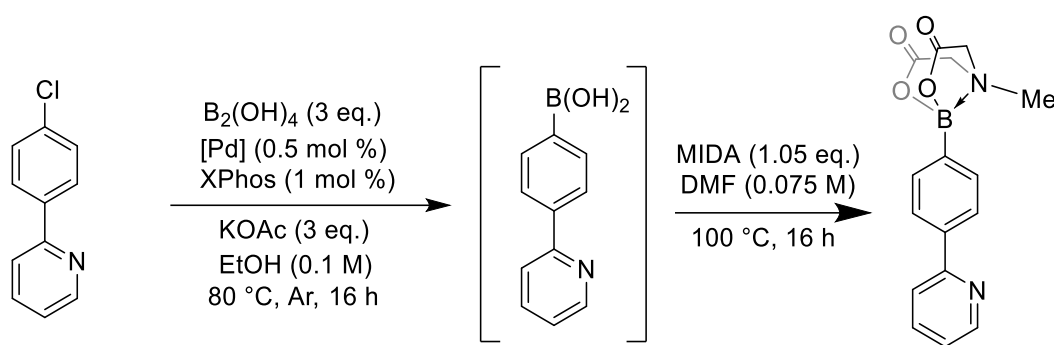
A 3-Neck round bottom flask was charged with 4-chlorophenyl boronic acid (9.42 g, 60 mmol, 1.2 eq.) and K<sub>2</sub>CO<sub>3</sub> (13.81 g, 100 mmol, 2 eq.), 1,4-Dioxane and Water was added (degassed, 0.3 M, 1.8:1, v:v = 107 mL: 60 mL), to this solution 2-Bromopyridine (7.9 g, 4.75 mL, 50 mmol, 1 eq.) was added and argon was bubbled through for 30 minutes. Bis(triphenylphosphine)palladium(II) chloride (0.35 g, 0.5 mmol, 1 mol%) was then added, and the reaction was heated to 80 °C. After 17 hours the reaction was cooled to room temperature and filtered through a celite plug with ether washings (100 mL). Aq. HCl (1 M, 150 mL, 150 mmol) was added and the organics layer was washed with aq. HCl (2 X 50 mL), the combined aqueous washings were basified with potassium carbonate. The organics were then extracted with DCM (3 X 100 mL), the combined organic layer was dried over MgSO<sub>4</sub>, filtered, and then dried *in vacuo*. The resulting crude was further purified by silica-gel chromatography (Et<sub>2</sub>O:Hexane:NEt<sub>3</sub>, 8:2:0.1) yielding the title product (6.1 g, 32.3 mmol, 65 %) as a white crystalline solid.



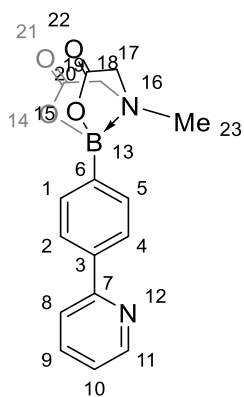
M.P. 54 – 57 °C. <sup>1</sup>H NMR (500 MHz, CDCl<sub>3</sub>) δ 8.68 (ddd, *J* = 4.8, 1.8, 1.0 Hz, 1H, C<sup>4</sup>-H), 7.94 (d, *J* = 8.7 Hz, 2H, C<sup>9,11</sup>-H), 7.75 (ddd, *J* = 7.9, 7.3, 1.8 Hz, 1H, C<sup>3</sup>-H), 7.69 (dt, *J* = 8.0, 1.1 Hz, 1H, C<sup>1</sup>-H), 7.44 (d, *J* = 8.7 Hz, 2H, C<sup>8,12</sup>-H), 7.24 (ddd, *J* = 7.3, 4.8, 1.3 Hz, 1H, C<sup>2</sup>-H). <sup>13</sup>C NMR (101 MHz, CDCl<sub>3</sub>) δ 156.35 (C<sup>6</sup>), 149.89 (C<sup>4</sup>), 137.94 (C<sup>7</sup>), 136.98 (C<sup>3</sup>), 135.23 (C<sup>10</sup>), 129.05 (C<sup>8,12</sup>), 128.29 (C<sup>9, 11</sup>), 122.49 (C<sup>2</sup>), 120.44 (C<sup>1</sup>). ATR-FTIR (cm<sup>-1</sup>) No major peaks



**8-(4-(2-pyridyl)phenyl)-4-methyl-2,6-dioxohexahydro-[1,3,2]-oxazaborolo-[2,3-b]-[1,3,2]-oxazaborol-4-ium-8-uide**

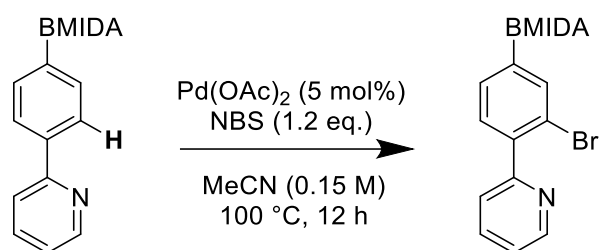


To an oven dried flask capable of sealing with a Teflon cap, was added 2-(4-chlorophenyl)pyridine (2.0 g, 10.6 mmol), XPhos Palladium(II) biphenyl preformed catalyst (40.9 mg, 0.5 mol%, 53  $\mu$ mol). Xphos (53.9 mg, 1.0 mol%, 106  $\mu$ mol), potassium acetate (3.11 g, 3 eq., 31.7 mmol) and tetrahydroxydiboron (2.85g, 3 eq., 31.7 mmol), the flask was sealed and the vessel evacuated and backfilled with argon four times. Ethanol (degassed, dried over 4Å MS, 106 mL, 0.1 M) was added and the resulting solution was stirred at 80 °C for 16 hrs. This was then cooled to ambient temperature and filtered through a short pad of celite, with EtOAc washings, the filtrate was then dried *in vacuo*. The resulting residue was dissolved in DCM (80 mL) and H<sub>2</sub>O (80 mL) was added. The aqueous layer was washed with DCM (3 X 40 mL), the combined organic washes were then dried over MgSO<sub>4</sub>, filtered, and dried *in vacuo*. To the remaining residue, *N*-methyliminodiacetic acid (1.64 g, 1.05 eq., 11.1 mmol) was added and dissolved in DMF (140 mL, 0.075 M), this was stirred at 100 °C for 18 hrs, after which the solvent was removed *in vacuo*. The remaining residue was purified by silica-gel chromatography (Et<sub>2</sub>O:Hexane:NEt<sub>3</sub> 7:3:0.1 then THF(BHT-free):Acetone:NEt<sub>3</sub> 9:1:0.1) yielding the title compound (1.59 g, 5.13 mmol, 48 %) as a white crystalline solid.



M.P. 212 -216 °C. R<sub>f</sub> (100% THF) 0.2. <sup>1</sup>H NMR (400 MHz, *d*<sub>6</sub>-DMSO) δ 8.68 (ddd, *J* = 4.8, 1.8, 1.0 Hz, 1H, C<sup>11</sup>-H), 8.08 (d, *J* = 8.3 Hz, 2H, C<sup>2,4</sup>-H), 7.99 (dt, *J* = 8.0, 1.0 Hz, 1H, C<sup>8</sup>-H), 7.89 (ddd, *J* = 8.0, 7.4, 1.8 Hz, 1H, C<sup>9</sup>-H), 7.57 (d, *J* = 8.3 Hz, 2H, C<sup>1,5</sup>-H), 7.36 (ddd, *J* = 7.4, 4.8, 1.0 Hz, 1H, C<sup>10</sup>-H), 4.37 (d, *J* = 17.2 Hz, 2H, C<sup>17,18</sup>-HH), 4.16 (d, *J* = 17.2 Hz, 2H, C<sup>17,18</sup>-HH), 2.55 (s, 3H, C<sup>23</sup>-H<sub>3</sub>). <sup>1</sup>H NMR (400 MHz, *d*<sub>3</sub>-MeCN) δ 8.66 (ddd, *J* = 4.8, 1.8, 1.0 Hz, 1H), 8.06 (d, *J* = 8.3 Hz, 2H), 7.90 – 7.80 (m, 2H), 7.62 (d, *J* = 8.2 Hz, 2H), 7.30 (ddd, *J* = 7.3, 4.8, 1.4 Hz, 1H), 4.09 (d, *J* = 17.1 Hz, 2H), 3.92 (d, *J* = 17.1 Hz, 2H), 2.55 (s, 3H). <sup>11</sup>B NMR (160 MHz, *d*<sub>6</sub>-DMSO) δ 11.83. <sup>11</sup>B NMR (128 MHz, *d*<sub>3</sub>-MeCN) δ 11.38. <sup>13</sup>C{<sup>1</sup>H} NMR (126 MHz, *d*<sub>6</sub>-DMSO) δ 169.40 (C<sup>19,20</sup>), 156.03 (C<sup>7</sup>), 149.56 (C<sup>11</sup>), 139.06 (C<sup>3</sup>), 137.22 (C<sup>9</sup>), 132.86 (C<sup>1,5</sup>), 125.73 (C<sup>2, 4</sup>), 122.64 (C<sup>10</sup>), 120.25 (C<sup>8</sup>), 61.83 (C<sup>17,18</sup>), 47.62 (C<sup>23</sup>). 11 of 12 signals observed with the quaternary C<sup>6</sup> carbon resonance identified to be absent, a correlation in the HMBC indicates a resonance at 139 ppm. <sup>13</sup>C NMR (101 MHz, *d*<sub>3</sub>-MeCN) δ 169.53, 157.60, 150.61, 137.96, 133.87, 127.05, 123.45, 121.30, 62.78, 48.47. 11 of 12 signals observed. ATR-FTIR (cm<sup>-1</sup>) 1746 (C=O stretch). HRMS calculated for C<sub>16</sub>H<sub>17</sub>BN<sub>2</sub>O<sub>4</sub> [M + H<sup>+</sup>] 312.1270; found 312.1284

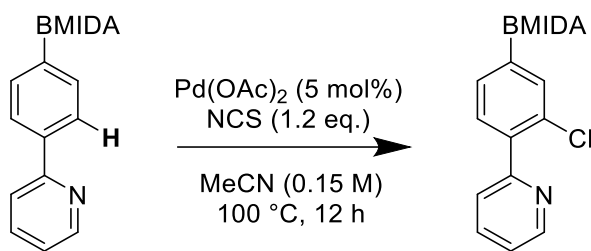
**8-(3-Bromo-4-(2-pyridyl)phenyl)-4-methyl-2,6-dioxohexahydro-[1,3,2]-oxazaborolo-[2,3-b]-[1,3,2]-oxazaborol-4-ium-8-uide**



2-(4-BMIDA-Phenyl)Pyridine (62 mg, 0.2 mmol, 1.0 eq.),  $\text{Pd}(\text{OAc})_2$  (2.2 mg, 5 mol%) and *N*-bromosuccinimide (43 mg, 0.24 mmol, 1.2 eq.) were dissolved in acetonitrile (1.3 mL, 0.15 M) and heated to  $100\text{ }^\circ\text{C}$  with stirring. After 16 hours the reaction was cooled to room temperature and filtered through a short celite pad with acetonitrile washings. Solvent was then removed *in vacuo*. The remaining residue was subjected to silica gel chromatography, first eluting with ether then THF realising the desired product (31.0 mg, 0.08 mmol, 40 %) as a 1.0:8.3 mixture of starting material to product.

$R_f$  (100 % THF) 0.2.  $^1\text{H}$  NMR (400 MHz,  $d_3$ -MeCN)  $\delta$  8.66 (ddt,  $J = 4.8, 1.8, 0.9$  Hz, 1H), 7.90 – 7.78 (m, 2H), 7.64 – 7.48 (m, 3H), 7.37 (ddd,  $J = 7.6, 4.8, 1.2$  Hz, 1H), 4.11 (d,  $J = 16.8$  Hz, 2H), 3.95 (d,  $J = 16.8$  Hz, 2H), 2.60 (s, 3H).  $^{13}\text{C}$  NMR (101 MHz,  $d_3$ -MeCN)  $\delta$  169.42, 159.26, 150.32, 143.11, 138.05, 137.13, 132.78, 132.07, 125.55, 123.72, 63.04, 48.73. 12 of 13 resonances observed. ATR-FTIR ( $\text{cm}^{-1}$ ) 2356, 1755 (C=O stretch) HRMS calculated for  $\text{C}_{16}\text{H}_{16}\text{B}^{79}\text{BrN}_2\text{O}_4$  [ $\text{M} + \text{H}^+$ ] 389.0303; found 389.0266.

**8-(3-Chloro-4-(2-pyridyl)phenyl)-4-methyl-2,6-dioxohexahydro-[1,3,2]-oxazaborolo-[2,3-b]-[1,3,2]-oxazaborol-4-ium-8-uide**

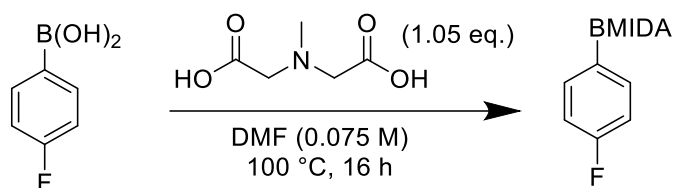


2-(4-BMIDA-Phenyl)Pyridine (62 mg, 0.2 mmol, 1.0 eq.), Pd(OAc)<sub>2</sub> (2.2 mg, 5 mol%) and *N*-chlorosuccinimide (32 mg, 0.24 mmol, 1.2 eq.) were dissolved in acetonitrile (1.3 mL, 0.15 M) and heated to 100 °C with stirring. After 16 hours the reaction was cooled to room temperature and filtered through a short celite pad with acetonitrile washings. Solvent was then removed *in vacuo*. The remaining residue was subjected to silica gel chromatography, first eluting with ether then THF realising the desired product (10.8 mg, 0.032 mmol, 16 %) as a 1.0:1.3 mixture of starting material to product.

R<sub>f</sub> (100 %THF) 0.2. <sup>1</sup>H NMR (500 MHz, *d*<sub>3</sub>-MeCN) δ 8.68 (ddd, *J* = 4.8, 1.8, 1.0 Hz, 1H), 7.89 – 7.79 (m, 1H), 7.68 – 7.49 (m, 4H), 7.37 (ddd, *J* = 7.6, 4.8, 1.2 Hz, 1H), 4.11 (d, *J* = 16.8 Hz, 2H), 3.95 (d, *J* = 16.8 Hz, 2H), 2.60 (s, 3H). <sup>13</sup>C{<sup>1</sup>H} NMR (101 MHz, *d*<sub>3</sub>-MeCN) δ 169.35, 157.68, 150.40, 140.94, 137.07, 134.80, 133.00, 132.15, 125.60, 123.64, 62.94, 48.63. 12 of 13 resonances observed. ATR-FTIR (cm<sup>-1</sup>) 2358, 1752 (C=O stretch). HRMS calculated for C<sub>16</sub>H<sub>16</sub>BClN<sub>2</sub>O<sub>4</sub> [M + H<sup>+</sup>] 345.0808; found 345.0859.

**8-(4-fluorophenyl)-4-methyl-2,6-dioxohexahydro-[1,3,2]-oxazaborolo-  
[2,3-b]-[1,3,2]-oxazaborol-4-ium-8-uide**

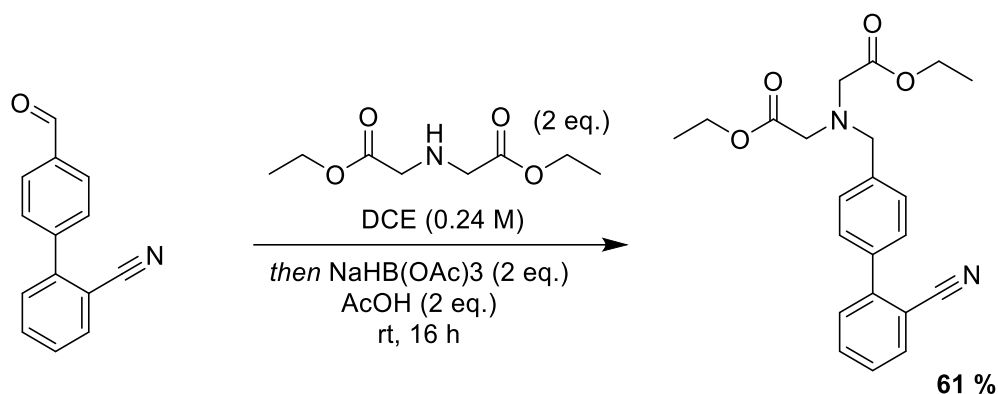
Angew. Chem. Int. Ed. 2021, 60, 24510–24518



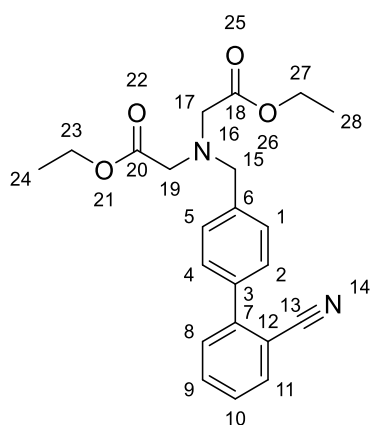
4-Fluorophenyl boronic acid (0.5 g, 3.6 mmol, 1.0 eq.) and *N*-methyl iminodiacetic acid (0.55 g, 3.7 mmol, 1.05 eq.) were dissolved in DMF (48 mL, 0.075 M) and stirred at 100 °C. After 16 hours, DMF was removed *in vacuo* and the remaining residue was triturated with diethyl ether, a precipitate was collected with diethyl ether washings yielding the title compound (0.85 g, 3.4 mmol, 95%) as an off-white solid.

M.P. 229 - 231 °C.  $R_f$  (100 %THF) 0.2.  $^1\text{H}$  NMR (400 MHz,  $d_3$ -MeCN)  $\delta$  8.13 – 7.95 (m, 2H), 7.75 – 7.57 (m, 2H), 4.62 (d,  $J$  = 17.1 Hz, 2H), 4.44 (d,  $J$  = 17.1 Hz, 2H), 3.06 (s, 3H).  $^1\text{H}$  NMR (400 MHz, DMSO- $d_6$ )  $\delta$  7.51 – 7.44 (m, 2H), 7.23 – 7.12 (m, 2H), 4.34 (d,  $J$  = 17.2 Hz, 2H), 4.12 (d,  $J$  = 17.2 Hz, 2H), 2.50 (s, 6H).  $^{11}\text{B}$  NMR (128 MHz,  $d_3$ -MeCN)  $\delta$  11.93.  $^{11}\text{B}$  NMR (128 MHz, DMSO)  $\delta$  11.65.  $^{19}\text{F}\{^1\text{H}\}$  NMR (376 MHz,  $d_3$ -MeCN)  $\delta$  -113.68.  $^{19}\text{F}\{^1\text{H}\}$  NMR(376 MHz, DMSO)  $\delta$  -113.01.  $^{13}\text{C}$  NMR (101 MHz,  $d_3$ -MeCN)  $\delta$  286.40, 281.77 (d,  $J$  = 245.4 Hz), 252.68 (d,  $J$  = 7.9 Hz), 232.63 (d,  $J$  = 20.2 Hz), 179.78, 165.45. 6 of 7 resonances observed. ATR-FTIR ( $\text{cm}^{-1}$ ) 3014, 1743 (C=O stretch).

## *N,N*-bis(ethoxycarbonylmethyl)-4-(2-cyanophenyl)benzylamine

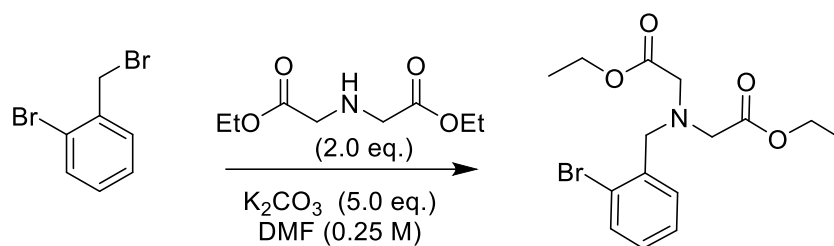


4-(2-cyanophenyl)benzaldehyde (1.04 g, 4.8 mmol) and diethyl iminodiacetate (1.76 mL, 9.6 mmol, 2 eq.) were dissolved in DCE (20 mL, 0.24 M), acetic acid was added (0.6 mL, 10.4 mmol, 2 eq.) and the reaction was stirred at ambient conditions for 1 hour. Sodium triacetoxyborohydride (2.12 g, 9.6 mmol, 2 eq.) was then added and the reaction was allowed to stir for 16 hours under ambient conditions. The reaction was quenched with sat.  $\text{NaHCO}_3$  (aq.) and the product was extracted with DCM (3 X 50 mL), the combined organic washings were then dried over  $\text{MgSO}_4$ , filtered and dried *in vacuo*. The resulting residue was subjected to silica gel chromatography (10 % EtOAc:Hexane to 30 % EtOAc:Hexane) yielding the title compound (1.1 g, 2.9 mmol, 60 %) as a colourless oil.



$R_f$  (30 % EtOAc/Hexane) = 0.3.  $^1\text{H}$  NMR (500 MHz,  $\text{CDCl}_3$ )  $\delta$  7.76 (d,  $J = 7.8$  Hz, 1H, C<sup>8</sup>-H), 7.63 (t,  $J = 7.7$  Hz, 1H, C<sup>9</sup>-H), 7.53-7.50 (m, 5H, C<sup>1,5</sup>-H, C<sup>2,4</sup>-H and C<sup>11</sup>-H), 7.43 (t,  $J = 7.6$  Hz, 1H, C<sup>10</sup>-H), 4.18 (q,  $J = 7.1$  Hz, 4H, C<sup>23,27</sup>-H<sub>2</sub>), 3.99 (s, 2H, C<sup>15</sup>-H<sub>2</sub>), 3.58 (s, 4H, C<sup>19,17</sup>-H<sub>2</sub>), 1.28 (t,  $J = 7.1$  Hz, 6H, C<sup>24,28</sup>-H<sub>3</sub>).  $^{13}\text{C}$  NMR (126 MHz,  $\text{CDCl}_3$ )  $\delta$  171.33 (C<sup>18,20</sup>), 145.42 (C<sup>7</sup>), 139.27 (C<sup>6</sup>), 137.32 (C<sup>3</sup>), 133.92 (C<sup>8</sup>), 132.93 (C<sup>9</sup>), 130.20 (C<sup>11</sup>), 129.39 (C<sup>1,5</sup>), 128.93 (C<sup>2,4</sup>), 127.59 (C<sup>10</sup>), 118.90 (C<sup>13</sup>), 111.32 (C<sup>12</sup>), 60.64 (C<sup>27,23</sup>), 57.65 (C<sup>15</sup>), 54.49 (C<sup>19,17</sup>), 14.39 (C<sup>28,24</sup>). ATR-FTIR ( $\text{cm}^{-1}$ ) 2981 (C-H Stretch), 2224 (C $\equiv$ N stretch), 1731 (C=O Stretching). HRMS calculated for  $\text{C}_{21}\text{H}_{23}\text{N}_2\text{O}_4$  [ $\text{M} + \text{H}^+$ ] 367.1652; found 367.1600.

### ***N,N*-bis(ethoxycarbonylmethyl)-2-bromo-benzylamine**



2-Bromobenzyl bromide (1.0 g, 4.0 mmol, 1.0 eq.) and potassium carbonate (1.66 g, 8.0 mmol, 3 eq.) was dissolved in dimethyl formamide (16 mL, 0.25 M) with stirring, diethyl iminodiacetate (1.51 g, 1.4 mL, 8.0 mmol, 2 eq.) was added and the reaction was heated to 70 °C for 16 hours. The reaction was then cooled to room temperature and diluted with water (50 mL), the product was then extracted with ethyl acetate (3 X 50 mL), the combined organic washings were then washed with a 50% brine solution (50 mL), dried over magnesium sulfate, filtered, and dried *in vacuo*. The resulting residue was purified by column chromatography (5% to 20% EtOAc/PE) to yield the title compound (0.92 g, 2.6 mmol, 65%) as a colourless oil.

$R_f$  (10 % EtOAc/PE) = 0.3.  $^1H$  NMR (500 MHz,  $CDCl_3$ )  $\delta$  7.70 (d,  $J$  = 7.5 Hz, 1H), 7.52 (d,  $J$  = 8.0 Hz, 1H), 7.31 (t,  $J$  = 7.5 Hz, 1H), 7.12 (t,  $J$  = 7.6 Hz, 1H), 4.17 (q,  $J$  = 7.1 Hz, 4H), 4.11 (s, 2H), 3.65 (s, 4H), 1.27 (t,  $J$  = 7.1 Hz).  $^{13}C$  NMR (126 MHz,  $CDCl_3$ )  $\delta$  170.51, 136.67, 132.76, 131.34, 129.12, 127.69, 124.44, 60.78, 57.35, 54.15, 14.20. ATR-FTIR ( $cm^{-1}$ ) 2979 (C-H), 1734 (C=O).